

Calcium Channel Distribution in the Arterial Vascular Tree and its Relation to Function

Christine June Ball, BSc (Hons)

A thesis submitted for the degree of

Doctor of Philosophy

Cardiology Unit

The Queen Elizabeth Hospital

Department of Medicine

Faculty of Health Sciences

The University of Adelaide

December 2009

TABLE OF CONTENTS

DECLARATION	xi
ACKNOWLEDGEMENTS	xii
THESIS-RELATED PUBLICATIONS	xiv
PUBLISHED ABSTRACTS	xv
PRESENTATIONS AT NATIONAL AND INTERNATIONAL CONFERENCES	xvi
AWARDS AND SCHOLARSHIPS	xviii
ABBREVIATIONS	xix
ABSTRACT	xxii
<u>SECTION A – INTRODUCTION</u>	1
A.1 SCOPE	2
A.2 THE VASCULATURE	3
A.2.1 Vascular Anatomy	3
A.2.1.1 ARTERIAL SYSTEM	
A.2.1.2 VENOUS SYSTEM	
A.2.1.3 MICROCIRCULATION	
A.2.2 Functional Anatomy	6
A.2.3 Vascular Histology	6
A.2.3.1 INTIMA	
A.2.3.2 MEDIA	
A.2.3.3 ADVENTITIA	

A.3	VASCULAR PHYSIOLOGY	8
A.3.1	Haemodynamic Principles	8
A.3.2	Regulatory Influences of Vascular Tone	9
A.3.2.1	ENDOTHELIAL INFLUENCES	
A.3.2.1.1	Nitric Oxide	
A.3.2.1.2	Prostacyclin	
A.3.2.1.3	Endothelium Derived Hyperpolarising Factor	
A.3.2.1.4	Endothelin	
A.3.2.2	HUMORAL INFLUENCES	
A.3.2.2.1	Catecholamines	
A.3.2.2.2	Bradykinin	
A.3.2.3	NEUROGENIC INFLUENCES	
A.3.2.3.1	Cholinergic Innervation	
A.3.2.3.2	Adrenergic Innervation	
A.3.2.3.3	Noncholinergic-Nonadrenergic Innervation	
A.4	VASCULAR CELL BIOLOGY	26
A.4.1	The Actin-Myosin Contractile Apparatus	26
A.4.2	Regulation of Myosin Light Chain Phosphorylation	27
A.4.2.1	MYOSIN LIGHT CHAIN KINASE AND IT'S REGULATION IN THE CONTEXT OF VASCULAR CONTRACTION	

A.4.2.2	MYOSIN LIGHT CHAIN PHOSPHATASE AND ITS REGULATION IN THE CONTEXT OF VASCULAR CONTRACTION	
A.5	REGULATION OF CYTOSOLIC CALCIUM	33
A.5.1	Voltage-Operated Calcium Channels	34
A.5.1.1	VOLTAGE-OPERATED CALCIUM CHANNEL SUBUNIT COMPOSITION AND FUNCTION	
A.5.1.2	VOLTAGE-OPERATED CALCIUM CHANNEL SUBGROUPS	
A.5.1.2.1	L-type Calcium Channels	
A.5.1.2.2	T-type Calcium Channels	
A.5.1.2.3	P/Q-, N- and R-type Channels	
A.5.1.3	VOLTAGE-OPERATED CALCIUM CHANNEL ANTAGONISTS	
A.5.2	Receptor-Operated Calcium Channels	49
A.5.3	Store-Operated Calcium Channels	50
A.5.4	Potassium Channels	51
A.5.5	Chloride Channels	53
A.6	VASCULAR PATHOPHYSIOLOGY	54
A.6.1	Pathophysiology Triad	54
A.6.2	Clinical Syndromes: Large Conduit Vessel Disorders vs. Small Resistance Vessel Disorders	56
A.6.2.1	LARGE CONDUIT VESSEL DISORDERS	
A.6.2.1.1	Coronary Artery Disease	

A.6.2.1.1	Peripheral Artery Disease	
A.6.2.2	SMALL RESISTANCE VESSEL DISORDERS	
A.6.2.2.1	Coronary Microvascular Disorders	
A.6.2.2.2	Hypertension	
A.6.2.2.3	Cerebral Microvascular Disorders	
A.6.3	Clinical Role of Calcium Channel Blockers	60
A.7	SUMMARY AND AIMS	61
<u>SECTION B – Ca⁺⁺ L- AND T- CHANNEL BLOCKADE IN</u>		
<u>RAT AND HUMAN VESSELS</u>		
B.1	BACKGROUND	64
B.1.1	Ca ⁺⁺ Channel Blocker Classifications	64
B.1.2	T-Channel Blockers in the Microcirculation	65
B.1.3	Study Objectives	66
B.2	METHODS	67
B.2.1	Vascular Preparations	67
B.2.1.1	RAT VESSELS	
B.2.1.2	HUMAN VESSELS	
B.2.2	Chronic Endothelin Infusion Model	69
B.2.2.1	MINI-OSMOTIC PUMP AND CANNULA PREPARATION	
B.2.2.2	MINI-OSMOTIC PUMP IMPLANTATION	
B.2.2.2	BLOOD PRESSURE MEASUREMENT	
B.2.3	Small Vessel Myograph Assessment of Vascular Reactivity	72

B.2.3.1	SMALL VESSEL MYOGRAPH BACKGROUND	
B.2.3.2	TISSUE HANDLING AND DISSECTION	
B.2.3.3	VESSEL MOUNTING	
B.2.4	Standardisation of Vascular Responses	75
B.2.4.1	VESSEL CALIBRE NORMALISATION	
B.2.4.2	NORMALISATION FOR DEPOLARISATION RESPONSE	
B.2.4.3	DEPOLARISING WITH POTASSIUM	
B.2.5	Endothelial Integrity	78
B.2.6	Study Reagents	78
B.2.6.1	VASOCONSTRICTORS	
B.2.6.2	VASODILATORS	
B.2.6.3	Ca ⁺⁺ CHANNEL BLOCKERS	
B.2.7	Data Analysis	80
B.2.7.1	CONCENTRATION-RESPONSE CURVE CHARACTERISTICS	
B.2.7.2	STATISTICAL ANALYSIS	
B.2.8	Study Protocol	82
B.3	RESULTS	84
B.3.1	Ca⁺⁺ Channel Blocker Dose Ranging Study	84
B.3.2	Inhibition of Rat Constrictor Responses by Ca⁺⁺ Channel Blockers at Therapeutic Equivalent Concentrations	86
B.3.2.1	ENDOTHELIN-1-MEDIATED CONSTRICTION	
B.3.2.1.1	Rat Microvascular Responses	

B.3.2.1.2	Rat Aortic Vessel Responses	
B.3.2.2	HIGH POTASSIUM-MEDIATED DEPOLARISATION	
B.3.2.2.1	Rat Microvascular Responses	
B.3.2.2.2	Rat Aortic Vessel Responses	
B.3.3	Inhibitory Effect of Efonidipine in Rat Microvessels with Maximal L-Channel Blockade	92
B.3.4	Inhibition of Rat Constrictor Responses by Ca⁺⁺ Channel Blockers at Therapeutic-Equivalent Concentrations in the Presence of Chronic Et-1 Receptor Activation	94
B.3.4.1	SHAM AND ET-1 RAT BLOOD PRESSURE DURING CHRONIC ET-1 TREATMENT	
B.3.4.2	RAT MICROVASCULAR RESPONSES IN THE PRESENCE OF CHRONIC ET-1	
B.3.4.3	RAT AORTIC RESPONSES IN THE PRESENCE OF CHRONIC ET-1	
B.3.5	Human Subcutaneous Microvascular Response	99
B.4	DISCUSSION	100
B.4.1	Heterogeneity in Vascular Responses to L- and Combined L- and T-type Ca⁺⁺ Channel Blockers	100
B.4.2	Vascular T-Channel Blockade	103
B.4.3	Implications	106
B.5	CONCLUSIONS	106

SECTION C – QUANTITATION OF L- AND T-TYPE Ca⁺⁺

<u>CHANNELS IN LARGE AND SMALL VESSELS</u>	107
C.1 BACKGROUND	108
C.1.1 Ca⁺⁺ Channels	108
C.1.2 T-Channel Molecular Biology	110
C.1.3 Ca⁺⁺ Channel Distribution in the Vasculature	111
C.1.4 Study Objectives	113
C.2 METHODOLOGY	114
C.2.1 Isolated Vessel Preparations	114
C.2.1.1 RAT MESENTERIC AND AORTIC VESSELS	
C.2.1.1 TISSUE HANDLING AND DISSECTION	
C.2.2 Quantitation of the mRNA Encoding the Pore-Forming Subunits of Ca⁺⁺ Channels Using Real-Time PCR	115
C.2.2.1 RNA EXTRACTION	
C.2.2.2 REVERSE TRANSCRIPTION	
C.2.2.3 REFERENCE CONTROL GENES (HOUSEKEEPING GENES)	
C.2.2.4 QUANTITATIVE PCR PROTOCOL	
C.2.2.4.1 Primers	
C.2.2.5 DATA ANALYSIS	
C.2.2.5.1 Statistical Analysis	
C.2.2.6 STUDY PROTOCOL	
C.2.3 Ratiometric Quantitation of the Proteins Comprising the Pore Forming Subunits of L- and T-Channels	118

C.2.3.1	ANTIBODIES	
C.2.3.2	PROTEIN ISOLATION	
C.2.3.3	SDS-PAGE AND WESTERN BLOTTING PROTOCOL	
C.2.3.4	PROTEIN QUANTITATION	
C.2.3.4.1	Establishing the Linear Range of Detection	
C.2.3.5	DATA ANALYSIS	
C.2.3.5.1	Statistical Analysis	
C.3	RESULTS	126
C.3.1	Quantitation of Ca⁺⁺ Channel mRNA	126
C.3.1.1	mRNA EXPRESSION OF L- AND T-CHANNELS IN RAT AORTA AND MESENTERIC VESSELS	
C.3.1.2	MELT CURVE ANALYSIS OF PCR PRODUCTS FOLLOWING QUANTIATIVE PCR: IDENTIFICATION OF EFFICIENCY	
C.3.2	Relative Quantitation of Ca⁺⁺ Channel Protein	127
C.3.2.1	LINEAR QUANTITATION OF L- AND T-CHANNELS IN RAT AORTA AND MESENTERIC MICROVESSELS	
C.3.2.2	L-CHANNEL VS. T-CHANNEL ABUNDANCE	
C.4	DISCUSSION	130
C.4.1	Heterogeneity in Channel Distribution According to Vessel Size	131

C.4.2	The Ca⁺⁺ T-Channel in the Microvasculature	132
C.4.3	Clarifications	133
C.5	CONCLUSIONS	134
 <u>SECTION D – CONCLUSIONS AND OVERVIEW</u>		135
 <u>APPENDICES</u>		141
 <u>REFERENCES</u>		156

DECLARATION

This thesis contains no material which has been accepted for the award of any other degree or diploma in any university or other tertiary institution and, to the best of my knowledge and belief, contains no material previously published or written by another person, except where due reference has been made in the text.

I give consent to this copy of my thesis when deposited in the University Library, being made available for loan and photocopying, subject to the provisions of the Copyright Act 1968.

The author acknowledges that copyright of published works contained within this thesis (as listed on page xiv) resides with the copyright holder(s) of those works

Christine J Ball

(March 2010)

ACKNOWLEDGEMENTS

The contents of this thesis cover my research studies over the past 4 years. During this period I have primarily been funded by a Queen Elizabeth Hospital Research Foundation/Faculty of Health Sciences Postgraduate Research Scholarship. At various times I have also been funded by an International Society for Heart Research (Australian Section) and Ivan de la Lande Memorial (Queen Elizabeth Hospital) Travel Grants. Without the support of the above funding agencies and the patience of my supervisors and colleagues this research would not have been possible.

Firstly, I would like to express my sincerest thanks to the principal supervisor of this thesis, A/Prof John Beltrame. His relentless enthusiasm for “bench to bedside” research has been a constant source of encouragement which I will always be thankful for. Without all of your help and support this thesis would never have eventuated. I have learnt so very much from you and thank you.

I would also like to thank my co-supervisors A/Prof David Saint and Dr David Wilson. Your many years of physiology and research experience have been invaluable throughout my PhD and have provided me with a sound basis for developing research practices and always thinking “two steps ahead”.

The component of this thesis which examined human subcutaneous microvessel reactivity required a close collaboration with the vascular surgical team at The Queen Elizabeth Hospital headed by Professor Rob Fitridge. I thank them for their support

and assistance in this area. A special acknowledgment must also be made to Mrs. Irene Stafford for her help and assistance with the technical aspects of my microvascular studies.

On a personal note, to my husband, Daniel, a special thanks. It takes a special person to tolerate the long hours and stress related with research and the production of a thesis. Your love and support throughout this period has meant more to me than I could ever express.

Finally, I must thank my parents and sisters. Firstly to my sisters I want to thank you for all your support and encouragement over the past 4 years. To my parents since my childhood you have always encouraged me to aim high and dream big and have always supported me, and believed without doubt, that I would achieve all my academic goals. Thank you all for your love and support.

PUBLICATIONS

Ball C, Wilson D, Turner S, Saint D, Beltrame J. Heterogeneity of L- and T-Channels in the Vasculature: a Rationale for the Efficacy of Combined L- and T-Blockade. *Hypertension* 2009; 53(4):654-660. (Appendix 1)

Wilson D, Ball C, Turner S, Saint D, Beltrame J. Response to Is Combined L- and T-Channel Blockade Better Than L-Channel Blockade in Therapy. *Hypertension* 2009; 54:e4. (Appendix 2)

PUBLISHED ABSTRACTS

Ball C, Saint D, Wilson D, Beltrame J. Heterogeneity in vasomotor responses to L- and T-type calcium channel blockers. *Journal of Molecular and Cellular Cardiology* 2008;44(4):817-818

Ball C, Saint D, Beltrame J, Wilson D. The role of L- and T- channels in the large and microvasculature. *Heart, Lung and Circulation* 2008;17(3):S241

Ball C, Saint D, Wilson D, Beltrame J. Heterogeneity in vasomotor responses to L- and T-type calcium channel blockers. *Heart, Lung and Circulation* 2007;16(2): S212-S213

Ball C, Saint D, Beltrame J. The effect of efonidipine hydrochloride on human subcutaneous microvascular constrictor responses. *Journal of Molecular and Cellular Cardiology* 2006;41(4):733

PRESENTATIONS AT NATIONAL AND INTERNATIONAL CONFERENCES

2009

- National Heart Foundation of Australia, Brisbane

2008

- International Society for Heart Research Congress, Greece
- International Society for Heart Research, Adelaide

2007

- International Society for Heart Research, New Zealand
- Frontiers in Vascular Medicine, Melbourne
- The Queen Elizabeth Hospital Research Day, Adelaide

2006

- National Health and Medical Research Congress, Melbourne
- International Society for Heart Research, Canberra
- The Queen Elizabeth Hospital Research Day, Adelaide
- Australian Society for Medical Research, Adelaide

2005

- European Society of Cardiology, Sweden
- Cardiac Society of Australia and New Zealand, Perth
- The Queen Elizabeth Hospital Research Day, Adelaide

AWARDS AND SCHOLARSHIPS

2008

- International Society for Heart Research Young Investigator of the Year Recipient (Australasian Section)

2007

- The Queen Elizabeth Hospital Research Day Ivan De LaLande Memorial Travel Fund
- International Society for Heart Research Young Investigator Finalist
- International Society for Heart Research Travel Grant (Australasian Section)
- Frontiers in Vascular Medicine Young Investigator Finalist

2006

- The Queen Elizabeth Hospital Research Day Oral Presentation Award Recipient

2005

- The University of Adelaide, Faculty of Health Sciences Postgraduate Research Scholarship

ABBREVIATIONS

5HT	5-Hydroxytryptamine (commonly known as Serotonin)
ACh	Acetylcholine
Ang-II	Angiotensin II
ANP	Atrial Natriuretic Peptide
ATP	Adenosine Triphosphate
BK	Bradykinin
Ca ⁺⁺	Ionic Calcium
CaM	Calmodulin
cAMP	Cyclic Adenosine Monophosphate
CCB	Calcium Channel Blocker
cDNA	Complimentary Deoxyribonucleic Acid
cGMP	Cyclic Guanosine Monophosphate
cGRP	Calcitonin Gene-Related Peptide
Cl ⁻	Ionic Chloride
CSFP	Coronary Slow Flow Phenomenon
DAG	Diacyl Glycerol
DNA	Deoxyribonucleic Acid
E _{max}	Maximal Contractile Response
EC ₅₀	Concentration Required for 50% Maximal Response
EDHF	Endothelium Derived Hyperpolarising Factor
EDRF	Endothelium Derived Relaxing Factor
eNOS	Endothelial Nitric Oxide Synthase

Et-1	Endothelin-1
K ⁺	Ionic Potassium
KCl	Potassium Chloride
KPSS	Potassium Physiological Salt Solution
HVA	High Voltage-Activated
iNOS	Inducible Nitric Oxide Synthase
IP ₃	1,4,5-triphosphate
LVA	Low Voltage-Activated
MLC	Myosin Light Chain
MLCK	Myosin Light Chain Kinase
MLCP	Myosin Light Chain Phosphatase
mRNA	Messenger Ribosomal Nucleic Acid
nNOS	neuronal NOS
NO	Nitric Oxide
NOS	Nitric Oxide Synthase
NPY	Neuropeptide Y
OD	Optical Density
PCR	Polymerase Chain Reaction
PE	Phenylephrine
PKC	Protein Kinase C
PLC	Phospholipase C
RNA	Ribosomal Nucleic Acid
ROCC	Receptor-Operated Ca ⁺⁺ Channel
ROK	Rho-kinase

RyR	Ryanodine Receptor
SDS	Sodium Dodecyl Sulfate
SDS-PAGE	Sodium Dodecyl Sulfate Polyacrylamide Gel Electrophoresis
SOCC	Store-Operated Ca ⁺⁺ Channel
SR	Sarcoplasmic Reticulum
TBS-T	Tris Buffered Saline with Tween 20
VOCC	Voltage-Operated Ca ⁺⁺ Channel
VSM	Vascular Smooth Muscle
VSMC	Vascular Smooth Muscle Cell

ABSTRACT

Clinical evidence in microvascular disease suggests that T-type Ca^{++} channel blockers (CCBs) have benefits over conventional L-type CCBs, however the basis for this remains largely unknown. The objective of this study was to examine vascular reactivity utilising both pharmacological and molecular techniques. This thesis is composed of three sections including (A) an Introduction, (B) Functional Vascular Studies and (C) Molecular Vascular Studies.

Section A summarised fundamental principles of the vasculature including an outline of the vascular system, vascular physiology, vascular cell biology, regulation of cytosolic Ca^{++} and vascular pathophysiology.

Section B utilised isolated vessels and wire myography to determine the effect of pre-treatment with L-type CCBs (verapamil and nifedipine) and combined L- and T-type CCBs (mibefradil and efonidipine) on endothelin-1 (Et-1) and K^{+} -mediated contractile responses in large (rat aorta) and small (rat mesenteric and human subcutaneous) vessels. All four CCBs inhibited both Et-1 and K^{+} -mediated contractile responses to a similar extent in large rat vessels, however in rat microvessels the combined L- and T-channel blockers produced significantly greater inhibition of contraction than L-channel blockers alone. The significance of this differential T-channel effect in microvessels was further supported by: (1) demonstration of divergent CCB responses in human microvessels, (2) incremental inhibition of constrictor responses with a combined L- and T- CCB despite maximal

L-channel blockade, (3) utilisation of structurally diverse CCBs with varied affinity for L- and T-channels, (6) use of pharmacodynamically and therapeutically appropriate CCB concentrations, (7) confirmation of contractile agonist independent responses, (8) consistent results even in the presence of an altered microvascular physiology in the form of chronic Et-1 activation and (9) exclusion of an endothelium-dependent mechanism.

Section C utilised the molecular techniques of quantitative polymerase chain reaction (PCR) and ratiometric western blotting to examine the distribution of the pore-forming subunits $Ca_v1.2$, $Ca_v3.1$ and 3.2 in both large (rat aorta) and small (rat mesenteric) vessels. The PCR data was equivocal with no difference noted in the distribution of the L- and T-channels between large and small vessels. In contrast to this, quantitative western blot analysis revealed that while there is a similar distribution of the three subunits in the large vessel, there is a significantly increased expression of both T-channel pore-forming subunits in microvessels ($Ca_v3.1$: $112 \pm 38\%^*$, $Ca_v3.2$: $168 \pm 48\%^*$ relative to L-channel expression, $*p < 0.05$).

Considered together these ‘functional’ and ‘structural’ studies indicate the important role of the Ca^{++} T-channel in regulating contractile responses in the microvasculature and their therapeutic potential.

SECTION A

INTRODUCTION

A.1 SCOPE

Calcium (Ca^{++}) channels in the vasculature are responsible for the ability of blood vessels to constrict and relax, thereby controlling blood flow and vascular tone. Specifically, the smaller vessels of the vasculature - the microvessels - have the greatest impact on this vascular tone. These microvessels control the resistance of the vasculature and consequently have been termed the resistance microvessels. Situated within the walls of the blood vessels are the vascular smooth muscle cells (VSMCs), and these are directly responsible for regulating tone.

The constriction and relaxation of vessels are regulated by a plethora of mediators that influence the tone of the vessels. Specifically, the endothelial, humoral and neurogenic groups contain several important mediators. Ca^{++} plays a vital role in the constriction of the VSMCs of blood vessels to the extent that the greater the concentration of Ca^{++} the greater the constriction. Ca^{++} is able to enter the cell through receptors located on the plasma membrane of a cell, the Ca^{++} channels. There are many types of Ca^{++} channels including voltage-operated Ca^{++} channels, receptor-operated Ca^{++} channels and store-operated Ca^{++} channels.

Any disturbance in the above regulatory mechanisms can result in the manifestation of many cardiovascular syndromes including large conduit vessel disorders (including coronary artery disease and peripheral artery disease) and small resistance vessel disorders (including coronary microvascular disorders, hypertension and cerebral microvascular disorders).

Although there is an abundance of knowledge in the field of cardiovascular physiology I will be restricting this introduction to the areas pertinent to this thesis. Specifically, the vasculature, calcium channels and the pathophysiology of certain cardiovascular disorders.

A.2 THE VASCULATURE

A.2.1 Vascular Anatomy

Within each circulatory bed there are both large conduit vessels and the resistance microvasculature. The large conduit vessels include large arteries which have an internal diameter greater than 500 μ m. All vessels less than 500 μ m in diameter form the resistance microvasculature which can be further subdivided, according to size, into the pre-arterioles (500 – 100 μ m), arterioles (100 μ m) and capillaries (10 μ m) (Figure 1).

NOTE:
This figure is included on page 3
of the print copy of the thesis held in
the University of Adelaide Library.

Figure 1: Pressure drop, relative to vessel size, in the hamster cheek pouch circulation. The division between different vessel types within the same vascular bed as determined by internal diameter. Modified from Davis *et al.* 1986¹.

The vasculature can be divided into three main systems, these being the arterial system, venous system and microcirculation.

A.2.1.1 ARTERIAL SYSTEM

The arterial system is the network of vessels responsible for providing oxygenated blood to peripheral tissues. This system consists of the aorta, smaller arteries and arterioles. The resistance of the arterial system is primarily focused at the arteriolar and pre-arteriolar level, and controls the flow of blood to the capillaries. When the arteries reach the tissue to which they supply blood, they branch into smaller arterioles and then into capillaries to allow for the transfer of oxygen and nutrients into the target tissue (Figure 2).

A.2.1.2 VENOUS SYSTEM

While the arterial system is responsible for carrying oxygenated blood to the tissues, the venous system is responsible for returning de-oxygenated blood and waste materials to the right heart chambers. From here it is pumped to the lungs for re-oxygenation before returning to the left heart chambers for subsequent peripheral circulation. The vessels involved in this transfer begin after the capillaries, which merge to form venules and then veins (Figure 2).

A.2.1.3 MICROCIRCULATION

The vascular network, which lies between the arteries and veins, defines the microcirculation. The vessels involved in this system are generally smaller than 500 μ m and includes the pre-arterioles, arterioles, capillaries and venules (Figure 2);

each has a unique function. The arterioles contain a large amount of vascular smooth muscle (VSM) and as such are responsible for delivering blood to tissues and regulating the rate of delivery. The capillaries have a very thin wall making them ideal for the exchange between blood and tissue. Finally, the venules then return this blood from the capillaries back to the heart via the venous system².

The microvasculature, including the pre-arterioles and arterioles, plays a vital role in determining vascular resistance. These vessels can substantially alter their calibre in terms of regulating blood flow into the capillary bed. The arterioles are able to dilate up to 50% from normal levels in response to stimuli and are therefore well suited to regulating blood flow². Conversely they can strongly vasoconstrict with the distal arterioles capable of closing completely under maximal stimulation³.

NOTE:
This figure is included on page 5
of the print copy of the thesis held in
the University of Adelaide Library.

Figure 2: Illustration of the circulatory system showing the progression from artery → arteriole → capillary → venule → vein. Modified from The Merck Manual⁴.

A.2.2 Functional Anatomy

Figure 1 from Davis' work indicates that 50% of the total pressure drop occurs in the small arteries of the microvasculature, specifically those vessels between 300 μ m - 100 μ m in diameter^{1, 5}. These vessels play a significant role in regulating resistance and blood flow. Furthermore, myogenic responsiveness in these vessels increased with decreasing vessel size. Maximum responsiveness was reached at the level of "intermediate-sized" arterioles rather than in more terminal arterioles⁶. The pressure-diameter relationship in Figure 1 is not unique to the hamster cheek pouch, with it described in other regional circulations including the mesenterics⁷, the intestinal wall⁸ and cremaster muscle⁹.

A.2.3 Vascular Histology

Histologically, blood vessels have three separate layers:

- (1) An intimal layer having an internal elastic membrane with an endothelial lining and a subendothelial layer of connective tissue.
- (2) The media, composed primarily of circularly arranged smooth muscle layers interspersed with elastic and collagenous fibres.
- (3) The adventitia which, consisting of connective tissue, is defined by its external elastic membrane.

A.2.3.1 INTIMA

Originally, the endothelium was considered to be an inactive, single layer of cells which existed only as a boundary between the reactive smooth muscle cells of the media and the circulation. However, this was revised when Furchgott and Zawadzki¹⁰

demonstrated a consistent vasomotor response to acetylcholine in rabbit aorta when the endothelium was removed. Since their original demonstration it has been shown that the endothelium releases a vast number of substances including: (a) vasoactive factors^{11, 12}, (b) inflammatory modulators¹³ and (c) haemostatic factors¹⁴. The endothelium has a variety of functions which it achieves via these endothelial substances. These include regulation of: (a) vascular permeability¹⁵, (b) vascular tone^{11, 16, 17}, (c) vascular growth and repair¹⁸, (d) leukocyte and platelet adhesion¹⁹, (e) thrombosis and fibrinolysis^{20, 21}, (f) inflammation^{22, 23}, (g) lipid oxidation^{24, 25}, and (h) myocardial ischaemia²⁶. Thus, it can be seen that the endothelium plays an important part in many physiological and pathophysiological states beyond its original role.

A.2.3.2 MEDIA

The VSMCs are arranged in either a circular or spiral fashion within the media layer and are connected by collagen fibrils. Although the principal role of the VSMCs in vascular tissue is to modulate vasomotor tone²⁷ they have a number of other important roles. Smooth muscle cells are the most abundant cell type in the arterial wall and thus their response to certain trophic substances impacts on vascular responses. In hypertension, for example, smooth muscle cell hyperplasia has important consequences in arterial compliance²⁸ through the production of extracellular matrix products including collagen^{29, 30} and proteoglycans^{31, 32}. In atherosclerosis, migration of smooth muscle cells to the intima results in plaque formation which may eventually impinge on the vessel lumen to such an extent that it increases vascular resistance³³.

A.2.3.3 ADVENTITIA

The adventitia is a collection of loose connective tissue between the perivascular tissue and fluid layers. The larger arteries, however, contain perivascular nerves³⁴ as well as the vasa vasorum³⁵. Inflammatory cells may also be found here yet they are generally sparse^{36, 37}. This adventitial layer may be significant as it may be involved in regulating vasomotor tone. Specifically the adventitia has been shown to have the capacity to contract and relax in response to vasoconstricting and vasodilating drugs^{38, 39}.

A.3 VASCULAR PHYSIOLOGY

A.3.1 Haemodynamic Principles

The principle haemodynamic law of blood flow from Darcy⁴⁰ is derived from Ohm's law, relating to electricity. Expressed in relation to the cardiovascular system this states that the total volume of blood flowing through the vessel per unit time, flow (Q), is proportional to the pressure gradient across the vessel (P) divided by the resistance (R):

$$Q = \Delta P / R$$

Using Darcy's formula this equates to:

$$CO = 80 \times ((MAP - RAP) / TPR)$$

where RAP represents mean right atrial pressure and TPR is total peripheral resistance.

Poiseuille's equation of fluid dynamics states:

$$Q = (\Delta P \times r^4) / (\eta \times l \times 8)$$

where P = the pressure gradient, r = vessel radius, η = fluid viscosity and l = vessel length.

By combining Poiseuille's equation with Ohm's law it is possible to identify factors that influence the resistance within a blood vessel:

$$R = (\eta \times l \times 8) / r^4$$

The major determinant of resistance is the radius of the vessel since both blood viscosity and vessel length are relatively fixed. The radius inversely influences the resistance to the fourth power; as such a small change in vessel diameter results in a large change in blood flow. Hence, blood flow can be dramatically regulated by influencing vascular tone.

A.3.2 Regulatory Influences of Vascular Tone

There are many regulatory determinants within the vasculature which contribute to the regulation of blood flow. These include endothelial, humoral and neurogenic influences.

A.3.2.1 ENDOTHELIAL INFLUENCES

As mentioned above Furchgott and Zawadzki¹⁰ first described the primary role of the endothelium in vasomotor control and hypothesised the existence of an endothelial-derived vasodilating factor (EDRF). EDRFs induce the relaxation of VSMCs and this consequently results in vessel dilation. The EDRFs considered to be most important

were later identified as nitric oxide^{41, 42}, prostacyclin⁴³ and endothelium-derived hyperpolarising factor (EDHF)⁴⁴.

A.3.2.1.1 Nitric Oxide

Nitric oxide (NO) is synthesised in endothelial cells from the amino acid L-arginine by nitric oxide synthase (NOS). In most vessels NO results in vessel dilation through the activation of soluble guanylate cyclase, which increases cellular levels of cyclic guanosine monophosphate (cGMP). This process activates protein kinase G (PKG) and in turn elicits a decrease in intracellular Ca⁺⁺ concentration⁴⁵.

There are three different forms of NOS which may be involved in the synthesis of NO: firstly, neuronal NOS (nNOS); secondly, endothelial NOS (eNOS); and thirdly, inducible NOS (iNOS). Neuronal NOS (nNOS) is primarily located in the central⁴⁶ and peripheral nervous systems⁴⁷ but has recently been identified as assisting with the regulation of vascular tone and blood flow^{48, 49}, purportedly through vasodilation⁵⁰. The second form of NOS is endothelial NOS (eNOS) which is a Ca⁺⁺-calmodulin dependent enzyme predominantly found in the endothelial cells^{51, 52}, cardiac myocytes⁵³ and platelets⁵⁴. In a recent study in mice, the large conduit vessels' eNOS produces NO to generate smooth muscle cell relaxation. In comparison the small resistance vessels' eNOS produces EDHF to stimulate relaxation⁵⁵ (Figure 3).

NOTE:

This figure is included on page 11 of the print copy of the thesis held in the University of Adelaide Library.

Figure 3: Differential role of NOS as determined by vessel size. In the larger conduit artery eNOS acts to produce NO which diffuses into the underlying VSMCs. This increases cyclic GMP and leads to relaxation. In the small resistance vessels, however, eNOS initiates a cascade of reactions ultimately producing EDHF and smooth muscle cell relaxation. Modified from Takaki *et al.* 2008⁵⁵.

The third form of NOS is the Ca⁺⁺-independent inducible NOS (iNOS). iNOS is induced in response to cytokines and bacterial agents in inflammatory and tissue cells^{56, 57}. Interestingly, even though iNOS is considered Ca⁺⁺ independent, iNOS expression may be regulated by intracellular Ca⁺⁺ concentration⁵⁸. An increase in intracellular Ca⁺⁺ concentration at low levels of lipopolysaccharide (LPS) stimulates iNOS expression, whereas at high LPS levels iNOS expression is reduced⁵⁸.

Acetylcholine to Assess Endothelial Function

Acetylcholine (ACh) has long been used to assess endothelial integrity as it elicits the production of NO. Furchgott and Zawadzki first noted that ACh acted on the

muscarinic receptors, stimulating the release of relaxing factors. Furthermore, they demonstrated that endothelial cells were required for relaxation in VSM¹⁰.

Vasodilation in response to ACh occurs through one of the following pathways, or a combination of the three:

- (1) The release of the endothelium-derived relaxing factor (EDRF) synthesised from NO, which diffuses to and subsequently relaxes the nearby VSM^{10, 59}.
- (2) Prostaglandin I₂ (PGI₂) produced by the activation of cyclooxygenase^{60, 61}.
- (3) The release of endothelium-derived hyperpolarising factor (EDHF) – EDHF is responsible for the persistent dilation and hyperpolarisation of the VSMCs⁶².

A.3.2.1.2 Prostacyclin

Prostacyclin was first described as an EDRF by Moncada *et al.*⁴³ who reported high prostacyclin concentrations in the endothelium. The main functions of prostacyclin are vasodilation^{16, 17} and inhibition of platelet aggregation^{63, 64}. Other roles of prostacyclin include a cytoprotective role concerning the gut^{65, 66}, liver^{67, 68}, heart^{69, 70} and mediation of haemorrhagic⁷¹ and endotoxic shock⁷². Furthermore it possibly inhibits atherosclerosis by preventing growth factor release and cholesterol uptake^{73, 74}.

Interestingly, the interaction between prostacyclin and NO has a synergistic effect on the VSM. NO inhibits a particular cyclic adenosine monophosphate (cAMP) phosphodiesterase, which is responsible for cAMP breakdown. This inhibition of cAMP breakdown consequently prolongs prostacyclin's vasodilating effects^{75, 76}.

A.3.2.1.3 Endothelium-Derived Hyperpolarising Factor

Many studies have demonstrated the existence of another endothelium-derived vasodilating factor independent of EDRF known as endothelium-derived hyperpolarising factor (EDHF). Chen *et al.*⁶² showed that not all endothelium-dependent relaxations could be explained by NO or prostacyclin. Instead, there appeared to be another substance, which resulted in the hyperpolarisation, and subsequently, relaxation of VSMCs.

The specific regulation of EDHF-dependent vascular tone is still debated, with several suggested mediators including hydrogen peroxide^{77, 78}, natriuretic peptide receptor-C^{79, 80} and arachidonic acid metabolites^{81, 82}. Potassium (K⁺) is also believed to be involved with the EDHF phenomenon⁸³, however its action is not consistent⁸⁴. Specific to K⁺, the small-conductance and intermediate-conductance Ca⁺⁺-activated K⁺ channels have been implicated in mediating EDHF vascular tone⁸⁵⁻⁸⁸. The observed relaxation response is often sustained whilst the initiating hyperpolarisation is only transient. Initially this prompted speculation that EDHF initiated smooth muscle cell relaxation by indirectly reducing Ca⁺⁺ movement through the voltage-dependent channels. However, Drummond *et al.* demonstrated that EDHF-induced relaxation was not mediated via the voltage-operated Ca⁺⁺ channels in isolated

bovine coronary artery⁸⁹. Instead, EDHF is released via a calcium-dependent mechanism^{86,90} possibly involving calmodulin⁹¹. The interactions between EDRF and EDHF are not completely clear, however they are often co-released.

EDHF has recently been investigated in relation to small vessel physiology. Specifically, while relaxation in large arteries is due to the combined effects of the EDRFs (NO, EDHF and prostacyclin) and EDHF, EDHF alone is responsible for relaxation of small resistance arteries^{85,92-94}.

A.3.2.1.4 Endothelin

Apart from endothelium-derived vasodilating factors there are endothelium-derived constricting factors to consider. One of the most potent endothelium-derived constricting factors is the 21 amino acid peptide, endothelin. Preproendothelin is the precursor for proendothelin which is cleaved to form the 3 endothelin isoforms – endothelin-1 (Et-1), endothelin-2 (Et-2) and endothelin-3 (Et-3)⁹⁵.

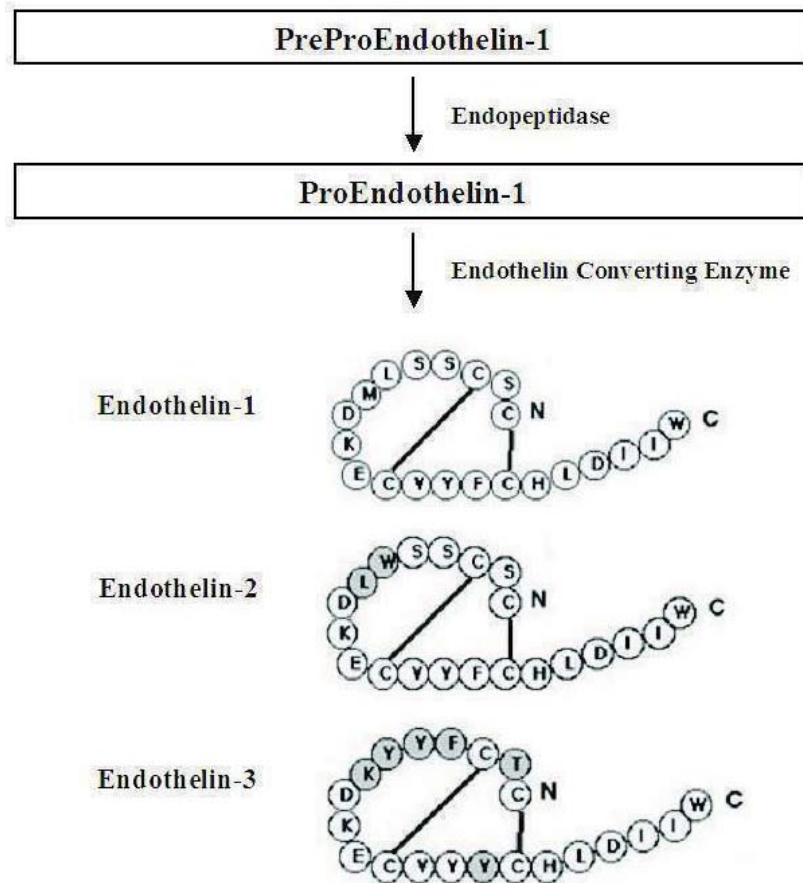


Figure 4: Biosynthesis and amino acid sequence of Et-1, Et-2 and Et-3. PreProEndothelin-1 is cleaved by endopeptidases into ProEndothelin which is then converted into the different isoforms of endothelin via Endothelin Converting Enzymes. Modified from Fagan *et al.* 2001⁹⁶.

The Et-1 isoform is a potent vasoconstrictor⁹⁷⁻⁹⁹ and the only isoform released by the endothelial cells¹⁰⁰. Et-2 is predominantly expressed in the pituitary¹⁰¹ and gastrointestinal tract¹⁰² and Et-3 is found in the brain¹⁰³, kidney¹⁰⁴ and gastrointestinal tract¹⁰³.

Two endothelin receptors have been identified - ET-A and ET-B receptors^{105, 106} - both of which are G-protein linked. Although ET-A receptors are widely abundant (see Table 1) high concentrations are found in cardiac myocytes and VSMCs¹⁰⁷.

Upon binding to the ET-A receptor, Ca^{++} channels are activated, resulting in a cascade in which phospholipase C (PLC) is activated. This generates 1, 4, 5-inositol triphosphate (IP_3) which liberates Ca^{++} from the sarcoplasmic reticulum (SR), thereby increasing intracellular Ca^{++} content. In VSMCs this Et-1-mediated pathway has a potent vasoconstricting effect⁹⁹. Other known effects of ET-A stimulation include: (a) stimulation of protein kinase C (PKC) which promotes vascular mitogenesis¹⁰⁸; (b) inhibition of chloride channel activation, therefore preventing catecholamine-induced arrhythmias¹⁰⁹; (c) activation of some K^+ channels¹⁰⁹; and (d) inhibition of the activation of L-type Ca^{++} channels¹⁰⁹.

ET-B receptors, however, are in abundance on endothelial cells and to a lesser extent on the smooth muscle cells¹⁰⁰ (see Table 1). Stimulating these ET-B receptors results in the activation of PLC and subsequent generation of IP_3 ^{110, 111} possibly through the activation of the L-type Ca^{++} channels¹¹¹. However, the ET-B receptors have an important functional difference in that they are also linked to an inhibitory G-protein which may activate the Na^+/H^+ transporter^{112, 113} and inhibit the production of cAMP^{114, 115}. The ET-B receptors have also been shown to release nitric oxide^{116, 117}.

NOTE:
This figure is included on page 17
of the print copy of the thesis held in
the University of Adelaide Library.

Table 1: Expression of ET-A and ET-B receptors in normal physiology. Modified from Kedzierski and Yanagisawa, 2001¹⁰⁷.

Several investigators have researched the roles of the ET-A and ET-B receptors in the human coronary artery. In isolated human coronaries, Et-1 is seen to be 10 times more potent in the small, distal vessels than in the larger proximal segments. It is a response that was antagonised by the ET-A receptor blocker BQ123. It can be presumed that the endothelin-based constriction seen in these small vessels must be mediated through the ET-A receptors with other receptors controlling large vessel constriction¹¹⁸. Consistent with this, it is proposed that coronary vasoconstriction mediated by Et-1 is due to activation of the ET-A receptors with no involvement of the ET-B receptors¹¹⁹.

A.3.2.2 HUMORAL INFLUENCES

There are many humoral mediators, including autacoidal and hormonal, which interact to regulate blood flow in the vasculature. The table below summarises those humoral influences are not directly relevant to this current thesis (Table 2):

Mediator	Receptor	Site	Action
Histamine	H ₁	Blood vessels	High doses → Vasoconstriction ¹²⁰ Low doses → Vasodilation ¹²⁰
	H ₂		Vasodilation ¹²¹
Serotonin	5HT _{1B}	Coronary ECs	Vasoconstriction ^{122, 123}
	5HT _{2A}	VSM & Platelets	Vasoconstriction ^{124, 125}
	5HT _{2B}	VSM	Vasoconstriction ^{126, 127}
	5HT ₇	Blood vessels, Brain & GI	Vasodilation ¹²⁸
Vasopressin	1 _A	VSM, Platelets, Hepatocytes, Brain Cells & Uterine Cells	Large Vessel Dilation and Microvascular Constriction ¹²⁹
Atrial Natriuretic Peptide	ANP _A & ANP _B	Atrial myocytes	Vasodilation ^{130, 131}
Angiotensin II	AT1	VSM, Brain, Lungs & Adrenals	Vasoconstriction ^{132, 133}

Table 2: Humoral mediators involved in the regulation of blood flow in the vasculature. VSM – vascular smooth muscle, ECs – endothelial cells, GI – gastrointestinal tract.

There are two important humoral influences that are involved with the regulation of blood flow – catecholamines and bradykinin. Furthermore, they are directly relevant to this study.

A.3.2.2.1 Catecholamines

There are two primary resources from which circulating catecholamines arise, the adrenal medulla and the sympathetic nerve terminals. The effects of catecholamines are mediated via α - and β - receptors. In particular those catecholamines produced by the adrenal medulla are important during exercise with the α -receptors being of importance¹³⁴. Specifically, blood flow in intact and sympathectomised regions in the presence and absence of α - and β -adrenergic antagonists was measured. During exercise, in both the intact and sympathectomised regions, coronary resistance significantly rose during combined α - and β -block compared to β -block alone¹³⁴.

One synthetic catecholamine is the α_1 agonist, phenylephrine (PE). Specifically, PE activates the α receptor which stimulates the G_{q11} pathway. This pathway initiates a cascade in which phosphatidylinositol biphosphate (PIP₂) is cleaved to form of IP₃ and diacyl glycerol (DAG)¹³⁵. IP₃ liberates Ca⁺⁺ from the sarcoplasmic reticulum (SR)¹³⁶ which is then able to activate myosin light chain kinase (MLCK) phosphorylation¹³⁷ and contraction via the binding of Ca⁺⁺ to calmodulin (CaM). DAG activates PKC which acts to inhibit CPI-17 and therefore inhibits the relaxing effect of myosin phosphatase¹³⁸, also known as myosin light chain phosphatase (MLCP), thus favouring contraction. Furthermore, PE sensitises the contractile

proteins for Ca^{++139} . All of these processes work together resulting in vessel contraction (Figure 5).

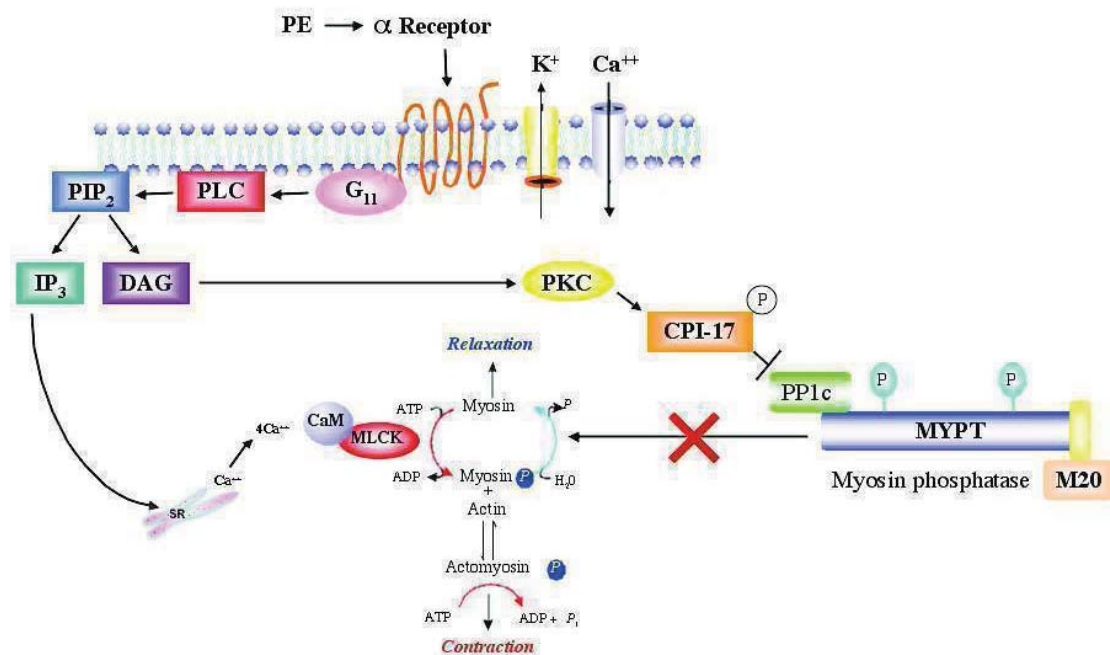


Figure 5: Diagrammatic representation of VSMC contraction through the binding of PE to the G_{q11} receptor. PE binds to the G_{q11} receptor which activates phospholipase C (PLC) and subsequently activates PIP_2 . PIP_2 cleaves to form IP_3 and DAG. IP_3 releases Ca^{++} from the SR which binds to calmodulin and activates Ca^{++} -CaM-MLCK resulting in contraction. DAG activates PKC which in turn phosphorylates CPI-17. MLCK is inhibited and this favours contraction. Adapted from the work of Kemp *et al.* 1961¹³⁵, Iino 1999¹³⁶, Ward and Kam 2004¹³⁷ and Kitazawa *et al.* 2000¹³⁸.

A.3.2.2.2 Bradykinin

Bradykinin (BK) is synthesised from the plasma α -globulin, kininogen, by the plasma enzyme kallikrein through the kallikrein-kinin cascade¹⁴⁰. BK has many actions involving vasodilation¹⁴¹⁻¹⁴³, increased vascular permeability¹⁴⁴⁻¹⁴⁶ and activation of phospholipase A_2 ¹⁴⁷. BK elicits its effects by binding to, and activating, the G-coupled B_1 and B_2 receptors. Of these B_2 appears to be the mediator of the majority of BK's vascular activities^{142, 143, 148-150}.

B₁ receptor

The B₁ receptor is typically expressed as a result of tissue injury^{151, 152} and upon activation mediates chronic pain^{153, 154} and inflammation^{151, 155, 156}. More recently the B₁ receptor has also been shown to mediate neutrophil recruitment^{157, 158}.

B₂ receptor

The B₂ receptor mediates most of BK's vascular actions and in particular its role in vasodilation. The vasodilating effect of BK is modulated by an endothelium-dependent mechanism¹⁴⁸ possibly the release of NO^{142, 143, 149} and/or the release of EDHF¹⁵⁰.

In the canine coronary circulation BK increased coronary blood flow, particularly in the subendocardial layers. B₂ receptor antagonists and NOS inhibitors suppress this response¹⁴². In isolated porcine coronary arteries BK-induced endothelium-dependent vasodilation occurs via both NO dependent and independent mechanisms¹⁴³. In human coronary arteries BK endothelium-dependent vasodilation is mediated by both NO¹⁴⁰ and EDHF mechanisms¹⁵⁰.

Assessing Endothelial Function

BK is a useful tool for assessing the endothelial function of vessels. When there is a functional and intact endothelium present the administration of BK will result in vessel relaxation or dilation¹⁵⁹. The BK precursor, high molecular weight kininogen, binds to endothelial cells thus converting prekallikrein into kallikrein^{140, 160}, subsequently releasing BK from the endothelial cells^{160, 161} (Figure 6).

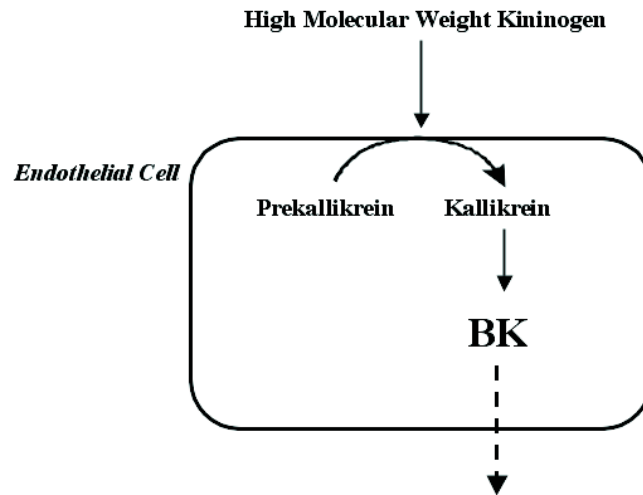


Figure 6: Diagrammatic representation of the production of BK. High Molecular Weight Kininogen binds to the endothelial cell which converts prekallikrein to kallikrein thus releasing BK. BK then diffuses out of the endothelial cells.

A.3.2.3 NEUROGENIC INFLUENCES

The autonomic nervous system is comprised of the sympathetic and parasympathetic nervous systems. Parasympathetic innervation originates in the medulla oblongata before passing through both the right and left vagal nerves. Sympathetic innervation originates in the medullary vasomotor center before passing through the spinal cord to its exit at the thoracic ganglia.

A.3.2.3.1 Cholinergic Innervation

Acetylcholine (ACh) mediates most cholinergic responses operating via 5 types of muscarinic receptor types, $M_1 - M_5$ ¹⁶²⁻¹⁶⁴. M_1 , M_3 and M_5 mediate the activation of PLC but do not inhibit adenylyl cyclase while the M_2 and M_4 receptors have the opposite effect mediating the inhibition of adenylyl cyclase without stimulating PLC^{165, 166}. However, when expressed at high levels, within certain cell types, the M_2 and M_4 receptors are able to weakly couple to PLC¹⁶⁷. In VSM the vasodilation in

response to muscarinic receptor activation appears to be mainly mediated via the M_3 receptor while the M_1 receptor mediates constriction¹⁶⁸. Furthermore, while the endothelium is intact the expression of M_1 receptors is downregulated¹⁶⁸.

A.3.2.3.2 Adrenergic Innervation

While cholinergic innervation highlights parasympathetic cardiovascular effects, adrenergic innervation produces the equally well-recognized sympathetic effects. Adrenergic nerves release noradrenaline from their nerve terminals which binds to G-proteins that are coupled to the α -adrenoceptor and the β -adrenoceptor:

- (a) The α -adrenoceptors can be subdivided into α_1 - and α_2 -adrenoceptors. Activation of either of the α -adrenoceptors (i.e. α_1 and α_2) will induce contraction of the VSM resulting in vasoconstriction. However, the ratio for α_1 and α_2 adrenoceptors varies between large and small vessels. Specifically the α_1 -adrenoceptor plays a greater role in large arteries whereas the α_2 -adrenoceptor primarily exerts its effect in the smaller arteries and veins^{169, 170}. The α_1 -adrenoceptors are further subdivided into α_{1A} and α_{1B} . While α_{1A} is primarily involved in the regulation of basal vascular tone, α_{1B} is involved with responses to exogenous agonists¹⁷¹. Likewise the α_2 -adrenoceptors are further subdivided into $\alpha_{2A/D}$, α_{2B} and α_{2C} . $\alpha_{2A/D}$ and α_{2B} are involved with arterial contraction and α_{2C} with venous contraction¹⁷¹.
- (b) β -adrenoceptors can be subclassified into β_1 , β_2 and β_3 adrenoceptors, all of which lead to vasodilation¹⁷²⁻¹⁷⁴. These β -adrenoceptors are found in both small and large coronary arteries. In the large canine arteries β_1 -

adrenoceptors effect a dilatory response¹⁷⁴, whereas the β_2 -adrenoceptors are the main activators in the small resistance vessels¹⁷⁵. Furthermore, the β_1 -adrenoceptors of the heart increase heart rate which will also influences blood flow¹⁷⁶.

Receptor	Direct Vasoconstriction	Direct Vasodilation	Endothelium-Dependent Vasodilation
α_1	+		
α_2	+		+
β_1		+	
β_2		+	+
β_3		+	+

Table 3: Adrenergic adrenoceptors expressed in the vasculature. Modified from Watts *et al.* 2008¹⁷⁷.

Interestingly, in many vascular beds, sympathetic activation will result in two conditions: firstly, α_1 -adrenoceptor dependent vasoconstriction in vessels larger than 100 μ m in diameter; and secondly, β -adrenoceptor dependent vasodilation of the small arterioles¹⁷⁸.

A.3.2.3.3 Noncholinergic-Nonadrenergic Innervation

These cholinergic and adrenergic fibres are not the only ones responsible for controlling blood flow. Neurotransmitters such as dopamine, serotonin, ATP and a variety of other peptides, which are released from alternative noncholinergic-nonadrenergic fibres located within the cardiac nerves, are also involved.

As with several of the humoral mediators, these neurogenic mediators are not directly relevant to the current study and therefore are summarised in the table below (Table 4).

Mediator	Receptor	Site	Action
Dopamine	D ₁ & D ₂	Smooth muscle	Suppressing an increasing myocardial demand ¹⁷⁹ , Stimulating dopamine receptors ¹⁸⁰ , Releasing NA to interact with the α - and β -adrenoceptors ¹⁸¹
Adenosine	P ₁ : A ₁	Symp. Nerves	Inhibit NA release ¹⁸²
Triphosphate	P ₁ :A ₂	VSM	Vasodilation ¹⁸³
	P ₂ : P _{2X}	VSM	Vasoconstriction ¹⁸⁴
	P ₂ : P _{2Y}	Endothelial Cells	Vasodilation ¹⁸⁵
Neuropeptide Y	Y ₁ – Y ₅	Cardiac nerves & Coronary vessels	Microvascular constriction ¹⁸⁶⁻¹⁸⁸
Substance P	NK-1 or SPR	Coronary vessels	Vasodilation ^{189, 190}
Calcitonin Gene Related Peptide	CLR	Nervous tissue	Microvascular dilation ^{191, 192} and Cardiovascular protection ^{193, 194, 193}

Table 4: Neurogenic mediators involved in the regulation of blood flow in the vasculature. NA – noradrenaline, Symp. – sympathetic, VSM – vascular smooth muscle.

A.4 VASCULAR CELL BIOLOGY

A.4.1 The Actin-Myosin Contractile Apparatus

In VSMCs actin is the major component of the thin filaments which, together with myosin (which forms the thick filaments), are arranged into actomyosin myofibrils; these form the mechanism of contraction. The actin-myosin contractile apparatus is solely responsible for contraction and relaxation through the following signalling cascade^{195, 196}:

- (1) Intracellular Ca^{++} concentration increases either through Ca^{++} entry following activation of the voltage-operated channels or Ca^{++} release from the SR.
- (2) In the pathway of release from the SR, the activated receptor interacts with a G-protein which in turn activates PLC. Activated PLC ultimately produces IP_3 which binds to its receptor on the surface of the SR. The result is a further Ca^{++} release from the SR.
- (3) This Ca^{++} combines with the protein calmodulin (CaM).
- (4) This Ca^{++} -CaM complex activates MLCK.
- (5) MLCK then phosphorylates the protein myosin light chain (MLC) which is bound to myosin.
- (6) The phosphorylated myosin filaments combine with actin filaments and the muscle contracts.

A.4.2 Regulation of Myosin Light Chain Phosphorylation

The phosphorylation of myosin is the major regulatory mechanism in VSM contractile responses. The level of myosin phosphorylation is directly regulated by the ratio of MLCK and MLCP.

A.4.2.1 MYOSIN LIGHT CHAIN KINASE AND ITS REGULATION IN THE CONTEXT OF VASCULAR CONTRACTION

In smooth muscle MLCK is required to generate muscle contraction^{197, 198}. In VSMCs Ca⁺⁺ entry activates Ca⁺⁺-CaM-dependent MLCK. In its active form MLCK is able to phosphorylate the MLC which then enables actin-myosin cross-bridge cycling and subsequent contraction^{197, 199}. It is the phosphorylation status of MLC by MLCK which controls the rate of actin-myosin cross-bridge cycling.

MLCK has been reported in modest amounts on endothelial cells²⁰⁰ enabling a counter-balancing role with MLCK-activated Ca⁺⁺ entry into endothelial cells releasing both NO and EDRF. Consequently this results in vasodilation. It has been suggested that MLCK results in vasoconstriction by having a direct effect on smooth muscle cells while its vasodilatory role is through its impact on the endothelial cells²⁰¹. Unlike the smooth muscle contractile apparatus MLCK, the endothelial cell MLCK mediates the release of NO and EDRF.

Cytosolic Calcium

Cytosolic Ca⁺⁺ is fundamental in the regulation of vasomotor responses. For contraction an increase in cytoplasmic Ca⁺⁺ is required, which is provided for by a

flux of Ca^{++} into the cell. There are two different sources for this activator Ca^{++} , these being the extracellular space and the SR:

(1) Extracellular Space

There is an abundant supply of Ca^{++} which may come from the extracellular space. This supply is regulated by the kinetics of the transmembrane Ca^{++} channels either by membrane depolarisation and/or messenger molecules. They may originate from the cell's exterior or alternatively from cytoplasmic second messengers²⁰².

(2) Sarcoplasmic Reticulum (SR)

There are two different ways in which Ca^{++} release from the SR may occur. The first of these is through Ca^{++} -induced Ca^{++} -release through the Ryanodine receptors (RyR)²⁰³, or secondly via IP_3 -induced Ca^{++} release¹³⁶ initiated by PLC (Figure 7).

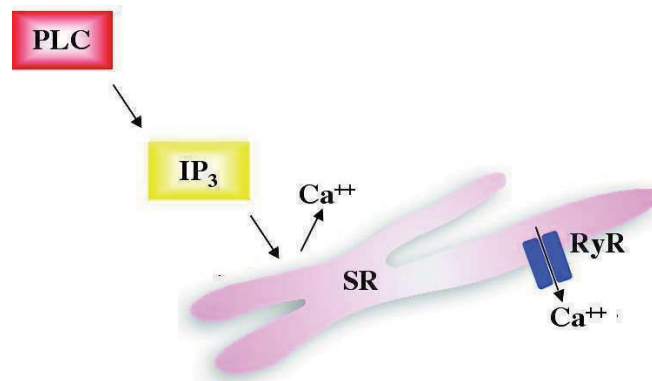


Figure 7: Ca^{++} release from the SR. There are two ways in which Ca^{++} may be released from the SR; either the PLC- IP_3 pathway or the RyRs.

Calmodulin

CaM is a Ca^{++} -binding protein important in transducing Ca^{++} signals and regulating contraction through its interaction with MLCK²⁰⁴⁻²⁰⁶. The primary role of CaM is to

bind Ca^{++} to initiate VSMC contraction. CaM has four Ca^{++} binding sites (see Figure 8) and when three or more sites are bound there is a significant conformational change²⁰⁷ enabling CaM to wrap around the target protein. Once Ca^{++} and CaM are bound together this complex interacts with MLCK, phosphorylating MLC. Actin-myosin interaction is initiated and subsequently smooth muscle contraction occurs.



Figure 8: Three-dimensional image of CaM demonstrating the positioning of the four Ca^{++} binding sites (green circles). Modified from Clapperton *et al.* 2002²⁰⁸.

A.4.2.2 MYOSIN LIGHT CHAIN PHOSPHATASE AND ITS REGULATION IN THE CONTEXT OF VASCULAR CONTRACTION

The other component involved with the regulation of MLC phosphorylation is MLCP. In particular the sensitivity of MLC to Ca^{++} is modulated, thus regulating the level of smooth muscle cell contraction; this is referred to as Ca^{++} sensitisation. The mechanism behind this modulation of Ca^{++} sensitisation is the inhibition of smooth muscle MLCP. Three important pathways involved in the inhibition of MLCP are protein kinase C (PKC)²⁰⁹⁻²¹¹, CPI-17^{212, 213} and Rho-kinase^{209, 214, 215}.

Protein Kinase C

PKC is a widely distributed protein serine-threonine kinase within the smooth muscle, which has been implicated as a key player in smooth muscle cell contraction^{210, 216} through a number of pathways. The three main pathways through which PKC mediates VSM contraction are as follows:

- (1) Enhanced Ca^{++} influx through activation of the L-type Ca^{++} channels activating MLCK phosphorylation¹³⁷.
- (2) Through the release of arachidonic acid which may interact directly with MLCP or alternatively activates a kinase known to phosphorylate, and accordingly, inhibit MLCP²¹⁷.
- (3) Through the phosphorylation and therefore activation of CPI-17, an inhibitory modulator of MLCP¹³⁷.

Often, the activation of PKC requires translocation from the cytosol to the membrane, particularly in VSMCs²¹⁸⁻²²⁰. It has been proposed that to become active a pseudosubstrate binds to the protein substrate binding site of PKC. Binding of DAG or other lipid activators then produces a conformational change, which dislodges the pseudosubstrate and leaves the kinase active²²¹. Once in its active form PKC is able to act on CPI-17.

CPI-17

CPI-17 is a smooth muscle phosphoprotein which potently inhibits MLCP^{212, 222}, an important regulator of smooth muscle contraction¹³⁸. PKC phosphorylates CPI-17 and it is this phosphorylated form of CPI-17 that inhibits MLCP¹³⁸ (see Figure 9).

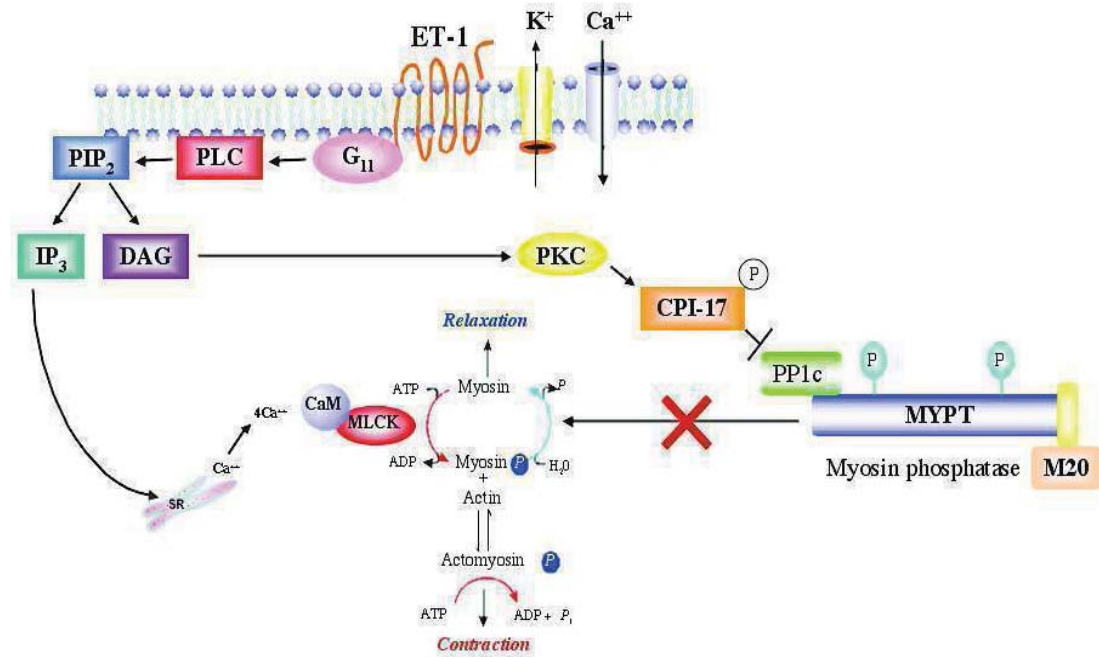


Figure 9: Diagrammatic representation of VSMC contraction through the PKC/CPI-17 pathways. An agonist (e.g. Et-1) binds to the Gq₁₁ receptor which activates PLC and in turn activates PIP₂. PIP₂ then cleaves to form IP₃ and DAG. IP₃ releases Ca⁺⁺ from the SR which binds to calmodulin and activates Ca⁺⁺-CaM-MLCK resulting in contraction. DAG activates PKC which in turn phosphorylates CPI-17. MLCP is inhibited and this action favours contraction. Adapted from the work of Kemp *et al.* 1961¹³⁵, Iino 1999¹³⁶, Ward and Kam 2004¹³⁷ and Kitazawa *et al.* 2000¹³⁸.

The expression of CPI-17 is seen to vary greatly depending on the type of muscle and the animal species (for example it is noticeably absent from chicken²²³). VSMs are seen to have more CPI-17 than visceral smooth muscles²¹⁰, microvessels also appear to have a greater abundance of CPI-17²¹⁰. Additionally, there is a difference between tonic and phasic muscles with the tonic femoral artery having 8 times more CPI-17 than the phasic vas deferens²¹⁰.

Rho-kinase

Rho-kinase (ROK) acts as a secondary regulatory unit in modulating smooth muscle cell contractility via the inhibition of MLCP^{215, 224, 225}. Specifically, agonist activation

of the G_{q13} receptor activates ROK resulting in the phosphorylation of MLCP at the Threonine 855 site with this phosphorylation favouring smooth muscle contraction²²⁵.²²⁶. The direct link between ROK and the contractile apparatus occurs through its translocation to the cell membrane²²⁷ (Figure 10).

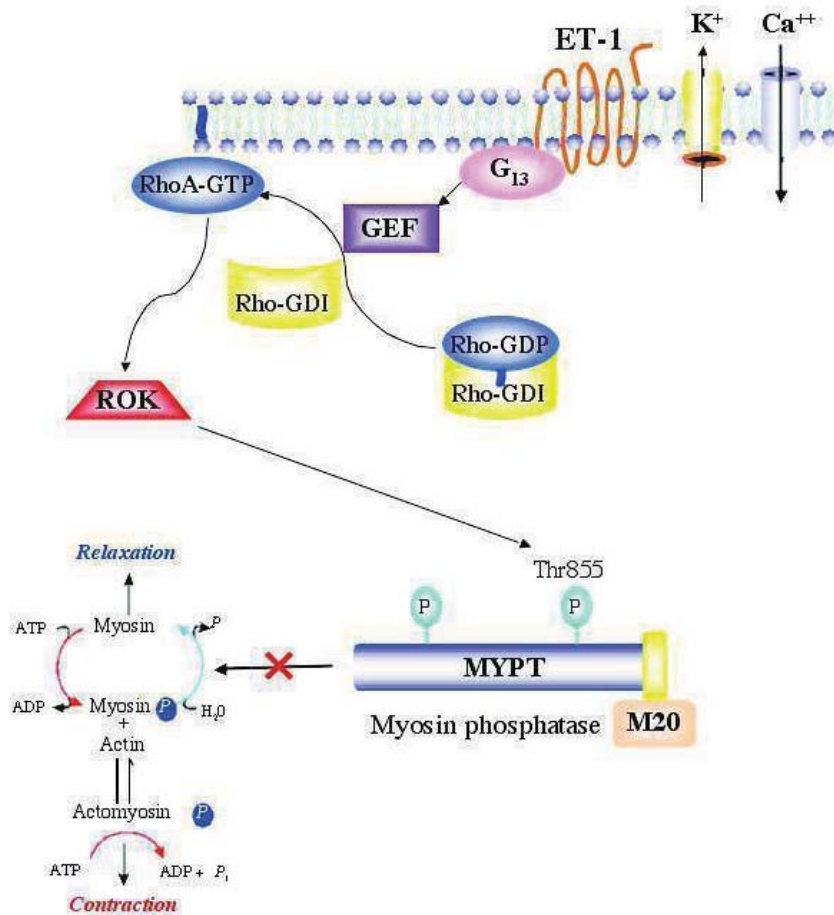


Figure 10: Diagrammatic representation of VSMC contraction through the ROK pathway. An agonist (e.g. Et-1) binds to the G_{q13} receptor initiating a cascade of reactions from the activation of guanidine exchange factor (GEF) to the subsequent activation of ROK. Once active ROK phosphorylates the threonine 855 site of MYPT thus resulting in inhibition of MLCP, favouring contraction. Adapted from the work of Wang *et al.* 2009^{215, 224, 225}, Wilson *et al.* 2005^{225, 226} and Leung *et al.* 1995²²⁷.

ROK has also been shown to phosphorylate CPI-17^{228, 229}, providing a further inhibition of MLCP enhancing contraction. Specifically, this ROK-mediated phosphorylation of CPI-17 is seen to occur during the late phase of contraction and is

much slower than agonist induced phosphorylation (for example, by PE)²³⁰.

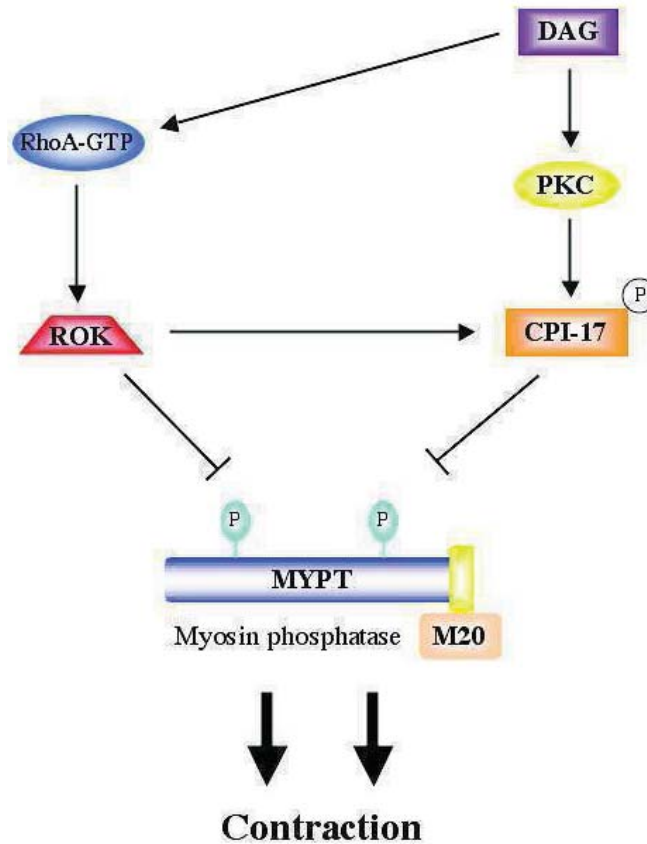


Figure 11: Diagrammatic illustration of the pathways leading to MLCP inhibition, and consequently contraction, including the interaction between RhoA and CPI-17 phosphorylation. Adapted from Hirano 2007²³¹.

A.5 REGULATION OF CYTOSOLIC CALCIUM

In VSM the regulation of cytosolic Ca^{++} is essential because high levels are toxic for the cell. The cytosolic Ca^{++} concentration in smooth muscle is around 100nM, much lower than the extracellular concentration of approximately 1.5mM. Ca^{++} channels play an important role in regulating and maintaining this critical cytosolic Ca^{++} concentration.

A.5.1 Voltage-Operated Calcium Channels

The voltage-operated Ca^{++} channels (VOCCs), sometimes referred to as voltage-gated calcium channels, allow for an influx of Ca^{++} into the cell upon channel activation. Specifically, depolarisation of the cell membrane potential increases the open possibility of VOCCs²³²⁻²³⁵. Through their regulation of Ca^{++} entry VOCCs play an important role in regulating vascular tone^{236, 237}. Myogenic responses are classically accompanied by a membrane depolarisation and an increase in intracellular Ca^{++} concentration, which is achieved by an influx of extracellular Ca^{++} through these VOCCs²³⁸.

A.5.1.1 VOLTAGE-OPERATED CALCIUM CHANNEL SUBUNIT COMPOSITION AND FUNCTION

VOCCs are a plasma membrane spanning protein comprised of five separate subunits, α_1 , α_2 , β , γ and δ (Figure 12).

NOTE:
This figure is included on page 34
of the print copy of the thesis held in
the University of Adelaide Library.

Figure 12: Molecular architecture of the VOCC depicting the α_1 pore forming, α_2/δ , β and γ subunits and their specific structure. Modified from Hoffman *et al.* 2004²³⁹.

Of these subunits only the α_1 subunit acts as the Ca^{++} channel²⁴⁰ as it contains the “voltage-sensing machinery”. The auxiliary subunits α_2 , β , γ and δ are responsible for regulating channel gating^{241, 242, 243, 244, 245, 246}.

The α_2 and δ subunits ($\alpha_2\delta$) are linked together by a disulfide bond with the δ subunit anchoring the protein in the plasma membrane²⁴² while the α_2 part provides the structural elements required for channel activation²⁴³. The δ subunit also contains the regions important in controlling the shift in voltage-dependent activation and steady state inactivation along with the inactivation kinetics²⁴⁷. The $\alpha_2\delta$ subunit also has a role in increasing the density of Ca^{++} channels activated by high voltage at the plasma membrane²⁴⁴.

The β subunit has many roles within the Ca^{++} channel. It regulates current density by controlling the amount of α_1 expressed at the cell membrane, regulates activation and inactivation kinetics, and hyperpolarises the voltage-dependent activation of the α_1 pore allowing for smaller depolarisations^{245, 246}. There are four different isoforms on the β subunit, β_1 - β_4 , which interact with the α_1 subunit producing these effects²⁴².

Finally the γ subunit is primarily associated with skeletal muscle VOCCs²⁴⁸. Various subunits of the γ subunit, however, have been noted in the brain, liver, kidney, heart and lung^{249, 250}. The γ subunit is yet to be described in VSM. The γ subunits are believed to have a modest influence on Ca^{++} current properties²⁵¹ with its primary role in interactions with other membrane proteins²⁴².

A.5.1.2 VOLTAGE-OPERATED CALCIUM CHANNEL SUBGROUPS

VOCCS can be classified into two subgroups on the basis of their biophysical and pharmacological properties. On the basis of their activation voltage the Ca⁺⁺ channels are divided into two groups, the high voltage-activated (HVA) channels and the low voltage-activated (LVA) channels (Figure 13):

(1) High Voltage-Activated Channels

The HVA channels are defined by their requirement of a large depolarisation from about -80mV to -30mV to induce Ca⁺⁺ channel opening, a large conductance (23 to 25pS) and rapid inactivation^{242, 252, 253}. These HVA channels have been further classified into L-, N-, P/Q- and R- subtypes. While these subtypes differ in their voltage dependence of activation, inactivation and deactivation²⁵⁴, they are primarily classified on the basis of pharmacological sensitivity.

(2) Low Voltage-Activated Channels

The LVA channels, however, are activated by a depolarisation of \geq -60mV, are characterised by the lowest single channel conductance of all the VOCCs (3.5 to 7pS) and inactivate slowly²⁵⁵⁻²⁵⁷. The only characterised LVA channel to date is the T-channel subtype^{255, 258, 259}.

When first discovered the α_1 subunits were named according to the well accepted nomenclature of the time, specifically α_{1S} for the original skeletal muscle isoform and α_{1A-I} for those discovered subsequently^{260, 261}. However, in 2000 the Ca_v classification was adopted in line with the well-defined K⁺ channel nomenclature²⁶¹.

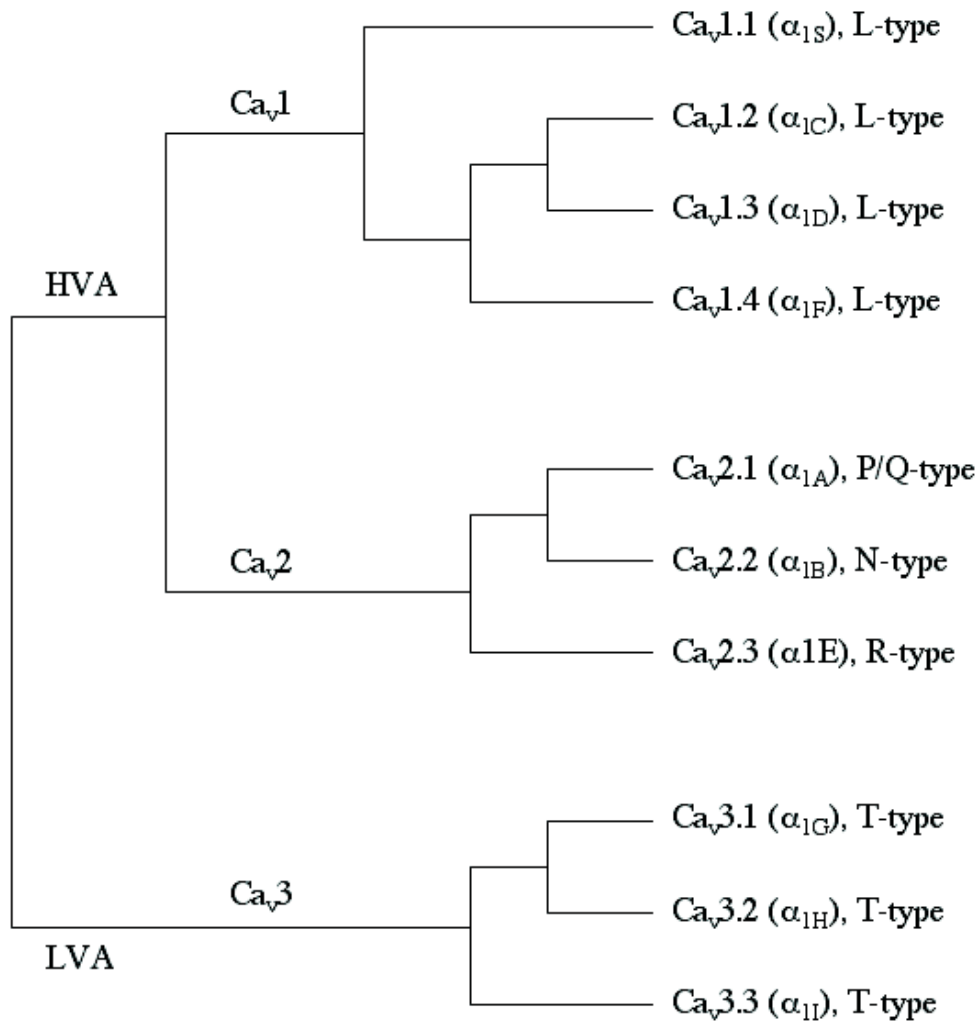


Figure 13: Division of the VOCCs into the HVA and LVA subgroups, the Ca_v1 , Ca_v2 and Ca_v3 families and their individual L-, P/Q-, N-, R and T-type. Modified from Perez-Reyes, 2003²⁵⁵.

A.5.1.2.1 L-type Calcium Channels

The L-type Ca^{++} channels belong to the class of HVA channels which activate and inactivate at more positive membrane potentials, inactivate slowly and have long-lasting effects^{242, 252, 253}. These L-channels are well characterised and play an essential role in excitation-contraction coupling in VSM, skeletal muscle and cardiac muscle²⁶²⁻²⁶⁶. Originally, the L-channels were classified as α_{1C} , α_{1D} , α_{1F} and α_{1S} , however with the new nomenclature system being adopted in 2000 the L-channels

are now classified as Ca_v1 and further subdivided into four groups, Ca_v1.1-1.4²⁶⁷. These subdivisions largely depend on their tissue distribution.

Ca_v1.1

Ca_v1.1 (formerly α_{1S}) is located primarily in skeletal muscle and linked to RyRs on the SR²⁶⁸. Ca_v1.1 primarily acts as a voltage-sensor releasing intracellular Ca⁺⁺ following depolarisation. The link between this depolarisation and the channel opening, however, is very inefficient as the Ca_v1.1 open with slow kinetics²⁶⁹.

Ca_v1.2

The Ca_v1.2 group (formerly α_{1C}) is expressed in vascular smooth muscle^{270, 271}, ventricular cardiac muscle^{270, 272}, pancreatic cells²⁷³, fibroblasts²⁷⁴ and neurons²⁷⁵. These Ca_v1.2 channels are primarily Ca⁺⁺ ion channels and play an important role in initiating smooth and cardiac muscle contraction^{263, 276}.

Ca_v1.3

Ca_v1.3 channels (formerly α_{1D}) have been identified in neurons²⁷⁷, pancreatic beta cells²⁷⁸, neuroendocrine cells²⁷⁹, photoreceptors²⁸⁰, amacrine cells²⁸¹ and inner ear hair cells²⁸². In the heart Ca_v1.3 is found in atrial tissue where it contributes to the pace-making activity of the heart^{283, 284}.

Ca_v1.4

Finally, Ca_v1.4 (formerly α_{1F}) have been identified primarily in the retina²⁸⁵ and dorsal root ganglia²⁸⁶. The Ca_v1.4 group has no direct vascular effects.

Further analysis of these L-channels has shown that they are in fact a functionally heterogeneous family²⁶⁷:

- (1) Firstly, not all of the L-channels require a strong depolarisation for activation. Specifically, the $\text{Ca}_v1.3$ ^{287, 288} and $\text{Ca}_v1.4$ ²⁸⁹ channels have a relatively low activation threshold compared to $\text{Ca}_v1.2$ and $\text{Ca}_v1.1$ channels .
- (2) While L-type channels are generally described as being sensitive to dihydropyridines, their sensitivities differ with the $\text{Ca}_v1.3$ ^{287, 288} and $\text{Ca}_v1.4$ ²⁹⁰ subtypes less sensitive.
- (3) Their activation kinetics also vary with $\text{Ca}_v1.2$ ²⁹¹ and $\text{Ca}_v1.3$ ²⁸⁷ activating faster while $\text{Ca}_v1.4$ ²⁸⁹ opens at a relatively slow rate.
- (4) Finally, only $\text{Ca}_v1.4$ shows Ca^{++} -independent inactivation²⁹⁰.

A.5.1.2.2 T-type Calcium Channels

In contrast to the L-channels the T-type Ca^{++} channels belong to the class of LVA channels meaning they activate and inactivate at more negative membrane potentials, are more transient²⁵⁵⁻²⁵⁷. Furthermore, they are highly sensitive to agents such as mibefradil and efonidipine, known T-channel blockers²⁹²⁻²⁹⁶.

Efonidipine^{292, 294} and mibefradil²⁹⁷ inhibit T-channel currents significantly more than the L-channel currents in isolated VSM preparations. Other investigators have also suggested that T-channel blockade with mibefradil may be more effective in the microvasculature. Kung *et al.* demonstrated that mibefradil dilates endothelin-contracted porcine small coronary vessels more effectively than large coronary

arteries²⁹⁸ while VanBavel *et al.* showed that mibefradil is more potent than verapamil in inhibiting myogenic tone in rat cremasteric muscle arterioles²⁹⁹.

As with the L-channels, the T-channels also are encoded for by a family of related genes, Ca_v3.1, Ca_v3.2 and Ca_v3.3²⁵⁵.

Ca_v3.1

The Ca_v3.1 channel (formerly α_{1G}) is primarily expressed in the vascular smooth muscle^{300, 301}, brain^{257, 302, 303} and heart^{304, 305} with low levels also detected in the kidney³⁰⁶. Although the exact role of Ca_v3.1 is yet to be fully elucidated it is believed to be involved with vascular contraction³⁰⁷, pace-making activity of the heart^{308, 309}, neuronal firing^{310, 311}, aldosterone secretion³¹² and/or fertilization³¹³.

Ca_v3.2

The mRNA for Ca_v3.2 (formerly α_{1H}) is predominantly expressed in the kidney^{256, 314}. In addition Ca_v3.2 is also found in the heart^{304, 314, 315}, brain^{302, 316}, liver³¹⁴, smooth muscle^{301, 306} and the adrenal cortex³¹⁷. Ca_v3.2 has several roles throughout the body including that of smooth muscle contraction³¹⁸, proliferation³¹⁹, aldosterone secretion³²⁰ and cortisol secretion³²¹.

Ca_v3.3

The Ca_v3.3 (formerly α_{1I}) subunit differs from the other two T-channel subunits in that while they have a varying distribution among a number of different tissue types, Ca_v3.3 is largely expressed in the brain with little found elsewhere³²²⁻³²⁵. Due to their

almost exclusive expression in the brain the Ca_v3.3 subunit is involved with thalamic oscillations²⁵⁵. An interesting feature of the Ca_v3.3 subunit is that it deactivates at a much slower rate than Ca_v3.1 and Ca_v3.2, enabling them to produce long-lasting bursts of firing³²⁶.

A.5.1.2.3 P/Q-, N- and R-type Channels

Apart from the L- and T-channels there are four other Ca⁺⁺ channels with functional and structural physiological importance. These include the P/Q-, N- and R- types, all of which are not thought to be in VSMCs³²⁷.

P/Q-type Channels

The P/Q-type Ca⁺⁺ channels, also known as the Ca_v2.1 channels (formerly α_{1A}), are so called that because they were first located in Purkinje cells. However, since their discovery they have also been noted in neurons³²⁸⁻³³⁰, cardiac neurons³³¹, pancreas^{332, 333} and pituitary³³⁴. These channels are involved with neurotransmitter release^{335, 336} and excitation-secretion coupling in pancreatic β cells³³³.

N-type Channels

The N-type Ca⁺⁺ channels, also known as Ca_v2.2 (formerly α_{1B}), are so called because they are predominantly expressed in neurons³³⁷⁻³³⁹. The N-type channels have a few different physiological functions including a role in neurotransmitter release³³⁸, pain transmission³⁴⁰ and sympathetic regulation of the circulatory system³³⁷.

R-type Channel

The last type of Ca⁺⁺ channel is the R-type, also known as the Ca_v2.3 (formerly α_{IE}). As with Ca_v2.1 and 2.2 these channel subtypes are expressed in neurons^{341,342}, as well as the heart^{343, 344} and pituitary³⁴⁵. Due to their distribution within these tissue types, the Ca_v2.3 channels have been implicated in neurotransmitter release^{342,346}, repetitive firing³⁴², long-term potentiation³⁴⁷ and neurosecretion^{348,349}.

A.5.1.3 VOLTAGE-OPERATED CALCIUM CHANNEL ANTAGONISTS

This thesis focuses primarily on L-type Ca⁺⁺ channel blockers and the combined L- and T-type Ca⁺⁺ channel blockers and as such only these will be described in this section.

CCBs are categorised according to: (1) chemical structure, (2) specificity of slow current inhibition, (3) tissue selectivity, (4) receptor specificity, or (5) clinical properties (dihydropyridines and non-dihydropyridines). The conventional CCBs include the phenylalkylamines, benzothiazepines and dihydropyridines which bind to separate sites on the L-type (or long-lasting, high voltage-activated) Ca⁺⁺ channel. Of specific relevance to this thesis are verapamil (phenylalkamine) and nifedipine (dihydropyridine). There are, however, CCBs which block not only the L-channel but also the T-channel. Two specific drugs belonging to this category are efonidipine (dihydropyridine) and mibefradil (a tetralol derivative) (Figure 14).

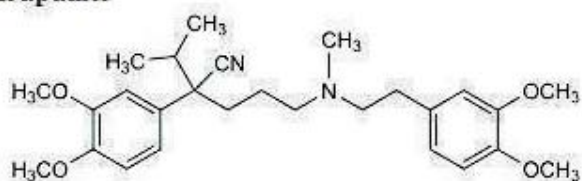
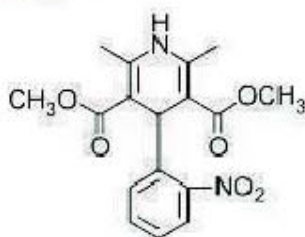
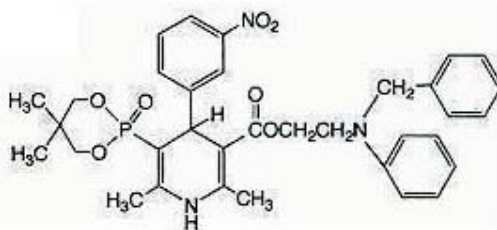
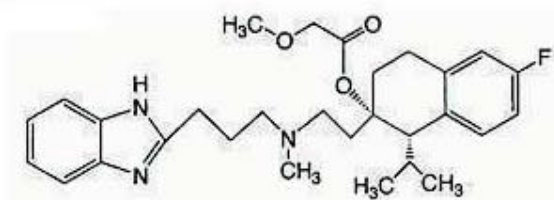
Verapamil**Nifedipine****Efonidipine****Mibefradil**

Figure 14: The chemical structure of the CCBs verapamil, nifedipine, efonidipine and mibefradil. Adapted from Triggle, 1998³⁵⁰ and Tanaka and Shigenobu, 2002²⁹⁴.

Verapamil

Verapamil blocks the Ca⁺⁺ L-channel and is of the phenylalkamine class of CCBs. The phenylalkamines differ from the other CCBs with their α binding site, located intracellularly at the S6 domain of segment IV (IVS6)³⁵⁰. Interestingly, the specific

location of the verapamil binding site corresponds to the local anaesthetic binding region of the sodium channel, and verapamil is a potent local anesthetic^{350, 351}.

Verapamil's primary application is to block the VOCCs for the management of cardiovascular conditions. Vascular constriction is dependent on Ca^{++} entry through the VOCCs located on the VSM of blood vessels²³⁷. Therefore, blocking these VOCCs will decrease the amount of Ca^{++} entering the VSMCs thereby promoting vasodilation. This vasodilatory effect is of therapeutic benefit in the treatment of hypertension^{352, 353}, angina^{354, 355} and primary pulmonary hypertension^{356, 357}. Another cardiovascular condition in which verapamil is therapeutically beneficial is treatment of cardiac arrhythmia, specifically atrial fibrillation^{358, 359}. Ca^{++} channels are highly concentrated throughout the sinoatrial and atrioventricular nodes. As such verapamil can decrease the conduction of impulses through the atrioventricular node, protecting the ventricles from atrial tachycardia^{358, 359}.

In addition to its Ca^{++} channel blocking effects, verapamil has many other "off target" effects including:

(1) *$\alpha 1$ Antagonist*

Verapamil inhibits adrenalin-induced platelet aggregation at the level of the $\alpha 1$ -adrenergic receptor^{360, 361}.

(2) *Inhibitor of Drug Efflux Pump Protein P-glycoprotein*

Many tumour cells over-express these drug efflux pumps, which limits the effectiveness of cytotoxic drugs. Specifically, P-glycoprotein removes the drugs from the cells before they can have their cytotoxic

effects. However, there is evidence that verapamil inhibits these pumps, thus increasing the effectiveness of treatment³⁶².

(3) *Verapamil/Chloroquine Treatment of Malaria*

The resistance to chloroquine, which is used to treat malaria, is characterised by the parasitic cells' ability to expel the drug from its digestive vacuole. Treatment with a combination of verapamil and chloroquine accumulates chloroquine within the digestive vacuole. This makes the parasite more susceptible to death³⁶³.

Nifedipine

Nifedipine differs from verapamil in that it belongs to the dihydropyridine class of CCBs with its binding site, IIS6 and IVS6, located extracellularly^{350,364}.

The binding of nifedipine to the VOCCs on the VSM membrane inhibits the entry of Ca^{++} . This reduction in Ca^{++} influx by nifedipine causes arterial vasodilation and decreased peripheral vascular resistance. The result is reduced arterial blood pressure. Due to these effects the main uses of nifedipine are in the treatment of angina (particularly Prinzmetal's angina, or variant angina)^{365,366}, hypertension^{367,368} and Raynaud's phenomenon³⁶⁹. Nifedipine does have some side effects, resulting from reflex sympathetic nervous system activation, including flushing, tachycardia, worsening myocardial ischaemia and cerebrovascular ischaemia. The use of long acting formulations, however, has reduced these effects^{370,371}.

Nifedipine is also used in the treatment of other conditions which are unrelated to its CCB effects, including:

(1) *Tocolytic*

Nifedipine has frequently been used to delay premature labour. Furthermore, it is also seen to have fewer negative side effects than other agents used in this manner³⁷².

(2) *High altitude pulmonary oedema*

Nifedipine is also used as a high altitude medicine in the treatment of high altitude pulmonary oedema^{373, 374}.

Mibefradil

Mibefradil is described as being non-selective because it binds to the phenylalkylamine and benzothiazepine L-channel binding sites. Yet, it does not bind to the dihydropyridine site. Mibefradil is in its own class - benzimidazole. One significant feature of mibefradil is that it has been shown to block not only the Ca⁺⁺ L-channel but also the Ca⁺⁺ T-channel^{297, 375}. Binding studies have demonstrated that mibefradil has a 10 – 15 times higher affinity for the T-channel than the L-channel³⁷⁶. Furthermore, T-channels are completely blocked at concentrations of 1-10µM mibefradil which blocks only 25 – 70% of L-channels²⁹⁷.

Due to its unique pharmacological profile mibefradil has an important therapeutic benefit in the treatment of hypertension^{377, 378} and angina^{377, 379, 380}. One condition in which mibefradil is seen to be especially efficacious is the small vessel disorder, the Coronary Slow Flow Phenomenon (CSFP). With CSFP patients L-channel blockers

are ineffective while the T-channel blocker mibefradil is beneficial³⁸¹. One additional benefit of mibefradil treatment of hypertension and angina is the absence of leg oedema, which has been seen to develop following treatment with the dihydropyridine CCBs^{377,382}.

Mibefradil also plays an interesting role in the prevention of neointima formation; a neointima forms in response to vascular injury. By preventing smooth muscle proliferation mibefradil is able to prevent the formation of a neointima³¹⁹. There is however some conjecture regarding whether this effect is actually mediated by the CCB effect of mibefradil³¹⁹.

Studies with the carotid, femoral and basilar arteries of dogs and rat aorta have shown that the effects of mibefradil may be endothelium-dependent. Specifically, the response to mibefradil during contractions to PE and Et-1 were abolished in these large vessels with no endothelium³⁸³.

One non-vascular condition in which mibefradil is effective (though the mechanism of action could be considered vascular) in the treatment of various types of cancer. Specifically, there is evidence that mibefradil inhibits cell proliferation in various cancers³⁸⁴⁻³⁸⁶.

Efonidipine

Efonidipine is another combined L- and T- Ca⁺⁺ channel antagonist²⁹⁴. Like nifedipine, efonidipine works through the dihydropyridine receptor, however it

differs from most DHPs in having a phosphate moiety in the position of the DHP ring²⁹⁴ (see Figure 14 above). Originally developed as an antianginal and antihypertensive drug, efonidipine has a relatively slow onset and long duration of action^{387, 388}.

In vitro studies of efonidipine have demonstrated that like the phenylalkamines it has relatively strong negative chronotropic activity with only weak negative inotropic effects³⁸⁹. Similar to the dihydropyridines efonidipine has been shown to produce potent vasodilation³⁸⁹. The phosphate moiety at the C5 position of structure of efonidipine may explain its strong negative chronotropic action and its slow onset of vessel relaxation³⁹⁰.

Efonidipine has a unique pharmacological profile characterised by its ability to block not only the Ca⁺⁺ T-channel but also the Ca⁺⁺ L-channel²⁹⁴. Specifically, the *S*(+)-efonidipine isomer exerts blocking actions of both the L- and T-channel types with no effect on the N-, P/Q- and R-type Ca⁺⁺ channels. In contrast the *R*(-)-efonidipine isomer selectively inhibits the Ca⁺⁺ T-channel³⁹¹.

As mentioned previously, two cardiovascular conditions in which efonidipine is seen to work are hypertension³⁹²⁻³⁹⁵ and angina^{394, 396, 397}. Furthermore, treatment of hypertensive, diabetic patients with efonidipine can lower their risk of developing other cardiovascular complications³⁹⁸. More recently the use of efonidipine in reducing proteinuria in renal patients^{399, 400} and improving renal function^{399, 401} has also been highlighted.

A.5.2 Receptor-Operated Calcium Channels

Receptor-operated Ca^{++} channels (or ROCCs) comprise a range of structurally and functionally diverse channels that are Ca^{++} permeable and non-voltage gated. The term receptor-operated was put forward to define any plasmalemmal channel which opened in response to an agonist binding to the receptor independent of any change in membrane potential^{402, 403}. Unlike the VOCCs which undergo a conformational change upon membrane depolarisation leading to channel opening, binding of an agonist to the receptor induces a conformational change which opens an ion-selective pathway intrinsic to that receptor⁴⁰⁴.

ROCCs are activated by agonists (for example, PE) acting on a seven transmembrane domain receptor coupled to a heterotrimeric G-protein^{233, 405}. This essential G-protein receptor role of activation and channel opening has been demonstrated in a variety of VSM preparations^{406, 407}. While some details on the transduction pathway of ROCCs remains unclear, recent evidence has shown that ROCC current can be increased through a number of signalling pathways. These pathways include Ca^{++} -CaM⁴⁰⁸, MLCK⁴⁰⁹, tyrosine kinase⁴¹⁰ and PKC⁴¹¹, which has also been shown to inhibit ROCC activity⁴¹².

Recently, the transient receptor potential cation (TRPC) channels have been shown to play an important role in modulating receptor-operated Ca^{++} entry into various cell types including VSM^{413, 414}. TRPC channels belong to a 'superfamily' of hexahelical cation channels which are subdivided into TRPC 1, 2, 3, 4, 5, 6, and 7. It is the TRPC 3, 6 and 7 subfamilies that are believed to form the store-independent ROCCs⁴¹⁵.

Ultimately, ROCCs are involved in modulating cytosolic Ca^{++} levels, which regulate several cellular processes including smooth muscle cell contraction^{416, 417}, cell proliferation⁴¹⁸, apoptosis^{419, 420} and neurotransmitter release^{420, 421}.

A.5.3 Store-Operated Calcium Channels

Store-operated calcium channels (SOCCs) are another Ca^{++} permeable channel, located on the plasma membrane of smooth muscle, which are not activated by membrane depolarisation. Instead a depletion of the internal stores of Ca^{++} activates a Ca^{++} influx mechanism, the SOCC^{405, 422}. This was first documented by Casteels and Droogmans who noted that, following depletion of the internal Ca^{++} stores of VSM, there was an increase in uptake of Ca^{++} into the cell⁴²³.

With SOCCs the mechanism of Ca^{++} entry is released from the SR due to activation of either the IP_3 receptor or RyR⁴²⁴. In the SR of muscle cells there is a limited capacity for Ca^{++} storage. Thus SOCCs provide cells with the means to renew depleted intracellular Ca^{++} concentrations.

As with ROCCs the TRPC proteins have also been implicated in the role of SOCCs. In particular TRPC1 is involved with store-operated Ca^{++} entry in VSMCs^{414, 425-427}. It has also been suggested that TRPC5 is involved⁴²⁸. The single membrane-spanning protein termed STIM1 is another mediator of SOCCs acting as a Ca^{++} sensor within the stores⁴²⁹. Furthermore, STIM1 may interact with TRPC1 and is involved in with store-operated Ca^{++} entry⁴³⁰. Another protein involved with SOCCs is Orai1 which acts as a pore subunit of the store-operated Ca^{2+} release-activated Ca^{2+} channels^{431, 432}.

A.5.4 Potassium Channels

Potassium (K^+) channels contribute to the regulation of membrane potential in VSMCs. Membrane hyperpolarisation occurs because there is an efflux of K^+ ions following opening of the K^+ channel in the VSM. This hyperpolarisation is followed by the closure of the VOCCs which decreases Ca^{++} entry into the cell consequently resulting in vasodilation⁴³³. Conversely, inhibition of the K^+ channels will result in cell depolarisation, subsequent Ca^{++} channel activation and Ca^{++} entry leading to vasoconstriction. Within the vascular smooth muscle four different K^+ channels have been identified. These are the voltage-dependent K^+ channel (K_v), large-conductance Ca^{++} -activated K^+ channel (BK_{Ca}), the ATP-sensitive K^+ channel (K_{ATP}) and the inward rectifier K^+ channel (K_{ir}).

Voltage-Dependent K^+ Channel

Voltage-dependent K^+ channel (K_v) expression has been identified in VSMCs⁴³⁴⁻⁴³⁷. K_v channels open to allow for an efflux of K^+ in response to membrane depolarisation, resulting in a repolarisation event and subsequent return to resting membrane potential. Specifically, in the VSMCs depolarisation of the membrane results in an influx of Ca^{++} through the Ca^{++} channels²³²⁻²³⁵. The influx activates MLCK leading to contraction (see Section A.4.2.1). Ultimately the K_v channels function to limit membrane depolarisation and therefore maintain resting vascular tone^{433, 438-440}.

Large-Conductance Ca^{++} -Activated K^+ Channel

The Large-Conductance Ca^{++} -Activated K^+ Channel, or the BK_{Ca} channel, also

features in VSM⁴⁴¹⁻⁴⁴³. The BK_{Ca} channel is a voltage-sensitive channel with the open probability increased by membrane depolarisation⁴⁴⁴⁻⁴⁴⁶. Under normal conditions BK_{Ca} channels are not believed to contribute to resting membrane potential^{447, 448}. They do, however, act as a negative feedback system during agonist and stretch-induced vasoconstriction⁴⁴⁹. Any increase in pressure due to membrane depolarisation or intracellular Ca⁺⁺ concentration (which result in the vasoconstriction) would activate the BK_{Ca} channels in an attempt to return the cell to resting membrane potential⁴⁵⁰.

ATP-sensitive K⁺ channel (K(ATP))

The third K⁺ channel identified in VSM is the ATP-sensitive K⁺ channel (K_{ATP}) so named because they close in response to increasing levels of ATP⁴⁵¹. Originally K_{ATP} channels were described in cardiac muscle^{452, 453}, however they have now been found in a variety of tissue types including VSM^{433, 454, 455}. The potential role of K_{ATP} channels and various pathophysiological responses have been noted, specifically coronary artery dilation in hypoxia⁴⁵⁶, reactive hyperemia⁴⁵⁷ and endotoxic shock-induced hypotension⁴⁵⁸.

Inward Rectifier K⁺ channel (Kir)

The inward rectifier K⁺ channels, or Kir_s, are primarily located within the resistance microvessels⁴⁵⁹⁻⁴⁶¹ although they are also present in coronary⁴⁶² and cerebral⁴⁶³ arteries. To date, the exact function of the Kir channels is unknown. Two functions have, however, been hypothesised. The first of these is that the Kir is involved in regulating resting membrane potential, and therefore resting tone, in microvessels⁴⁶⁴.

⁴⁶⁵. The second proposed function is that Kirs may hyperpolarise the cell in response to moderate increases in extracellular K^+ thus producing vasodilation. This is based on data which has shown that vasodilation cannot be prevented in the presence of inhibitors of other K^+ channels⁴⁶⁶⁻⁴⁶⁸.

A.5.5 Chloride Channels

Chloride (Cl^-) channels also play an important role in regulating vascular tone⁴⁶⁹. There are 3 gene families of Cl^- channels which have been identified. These are the Ca^{++} -activated Cl^- channels (CaCCs), the cystic fibrosis transmembrane conductance regulator (CFTR) and the ligand-gated GABA- and glycine-receptor channel. Concerning the regulation of membrane excitability the CaCCs play a large role because they are located on VSM^{470, 471}, cardiac cells^{472, 473}, neurons^{474, 475}, blood cells^{476, 477} and epithelial cells⁴⁷⁸.

Cl^- channels are activated by cytosolic Ca^{++} concentrations generally in the range of $0.2-5\mu M$ ⁴⁷⁹. In smooth muscle cells the activation of CaCCs occurs either by Ca^{++} entry through the VOCCs or by Ca^{++} release from intracellular stores⁴⁸⁰. Opening these CaCCs and the subsequent efflux of negative Cl^- ions depolarises the plasma membrane. This depolarisation increases the open probability of the VOCCs, thus further enhancing Ca^{++} entry and consequently smooth muscle cell contraction^{470, 481}.

A.6 VASCULAR PATHOPHYSIOLOGY

A.6.1 Pathophysiology Triad

When considering vascular pathophysiology it is important to recognise that there are three factors to be considered – atheroma, thrombosis and vascular reactivity. Together they form an integrated pathophysiological triad (Figure 15). While these factors can occur individually, there is also an element of overlap between each of the factors.

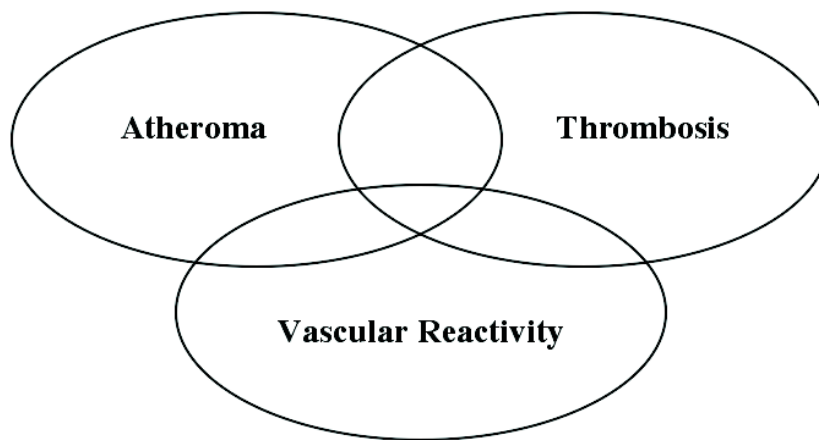


Figure 15: The pathophysiology triad involving atheroma, thrombosis and vascular reactivity.

Vasomotor Reactivity

The endothelium plays a central role in regulating vasomotor tone through the release of vasodilating and vasoconstricting factors^{148, 482}. A key factor of endothelial dysfunction is inadequate or inappropriate vasodilation or constriction. In healthy conditions the release of these substances occurs harmoniously to regulate vasomotor tone. However, in certain conditions this balance may be altered so that either the vasodilating or vasoconstricting substances are preferentially produced and released, resulting in altered vasomotor tone. Cardiovascular risk factors contributing to the

development of endothelial dysfunction, include hypercholesterolemia, smoking, hypertension and hyperglycaemia⁴⁸².

Platelet Reactivity

Platelets are essential in haemostasis and thrombosis. Platelet dysfunction plays an important role in many clinical disorders, manifesting as hypo- or hyper-coagulable states. *Ex vivo* studies have demonstrated the coagulation protease, thrombin, to be a potent activator of platelets⁴⁸³ and thus thrombin directly contributes to the formation of a platelet plug. While thrombin-mediated platelet activation is critical for homeostasis, and may also result in thrombosis, the signalling pathway involved with this remains unclear⁴⁸⁴.

Atherosclerosis

Atherosclerosis is an inflammatory process where the vascular intima becomes thickened with atheroma and connective tissue^{485, 486}. The risk factors for atherosclerosis include hypertension, diabetes mellitus, high cholesterol, cigarette smoking and a positive family history⁴⁸⁷.

Endothelial dysfunction has been implicated as one of the first steps in the pathogenesis of atherosclerosis⁴⁸⁸. Endothelial dysfunction contributes to the formation of vasoactive molecules^{11, 12}, cytokines⁴⁸⁹ and growth factors⁴⁹⁰, which activate the inflammatory response to remove these agents. If removal is not initially successful the inflammatory response may continue indefinitely, thus stimulating migration and proliferation of smooth muscle cells. They may become intermixed

with the area forming an intermediate lesion⁴⁸⁵. Once more, if this process continues unabated the arterial wall gradually thickens, which is compensated for by a parallel arterial dilation – a process referred to as “arterial remodeling”⁴⁸⁵. These cycles of accumulation, migration and proliferation continue until the artery is no longer able to compensate by dilation. Eventually an atherosclerotic plaque forms and it intrudes into the lumen and restricts or prevents the flow of blood.

A.6.2 Clinical Syndromes: Large Conduit Vessel Disorders vs. Small Resistance Vessel Disorders

When there is a negative alteration to the ‘normal’ physiology, such that blood flow is compromised there are two outcomes – ischaemia and infarction. Ischaemia is characterised by an imbalance between supply and demand with a transient interruption of blood flow being the most common mechanism. In ischaemia, cellular dysfunction but not necrosis occurs, whereas tissue necrosis does occur with infarction.

A.6.2.1 LARGE CONDUIT VESSEL DISORDERS

A.6.2.1.1 Coronary Artery Disease

Stable angina is primarily a result of obstructive coronary artery disease^{491, 492} with ischaemia occurring when myocardial demand is increased due to an increased heart rate. Accordingly, therapy is primarily focused on reducing heart rate. In contrast, in variant angina⁴⁹³ and acute coronary syndromes^{494, 495}, spasm^{496, 497} and thrombosis⁴⁹⁸ play a substantial role, respectively, so that therapies include the use of CCBs, nitrates or anti-platelet agents.

A.6.2.1.2 Peripheral Artery Disease

Peripheral artery disease (PAD) occurs in the peripheral tissues of the body and is characterised by interrupted or occluded blood flow. PAD primarily occurs secondary to cardiovascular disease. Two PAD conditions include intermittent claudication and gangrene.

Intermittent claudication (IC) is an ischaemic condition that presents as muscular pain during exercise and is the primary symptom of PAD⁴⁹⁹. The ischaemia occurs when the tissue metabolic demand (during exercise) exceeds the limited supply to the obstructed atherosclerotic large vessels^{500, 501}. Treatment of this condition has largely focused on revascularisation therapies, which entails dilating the obstructive lesion by angioplasty/stenting or bypassing it surgically. CCBs may be useful if a component of spasm is involved.

Gangrene is a condition where large vessel occlusion occurs, resulting in tissue necrosis. Thrombosis is frequently involved⁵⁰² and anti-platelet and anti-coagulation therapy may be beneficial for revascularisation of viable tissue. However, amputation is normally required for necrotic tissue.

A.6.2.2 SMALL RESISTANCE VESSEL DISORDERS

Since the smaller vessels within the vasculature play a major role in regulating vascular tone and blood flow (Section A.2.2), they also play a role in many cardiovascular conditions.

A.6.2.2.1 Coronary Microvascular Disorders

Microvascular disorders are characterised by coronary microvascular spasm resulting in a decreased oxygen supply and consequently debilitating pain. To date, there are no effective treatments for managing these conditions with the conventional cardiovascular medications (nitrates and CCBs) targeting primarily the large coronary vessels. As suggested in the previous discussion the regulation of microvascular and large vessel tone involves different mechanisms and thus alternative therapies may need to be evaluated.

Coronary microvascular dysfunction may manifest as cardiac syndrome-X or the Coronary Slow Flow Phenomenon (CSFP). Cardiac syndrome-X is characterized by exertional chest pain and a positive exercise stress test indicative of myocardial ischaemia^{503, 504} but in the absence of epicardial coronary artery disease. Patients with the CSFP predominantly experience chest pain at rest and exhibit a delayed passage of angiographic contrast dye through the distal vasculature⁵⁰⁵ in the absence of obstructive coronary artery disease, implicating an increased distal vascular resistance⁵⁰⁵.

A.6.2.2.2 Hypertension

Hypertension refers to a consistently elevated systolic blood pressure of >140mmHg or a diastolic >90mmHg⁵⁰⁶. Second only to tobacco smoking, hypertension is a leading risk factor for the development of stroke^{507, 508} and coronary heart disease⁵⁰⁷. It is also a major contributor to chronic heart failure^{509, 510} and chronic kidney disease⁵¹¹. Hypertension is the result of increased peripheral vascular resistance and

is primarily managed with vasodilator therapy. In over 95% of hypertensive patients there is no identifiable cause for the increased resistance⁵⁰⁶. Current National Heart Foundation guidelines recommend CCBs, angiotensin-converting enzyme (ACE) inhibitors, renin-angiotensin-aldosterone blockers or diuretics as first-line pharmacological therapies to treat hypertension following appropriate lifestyle modifications⁵⁰⁶.

A.6.2.2.3 Cerebral Microvascular Disorders

Stroke is a disabling condition resulting from cerebrovascular dysfunction. While discussed in the resistance vessel section, strokes can also occur in the large arteries responsible for supplying the brain with oxygen and nutrients, these are referred to as carotid strokes. Lacunar strokes however are characterised by small vessel occlusion.

Lacunar strokes can be either occlusive (when blood flow through the vessel is obstructed) or hemorrhagic (due to uncontrolled bleeding from the vessel). Most occlusive strokes are due to atherosclerosis and thrombosis^{512, 513} whereas hemorrhagic strokes are generally associated with hypertension or aneurysms^{514, 515}. Either of these may occur at any age from many causes; however, many studies have shown an increased risk of stroke in the presence of other vascular disorders such as hypertension. One such study demonstrated an increased risk of stroke in middle-aged, hypertensive men compared with non-hypertensive men of similar age⁵¹⁶.

Intermittent changes in blood flow to certain parts of the brain resulting in ischemia and neurological dysfunction⁵¹⁷ are termed transient ischaemic attacks (TIAs). TIAs

commonly result from disruption of an atherosclerotic plaque and thrombosis, commonly known as atherothrombosis^{498, 518, 519}. Symptoms can vary, however, they manifest themselves in a similar way to stroke, including temporary loss of vision, difficulty in speaking, weakness on one side of the body and numbness or tingling usually on one side of the body. TIAs can be considered a warning sign for stroke with 15-20% of stroke patients suffering a TIA in the preceding hours or days^{517, 520}.

A.6.3 Clinical Role of Calcium Channel Blockers

As discussed in Section A.6.2.2.2 hypertension is prevalent in the Australian community and is associated with many other cardiovascular conditions. Furthermore, hypertension is responsible for more disease and deaths worldwide than any other biomedical risk factor⁵²¹. CCBs play an important role in the initial treatment and management of hypertension and are one of the most commonly used medications. This is indicated by their increasing use over the last 15 years⁵²². The National Heart Foundation of Australia Guide to the Management of Hypertension 2008 recommends the use of dihydropyridine CCBs, ACE inhibitors, angiotensin receptor blockers or low dose thiazide diuretics for the initial treatment of hypertension⁵⁰⁶. While the most effective combination treatment consists of a dihydropyridine CCB and an ACE inhibitor, other effective combinations include a dihydropyridine CCB and beta-blocker or a CCB and thiazide diuretic⁵⁰⁶.

As mentioned above, CCBs play a major role in the management of cardiovascular disorders. Not only do they ameliorate symptoms such as angina but also reduce cardiovascular events associated with acute coronary syndromes, hypertension and

strokes. While their therapeutic benefits have predominantly focused on large vessel dysfunction, the studies undertaken in this thesis will also evaluate their effects on the microvasculature.

A.7 SUMMARY AND AIMS

The coronary, cerebral and peripheral vasculatures play a major role in health and disease and are responsible for more deaths in Australia than any other disease process. Combined they account for 34% of male and 39% of female deaths in Australia⁴⁸⁷. Control of blood flow within these vascular beds involves multiple regulatory mechanisms with VSMC Ca^{++} fluxes being the major common pathway. This thesis will investigate the regulation of Ca^{++} fluxes via the L- and T-channels in both large and small vessels. Specifically the focus will be on the effects of L-channel blockers and combined L- and T-channel blockers. Furthermore, this thesis will quantitatively examine the protein distribution of L-channels and T-channels in both large and small vessels. These will be addressed in Sections B and C with an overall conclusion detailed in Section D.

In Section B wire myography will be used to determine if there are differences in the inhibition of contractile responses between combined L- and T-channel blockade compared to L-channel blockade alone. The emphasis will be on microvessels given the clinically observed differences related predominantly to dysfunction in small resistance vessels.

The objectives of Section C are to: firstly, quantify with Real-Time PCR the mRNA expression of the pore-forming subunits of Ca⁺⁺ L- and T-channels in small and large vessels; and secondly, using quantitative western blotting to compare the protein abundance of the pore-forming subunits of Ca⁺⁺ L- and T-channels in both small and large vessels.

SECTION B

L- AND T- CHANNEL BLOCKADE IN RAT AND HUMAN VESSELS

B.1 BACKGROUND

Ca⁺⁺ channel blockers (CCBs) play a major therapeutic role in the management of cardiovascular disorders, particularly as anti-hypertensive and anti-anginal agents. These clinical effects are mediated via the inhibition of transmembrane Ca⁺⁺ channels on vascular smooth muscle cells (VSMCs). They reduce Ca⁺⁺ ion influx and this results in reduced vascular smooth muscle (VSM) contraction and vascular tone, ultimately relaxing the blood vessels.

B.1.1 Ca⁺⁺ Channel Blocker Classifications

The conventional CCBs include phenylalkylamines (for example, verapamil), benzothiazepines (such as diltiazem) and dihydropyridines (for instance, nifedipine). These CCBs mediate their effects via a common mechanism, namely the inhibition of the long-acting voltage-dependent Ca⁺⁺ channels (L-channel). The dihydropyridines are identified as vasodilators with no negative chronotropic or inotropic properties⁵²³. The non-dihydropyridines, however, are vasodilators with negative chronotropic and inotropic properties⁵²³.

Some new generation CCBs have been developed which block not only the Ca⁺⁺ L-channel but have the additional effect of inhibiting the transient Ca⁺⁺ channel (T-channel). Mibefradil was the first such drug and had negative chronotropic but no significant inotropic properties^{524, 525}. Clinical trials have shown mibefradil is an effective treatment for Coronary Slow Flow Phenomenon (CSFP) related chest pain. Specifically, mibefradil reduced the total number of anginal episodes per week, the duration of these anginal episodes and sublingual nitrate consumption required for

pain management³⁸¹. However, mibefradil has since been voluntarily withdrawn from the market due to negative interactions with cytochrome P450 3A4, an effect unrelated to its T-channel blocking actions²⁹⁴. Efonidipine hydrochloride is a novel dihydropyridine with a unique pharmacological profile characterised by its ability to block Ca⁺⁺ T-channels²⁹⁴. Specifically, the *S*(+)-efonidipine isomer blocks both the L- and T-channels with no effect on the N-, P/Q- and R-type channels. In contrast, the *R*(-)-efonidipine isomer selectively inhibits the T-channels³⁹¹.

B.1.2 T-Channel Blockers and the Microcirculation

The new generation CCBs which have combined L- and T-channel blocking properties appear to have incremental clinical benefits over the conventional L-CCBs. These two CCB groups of agents differ in their pharmacodynamic responses at the small resistance vessel level. Since these blood vessels play a pivotal role in the regulation of blood pressure^{377,526}, coronary blood flow³⁸¹ and renal perfusion³⁰⁶ it is expected that these newer agents would have additional benefits for treating disorders relating to these circulations. For example, in a comparison of the anti-hypertensive effects of diltiazem (an L-channel blocker) and mibefradil, the combined L- and T-channel blocker reduced blood pressure to a greater extent than the L-channel blocker³⁷⁷. Another comparison of diltiazem and mibefradil reported similar anti-hypertensive effects of the dual L- and T-channel blocker⁵²⁶.

However, recent findings by Moosmang *et al.* in a conditional knockout mouse model, is in contrast to these findings. In embryonic stem cells Ca_v1.2 alleles are generated by Cre-mediated recombination. The animals in this study were made to

express the tamoxifen-dependent Cre recombinase, therefore treatment of these premutant mice with tamoxifen activates the recombinase which results in ablation of Ca_v1.2 in smooth muscle⁵²⁷. In these L-channel knockout animals they demonstrated that mibefradil's lowering of blood pressure and increased hind-limb perfusion effects were absent. It was therefore proposed that mibefradil's vascular effects were mediated via the L-channel only⁵²⁷.

The beneficial effects of the combined L- and T-channel blockers in the microvasculature are thought to be mediated through an increased presence of T-channels in the smaller vessels.

B.1.3 Study Objectives

The clinical and pharmacological data described above suggest that CCBs having T-channel blocking properties may differ from those exerting only L-channel blockade. The main objective of the studies in this chapter is to determine if there are differences in the inhibition of contractile responses between combined L- and T-channel blockade compared to L-channel blockade alone. The focus will particularly be on microvessels given that the clinically observed differences related predominantly to dysfunction in small resistance vessels.

To achieve the above objective, several preliminary sub-studies were undertaken to ensure a comprehensive evaluation. These include:

- (1) Establishing appropriate CCB concentrations.

- (2) Determining the effect of combined L- and T-channel blockers compared with L-channel blockers in large conduit vessels and microvessels, on constrictor responses mediated via: (a) a receptor-coupled vasoconstrictor agonist; and (b) a depolarising stimulus.
- (3) Assessing if combined L- and T-channel blockade produces incremental inhibition of constrictor responses in the presence of maximal L-channel blockade.
- (4) Determining the effect of combined L- and T-channel blockers compared with L-channel blockers in large conduit vessels and microvessels, on endothelin-1 (Et-1) constrictor responses in the presence of chronic Et-1 receptor activation.
- (5) Confirming if heterogeneity in CCB responses is evident in human microvessels.

The methods and findings from these sub-studies are summarised in the following sections.

B.2 METHODS

B.2.1 Isolated Vessel Preparations

B.2.1.1 RAT VESSELS

Six male Sprague Dawley rats weighing 400g each were anaesthetised using forthane inhalation anaesthetic and euthanased by exsanguination. Rats were placed in the supine position and a medium laparotomy performed. The small intestine was tied off with sutures, 3cm from the stomach and 3cm proximal to the colon, before removal of the small intestine with mesentery, including the superior mesenteric

artery. The vessels were immediately placed in ice cold Krebs at 4°C and bubbled with carbogen (95% oxygen, 5% carbon dioxide).

For large vessel preparations the thoracic aorta was harvested. The contents of the thoracic cavity, including the heart and lungs, were removed and immediately placed in ice cold Krebs at 4°C and bubbled with carbogen. The aorta was dissected free of the lungs and separated from the heart at the aortic branch.

This study was approved by the institutional ethics committees for animal research (approval M-04-2006, The University of Adelaide Animal Ethics Committee; approval 7/06, Institute of Medical and Veterinary Science/Central Northern Adelaide Health Service Animal Ethics Committee).

B.2.1.2 HUMAN VESSELS

Patients undergoing elective abdominal surgery were recruited into the study after completing informed consent, prior to the surgical procedure. The 17 subjects (55 ± 4 years, 11 females) recruited to the study had no known history of cardiovascular disease although several had cardiovascular risk factors including hypercholesterolemia (29%), hypertension (24%), cigarette smoking (29%) and diabetes (12%). No patient was being prescribed vasodilator or statin therapy (see Appendix 3 for Patient Information Sheet). Immediately following surgical removal the subcutaneous, abdominal sample was placed in ice cold Krebs at 4°C and bubbled with carbogen. The study was approved by the institutional ethics

committees for human research (approval 2005050, The Ethics of Human Research Committee, Central Northern Adelaide Health Service).

B.2.2 Chronic Endothelin Infusion Model

To investigate the effects of the CCBs in the presence of an increased microvascular tone, via chronic Et-1 receptor activation, a mini-osmotic pump model was chosen as these mini-pumps are able to infuse animals at a continuous rate for a prolonged period. Previous studies have validated the use of these pumps to infuse endothelin resulting in hypertension⁵²⁸.

B.2.2.1 MINI-OSMOTIC PUMP FILLING AND CANNULA PREPARATION

ALZET[®] mini-osmotic pumps model 1002 (ALZET[®] through Jomar Biosciences, Australia) were filled with 100µL of filtered 0.1mg/mL Et-1 prepared in Tris (1M) buffered saline (saline 9%). Holding the pump in the upright position a syringe was used to fill the pumps at the filling port. Care was taken during filling to avoid the introduction of air bubbles into the pump. Once full the accompanying flow modulator was attached to the pump so that the flange was flush with the top of the pump.

To construct the cannulae 2.5cm lengths of polyethylene tubing 0.03 inches internal diameter (Intramedic, Australia) were prepared with one end cut at a 45° angle. A 0.1cm length of tubing was placed around the cannula 2cm from the angled end – this additional piece of tubing provides an anchor for suturing the cannula to the

jugular. The cannulae were sterilised with ethanol and flushed with 9% saline before attaching to the pump

The ALZET[®] pumps are known to have a “start-up gradient” during which they regulate to body temperature, this may alter the infusion rate of the pump. To overcome this, pumps are “primed” prior to implantation. This is achieved by placing the pump in 9% saline at 37°C for a period of 4-6 hours. During priming it is important to keep the end of the cannula out of the saline to prevent mixing of the saline with the Et-1.

The levels of Et-1 used in the current study are consistent with previous published reports which document a significant increase in blood pressure⁵²⁸, through chronic receptor activation.

B.2.2.2 MINI-OSMOTIC PUMP IMPLANTATION

Four male Sprague Dawley rats were anaesthetised with forthane inhalation anaesthetic and unconsciousness confirmed by a lack of reflex response of the hind and forelimbs. Throughout the surgical procedure unconsciousness was maintained through the delivery of anaesthetic via a nose cone. All procedures were performed using a sterile technique and instruments.

Rats were placed in a supine position on a warmed 37°C surgical table facing away from the surgeon. The neck was shaved from the midline to 1cm beyond the jugular groove and cleaned with 70% ethanol swabs. Using sharp, curved scissors a 2cm

incision was made in the neck to the left of the midline penetrating the skin only. The main jugular vein was then isolated via blunt dissection. Blunt dissection was continued laterally to create a 7mm × 16mm pouch to house the mini-pump.

Two lengths of 4.0 suture were placed underneath the jugular – the first 2cm caudally and the other loosely positioned around the external jugular vein. The sutures were held tautly in place with haemostats. A 21-gauge needle was used to puncture the jugular vein providing an opening for insertion of the cannula. The cannula was advanced through the jugular vein 2cm caudally. Each of the sutures were tied with triplicate box knots; the caudally positioned suture was tied around the cannula to secure it in place and the second suture tied around the vein to secure the cannula and pump. The mini-osmotic pump was then placed in the subcutaneous pouch and the incision site closed with 3-4 sutures.

Sham rats ($n = 4$) underwent the same surgical procedure, however no Et-1 filled pump was inserted. Rather the jugular vein was tied off with 2 sutures.

Ibuprofen (15mg/kg; Nurofen, Australia) was administered post-operatively for pain management. Following surgery, and for the duration of the protocol, the rats were monitored twice daily and all notes recorded in clinical record sheets.

B.2.2.3 BLOOD PRESSURE MEASUREMENT

Blood pressure was recorded using a Non-invasive Blood Pressure (NIBP) Controller tail cuff (ADInstruments Pty Ltd., Australia). Blood pressure recordings were

documented on a computer (mini-Mac, Apple Inc.) utilising the Powerlab[®] Chart v5.02 program (ADInstruments Pty Ltd., Australia).

Three consecutive blood pressure measurements were recorded every morning to account for biological diurnal fluctuations. A pre-operative blood pressure reading was recorded prior to osmotic pump implantation. The rat was allowed to recover for 2 days post-operatively before daily blood pressure measurements.

B.2.3 Small Vessel Myograph Assessment of Vascular Reactivity

B.2.3.1 SMALL VESSEL MYOGRAPH BACKGROUND

In 1977 Mulvany and Halpern developed the small vessel wire myograph to allow for *in vitro* assessment of the mechanical and pharmacological properties of small vessels in a controlled environment⁵²⁹. The myograph technique allows small vessels to be mounted as a ring preparation and attached to two fixed wires to provide accurate measurements of vessel reactivity.

A 2mm length of vessel is dissected and two stainless steel wires (40µm diameter) are inserted through the vessel lumen, care being taken not to damage the delicate endothelial lining. One of these wires is then connected to a force transducer to measure the tension of the vessel and the other connected to a micrometer, which may be used to manually stretch and relax the vessel if required (Figure 1):

NOTE:

This figure is included on page 73 of the print copy of the thesis held in the University of Adelaide Library.

Figure 1: The established set-up of a Mulvany wire myograph as utilised for microvessel mechanical and pharmacological assessment.

Modified from http://www.dmt.dk/files/610m_setup.jpg.

The small vessel Mulvany wire myograph (Multi Myograph model 610M, Danish Myo Technology) consists of four independent 6ml chambers, each with a force transducer capable of detecting 0.01mN – 1N changes in vessel tension. Transducer recordings were documented on a computer (iMac, Apple Inc.) utilising the Powerlab[®] Chart v5.02 program (ADInstruments Pty Ltd., Australia).

B.2.3.2 TISSUE HANDLING AND DISSECTION

To prevent RNA and protein degradation, which may compromise tissue reactivity, immediately following dissection tissue samples were placed in ice cold Krebs solution at 4°C. Dissection of individual arterioles was conducted in Krebs solution on a bed of ice and bubbled with carbogen to maintain a pH of 7.34. Using a dissecting microscope 2mm segments of vessels were dissected free from the surrounding tissue and all traces of adventitia carefully removed.

For rat mesenteric arterioles a midline laparotomy was performed and ~10cm of proximal intestine, with mesentery and feeding vasculature to level of superior mesenteric artery, was removed. The specimen was mounted in a Silguard-based

petri dish and adjacent segments of 3rd order mesenteric vessels, 2mm in length, dissected for mounting.

For aortic vessels the thoracic aorta was removed and mounted in a Silguard-based petri dish and the surrounding layer of connective tissue removed. Rings of aorta, 2mm in length, were carefully dissected and washed repeatedly in clean Krebs to remove all traces of blood from the lumen.

For human subcutaneous arterioles a technique pioneered by Aalkjaer⁵³⁰ and modified by Hadoke¹⁴¹ was adopted. A subcutaneous tissue sample (2 (length) × 1(width) × 1(depth) cm) was obtained from the lower abdominal wall of patients undergoing routine surgical procedures involving an incision in the inguinal region or anterior abdomen. The procedure had no additional risk or cosmetic implications and was performed by the patient's surgeon. Small arteries were identified by distinct physical characteristics; arteries have a smooth adventitial surface, maintain their shape when removed from physiological salt solution and the vessel wall is sufficiently transparent to allow distinction between the media and lumen. Vessels were dissected free from the surrounding tissue and divided into 2mm segments for mounting.

B.2.3.3 VESSEL MOUNTING

The isolated 2mm mesenteric vessel segments were mounted in the myograph using two stainless steel wires (40µm diameter). The wires were inserted while the isolated vessel segment was continuously bathed in carbogen-gassed Krebs solution thereby

optimising tissue viability. The 2mm lengths of aorta were mounted directly onto the large myograph pins. Once the vessels were mounted the myograph bath was slowly warmed to 37°C over a 30 minute period before commencing the vasomotor studies.

B.2.4 Standardisation of Vascular Responses

B.2.4.1 VESSEL CALIBRE NORMALISATION

Prior to the commencement of any *in vitro* vessel experiment it is necessary to normalise the internal diameter of the vessels to ensure an initial equivalent tension. This ensures that appropriate comparisons are made between vessels that may not be identical in diameter. This normalisation procedure was first devised in 1977⁵²⁹ and is still the standard for wire myograph experiments.

The conventional conditions for lumen diameter calculation are based on an intravascular pressure equivalent to *in vivo* resting tension. While the pressure myograph can calculate accurate pressure values the wire myograph is not equipped for such measurements and as such they must be mathematically derived. This is achieved by calculating the point of intersection of the 100mmHg isobar using each individual vessels unique length-tension curve (for further details see Section B.2.4.2).

As mentioned earlier, *in vitro* vessel tension is measured directly via the wire connected to the force transducer with the following equations⁵²⁹. The vessel radius can be determined by measuring the internal circumference; if the wires have a

diameter 'w' and are separated from each other by 's' then the internal circumference 'c' of the vessel is shown by:

$$c = ((2 + \pi)(w)) + 2s$$

From this the internal diameter (ID) can be calculated as:

$$ID = c/\pi$$

With 'l' representing vessel length and 'f' force, then wall force per unit length is the passive wall tension (t) which is given as follows:

$$t = f/2l$$

By distending the vessel in a stepwise fashion, corresponding wall tension and vessel diameter (d) values are acquired. These data can be modeled to:

$$t = A \times \text{Exp}(B \times d)$$

where A and B are constants. As can be seen, the equation describes an exponential (Exp) curve. The constants can be derived by taking the logarithm of both sides of the equation and using linear regression.

The corresponding pressure (p) at any point on the passive diameter-tension curve can be calculated using the Laplace equation:

$$p = (2\pi t)/c$$

B.2.4.2 NORMALISATION FOR DEPolarisation RESPONSE

Vessels are normalised using the Danish Myo Technology (DMT) Normalisation program (AD Instruments Chart Module Series, Powerlab[®] System, Australia) whereby the vessels are progressively stretched in 3mN increments until a pressure

of 100mmHg is obtained with an exponential curve fitted to the tension/radius data. The point at which this length-tension curve intersects the 100mmHg isobar corresponds to the vessel circumference and is denoted as IC₁₀₀. The internal circumference is then set to 90% of this value which represents the optimum point of resting tension⁵³¹⁻⁵³³.

Once the tension of the vessels has been set and integrity of the vessels confirmed, vessel-drug interactions can be investigated with accurate comparisons made between vessel segments.

B.2.4.3 DEPolarising WITH POTASSIUM

Following vessel size normalisation there is a 30 minute equilibration period after which the experiment may begin. The standardised start procedure involves depolarising the vessels with 112mM potassium physiological salt solution (KPSS). The purpose of this KPSS exposure is to:

- Ensure vessel integrity
- Reactivate the mechanical and functional properties of the vessel which may have decreased during the dissecting, mounting and normalising stages
- Generate a standard contractile value to which subsequent responses may be expressed

This KPSS stimulation/washout procedure is repetitively analysed until reproducible results are obtained. An average of the final two stimulations is utilised for standardising subsequent responses.

B.2.5 Endothelial Integrity

Since the endothelium has a large influence on vasomotor responses endothelial integrity was assessed at the beginning of all experiments. This not only provides information on the native integrity of the endothelium but also indicates if it has been damaged during experimental preparation. Endothelial integrity was assessed using incremental doses of acetylcholine (ACh, 0.01 - 3 μ M) in rat vessels precontracted with phenylephrine (PE, EC₇₅ concentration), using a well-established protocol.

In human microvessels (<400 μ m) ACh has been shown to be an ineffective stimulus to assess the endothelial integrity of vessels¹⁴¹. For this reason bradykinin (BK, 0.001- 3 μ M) was utilised as the stimulus in these vessels. If the vessels relax by 80% or more then endothelial integrity is determined to be intact and the vessels included. If, however, the vessels fail to relax to the bradykinin they are discarded.

For the endothelium-denuded studies the endothelium was removed using the accepted method of gently rubbing the interior of the lumen with a thin piece of mounting wire. The loss of endothelial integrity was then confirmed by a lack of relaxation to ACh.

B.2.6 Study Reagents

The physiologic saline solution for all myograph experiments was Krebs which was continuously gassed with carbogen (95% O₂, 5% CO₂). The composition of the Krebs solution included (mM): NaCl (118), KH₂PO₄ (1.18), NaHCO₃ (25), 10% MgCl₂ (1.05), 40% CaCl₂ (2.34), 3.7mg/mL Na₂EDTA (0.01) and glucose (5.56), ph 7.4.

High potassium solution, potassium physiological salt solution (KPSS), was made by replacing the NaCl in Krebs with iso-osmolar KCl. Fresh Krebs was made daily with KPSS made fresh every second day.

B.2.6.1 VASOCONSTRICTORS

The vasoconstrictor agonists used in this study were:

- | | | |
|----|--------------------------|--------------------|
| 1) | Phenylephrine (PE) | 0.01 - 100 μ M |
| 2) | Endothelin-1 (Et-1) | 0.01 – 30nM |
| 3) | KPSS | 112mM |
| 4) | Potassium Chloride (KCl) | 87mM |

B.2.6.2 VASODILATORS

The endothelium-dependent vasodilator agonists used in this current study were:

- | | | |
|----|---------------------|-------------------|
| 1) | Acetylcholine (ACh) | 0.01 - 3 μ M |
| 2) | Bradykinin (BK) | 0.001 - 3 μ M |

B.2.6.3 Ca⁺⁺ CHANNEL BLOCKERS

The Ca⁺⁺ channel antagonists used in this study were:

- | | | |
|----|---------------------------|---------------|
| 1) | Verapamil | 1 μ M |
| 2) | Nifedipine | 1 μ M |
| 3) | Efonidipine Hydrochloride | 0.021 μ M |
| 4) | Mibefradil | 1 μ M |

Stock concentrations of each of the vasoconstrictors and vasodilators were prepared in double distilled water at a concentration of 100mM with the exception of Et-1 which was prepared in 180mM acetic acid at a concentration of 200µM. Sequential dilutions required for the concentration-response curves were prepared in double distilled water from the 100mM (or 200µM) stock. Sequential concentration stocks were stored at -20°C as 1mL aliquots and thawed as required.

The therapeutic plasma concentrations of each Ca⁺⁺ channel antagonists were used⁵³⁴⁻⁵³⁷. Verapamil and nifedipine are light sensitive and as such were appropriately shielded with aluminium foil during storage and the experimental procedure. A 1M stock concentration of efonidipine was prepared in dimethyl sulfoxide with dilution down to the working concentration made in double distilled water. A 1M stock solution of nifedipine was prepared in acetone with dilution down to the working concentration in double distilled water. Stocks (1M) of verapamil and mibefradil were prepared in double distilled water and diluted down to working concentration in double distilled water. All antagonist stocks were stored at -20°C as 1mL aliquots and thawed as required.

B.2.7 Data Analysis

B.2.7.1 CONCENTRATION-RESPONSE CURVE CHARACTERISTICS

Each vessel responses to 112mM KPSS were repetitively analysed until reproducible responses were obtained. A mean of the final two KPSS responses were then used as a reference value for all following contractile responses. Each vessel's responses were expressed as a percentage of their own averaged KPSS depolarising stimuli.

This acts to standardise individual vessel responses relative to a fixed contractile event. This also controls for any differences in contractility between individual vessel segments due to slight variances in vessel size.

Each Et-1 concentration-response curve was performed in separate vessel segments due to the possibility of tachyphylaxis, which has been noted with Et-1 contractions⁵³⁸. By performing these concentration-response curves in separate vessel segments, rather than consecutively in the same segment, we were able to obtain comparable responses between vessel segments with sustained Et-1 contractions and no evidence of spontaneous rundown (tachyphylaxis).

For all experiments a pre-incubation approach was used. Vessel segments were incubated with the appropriate concentration of the CCB or control for a period of 30 minutes. Following the CCB incubation concentration-response curves were performed for Et-1 or the vessels were depolarised with 87mM KCl. The decreased contraction seen in the treated vessels reflects the vessels inability to contract to the same extent as seen in control conditions.

All data were analysed and statistics performed using GraphPad Prism[®] v5.02. Data were fitted to the Hill equation with variable slopes by using Prism[®] with EC₅₀ and E_{max} values determined from the fit. The concentration required to produce a 50% maximal contraction or relaxation response is referred to as the EC₅₀ and is expressed as a log molar concentration; EC₅₀ values were determined with the following equation: $Y = \text{Minimum} + (\text{Maximum} - \text{Minimum}) / (1 + (X/EC_{50})^{\text{Hill coefficient}})$

where Y is the observed value, Minimum is the lowest observed value, maximum is the highest observed value, X is the logarithm of the concentration and the Hill coefficient provides the largest absolute value of the slope of the curve. With vasoconstrictor responses (Et-1) the E_{max} refers to the maximal level of contraction obtained. With the vasodilator responses (ACh and BK), however, the E_{max} value represents a percent relaxation of the vessels from a steady state pre-contractile response. Peak KCl contraction refers to the sharp depolarisation peak following KCl administration. These E_{max} , EC_{50} and peak KCl values were used to make comparisons between vessel segments.

B.2.7.2 STATISTICAL ANALYSIS

Comparisons between treatments were made for E_{max} , EC_{50} or peak KCl values for different agents as appropriate. Normal distribution of the data was validated using Prism[®] with $p > 0.10$ for each data set. Due to a normal distribution the data are expressed as mean \pm standard error of the mean (SEM). Where appropriate, comparisons between agents were performed using analysis of variance (ANOVA) with a Bonferroni's post-hoc test with $p < 0.05$ representing statistical significance. All blood pressure measurements however were analysed using Student's t-test with $p < 0.05$ representing statistical significance. n refers to the number of experiments taken from individual rats.

B.2.8 Study Protocol

The protocols for the individual sub-studies differed slightly as outlined below:

- (1) To ascertain the dose-range effects of the CCBs on rat mesenteric microvessels, each of the CCBs were assessed at either their therapeutic concentration, one log unit higher or one log unit lower than an Et-1 concentration-response curve performed. These experiments were designed to demonstrate the use of CCBs at near maximal concentrations.
- (2) To examine the effects of the CCBs on vessel constriction a pre-incubation method was followed. This involves the therapeutic plasma concentration of the Ca⁺⁺ channel antagonist (or the vehicle of the Ca⁺⁺ channel antagonist) being incubated with the vascular segments for 30 minutes followed by an Et-1 concentration-response curve. To determine the effect of the Ca⁺⁺ channel antagonists on depolarisation-mediated contraction, a KCl depolarisation post-incubation was also performed. Comparisons could then be made between the control and experimental baths for vessel reactivity to Et-1 and KCl.
- (3) A third sub-study was designed to determine any additional effects of efonidipine in the presence of maximal L-channel blockade. Rat mesenteric microvessels were incubated with verapamil or nifedipine (both 10µM) with efonidipine (0.21µM) for 30 minutes and an Et-1 concentration-response curve performed.
- (4) The effects of the CCBs were also examined in the presence of chronic Et-1 receptor activation. An osmotic mini-pump was inserted into the jugular vein and rats infused with 10ng/kg/min Et-1 for a period of 7 days. Rats were then sacrificed and mesenteric microvessels and aortic segments incubated with the therapeutic plasma concentration of either

efonidipine, verapamil or efonidipine and verapamil for 30 minutes followed by an Et-1 concentration-response curve.

- (5) To confirm if this divergent response is also present in human subcutaneous vessels, samples were obtained from patients undergoing elective non-cardiac surgery. As with the rat aortic and mesenteric vessels, segments were incubated with the CCB for 30 minutes followed by an Et-1 concentration-response curve.

New sets of vessels were used for each Ca⁺⁺ channel antagonist to avoid the possibility of residual effects of previous Ca⁺⁺ channel antagonists.

B.3 RESULTS

B.3.1 Ca⁺⁺ Channel Blocker Dose Ranging Study

As shown in Figure 2, incubation with the therapeutically-equivalent L-channel blocker concentrations produced a similar level of inhibition of the Et-1 contractile responses to those one log unit higher. This demonstrated that the therapeutic concentration produced near maximal effects (E_{max} : verapamil [1 μ M] = 82 \pm 6%, [10 μ M] = 72 \pm 3%, $p > 0.05$; nifedipine [1 μ M] = 76 \pm 3%, [10 μ M] = 67 \pm 2%, $p > 0.05$). Similarly for the combined L- and T-channel CCBs the therapeutic plasma concentrations utilised were also near maximal (E_{max} : efonidipine [0.021 μ M] = 45 \pm 2%, [0.21 μ M] = 41 \pm 4%, $p > 0.05$; mibefradil [1 μ M] = 36 \pm 4%, [10 μ M] = 29 \pm 2%, $p > 0.05$). Furthermore, there were no significant differences in the Et-1 EC_{50} s across the CCB concentration ranges for any of the CCBs. Several CCB concentration-response curves ($n = 2$) were also performed at two-fold greater log concentrations to the therapeutic concentrations, with the results identical to the one log unit greater

concentrations (data not shown). Hence comparisons between the L-channel blockers (verapamil and nifedipine) and the combined L- and T-channel blockers (efonidipine and mibefradil), at their respective therapeutic-equivalent concentrations used in this study are both therapeutically and pharmacodynamically appropriate.

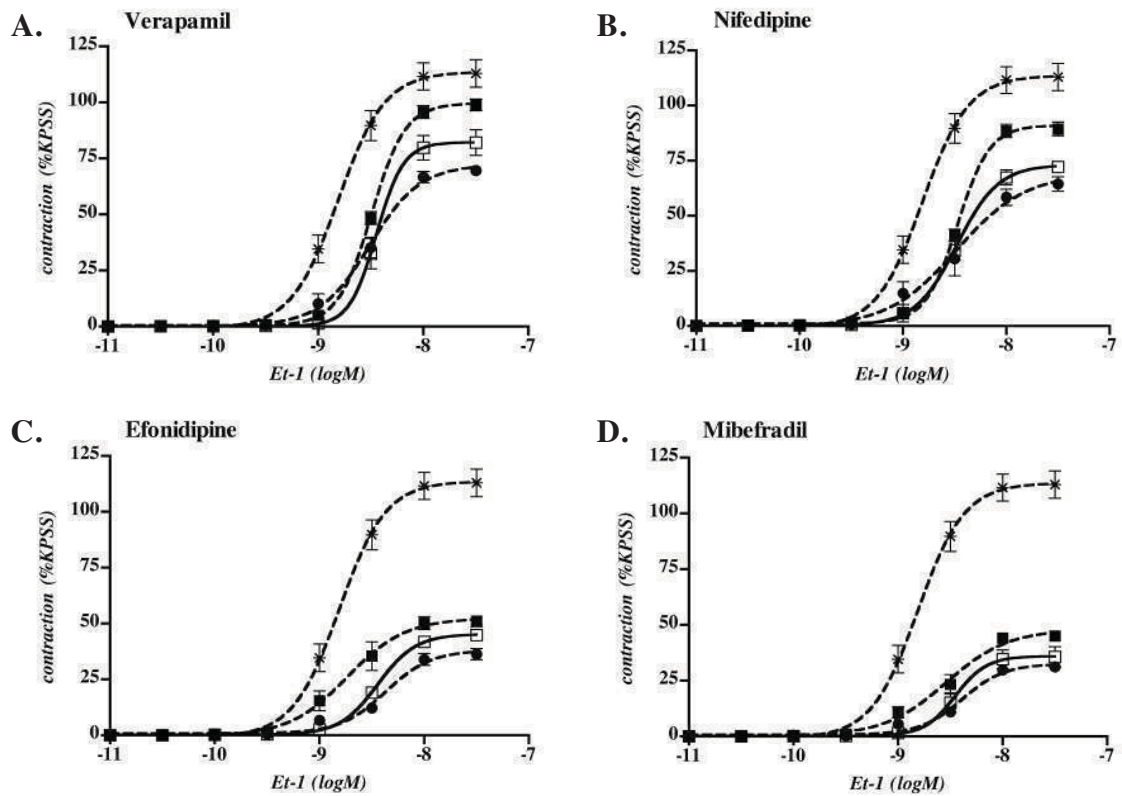


Figure 2: CCB dose-ranging study. Inhibition of individual Et-1 concentration-response curves by (A) verapamil, (B) nifedipine, (C) efonidipine, and (D) mibefradil, following 30 minutes pre-incubation at their respective therapeutic plasma concentrations (□), one log unit below (■) and above (●) this concentration or control (*), for rat mesenteric microvessels ($n = 5$ per CCB per concentration).

B.3.2 Inhibition of Rat Constrictor Responses by Ca⁺⁺ Channel Blockers at Therapeutic-Equivalent Concentrations

B.3.2.1 ENDOTHELIN-1-MEDIATED CONSTRICTION

B.3.2.1.1 Rat Microvascular Responses

Endothelium Intact

Rat mesenteric microvessels had a mean diameter of $304 \pm 7\mu\text{m}$ and intact endothelium-dependent vasodilator responses with a mean maximal ACh relaxation of $87 \pm 2\%$ ($n = 6$). Pre-treatment with verapamil, nifedipine, efonidipine or mibefradil inhibited Et-1 contractile responses (E_{max} : $82 \pm 6\%^*$, $76 \pm 3\%^*$, $45 \pm 2\%^{**}$ and $36 \pm 4\%^{**}$ respectively, $*p < 0.05$ vs. control, $**p < 0.05$ vs. L-channel blockade; see Figure 3 and 4). As summarised in Table 1, the combined L- and T-channel blockers (efonidipine and mibefradil) inhibited Et-1 contractile responses nearly twice as effectively as the L-channel blockers (verapamil and nifedipine) in these microvessels.

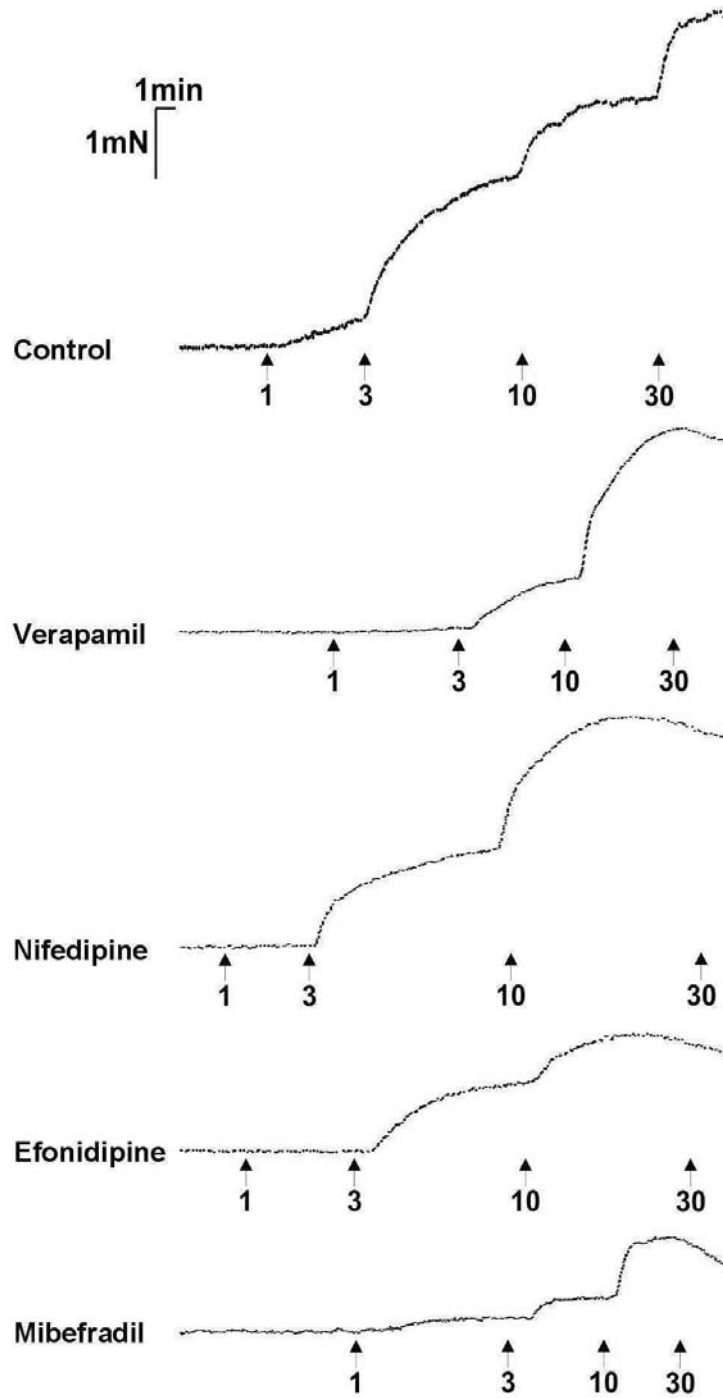


Figure 3: Et-1-mediated developed tension in rat mesenteric vessels in the presence of CCBs. A. Representative trace of concentration-response curves to Et-1 following 30 minute incubation with verapamil ($1\mu\text{M}$), nifedipine ($1\mu\text{M}$), efonidipine ($0.021\mu\text{M}$), mibefradil ($1\mu\text{M}$), or control.

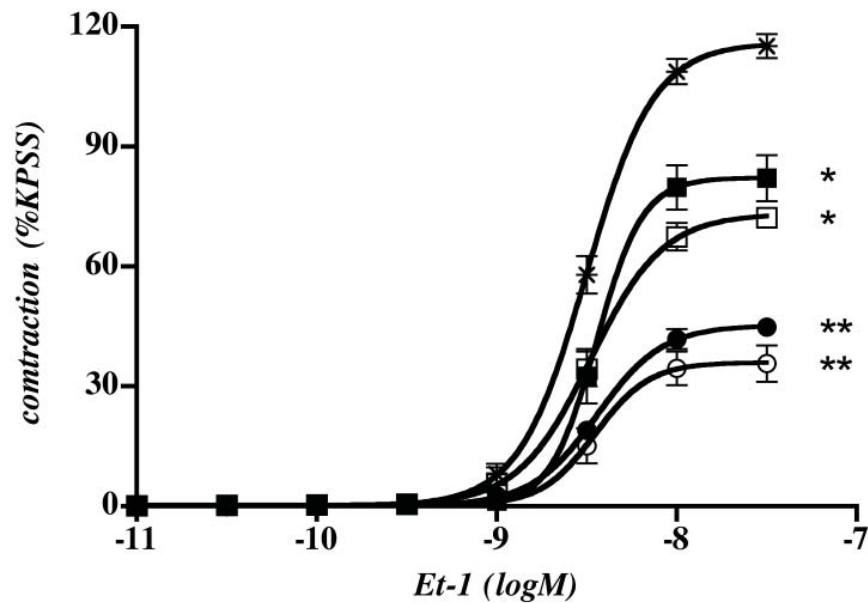


Figure 4: Et-1-mediated developed tension in rat mesenteric vessels in the presence of CCBs. Concentration-response curves to Et-1 following 30 minute incubation with verapamil ($1\mu\text{M}$, ■), nifedipine ($1\mu\text{M}$, □), efonidipine ($0.021\mu\text{M}$, ●), mibefradil ($1\mu\text{M}$, ○), or control (*). There was a significant inhibition of the Et-1 E_{max} by each of the CCBs. However, the combined L- and T-channel blockers produced greater inhibition than the L-channel blockers (* $p < 0.05$ vs. control, ** $p < 0.05$ vs. L-channel blockade, $n = 6$).

Endothelium Denuded

In 6 rats the endothelium was denuded from mesenteric microvessels (mean vessel diameter = $314 \pm 13\mu\text{m}$) and impaired endothelium-dependent vasodilatory responses confirmed with ACh. Pre-treatment with verapamil, nifedipine, efonidipine or mibefradil in these endothelium-denuded vessels, inhibited Et-1 contractile responses (E_{max} : $88 \pm 4\%^*$, $83 \pm 5\%^*$, $47 \pm 1\%^{**}$ and $45 \pm 3\%^{**}$ respectively, * $p < 0.05$ vs. control, ** $p < 0.05$ vs. L-channel blockade; see Figure 5). As shown in Figure 4 the combined L- and T-channel blockers (efonidipine and mibefradil) again inhibited Et-1 contractile responses almost twice as effectively as the L-channel blockers (verapamil and nifedipine) in these microvessels. Thus the divergent

responses between the combined L- and T-channel and the L-channel blockers in these microvessels are independent of endothelial function.

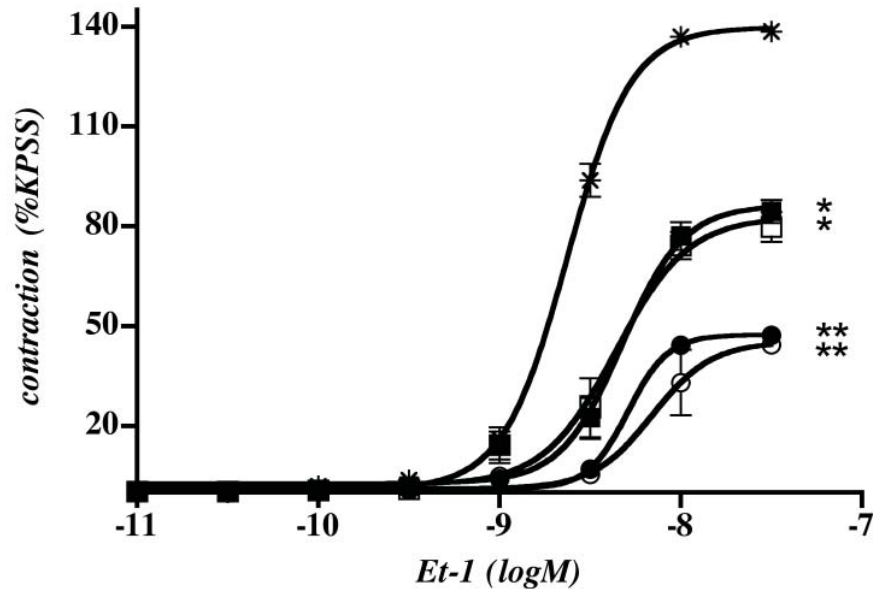


Figure 5: Et-1-mediated developed tension in rat mesenteric vessels in the presence of CCBs. Concentration-response curves to Et-1 following 30 minute incubation with verapamil (1 μ M, ■), nifedipine (1 μ M, □), efonidipine (0.021 μ M, ●), mibefradil (1 μ M, ○), or control (*). In endothelium-denuded rat mesenteric microvessels, the differential inhibitory effects of the combined L- and T-channel blockers compared with the L-channel blockers remained evident (* p <0.05 vs. control, ** p <0.05 vs. L-channel blockade, n = 6).

B.3.2.1.2 Rat Aortic Vessel Responses

The aortic rings had a mean diameter of $2055 \pm 35\mu\text{m}$ and intact endothelium-dependent vasodilator responses with a mean maximal ACh relaxation of $91 \pm 1\%$ (n = 7). As shown in Figure 6 and Table 1, pre-treatment with verapamil, nifedipine, efonidipine or mibefradil significantly reduced Et-1 contractile responses compared with control (E_{max} : $83 \pm 6\%^*$, $79 \pm 5\%^*$, $96 \pm 3\%^*$, $100 \pm 4\%^*$ vs. control $159 \pm 6\%$, respectively, * p <0.05).

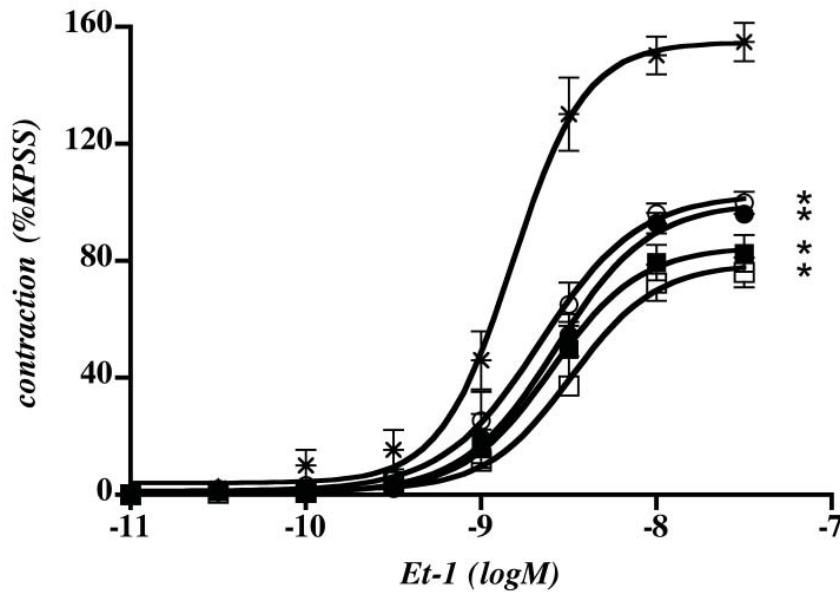


Figure 6: Et-1-mediated developed tension in rat aortic vessels in the presence of CCBs. Concentration-response curves to Et-1 following 30 minute incubation with verapamil (1 μ M, ■), nifedipine (1 μ M, □), efonidipine (0.021 μ M, ●), mibefradil (1 μ M, ○), or control (*). There was a significant inhibition of the Et-1 E_{max} between the control and each of the CCBs, although the extent of inhibition did not differ between the CCBs (* p <0.05 vs. control, n = 7).

As summarised in Table 1, in both rat microvessels and human microvessels (detailed in Section A.3.5) the combined L- and T-channel blockers inhibited Et-1 contractile responses to a greater extent than L-channel blockers.

ΔE_{max} (relative to control)	L-Channel CCB		L- & T-Channel CCB	
	Verapamil	Nifedipine	Mibefradil	Efonidipine
Rat Aorta	-69 \pm 1%	-75 \pm 1%	-68 \pm 9%	-65 \pm 9%
Rat Microvessel	-37 \pm 7%	-43 \pm 9%	-83 \pm 4%*	-77 \pm 7%*
Human Microvessel	-40 \pm 7%	-56 \pm 8%	-92 \pm 9%*	-86 \pm 8%*

Table 1: Change in maximal Et-1 contractile responses by various CCBs. Change in the maximal contractile response to Et-1 (%KPSS) following 30 minute incubation with verapamil (1 μ M), nifedipine (1 μ M), efonidipine (0.021 μ M) or mibefradil (1 μ M) in rat aorta (n = 7), rat mesenteric (n = 6) and human microvessels (n = 6). In rat aorta there was no difference between the CCBs in their maximal Et-1 contractile response changes. However, in both rat microvessels and human microvessels there was a significant reduction in Et-1 E_{max} by the combined L- and T-channel blockers compared with L-channel blockers (* p <0.05 compared with L-channel blockers).

B.3.2.2 HIGH POTASSIUM-MEDIATED DEPOLARISATION

B.3.2.2.1 Rat Microvascular Responses

Pre-treatment with verapamil, nifedipine, efonidipine or mibefradil significantly inhibited peak KCl contractile responses compared to control (KCl: $12 \pm 1\%^*$, $12 \pm 1\%^*$, $2 \pm 1\%^{**}$ and $3 \pm 2\%^{**}$, respectively, $*p < 0.05$ vs. control; $**p < 0.05$ vs. L-channel blockade; see Figure 7). Furthermore, as observed with agonist-mediated responses, the combined L- and T-channel blockers (efonidipine and mibefradil) inhibited KCl contractile responses to a greater extent than L-channel blockade alone (verapamil and nifedipine) in these microvessels.

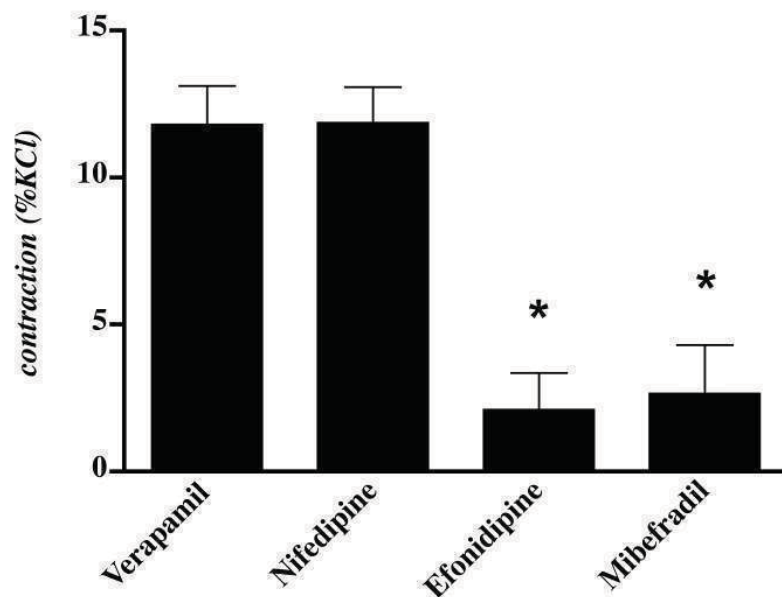


Figure 7: The role of L- and T-channels in depolarisation-mediated extracellular Ca⁺⁺ entry in rat mesenteric vessels. Peak KCl (87mM) contraction following 30 minute incubation with verapamil (1 μ M), nifedipine (1 μ M), efonidipine (0.021 μ M), mibefradil (1 μ M) or control. All CCBs significantly inhibited KCl contractile responses. Moreover, the combined L- and T-channel blockers (efonidipine and mibefradil) inhibited KCl responses more effectively than the L-channel blockers ($*p < 0.05$ L- and T-channel blockers vs. L-channel blockade alone, $n = 4$).

B.3.2.2.2 Rat Aortic Vessel Responses

As shown in Figure 8, pre-treatment with verapamil, nifedipine, efonidipine or mibefradil significantly reduced the peak KCl contractile responses compared to control (KCl: $20 \pm 1\%^*$, $20 \pm 2\%^*$, $17 \pm 2\%^*$, $18 \pm 1\%^*$, respectively, $*p < 0.05$). However, there was no difference between the CCBs regarding the extent of inhibition of contraction.

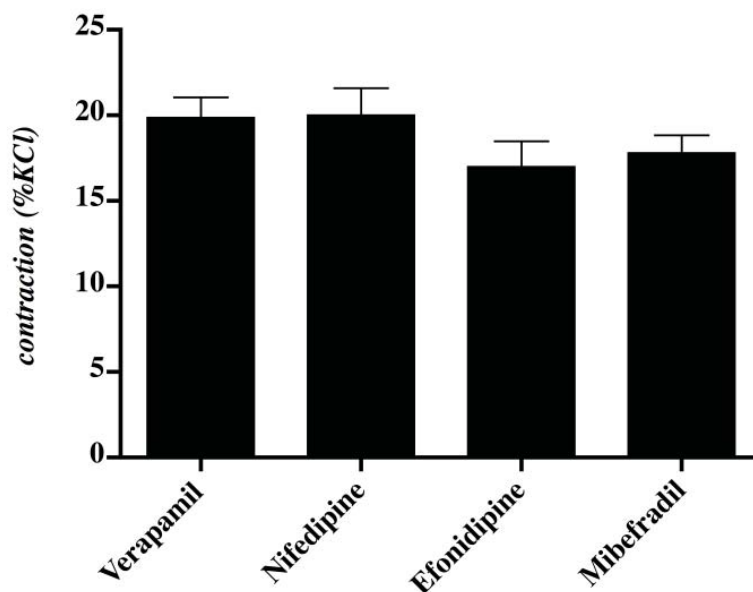


Figure 8: The role of L- and T-channels in depolarisation-mediated extracellular Ca⁺⁺ entry in rat aortic vessels. Peak KCl (87mM) contraction following 30 minute incubation with verapamil (1 μ M), nifedipine (1 μ M), efonidipine (0.021 μ M), mibefradil (1 μ M) or control. There was a significant inhibition of the peak KCl response between the control and individual CCBs but no difference between the CCBs ($n = 4$).

B.3.3 Inhibitory Effect of Efonidipine in Rat Microvessels with Maximal L-Channel Blockade.

Rat mesenteric vessels were treated with maximal L-channel blockade (either verapamil or nifedipine at 10 μ M) and efonidipine to ascertain if there was incremental inhibition of the constrictor response in the presence of the combined L- and T-channel blocker. Despite maximal L-channel blockade, efonidipine produced

incremental inhibition of Et-1 constrictor responses suggesting that mechanisms other than L-channel blockade were involved (E_{max} : verapamil alone = $-70 \pm 2\%^*$, verapamil with efonidipine = $38 \pm 4\%^{**}$, nifedipine alone = $66 \pm 2\%^*$, nifedipine with efonidipine = $36 \pm 4\%^{**}$, $*p < 0.05$ vs. control, $**p < 0.05$ vs. L-channel blockade, $n = 5$) (Figure 9).

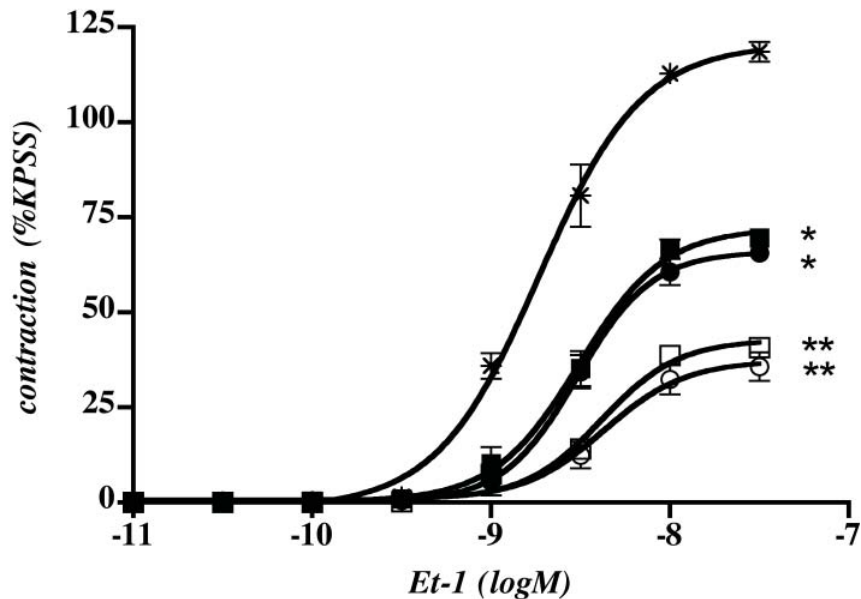


Figure 9: In the presence of maximal L-channel blockade efonidipine reduces developed tension in rat mesenteric vessels. Concentration-response curves to Et-1 in the presence of verapamil (10µM, ■), verapamil (10µM)/efonidipine (0.21µM) (□), nifedipine (10µM, ●), nifedipine (10µM)/efonidipine (0.21µM) (○) or control (*). Following incubation with the maximal verapamil or nifedipine concentration there was a significant inhibition of the Et-1 E_{max} compared to control. In the presence of maximal verapamil or nifedipine concentration with efonidipine there was a further significant inhibition of Et-1-mediated developed tension ($*p < 0.05$ vs. control, $**p < 0.05$ vs. verapamil or nifedipine alone, $n = 5$).

B.3.4 Inhibition of Rat Constrictor Responses by Ca⁺⁺ Channel Blockers at Therapeutic-Equivalent Concentrations in the Presence of Chronic Et-1 Receptor Activation

B.3.4.1 SHAM AND ET-1 RAT BLOOD PRESSURE DURING CHRONIC ET-1 TREATMENT

Following chronic Et-1 receptor activation, with a 7 day Et-1 infusion, there was a significant increase in mean systolic blood pressure from the pre-operative day 0 measurement of 157 ± 1 mmHg to 172 ± 0.5 mmHg* on day 7 of the protocol (* $p < 0.05$, $n = 4$ per group, see Figure 10). The mean systolic blood pressure of the sham surgery rats however remained the same for the duration of the study.

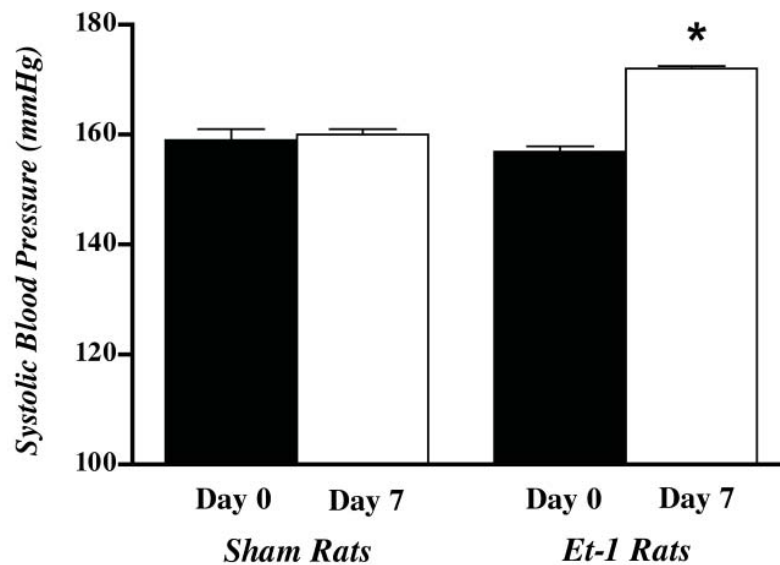


Figure 10: Pre-operative and day 7 mean systolic blood pressure in both sham and Et-1 rats. Following treatment with Et-1 for 7 days there was a significant increase in mean systolic blood pressure from the commencement of the protocol (Day 0) to completion (Day 7) in the Et-1 rats ($n = 4$). In the sham rats ($n = 4$) however, blood pressure remained unchanged throughout the study (* $p < 0.05$ compared to Day 0 Et-1 rats).

B.3.4.2 RAT MICROVASCULAR RESPONSES IN THE PRESENCE OF
CHRONIC ET-1

Sham rat mesenteric microvessels had a mean diameter of $311 \pm 10\mu\text{m}$ and intact endothelium-dependent vasodilator responses with a mean maximal ACh relaxation of $88 \pm 2\%$ ($n = 4$). The Et-1 rat mesenteric microvessels had a mean diameter of $307 \pm 6\mu\text{m}$ and intact endothelium-dependent vasodilator responses with a mean maximal ACh relaxation of $87 \pm 3\%$ ($n = 4$). In both groups pre-treatment with verapamil, efonidipine or efonidipine/verapamil inhibited exogenous Et-1 contractile responses (Sham E_{max} : $69 \pm 2\%^*$, $40 \pm 2\%^{**}$ and $36 \pm 2\%^{**}$ respectively; Et-1 E_{max} : $76 \pm 5\%^*$, $39 \pm 4\%^{**}$ and $39 \pm 2\%^{**}$ respectively; $*p < 0.05$ vs. control, $**p < 0.05$ vs. verapamil; see Figure 11). Furthermore, the Et-1 mesenteric EC_{50} values for the control, verapamil, efonidipine and efonidipine/verapamil vessels were significantly higher than the corresponding sham mesenteric microvessel EC_{50} values (Table 2).

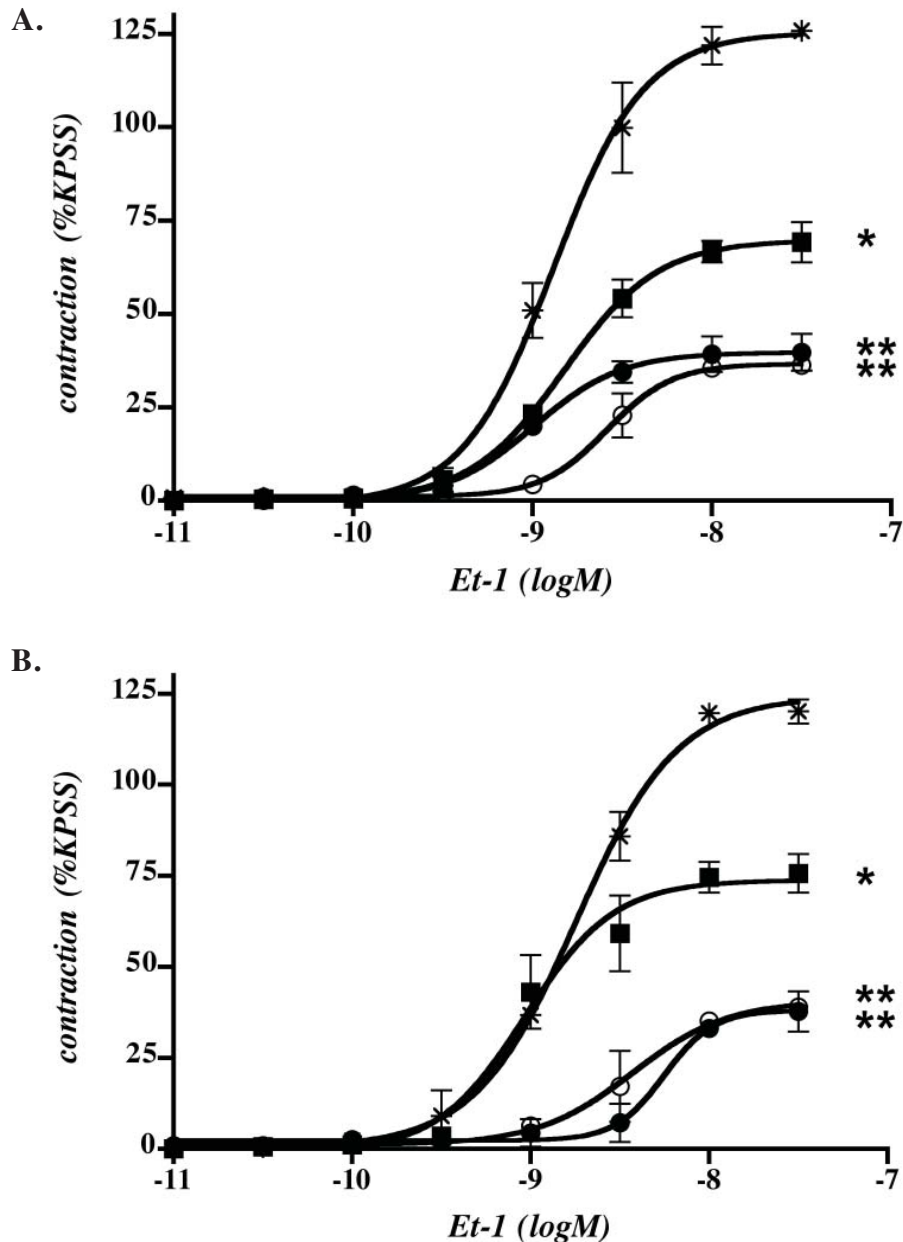


Figure 11: Et-1-mediated developed tension in rat mesenteric vessels in the presence of CCBS following chronic Et-1 receptor activation. Concentration-response curves to Et-1 following 30 minute incubation with verapamil ($1\mu\text{M}$, ■), efonidipine ($0.021\mu\text{M}$, □), efonidipine ($0.021\mu\text{M}$)/verapamil ($1\mu\text{M}$) (○), or control (*) in rat (A) sham and (B) chronic Et-1 vessels. In each group there was a significant inhibition of the Et-1 E_{max} by each of the CCBs. However, the combined L- and T-channel blocker, efonidipine, produced greater inhibition than the L-channel blocker, verapamil. Furthermore, combining efonidipine with verapamil produce no incremental inhibition compared to efonidipine alone (* $p < 0.05$ vs. control, ** $p < 0.05$ vs. verapamil alone, $n = 4$).

B.3.4.3 RAT AORTIC RESPONSES IN THE PRESENCE OF CHRONIC ET-1

Sham rat aortic vessels had a mean diameter of $2015 \pm 30\mu\text{m}$ and intact endothelium-dependent vasodilator responses with a mean maximal ACh relaxation of $89 \pm 2\%$ ($n = 4$). The Et-1 rat aortic microvessels vessels had a mean diameter of $2000 \pm 35\mu\text{m}$ and intact endothelium-dependent vasodilator responses with a mean maximal ACh relaxation of $88 \pm 2\%$ ($n = 4$). In both groups pre-treatment with verapamil, efonidipine or efonidipine/verapamil inhibited exogenous Et-1 contractile responses (Sham E_{max} : $80 \pm 2\%^*$, $80 \pm 2\%^*$ and $70 \pm 1\%^*$ respectively; Et-1 E_{max} : $81 \pm 1\%^*$, $77 \pm 1\%^*$ and $72 \pm 2\%^*$ respectively; $*p < 0.05$ vs. control; see Figure 12). Furthermore, the Et-1 aortic EC_{50} values for the control, verapamil, efonidipine and efonidipine/verapamil vessels were significantly higher than the corresponding sham EC_{50} aortic values (Table 2).

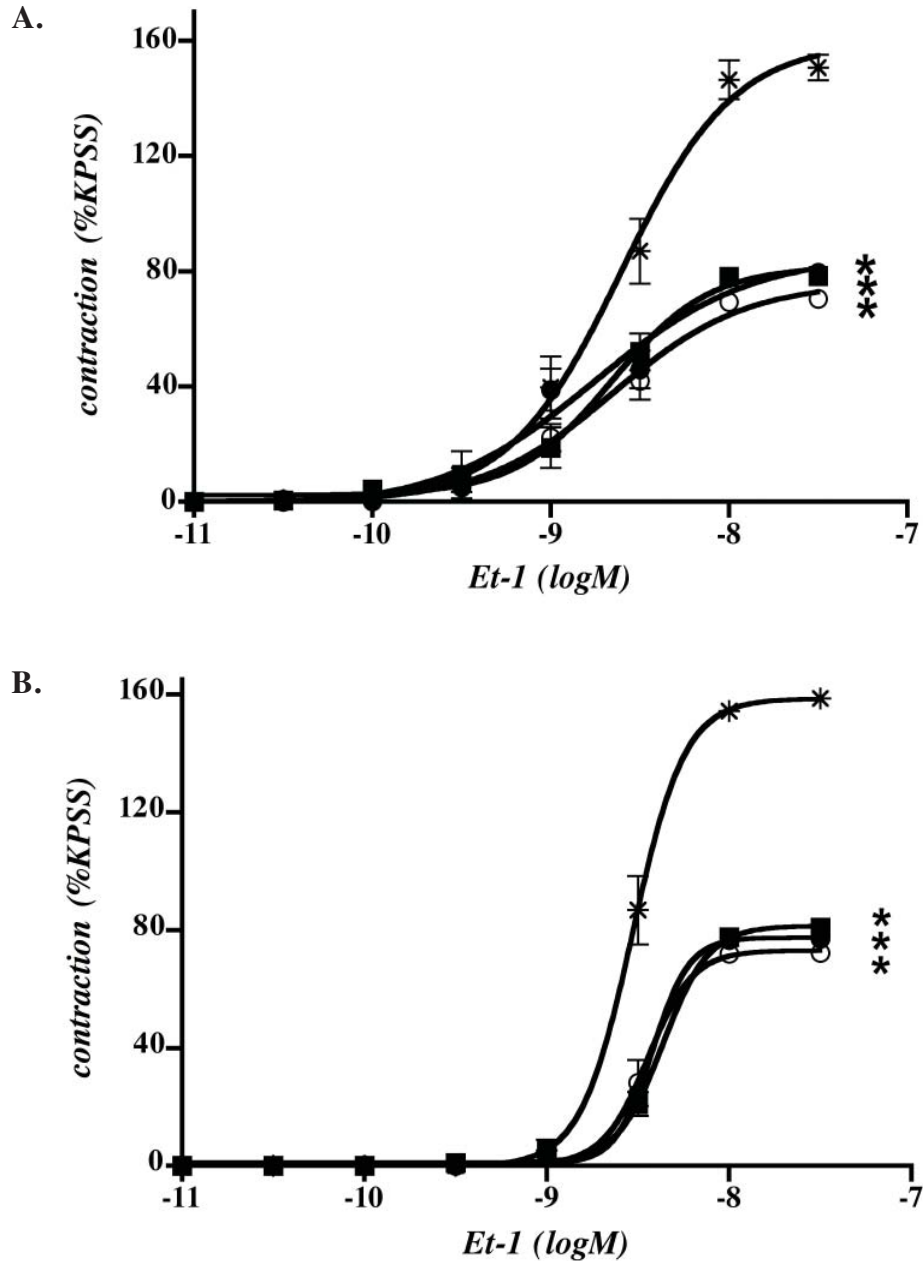


Figure 12: Et-1-mediated developed tension in rat aortic vessels in the presence of CCBs following chronic Et-1 receptor activation. Concentration-response curves to Et-1 following 30 minute incubation with verapamil (1 μ M, ■), efonidipine (0.021 μ M, □), efonidipine (0.021 μ M)/verapamil (1 μ M) (○), or control (*) in rat (A) sham and (B) chronic Et-1 vessels. In each group there was a significant inhibition of the Et-1 E_{max} by the CCBs. Furthermore, combining efonidipine with verapamil produce no incremental inhibition compared to efonidipine alone (* p <0.05 vs. control, ** p <0.05, n = 4).

	Rat Mesenteric		Rat Aorta	
	Sham	Et-1	Sham	Et-1
Control	1.5 (0.6, 3.1)	1.8 (1.6, 2.0)*	2.2 (2.1, 3.7)	3.0 (2.7, 3.2) [#]
Verapamil	1.6 (1.2, 2.4)	3.9 (2.5, 5.3)*	2.4 (1.5, 3.3)	4.4 (3.9, 4.8) [#]
Efonidipine	1.8 (1.5, 2.1)	3.7 (3.5, 5.8)*	2.2 (0.8, 3.5)	3.8 (3.7, 3.8) [#]
E & V	2.6 (1.7, 3.8)	3.5 (3.1, 4.2)*	2.3 (1.2, 4.1)	3.5 (3.1, 3.9) [#]

Table 2: EC₅₀ values in sham and chronic Et-1 rat mesenteric and aortic vessels. In rat mesenteric microvessels chronic Et-1 exposure significantly increased the control, verapamil, efonidipine and efonidipine/verapamil EC₅₀ values to exogenous Et-1 compared to sham mesenteric microvessels (*p<0.05 vs. sham, n = 4). Likewise, in rat aortic vessels chronic Et-1 exposure significantly increased the verapamil, efonidipine and efonidipine/verapamil EC₅₀ values to exogenous Et-1 compared to sham aortic vessels ([#]p<0.05 vs. sham, n = 4). *Note:* Data presented as mean with the range; E & V – efonidipine/verapamil.

B.3.5 Human Subcutaneous Microvascular Responses

Subcutaneous microvessels were obtained during non-cardiac surgery and mounted in the myograph (n = 6). The mean vessel diameter (at resting normalised tension) was 289 ± 14µm and endothelium-dependent vasodilator responses to BK intact in all vessels with a mean maximal BK relaxation of 87 ± 5%. The human microvascular responses to the CCBs were similar to those of the rat microvessels with a greater inhibitory effect on Et-1-mediated contractile responses by the combined L- and T- CCBs compared to L-channel blockade alone (Figure 13).

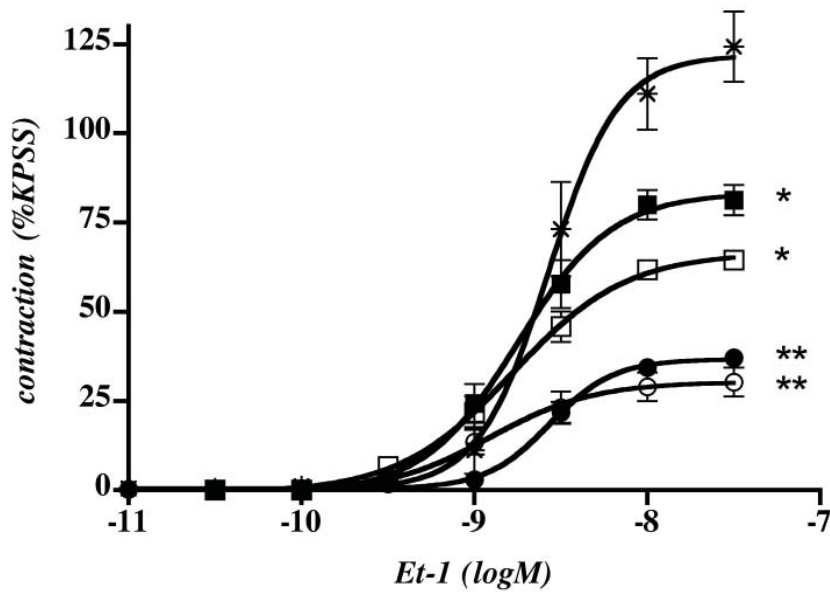


Figure 13: Effectiveness of L- and combined L- and T-channel blockade in human subcutaneous microvessels. Concentration-response curves to Et-1 in human subcutaneous microvessels following 30 minute incubation with verapamil (1 μ M, ■), nifedipine (1 μ M, □), efonidipine (0.021 μ M, ●), mibefradil (1 μ M, ○), or control (*). There was a significant inhibition of the Et-1 E_{max} between the control (123 \pm 8%) and each of the CCBs, verapamil (81 \pm 4%*), nifedipine (66 \pm 1%*), efonidipine (38 \pm 2%**), and mibefradil (30 \pm 4%**), (*p<0.05 vs. control, **p<0.05 vs. L-channel blockade, n = 6).

B.4 DISCUSSION

B.4.1 Heterogeneity in Vascular Responses to L- and Combined L- and T-type Ca⁺⁺ Channel Blockers

The above series of experiments demonstrate segmental heterogeneity in vascular responses between conventional L-channel blockers (verapamil and nifedipine) and the newer combined L- and T-channel blockers (efonidipine and mibefradil). More specifically, in the rat model there were no differences between the CCBs concerning the inhibition of contractile responses in the large aortic vessels. However, in the mesenteric microvessels, the combined L- and T-channel blockers exerted greater inhibition of contractile responses compared to L-channel blockade.

The significance of this observation was further supported by additional experiments:-

- (1) The concentrations of the CCBs were shown to be near maximal for each of the CCBs as well as equivalent to their therapeutic plasma levels (see Figure 2).
- (2) The phenomenon is independent of: (a) the vasoconstrictor stimulus used (i.e. agonist-mediated Et-1 or depolarisation-mediated KCl; Figures 4, 6, 7 and 8); (b) chemical class of CCB (ie. verapamil – phenylalkylamine; nifedipine and efonidipine – dihydropyridine; and mibefradil – benzimidazole); or (c) endothelial function (Figure 5).
- (3) Furthermore, we have shown that maximal L-channel blockade in the presence of efonidipine significantly reduces maximal constriction, compared to L-channel blockade alone, suggesting that efonidipine efficacy involves a mechanism other than L-channel blockade (Figure 9). This is consistent with clinical findings which found that the addition of mibefradil in the presence of the conventional L-channel blocker verapamil depressed microvessel constriction more than L-channel blockade alone³⁸¹.
- (4) In the presence of chronic Et-1 receptor activation, and consequently altered microvascular reactivity, the CCBs were still able to exert their effects (Figures 11 and 12). Specifically, in both sham and Et-1 rats the combined L- and T-channel blocker efonidipine was more effective at decreasing Et-1-mediated constriction than L-channel blockade alone (Figure 11).

- (5) Demonstration of a divergent CCB response in human subcutaneous microvessels (Figure 13).

It is important to note that even in the presence of altered microvascular reactivity, via chronic Et-1 receptor activation, the CCBs were still able to exert their effects. The Et-1 rats were seen to have a significantly elevated systolic blood pressure at the completion of the 7 days treatment period. We do note that the mean pre-operative blood pressure of 159 ± 2 mmHg in these rats was higher than the reported mean systolic blood pressure on 120 mmHg⁵²⁸. Further studies by my colleagues will be exploring the reason for the high baseline blood pressure in these rats. However, the model did demonstrate an increase in blood pressure for the Et-1 rats whereas this did not occur in the sham surgery rats.

Specifically, In the presence of chronic Et-1 receptor activation, via 7 days infusion through the jugular vein, the combined L- and T-channel blocker efonidipine was still able to inhibit maximal Et-1 constriction to a greater extent than the L-channel blocker verapamil in mesenteric microvessels. Furthermore, incubation of vessels with both efonidipine and verapamil provided no additional benefit compared to efonidipine alone (Figure 10). Vessels from rats infused with Et-1 for 7 days did however have an increased Et-1 EC50 compared to the control surgery rats (Table 2), suggesting that this chronic Et-1 exposure reduced vascular sensitivity to exogenous Et-1. Previous studies have demonstrated the binding of Et-1 to the ET-A receptors results in cellular internalisation of the receptor⁵³⁹ which may be a possible explanation for this reduced sensitivity. Once internalised there are two possibilities

for receptors, either then can dissociate from the ligand and move back to the surface⁵⁴⁰, or they can be degraded^{541, 542}. For Et-1, it is an established fact that dissociation of Et-1 from the ET receptors is difficult⁵⁴³. Therefore, if the Et-1 receptor is internalised and degraded then this would explain the increase in EC50 and increased time to reach maximal contraction (which was comparable to the sham surgery rats).

The findings regarding the combined L- and T-channel blockers, efonidipine, maintaining its effects in the presence of an altered physiology holds important therapeutic value. Furthermore, this is consistent with clinical studies demonstrating the benefit of combined L- and T-channel blockers in conditions involving an alteration in microvascular tone, such as hypertension and CSFP. Thus we propose that efonidipine and mibefradil's additional T-channel blockade may explain their differential response in the microvasculature in comparison to the conventional L-channel blockers.

B.4.2 Vascular T-Channel Blockade

Previously the role of vascular T-channels has been controversial. Moosmang *et al.* utilising a conditional L-channel knockout mouse model, showing no gross abnormalities, demonstrated a loss of mibefradil's vasomotor effects. These included impairment of its blood pressure lowering effect and a reduction in its inhibition of vasoconstrictor effects in a hind-limb perfusion model⁵²⁷. Appropriately, these researchers concluded that in their mouse model, mibefradil's vasomotor effects were mediated exclusively via the L-channel. We have pharmacologically

reproduced the inactivation of L-channels using a maximal concentration of the L-channel blockers (Figure 9). Our functional data with human and rat microvessels indicates that L-channel blockade inhibits contractile responses by approximately half. However, the addition of T-channel blockade in these microvessels results in a further 30% reduction in contractile responses. These data support the notion that there are species differences among both rodent models and humans.

Further support for our observations concerning the importance of vascular T-channels can be derived from previous experimental and clinical studies. Firstly, efonidipine^{292, 294} and mibefradil²⁹⁷ inhibit T-channel currents significantly more than the L-channel currents in isolated vascular smooth muscle preparations. In porcine small coronary vessels, mibefradil dilates Et-1-contracted vessels more effectively than in the larger coronary arteries²⁹⁸. Similarly, in rat cremasteric muscle arterioles, mibefradil is more potent than verapamil in inhibiting the myogenic tone of these vessels²⁹⁹. Studies of the glomerular microcirculation have demonstrated L-channels in the afferent but not the efferent arteriole, whereas T-channels are found in both types of glomerular microvessels³⁰⁶. Thus, while L-channel blockers predominantly dilate the afferent arteriole and may produce glomerular hypertension, T-channel blockade does not. This may explain why efonidipine and mibefradil have been shown to reduce proteinuria in hypertensive patients with renal impairment whereas L-channel blockers do not⁵⁴⁴.

Clinical studies of hypertension^{393, 526} and coronary microvascular dysfunction³⁸¹ have also demonstrated the benefits of the combined L- and T-channel blockers. A

randomised, double-blind, placebo controlled, cross-over study clearly demonstrated the anti-hypertensive effects of efonidipine. It also significantly lowered blood pressure and improved endothelial function³⁹³. The L-channel blocker nifedipine increases heart rate by baroreceptor reflexes which is undesirable in patients already suffering from hypertension. In contrast, efonidipine has potent bradycardic action when given in therapeutic doses²⁹⁴.

In the Posicor Reduction of Ischaemia During Exercise (PRIDE) study patients with stable angina were randomised to receive the maximum dose of either 100mg mibefradil or 360mg diltiazem (an L-channel blocker) to compare the anti-anginal effects of both drugs. The primary endpoint of this study was the time to symptom-limited exercise termination (i.e. chest pain onset) in comparison to that at the commencement of the study period 8 weeks earlier. In this study the combined L- and T-channel blocker mibefradil significantly increased both exercise duration and the time to ischaemia. An additional benefit noted with the treatment of mibefradil was a reduction in blood pressure to a greater extent than the L-channel blocker⁵²⁶.

The coronary slow flow phenomenon is a coronary microvascular disorder characterised by the delayed passage of contrast during angiography reflecting the increased downstream resistance⁵⁰⁵. Patients with this disorder on maintenance verapamil therapy, still exhibit the angiographic phenomenon. The addition of mibefradil, however, acutely improves angiographic flow³⁸¹. Furthermore, mibefradil was shown to alleviate the angina associated with this microvascular disorder.

Specifically, mibefradil decreased the number of anginal attacks, the duration of these attacks and the amount of nitrates required for pain management³⁸¹.

B.4.3 Implications

The above findings provide a clear rationale for the use of combined L- and T-channel blockers in microvascular dysfunction. The new generation CCBs which have combined L- and T-channel blocking properties appear to have incremental benefits over the conventional L-channel blockers. As demonstrated in this study, these two CCB groups of agents differ in their pharmacodynamic responses at the small resistance vessel level. Since these resistance vessels play a pivotal role in the regulation of blood pressure and coronary blood flow, additional benefits of the newer agents could be expected in disorders relating to these circulations. Therefore development of specific T-channel blockers has significant therapeutic potential in a clinical setting.

B.5 CONCLUSIONS

In summary, the incremental microcirculatory benefits of the combined L- and T-channel blockers, efonidipine and mibefradil, over the conventional L-channel blockers are possibly due to their additional T-channel blocking abilities. However, further studies are required to define the precise role of the T-channel with the newer CCBs and their role in regulating vascular tone, including its therapeutic application.

SECTION C

Quantitation of L- and T-type Ca⁺⁺ Channels in Large and Small Vessels

C.1 BACKGROUND

An improved understanding of the mechanisms regulating vascular tone may enable advances in the treatment of microvascular disorders. This section aims to quantitate the mRNA and protein abundance of the pore-forming subunits of the Ca⁺⁺ L- and T-channels in large and small blood vessels. Doing so may provide a structural basis for the differential pharmacological response to L- and T-channel blockers documented in Section B.

C.1.1 Ca⁺⁺ Channels

Structurally the L- and T-type Ca⁺⁺ channels are composed of several subunits including a unique α_1 pore-forming subunit, an α_2/δ subunit, a β subunit and a γ subunit (Figure 1).

NOTE:
This figure is included on page 108
of the print copy of the thesis held in
the University of Adelaide Library.

Figure 1: Molecular architecture of the VOCC depicting the α_1 pore-forming, α_2/δ , β and γ subunits. Modified from Hofmann *et al.*1994²³⁹.

The auxiliary subunits (α_2/δ , β and γ) regulate channel gating^{241, 242, 243, 244, 245, 246} whereas the α_1 pore-forming subunit contains the voltage sensor and as such determines the voltage selectivity of the channel expressed²⁴⁰.

The α_2 and δ subunits are linked by a disulfide bond with the δ subunit anchoring the protein in the plasma membrane²⁴². Importantly, the α_2 subunit provides the structural elements required for channel activation²⁴³. The $\alpha_2\delta$ subunit has a role in increasing the density of Ca⁺⁺ channels (activated by high voltage) at the plasma membrane²⁴⁴ with several studies demonstrating a significant increase in the number of functional HVA channels in the presence of $\alpha_2\delta$ ^{545, 546}. The exact mechanism behind this effect is unknown however it is proposed that $\alpha_2\delta$ facilitates proper insertion of the channel protein into the plasma membrane²⁴⁴.

The β subunit regulates current density by controlling the amount of α_1 subunit expressed at the cell membrane. Through its interaction with the α_1 pore the β subunit also regulates activation and inactivation kinetics, and hyperpolarises the voltage-dependent activation of the α_1 pore to allow for smaller depolarisations^{245, 246}.

Finally, the γ subunit is predominantly associated with skeletal muscle VOCCs²⁴⁸ with a primary role in interactions with other membrane proteins²⁴².

To date ten Ca⁺⁺ channel subtypes have been identified and classified (Figure 2). These subtypes can be further divided into three subfamilies (Ca_v1, 2 and 3) based on their amino acid sequence and electrophysiological properties. Three of these

channels have been identified as functionally important in VSM. These include $Ca_v1.2$ (α_{1C} subunit of the L-channel) and $Ca_v3.1$ and 3.2 (α_{1G} and α_{1H} subunits of the T-channel)^{300, 306, 307, 416}.

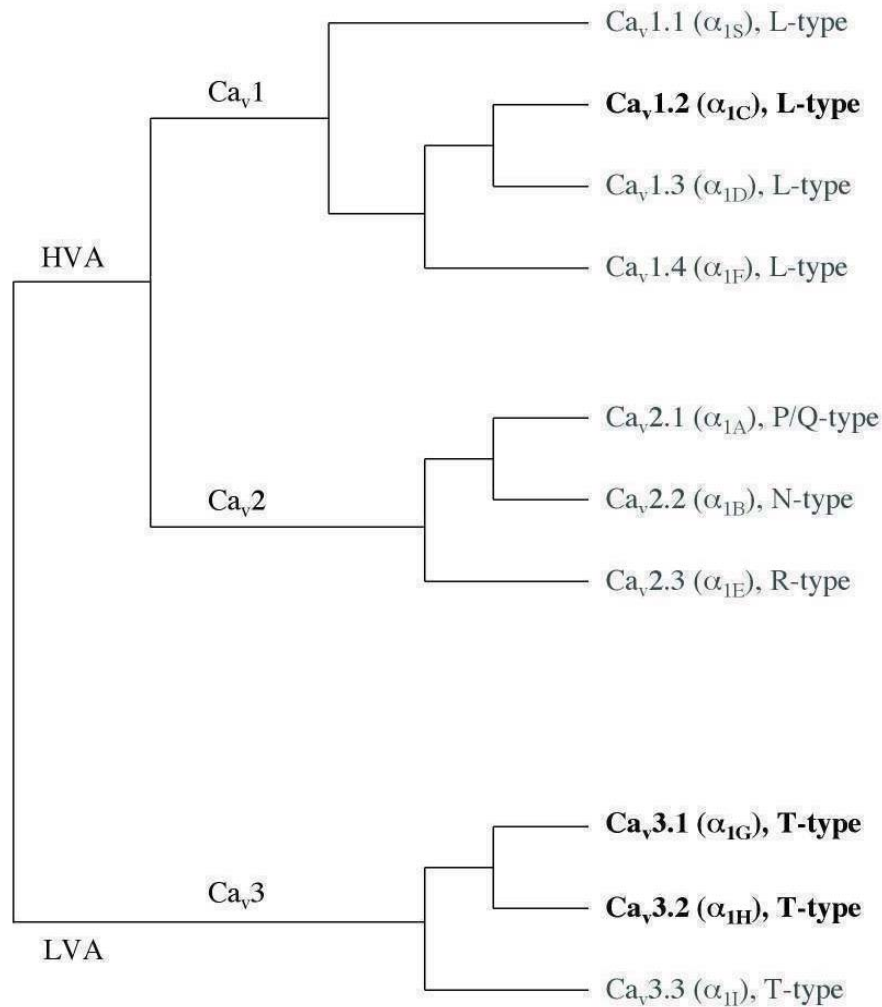


Figure 2: Division of the VOCCs into the HVA and LVA subgroups, the Ca_v1 , Ca_v2 and Ca_v3 families and their individual L-, P/Q-, N-, R and T-type. Modified from Perez-Reyes, 2003²⁵⁵

C.1.2 T-Channel Molecular Biology

The LVA T-channels have been further subclassified into 3 separate T-channels, based on the molecular architecture of the α_1 pore-forming subunit (Figure 2), each of which are encoded for on different genes. The genes encoding T-channels are designated as *Cacna1G*, *Cacna1H* and *Cacn1I* and code for $Ca_v3.1$, 3.2 and 3.3 ,

respectively. From the human genome project the three T-channels are known to be located on the long arm of chromosome 17 (Cacna1G/Ca_v3.1), the short arm of chromosome 6 (Cacna1H/Ca_v3.2) and the long arm of chromosome 22 (Cacna1I/Ca_v3.3)⁵⁴⁷. The genetic difference between these three T-channel types is quite large with a sequence homology of approximately 60%²⁵⁵.

The coding sequences for the T-channels were determined in 1998 by Perez-Reyes *et al.*²⁵⁷ who sequenced the T-channel by matching highly conserved genetic sequences from the L-channel to unknown genetic sequences contained within multiple animal species. Earlier functional studies in *Xenopus* oocytes also confirmed that these genes did encode for T-channels with the currents having the distinct low activating potential (≥ 60 mV), a small single channel conductance (3.5 – 7pS) and slow inactivation, all hallmarks of the T-channel²⁵⁵⁻²⁵⁷.

C.1.3 Ca⁺⁺ Channel Distribution in the Vasculature

In large vessels, L-channels regulate a large proportion of extracellular Ca⁺⁺ entry²³⁷ and therefore activation of Ca⁺⁺ CaM-dependent MLCK, myosin phosphorylation and vascular contraction⁵⁴⁸⁻⁵⁵⁰. Due to the role of L-channels in Ca⁺⁺ entry and vasoconstriction, blockade of this channel can be an effective form of treatment for large vessel vasospasm including angina^{354, 355, 365, 366}. More recently evidence has emerged that the T-type channels are important in several cardiovascular and renal pathologies^{306, 381, 551}.

Animal and human clinical studies have suggested that in the microvasculature there is a significant increase in the mRNA encoding the T-channel compared to the L-channel^{552, 553, 306, 301}. Using non-quantitative PCR, on extracts of rat mesenteric vessels less than 40µm in diameter, T-channel mRNA was readily detected whereas the level of L-channel mRNA was undetectable³⁰¹. Subsequent follow-up studies using both Ca⁺⁺ imaging and polymerase chain reaction (PCR) in isolated smooth muscle cells from rat and guinea pig mesenteric microvessels suggest that the Ca⁺⁺ channel activated during sustained depolarisation did not have properties of the HVA channel but were similar to the T-channel⁵⁵². Specifically, the pharmacology (nifedipine-insensitive Ca⁺⁺ currents) and physical ion pore properties (Ca⁺⁺ and barium permeability) suggested that these channels belonged to the class of LVA channels.

Studies in the renal microvasculature identified an equal distribution of L- and T-channel mRNA in the afferent arteriole, but a predominance of T-channel mRNA over L-channel mRNA in the efferent arteriole³⁰⁶. Consistent with this difference in expression level of the pore-forming subunits of these VOCCs both L- and T-channel antagonists are able to inhibit afferent vasoconstriction. However, only the T-channel antagonists can inhibit efferent vasoconstriction⁵⁵³. Additionally, T-type CCBs dilate both afferent and efferent glomerular arterioles whereas L-type CCBs dilate only the afferent arterioles⁵⁴⁴.

However, controversy over the importance of the T-channel in the microvasculature still exists. Although the above studies suggest a role for the T-channel in regulating

microvascular tone, a recent study by Moosmang *et al.*⁵²⁷ has sparked debate. Using a time and smooth muscle specific L-channel knockout mouse model to investigate blood pressure and hind limb blood flow, they found that the beneficial effects of the combined L- and T-channel blocker, mibefradil, were abolished. This suggests that the vasodilatory effects of mibefradil were actually mediated via the L-channel and not the T-channel (for more details refer to Section B.1.2).

C.1.4 Study Objectives

Efonidipine^{292, 294} and mibefradil³⁷⁵ have been identified as dual L- and T-channel blockers. Furthermore, they have been identified as more efficacious in attenuating microvascular constriction than the conventional L-channel blockers verapamil and nifedipine. This is the case even when complete L-channel blockade occurs. Furthermore, this phenomenon manifests itself in human subcutaneous microvessels and is independent of the agonist utilised or endothelial function (see Section B).

As outlined above previous studies have examined the mRNA distribution of L- and T-channels^{301, 544, 553}. However, these studies used non-quantitative PCR which is considered less reliable than quantitative PCR since the analysis is endpoint in nature. For example, if the products of the reaction have reached saturation by completion of the PCR reaction, no differences in mRNA expression will be detectable. The advantage of quantitative PCR is that it allows for kinetic analysis of channel expression during the linear phase of the polymerase chain reaction. This consequently enables one to more reliably detect any differences in mRNA expression. To date, however, no studies have quantitatively compared both mRNA

and protein abundance of L- and T-channels in large and small vessels. The current study provides a comprehensive evaluation of small and large vessel reactivity regarding various CCBs (Section B) coupled with the first quantitative molecular analysis of the structural components of L- and T-channels. The objectives of the current chapter are to: (1) quantify mRNA expression of the pore-forming subunits of Ca⁺⁺ L- and T-channels in rat thoracic aorta (>2000µm diameter) and mesenteric microvessels (<300µm diameter) and using quantitative PCR; and (2) compare the abundance of pore-forming subunits of Ca⁺⁺ L- and T-channels in rat thoracic aorta and mesenteric microvessels using quantitative radiometric western blot analysis.

C.2 METHODOLOGY

C.2.1 Isolated Vessel Preparations

C.2.1.1 RAT MESENTERIC AND AORTIC VESSELS

For vascular preparations information refer to Section B.2.1.1.

In these experiments, to provide sufficient tissue for analysis, ten 3rd order mesenteric vessels 5mm in length were dissected from an individual rat and pooled to form one sample.

This study was approved by the relevant institutional ethics committees for animal research (approval M-04-2006, The University of Adelaide Animal Ethics Committee; approval 7/06 Institute of Medical and Veterinary Science/Central Northern Adelaide Health Service Animal Ethics Committee).

C.2.1.2 TISSUE HANDLING AND DISSECTION

For tissue handling and dissection see Section B.2.3.2.

Specific to these experiments following dissection vessels were placed in 2mL eppendorf tubes and snap frozen in liquid nitrogen. Samples were stored at -80°C prior to mRNA and protein extraction and quantitative PCR and SDS-PAGE/western blot analysis.

C.2.2 Quantitation of the mRNA Encoding the Pore-Forming Subunits of Ca⁺⁺ Channels Using Real-Time PCR

C.2.2.1 RNA EXTRACTION

RNA extraction was performed using the Qiagen RNeasy Mini Kit (Qiagen Pty Ltd., Australia) with the extraction procedure outlined by the manufacturer.

The aortic vascular tissue (20-30mg) was homogenised in a liquid nitrogen-cooled mortar and pestle and placed in a 2mL eppendorf tube containing 600µL of the proprietary Qiagen extraction buffer RLT containing guanidine-thiocyanate. Due to their small size mesenteric segments were placed directly in a 2mL eppendorf tube containing 600µL of the extraction buffer. Following tissue lysis samples were centrifuged for 3 minutes at room temperature at 14 000g. The aqueous supernatant layer (~600µL) was removed and mixed with one volume of 70% ethanol. The samples were then passed through a Qiagen column where the RNA binds to the silica membrane of the column. To remove any contaminating DNA and/or salts the column was sequentially washed with buffers contained in the kit: Buffer RW1

(700µL × 1 wash) and Buffer RPE (500µL × 2 washes) as recommended by Qiagen. RNA was then eluted from the column, into a 1.5mL eppendorf tube, with 20µL of sterile water. Samples were stored at -80°C prior to reverse transcription and quantitative PCR.

C.2.2.2 REVERSE TRANSCRIPTION

cDNA was generated by reverse transcription of 3µL of the RNA samples using oligo dT (Invitrogen, Australia) and Superscript II polymerase (Invitrogen, Australia). Briefly, this included 1µL oligo dT (500ng/µL), 4µL 5× first strand buffer (Invitrogen, Australia), 2µL dithiothreitol (DTT, 100mM), 1µL deoxyribonucleotide triphosphate (dNTPs, 10mM) (Invitrogen, Australia), 1µL Superscript II polymerase (added last) and 8µL sterile water.

The reagents were mixed together by pipetting, centrifuged and incubated at 42°C for 90 minutes. The cDNA samples were then stored at -20°C until required for quantitative PCR.

C.2.2.3 REFERENCE CONTROL GENES (HOUSEKEEPING GENES)

Housekeeping genes provide a reference value and act as an internal reference standard when identifying expression of the same or different mRNAs between tissue types. Importantly, factors which inhibit reaction efficiency will do so for both the housekeeping and experimental reactions. Therefore, if the PCR efficiency of the housekeeping gene is reduced for a particular cDNA sample then it is likely the experimental cDNA sample will be similarly reduced⁵⁵⁴. This approach enables one

to identify relative expression of experimental cDNA in comparison to reference genes and thereby identify true differences in expression. In all experiments message for the 18s ribosomal subunit was used as the internal reference gene due to its wide and uniform expression in a variety of vascular tissues⁵⁵⁵.

C.2.2.4 QUANTITATIVE PCR PROTOCOL

The quantitative PCR protocol used specific primer-mediated amplification of DNA. The SYBR green polymerase master mix (Applied Biosystems, Australia), with 3 μ L of cDNA and 1 μ L of both the forward and reverse primers, was used in PCR reactions to enable real-time quantitation of PCR amplicon abundance. SYBR green intercalates between the major groove of the double stranded DNA and fluoresces. Thus, the level of fluorescence during the PCR protocol directly correlates to the amount of DNA present. Non-template controls, containing sterile water in place of cDNA, were included to verify there was no contaminating DNA present in the primers or SYBR green polymerase master mix.

A Corbett 3600 thermal cycler with fluorescence detector and accompanying Rotor-Gene 6 software (Corbett Research, Australia) was used to analyse all quantitative PCR reactions. Briefly the PCR protocol involved a 5 minute 95°C hot start followed by a maximum 40 amplification cycles with the following temperature protocol: denaturation of DNA at 95°C for 30 seconds, annealing at 55°C for 30 seconds and primer extension at 72°C for 30 seconds. At the end of the protocol there was a 2 minute hold at 40°C followed by melt analysis. Due to each double-stranded DNA amplicon having a specific melting point (Ca_v1.2 = 78°C, Ca_v3.2 = 82°C and 18s =

78°C) at which the strands separate, melt curve analysis identified the number of unique amplicons in each PCR reaction providing an index of primer specificity.

C.2.2.4.1 Primers

Each of the PCR primers were designed using the Primer3 Input Program (version 1.1.1) to generate amplicons between 20–24 base pairs and were synthesised by Sigma-Genosys, Australia (Table 1).

	Forward (5' – 3')	Reverse (5' – 3')
Ca_v1.2	AGTGATTGCCTACGGACTACTCTT	AAGCCCTACAACCACGATTATAAA
Amplicon Size	24	24
Ca_v3.2	CTGCCCAGAGAAGGAACAAG	CAGGCTCATCTCCACTGTCA
Amplicon Size	20	20
18s	GCCGCTAGAGGTGAAATTCTTG	CATTCTTGGCAAATGCTTTTCG
Amplicon Size	22	21

Table 1: Quantitative PCR primers. Real-Time PCR forward and reverse primers for Ca_v1.2, Ca_v3.2 and 18s housekeeping gene and the corresponding amplicon size.

C.2.2.5 DATA ANALYSIS

The threshold cycle (C_T), used for analysis, reflects the cycle number at which the fluorescence generated within a reaction crosses the threshold. The delta delta C_T formulae, 2^{-ΔΔC_T}, as described by Livak *et al.*⁵⁵⁶ was used to analyse and quantitate L- and T-channel mRNA data. To determine the expression of each of the channels the following formula was used:

$$\Delta\Delta C_T = (\text{channel} - 18s)_X - (\text{channel} - 18s)_O$$

where X represents the C_T of each individual sample at a chosen threshold and O represents the mean of these individual C_T values. The mean of each of these ΔΔC_T values for each channel was then taken and incorporated into 2^{-ΔΔC_T} to provide a final expression value for Ca_v1.2, Ca_v3.2 and 18s.

C.2.2.5.1 Statistical Analysis

The mRNA expression values for $Ca_v1.2$, $Ca_v3.2$ and 18s in both aorta and mesenteric tissue were examined using Student's t-test with $p < 0.05$ representing statistical significance. n refers to the number of individual samples taken from independent rats, such that an n of 4 would indicate individual samples were obtained from 4 separate rats.

C.2.3 Ratiometric Quantitation of the Proteins Comprising the Pore-Forming Subunits of L- and T-Channels

C.2.3.1 ANTIBODIES

All primary antibodies were prepared in 1% non-fat dried milk (NFDM) and Tris Buffered Saline (composition: 25mM Tris, 150mM NaCl) with 0.05% Tween 20. Commercially available polyclonal (rabbit IgG) antibodies were used: anti- $Ca_v1.2$, which recognises the 190kDa α_{1C} subunit⁵⁵⁷⁻⁵⁵⁹, at a 1:2000 dilution (Chemicon, Australia); anti- $Ca_v3.1$, which recognises the 250kDa α_{1G} subunit^{560, 561}, at a 1:500 dilution (Sigma-Aldrich, Australia); and anti- $Ca_v3.2$, which recognises the 230kDa α_{1H} subunit^{562, 563}, at a 1:500 dilution (Sigma-Aldrich, Australia).

The secondary antibody was an anti-rabbit IgG-horseradish peroxidase-conjugate (Santa Cruz Biotechnology® Inc., California) prepared in TBS-T at a dilution of 1:10 000.

C.2.3.2 PROTEIN ISOLATION

The α_1 subunits of the Ca⁺⁺ L-channel are known to be highly sensitive to proteases⁵⁶⁴. Therefore to prevent degradation of proteins, samples were extracted in the presence of Calpain Inhibitor 1 (Calbiochem[®], Australia) and a broad spectrum protease inhibitor cocktail (Complete Mini tablet, Roche Applied Science, Australia).

Protein extraction was performed using previously published, validated methods⁵⁶⁵. All mesenteric vessels were 3rd order and cut to a similar length. Each of the aortic segments were also cut to a similar size. All protein samples were extracted from snap-frozen vessels in a 60 μ L aqueous solution containing a 1:10 dilution of the calpain/protease inhibitor mix (5mg/mL), 1mM DTT, 50mM Tris pH 6.8, 30% glycerol, 0.001% bromophenol blue and 1% sodium dodecyl sulfate (SDS) (modified from Laemmli extraction buffer⁵⁶⁶). The samples were then heated for 5 minutes at 72°C, rather than 95°C, to maintain the solubility of the hydrophobic ion channels.

It is common practice to extract and measure total protein by a protein assay. However, many of the myofilament proteins are insoluble requiring high concentrations of SDS and DTT to completely solubilise these tissues. Unfortunately, this can make the sample incompatible for protein assay without a clean-up step which often results in loss of sample thus contributing to variability. To avoid incorrectly sub-sampling these proteins we opted to use vessels of the same size and number and the same sample volume for all protein extractions. This provides as good, or an arguably better, approach to standardising loading of vessel samples for western analysis and was validated by coomassie stain and densitometry.

C.2.3.3 SDS-PAGE AND WESTERN BLOTTING PROTOCOL

Protein extracts were analysed by SDS-PAGE, coomassie brilliant blue staining and western blot. Densitometric scanning of stained gels prior to running western blots enabled adjustment of sample volumes to ensure equal loading of samples, and importantly, to ensure samples were in the linear range for quantitative western blot analysis (Figure 3).

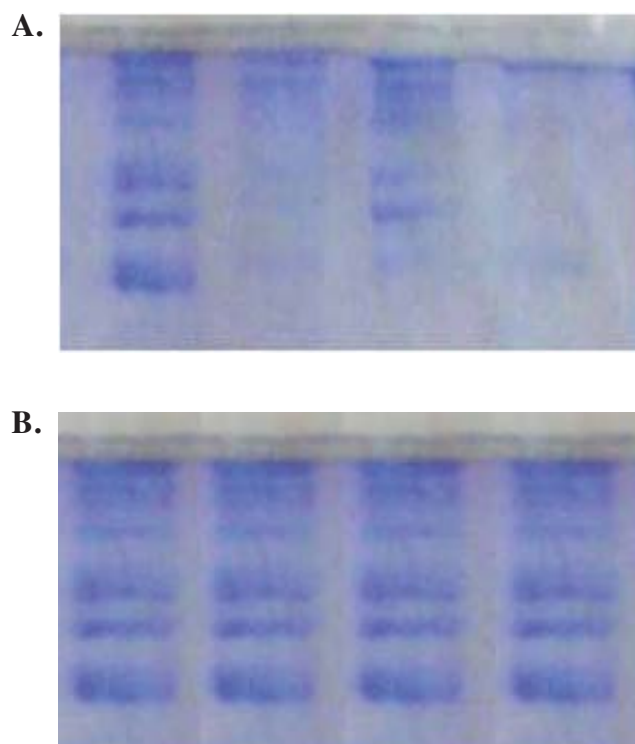


Figure 3: Adjustment of sample volume to ensure equal loading of vessel samples. A. Representative coomassie blue stained gel prior to sample adjustment where 20 μ L of samples were loaded. B. Representative coomassie blue stained gel after sample adjustment where samples of 8 μ L, which was within the linear range, were loaded.

Total protein extracts were analysed using 7.5% acrylamide gels with the Bio-Rad Mini-PROTEAN II Electrophoresis System in Running Buffer (composition: 25mM Tris, 192mM Glycine and 1% SDS) at 200 volts for 1 hour. Proteins were electrophoretically transferred onto 0.2 μ m nitrocellulose membranes with the Bio-

Rad Mini Trans-Blot Cell in Transfer Buffer (composition: 25mM Tris, 192mM Glycine, 20% methanol and 0.01% SDS) at 100 volts for 1 hour. To provide a molecular weight reference for each gel 2 μ L of the Fermentas PageRuler™ Prestained Protein Ladder Plus was loaded onto each gel (Fermentas, Australia).

To prevent non-specific antibody binding the nitrocellulose was incubated in a TBS-T solution containing 5% NFDM for 1 hour at room temperature with gentle shaking. Antibody detection of the pore-forming subunits of voltage sensitive Ca⁺⁺ channels was carried out for 1 hour at room temperature. Nitrocellulose membranes were washed three times in TBS-T followed by incubation with the anti-rabbit IgG-horseradish peroxidase-conjugated secondary antibody for 1 hour at room temperature. Nitrocellulose membranes were exposed to enhanced chemiluminescence reagents for 1 minute (GE Healthcare Life Sciences, Australia) and exposed to film for 5 minutes before developing. To avoid loss of antigen separate gels and blots were used for each of the three primary antibodies.

To quantify the relative abundance of the pore-forming subunit of each Ca⁺⁺ channel in the large and small vessels, the autoradiographic exposure of the western blots were scanned (BioRad GS-710 Imaging Densitometer, California) and the signal for each Ca⁺⁺ channel determined using QuantityOne software (BioRad, California). The coomassie blue stained gel was also scanned to confirm equivalent protein loading in each lane. The optical density value for the T-channel western blots was then divided by the L-channel value to give a ratio of optical density for T/L channel abundance for both aortic and mesenteric vessels.

C.2.3.4 PROTEIN QUANTITATION

To identify the abundance of the pore-forming subunits of the L- and T-channels ratiometric protein quantification was used because this provides an index of relative abundance of the protein. Importantly, when undertaking ratiometric analysis it is necessary to ensure the signal of each protein, in this case ion channel, is within the linear range (described below). Working in the linear range of detection provides the greatest sensitivity and accuracy to enable the identification of differences between test samples. For example, protein samples near saturation provide an under-representation of true differences which may exist between control and test samples (Figure 4).

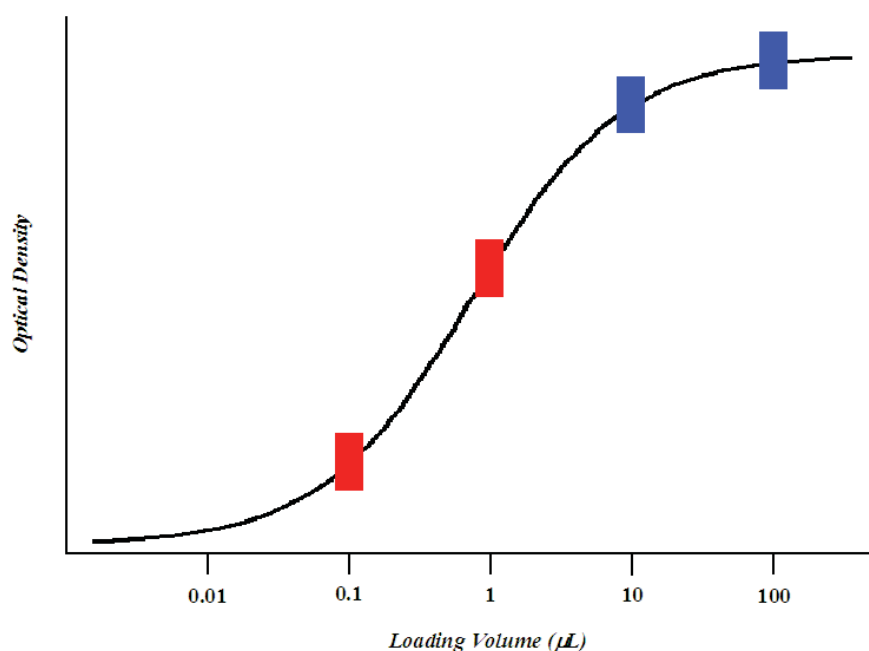


Figure 4: Representation of linear range detection. Samples between 0.1µL and 1µL (red rectangles) will reveal any differences in sample protein abundance as differences in protein band intensity will be more apparent. Samples at or near saturation, 10µL and 100µL (blue rectangles) will be less efficient at identifying any differences in sample protein abundance as both the protein bands will be of similar intensity.

C.2.3.4.1 Establishing the Linear Range of Detection

A series of experiments were performed to determine the volume of protein extract that should be loaded to ensure detection in the linear range. To achieve this objective 2µL, 5µL, 10µL and 20µL of protein extracts from each vessel type were subjected to SDS-PAGE/western blotting and detected using antibodies to the specific pore-forming subunits.

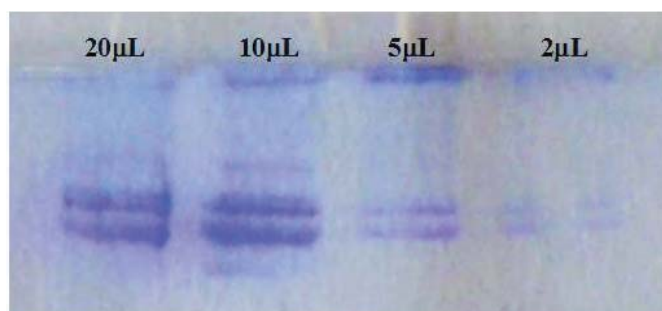


Figure 5: Establishing the linear range of detection. Representative coomassie blue stained gel with 20µL, 10µL, 5µL and 2µL (left → right respectively) of rat mesenteric microvessel sample to determine the volume load required to be within the linear range for mesenteric samples.

The optical density (OD) of the protein was plotted vs. protein load and regression analysis identified the linear range of detection. These analyses identified that 8µL was within the linear range for all the samples (Figure 8) and was therefore used for all subsequent ratio analyses:

$$\text{T-/L- ratio} = (\text{OD T-channel}/\text{OD L-channel}) \times 100$$

The protein profile composition varies between large and small vessels. Therefore, rather than normalising to total protein a ratio analysis was performed to account for any differences in vessel size and protein extraction efficiency. Linear range was set

over a single sample set, however, the T/L ratio was reproducible between independent protein extractions.

C.2.3.5 DATA ANALYSIS

The protein abundance measurements are represented as optical density (OD) readings. The complete data comparison values are represented as a percentage score normalised to the relative level of L-channel on the corresponding paired blot.

C.2.3.5.1 Statistical Analysis

Statistical differences in the protein abundance of each of the three channels in each tissue type were calculated using Student's t-test with $p < 0.05$ statistically significant. n refers to the number of samples taken from independent rats.

C.3 RESULTS

C.3.1 Quantitation of Ca^{++} Channel mRNA

C.3.1.1 mRNA EXPRESSION OF L- AND T-CHANNELS IN RAT AORTA AND MESENTERIC VESSELS

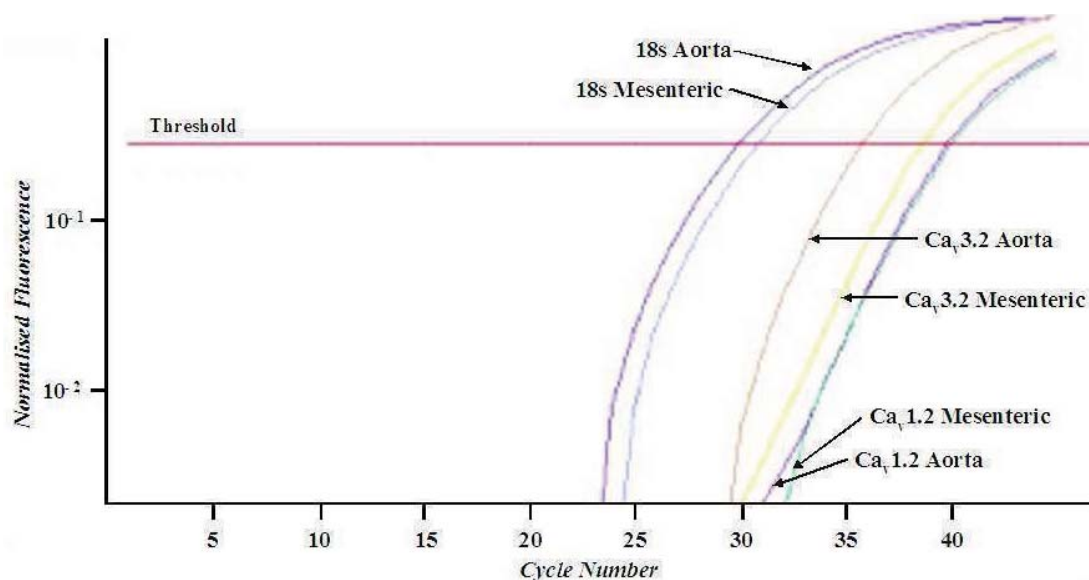


Figure 6: mRNA Expression of $Ca_v1.2$, $Ca_v3.2$ and 18s in Rat Aorta and Mesenteric Microvessels. The C_T required for double-stranded DNA amplification to reach threshold (as represented by the red line) were: Aorta – $Ca_v1.2$ = 39.94, $Ca_v3.2$ = 38.74, 18s = 30.09; Mesenteric – $Ca_v1.2$ = 40.15, $Ca_v3.2$ = 35.89, 18s = 31.01.

C.3.1.2 MELT CURVE ANALYSIS OF PCR PRODUCTS FOLLOWING QUANTITATIVE PCR: IDENTIFICATION OF EFFICIENCY

The efficiency of the quantitative PCR reactions were determined to be: $Ca_v1.2$ Aorta = 95%, Mesenteric = 95%; $Ca_v3.2$ Aorta = 93%, Mesenteric = 93%; 18s Aorta = 92%, and Mesenteric = 91%. The melting point analysis confirmed the presence of a single amplicon for each sample (Figure 7).

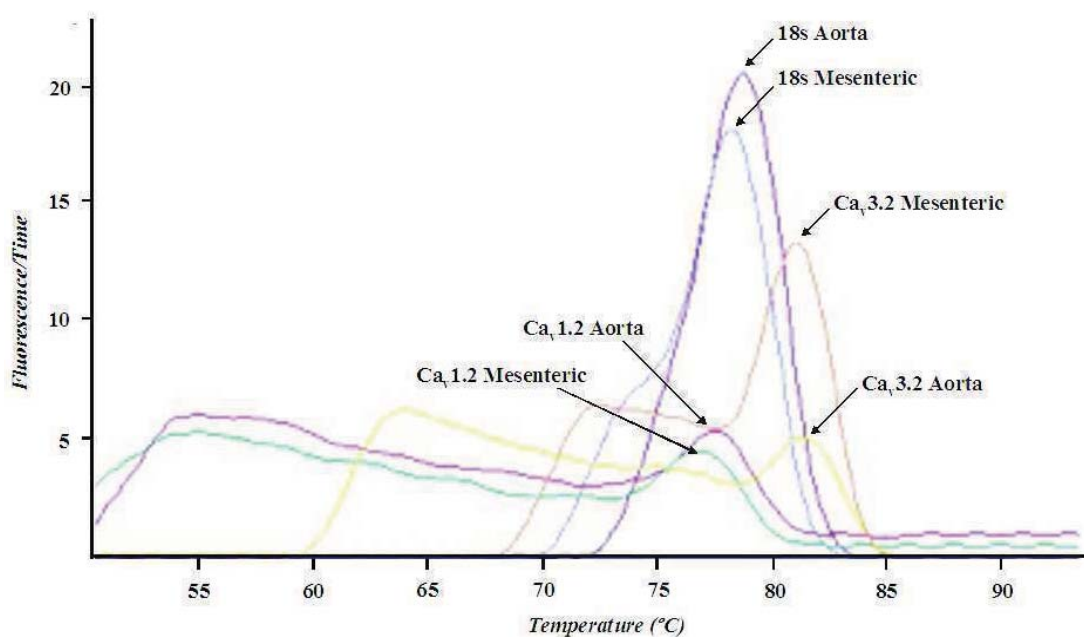


Figure 7: Melting point analysis of PRC amplicons. Melt curve analysis showed the presence of a single amplicon in each sample with correct melting temperatures of 78°C for Ca_v1.2 amplicons, 82°C for Ca_v3.2 amplicons and 78°C for 18s amplicons.

	Aorta	Mesenteric
T/L Ratio	1.28 ± 1.24	0.91 ± 0.70

Table 2: Relative ratio of T/L Ca⁺⁺ channel mRNA in rat aorta and mesenteric vessels. There was no difference in the T/L channel mRNA ratio between large and small vessels ($p > 0.05$, $n = 4$).

C.3.2 Relative Quantitation of Ca⁺⁺ Channel Protein

C.3.2.1 LINEAR QUANTITATION OF L- AND T-CHANNELS IN RAT AORTA AND MESENTERIC MICROVESSELS

Protein extraction of the pore-forming subunit of the L-channel Ca_v1.2 protein (~190kDa), T-channel Ca_v3.1 protein (~250kDa) and T-channel Ca_v3.2 protein (~230kDa) from rat aorta and mesenteric vessels was carried out in 60μL of sample buffer as described above (Section C.2.3.2). Aliquots of these samples were loaded in volumes of 2μL, 5μL, 10μL and 20μL. For each antibody the volumes of 2μL,

5 μ L and 10 μ L were linear with r^2 values ranging from 0.98 – 1.00. However, overloading with 20 μ L of sample resulted in non-linear signal detection and saturation.

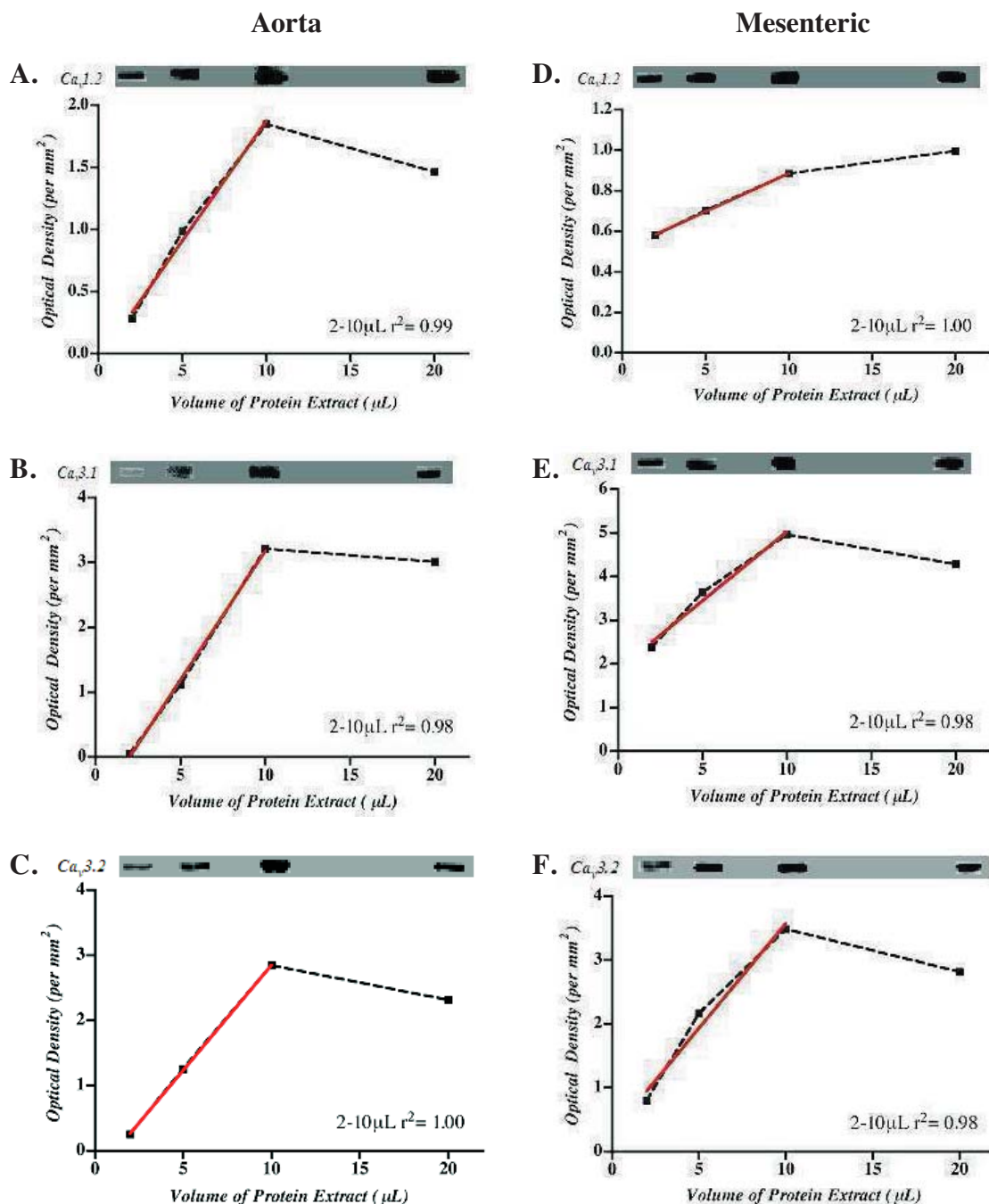


Figure 8: Identification of the Limits of Quantitative Detection of Ca_v1.2, Ca_v3.1 and Ca_v3.2 in Rat Aorta and Mesenteric Vessels. Linear range analysis of loading sample volumes of 2 μ L, 5 μ L, 10 μ L and 20 μ L of rat aorta (A, B and C) and mesenteric vessels (D, E and F) for Ca_v1.2, Ca_v3.1 and Ca_v3.2 protein analysis. Solid red line indicates linear regression for 2 - 10 μ L volumes.

C.3.2.2 L-CHANNEL VS. T-CHANNEL ABUNDANCE

Aorta: Relative Abundance of the Pore-Forming Subunits of Ca_v1.2, 3.1 and 3.2

Quantitative ratiometric western blot analysis identified that there was no difference between the relative abundance of the pore-forming subunits for the Ca_v1.2 protein band with an OD = 0.29 ± 0.1 , Ca_v3.1 protein band OD = 0.43 ± 0.29 and Ca_v3.2 protein band OD = 0.40 ± 0.17 in rat aorta ($p > 0.05$) (Figure 9).

Mesenteric Vessels: Protein Abundance of the Pore-Forming Subunits of Ca_v1.2, 3.1 and 3.2

In contrast to aorta, mesenteric vessels had a significant increase in the pore-forming subunits for the Ca_v3.1 protein band with an OD = $0.90 \pm 0.05^*$ and the Ca_v3.2 protein band with an OD = $1.23 \pm 0.18^*$ compared to the Ca_v1.2 protein band OD = 0.47 ± 0.17 ($p < 0.05$ vs. L-channel). Applying ratiometric analysis this reveals a significant increase in Ca_v3.1 of $112 \pm 38\%$ and Ca_v3.2 of $163 \pm 48\%$ when normalised to L-channel protein ($*p < 0.05$) (Figure 9).

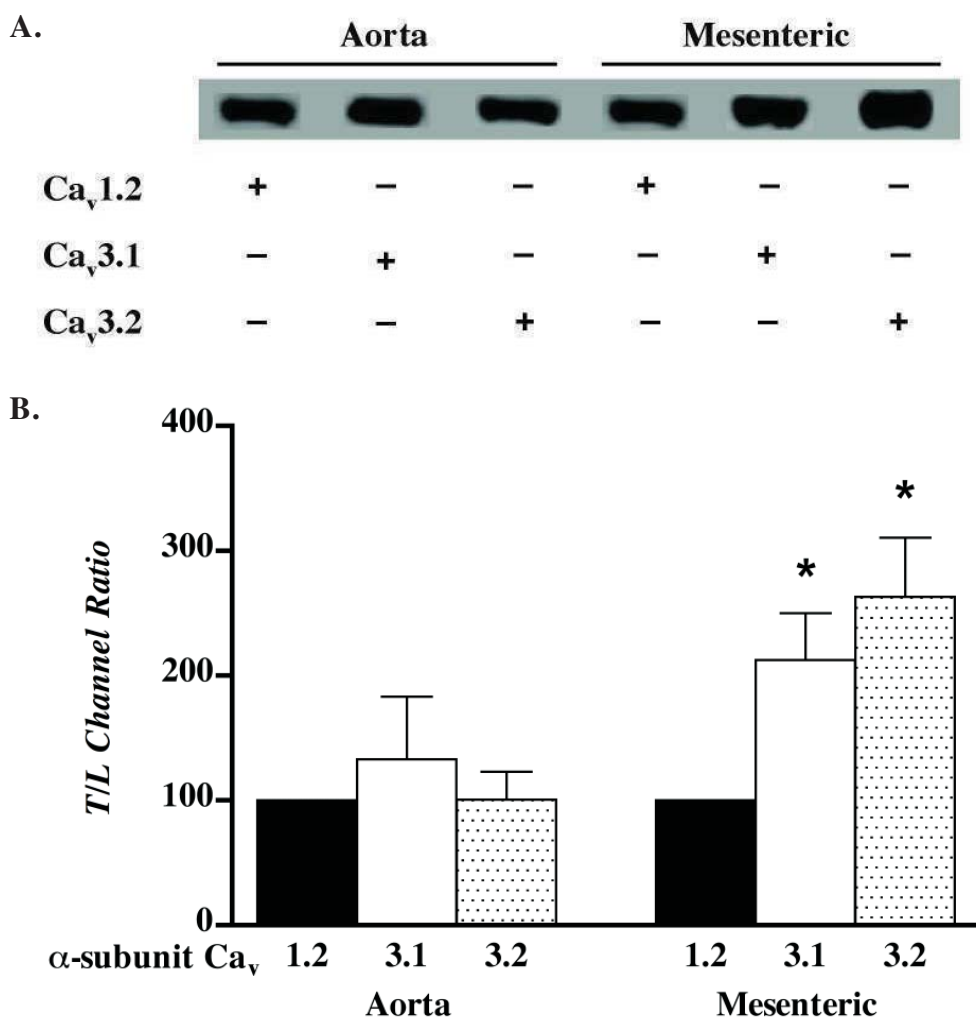


Figure 9: (A) Representative western blots using specific antibodies to the pore-forming subunits of Ca_v1.2, 3.1 or 3.2 in rat aorta and mesenteric vessels. (B) To account for any variations in loading levels data are expressed as a ratio of T/L channel abundance. There was a significant increase in the ratio of the pore-forming subunits of the two T-channels in the small mesenteric vessels but no difference in the large aortic vessels (*p<0.05, n = 4).

C.4 DISCUSSION

Previous clinical studies^{381, 526, 377} and current functional studies conducted with L- and T-channel blockers have demonstrated an increased efficacy of the combined L- and T- blockers (efonidipine and mibefradil) in the microvasculature when compared to the L-channel blockers (verapamil and nifedipine). In order to identify the

molecular basis underlying this function the mRNA and protein of the pore-forming subunits of the L- and T-channels were quantified in large and small vessels.

At the outset of this study there were no antibodies available to detect the Ca_v3.1 and 3.2 subunits of the T-channel, and consequently mRNA abundance was quantified as a possible index of channel abundance. However, when selective antibodies for the pore-forming subunits became available we opted to quantify the Ca_v1.2, 3.1 and 3.2 subunits as a more direct measure of Ca⁺⁺ channel abundance.

C.4.1 Heterogeneity in Channel Distribution According to Vessel Size

The data from our mRNA studies is equivocal with no difference noted in the distribution of Ca_v1.2 and Ca_v3.2 channels between large and small vessels. There is, however, a large standard error which may account for the equivocal nature of this result.

In rat aorta there was an even distribution of the protein for all three of the Ca⁺⁺ channel subunits, Ca_v1.2, 3.1 and 3.2. However, in the mesenteric microvessels there was a significantly increased expression of the protein for the two Ca⁺⁺ T-channel subunits consistent with the pharmacological results of Section B. For the Ca_v3.1 subunit there was an increase of $112 \pm 38\%$ and an even greater increase of $163 \pm 48\%$ for the Ca_v3.2 subunit (expressed relative to L-channel protein expression).

C.4.2 The Ca⁺⁺ T-Channel in the Microvasculature

Previous research using non-quantitative PCR provides evidence of an increase in T-channel mRNA in mesenteric microvessels^{301, 305} and efferent arterioles^{301, 306, 553}. Despite using quantitative PCR the mRNA data from the current study was equivocal. Although the means were different, which is consistent with other reports, the large variability resulted in no statistically significant difference between the means. This large amount of variation may in part be due to the factors discussed below (Section C.4.3) or experimenter error. Rather than continue with mRNA analysis, when antibodies for the T-channel proteins became available we opted to focus on investigating the abundance of the protein encoding the pore-forming subunits for Ca_v1.2, 3.1 and 3.2 as this would be a more direct measure of structural channels.

Our novel findings using this approach have enabled us to identify a significant increase in relative T/L protein ratio for both T-channel pore-forming subunits in the microvasculature. Importantly, this is consistent with pharmacological data (Section B) suggesting an increased abundance of T-channels in the microvasculature that may explain the enhanced sensitivity to T-channel blockade in small but not large vessels. This is consistent with the finding that the T-channel blocker mibefradil dilates small, porcine coronary vessels to a greater extent than the larger epicardial vessels²⁹⁸. Mibefradil is also more potent at inhibiting microvascular tone than the L-channel blocker verapamil in rat resistance vessels²⁹⁹.

Likewise a number of clinical studies indicate an increased efficacy of the combined L- and T-channel blockers over those that block only the L-channel. Studies of hypertension^{393, 526} suggest that combined L- and T-channel blockers have incremental benefits over L-channel blockers. A randomised, double-blind, placebo controlled, cross-over study clearly demonstrated the anti-hypertensive effects of efonidipine³⁹³. A comparison of diltiazem and mibefradil likewise highlighted the increased anti-hypertensive efficacy of mibefradil over diltiazem⁵²⁶. Furthermore, clinical studies in patients with microvascular disorders, on background verapamil therapy, have shown that mibefradil significantly decreases microvascular resistance³⁸¹. These data now provide a molecular basis for the functional and clinical findings wherein combined L- and T-channel blockers are more effective at attenuating small vessel vasospasm.

C.4.3 Clarifications

mRNA expression is often analysed as a surrogate of protein expression if no antibodies are available, or to investigate the regulation of protein abundance at the transcriptional level. However, the availability of antibodies made it possible to analyse the protein abundance, which was found to be consistent with both the functional pharmacology and clinical findings.

It is important to recognise that the level of mRNA does not always directly correlate with the level of protein in a cell. All cells contain ribonucleases which remove mRNAs from the cell once they have served their function⁵⁶⁷ as may be the case with the Ca⁺⁺ channel mRNAs. mRNA which is not being translated is generally degraded at a faster rate⁵⁶⁷. Furthermore, translation may be initiated at different rates and

therefore some mRNAs may have an increased translation rate⁵⁶⁸. Consequently, while there is an abundance of protein there may be little or no mRNA present as was seen in this current study.

Although quantitative western blotting is useful for identifying protein abundance there are many post-translational events, including protein modification and turnover, which can alter protein or ion channel function. Although our western blotting data is consistent with the functional pharmacological and clinical findings direct functional analysis of an ion channel, using patch-clamp techniques, is considered the most direct index of function. Ongoing patch-clamp studies of L- and T-channels by new members of our research group will directly identify the number of open channels in small and large vessels.

C.5 CONCLUSIONS

We have utilised ratiometric western blotting tools to show a differential expression of the L-type channels and T-type channels in both large and small vessels. Our functional data from Section B demonstrated an increased efficacy of the Ca⁺⁺ T-channel in the microvasculature, which is entirely consistent with the increased expression of the protein for the pore-forming subunits of the Ca⁺⁺ T-channel in the microvasculature. This has clearly been shown throughout this section. Finally, we have identified there is a significant increase in the relative abundance of T/L channels in the microvessels only. This is consistent with, and provides a molecular basis for, the incremental microcirculatory benefits of the combined L- and T-channel blockers, efonidipine and mibefradil over the conventional L-channel blockers.

SECTION D

OVERVIEW

and

CONCLUSIONS

This thesis investigated the heterogeneity of vascular Ca⁺⁺ channels in large and small arterial vessels. It has utilised functional reactivity studies to examine the effect of various Ca⁺⁺ channel blockers (CCBs) as well as molecular techniques to evaluate the relative distribution of the pore-forming subunits of L- and T-type channels. These findings have advanced our understanding of VSM Ca⁺⁺ channels.

Section B utilised the *in vitro* technique of myography to examine the effect of two L-channel blockers (verapamil and nifedipine) and two combined L- and T-channel blockers (efonidipine and mibefradil) on large and small vessel constriction. This study clearly demonstrated an increased efficacy of the combined L- and T-channel blockers in attenuating microvascular constrictor responses. The significance of this observation was further supported by: (1) consistent findings in both human and animal models, (2) reproducibility with mechanistically different vasoconstrictor stimuli (i.e., receptor-mediated Et-1 or depolarisation-mediated KCl), (3) incremental inhibition of contractile responses by efonidipine in the presence of maximal L-channel blockade, (4) pairing of CCBs with similar effects on Ca⁺⁺ channels but different chemical structure (verapamil – phenylalkylamine; nifedipine and efonidipine – dihydropyridine; and mibefradil – benzimidazole), (5) the use of CCB concentrations that are near-maximal for all the CCBs and equivalent to their therapeutic plasma levels, (6) consistent results even in the presence of an altered microvascular physiology in the form of chronic Et-1 receptor activation and (7) exclusion of an endothelium-dependent mechanism. These functional findings suggest that T-channels play a significant role in human microvascular tone and provided an explanation whereby combined L- and T-channel blockers have

additional therapeutic benefits over conventional L-channel blockers in microvascular disorders.

Section C explored a potential mechanism for this divergent CCB response, by examining if a differential distribution of the pore-forming subunits of Ca_v1.2, Ca_v3.1 and 3.2 existed between large and small vessels. To examine mRNA distribution quantitative PCR was undertaken and for protein abundance quantitative western blotting was used. While the PCR data revealed no difference in the T/L channel ratio between rat large aorta and mesenteric microvessels there was a large amount of variation in these data. In addition to these quantitative PCR experiments the recent availability of T-channel antibodies allowed for the examination of the protein abundance of the Ca⁺⁺ L- and T-channels in both large and small rat vessels. In the aorta there was a similar distribution of the protein for all three of the Ca⁺⁺ channel subunits. However, in the mesenteric microvessels there was a significantly increased expression of the T-channel Ca_v3.1 subunit of $112 \pm 38\%$ and an even greater increase of $163 \pm 48\%$ for the Ca_v3.2 subunit (expressed relative to L-channel protein expression). This increased expression of the two T-channel subunits in the microvasculature is consistent with our functional data showing an increased effectiveness of the combined blockers in these microvessels.

The divergence between the PCR data and the protein data could be due to a number of factors. Firstly, there was considerable variability in the PCR results as seen by the large standard errors. Another possible explanation for these diverse results is that there is not a perfectly linear relationship between mRNA and protein. For example,

some mRNAs are degraded following translation into protein therefore while you would see the protein there would be no detectable mRNA^{567, 568}. However, rather than focusing on lowering this variation to obtain a significant value we focused instead on protein levels as these are considered a more relevant measure of channel function.

The above studies provide us with greater insights into the regulation of microvascular tone and advance our understanding of microvascular disorders. The combined L- and T-channel blockers already been shown to differ to L-channel blockers in their clinical effects on blood pressure and renal perfusion. For example, in a comparison of the anti-hypertensive effects of diltiazem (an L-channel blocker) and mibefradil, the combined L- and T-channel blocker reduced blood pressure to greater extent than the L-channel blocker³⁷⁷. Similarly, in the Posicor Reduction of Ischaemia in Exercise (PRIDE) comparative study of diltiazem and mibefradil, mibefradil significantly increased both exercise duration and time to ischaemia while also lowering blood pressure⁵²⁶. Furthermore, efonidipine has also been shown to have these same anti-hypertensive effects³⁹³.

These anti-hypertensive effects of the combined L- and T-channel blockers are consistent with our functional studies examining the effect of the CCBs in the presence of chronic Et-1 exposure. These rats exposed to Et-1 for 7 days had a significantly increased blood pressure compared to sham surgery rats. In the mesenteric microvessels of these chronic Et-1, hypertensive rats, the combined L-

and T-channel blocker, efonidipine, was more effective at inhibiting contraction than the conventional L-channel blocker, verapamil.

Studies of the glomerular microcirculation have demonstrated L-channels in the afferent but not the efferent arteriole whereas T-channels are found in both types of glomerular microvessels³⁰⁶. Thus L-channel blockers predominantly dilate the afferent arteriole and may produce glomerular hypertension whereas T-channel blockade does not. This may explain why efonidipine and mibefradil have been shown to reduce proteinuria in hypertensive patients with renal impairment whereas L-channel blockers do not⁵⁴⁴.

In addition to its role in blood pressure and renal perfusion, the combined blockers also play a role in many coronary microvascular disorders. The coronary slow flow phenomenon is a coronary microvascular disorder characterised by the delayed passage of contrast during angiography reflecting the increased downstream resistance⁵⁰⁵. Patients with this disorder on maintenance verapamil therapy, still exhibit the angiographic phenomenon. However, the addition of mibefradil acutely improves angiographic flow³⁸¹. Furthermore, mibefradil was shown to alleviate the debilitating angina associated with this microvascular disorder³⁸¹. However, mibefradil has since been withdrawn from the market effectively leaving this group of patients with no effective therapies. Accordingly, the study supports the need for an alternative T-channel blocker.

The incremental microcirculatory benefits of the combined L- and T-channel blockers, efonidipine and mibefradil, over the conventional L-channel blockers are likely due to their additional T-channel blocking properties and the increased presence of T-channels compared with L-channels in the microvasculature of the rat. However, further studies aimed at quantifying L- and T-channels in the human vasculature and also defining the precise role of the T-channel with the newer CCBs and their role in the regulation of vascular tone are required. We believe these studies provide a rational explanation for the beneficial effects of combined L- and T-channel blockers and provide the necessary data to warrant further investigation of the therapeutic value of these agents in cardiovascular pathologies, particularly in those involving increased microvascular resistance.

APPENDIX 1

Hypertension

JOURNAL OF THE AMERICAN HEART ASSOCIATION



Heterogeneity of L- and T-Channels in the Vasculature: Rationale for the Efficacy of Combined L- and T-Blockade

Christine J. Ball, David P. Wilson, Stuart P. Turner, David A. Saint and John F. Beltrame

Hypertension 2009;53;654-660; originally published online Feb 23, 2009;

DOI: 10.1161/HYPERTENSIONAHA.108.125831

Hypertension is published by the American Heart Association, 7272 Greenville Avenue, Dallas, TX 72514

Copyright © 2009 American Heart Association. All rights reserved. Print ISSN: 0194-911X. Online ISSN: 1524-4563

The online version of this article, along with updated information and services, is located on the World Wide Web at:

<http://hyper.ahajournals.org/cgi/content/full/53/4/654>

Subscriptions: Information about subscribing to Hypertension is online at
<http://hyper.ahajournals.org/subscriptions/>

Permissions: Permissions & Rights Desk, Lippincott Williams & Wilkins, a division of Wolters Kluwer Health, 351 West Camden Street, Baltimore, MD 21202-2436. Phone: 410-528-4050. Fax: 410-528-8550. E-mail:
journalpermissions@lww.com

Reprints: Information about reprints can be found online at
<http://www.lww.com/reprints>

Heterogeneity of L- and T-Channels in the Vasculature Rationale for the Efficacy of Combined L- and T-Blockade

Christine J. Ball, David P. Wilson, Stuart P. Turner, David A. Saint, John F. Beltrame

Abstract—Clinical studies suggest that T-type Ca^{2+} channel blockade may have incremental benefits over conventional L-channel blockade, particularly in microvascular disorders. This study examined functional vasomotor differences in L- and T-channel blockade between large and small vessels and compared the abundance of the L- and T-type channels in these vessels. The inhibition of endothelin-1 and potassium-induced vascular contractile responses by L-channel blockers (verapamil and nifedipine) was compared with combined L- and T-channel blockers (mibefradil and efonidipine) in large (rat aorta) and small (rat mesenteric and human subcutaneous) vessels using wire myography. All 4 of the Ca^{2+} channel blockers inhibited contractile responses to a similar extent in large rat vessels; however, in rat microvessels, the combined L- and T-channel blockers produced significantly greater inhibition of contraction than L-channel blockers alone. The significance of this differential T-channel effect in microvessels was further supported by the following: (1) a greater abundance of T-channels compared with L-channels in microvessels but not in large vessels; (2) demonstration of divergent Ca^{2+} channel blocker responses in human microvessels; (3) incremental inhibition of constrictor responses with combined L- and T- Ca^{2+} channel blockers despite maximal L-channel blockade; (4) the use of structurally diverse Ca^{2+} channel blockers with varied affinity for L- and T-channels; (5) the use of pharmacodynamically and therapeutically appropriate Ca^{2+} channel blocker concentrations; (6) confirmation of contractile agonist independent responses; and (7) exclusion of an endothelium-dependent mechanism. We propose that T-type channels play an important role in regulating contractile responses in the microvasculature and, therefore, are a potential therapeutic target. (*Hypertension*. 2009;53:654-660.)

Key Words: calcium ■ calcium channel blockers ■ vessels ■ vasoconstriction ■ vasculature

Calcium (Ca^{2+}) channel blockers (CCBs) have a major therapeutic role in the management of cardiovascular disorders, particularly as antihypertensive and antianginal agents. These clinical effects are mediated via the inhibition of transmembrane Ca^{2+} channels on vascular smooth muscle cells, thus reducing Ca^{2+} ion influx, resulting in reduced vascular smooth muscle contraction and vascular tone. Although chemically diverse, clinically established CCBs such as nifedipine (a dihydropyridine CCB) and verapamil (a phenylalkylamine CCB) mediate their effects via a common mechanism, namely the inhibition of the long-acting voltage-dependent Ca^{2+} channels (L-channel). In contrast, some new-generation CCBs, eg, mibefradil and efonidipine, have additional effects, such as inhibition of the transient Ca^{2+} channel (T-channel).¹

Although the clinical benefits of L-channel blockade are well established, the benefits of T-channel blockade remain less clear. Previous clinical studies have suggested that T-channel blockade may have incremental antianginal benefits over L-channel blockade alone. For example, the Posicor Reduction of Ischaemia During Exercise Study² demonstrated improved exercise treadmill parameters with mibefradil compared with diltiazem (a

benzothiazepine L-CCB). Moreover, in patients with microvascular dysfunction, on background verapamil therapy, a single dose of mibefradil substantially improved coronary angiographic flow.³ Similarly, the antihypertensive literature reports unique benefits of efonidipine in reducing proteinuria in hypertensive patients with renal impairment, unlike conventional L-CCBs.⁴ Consistent with this renal effect, Hayashi et al⁵ have demonstrated that T-CCBs dilate both afferent and efferent glomerular arterioles, whereas L-CCBs dilate only the afferent microvessels, thereby explaining the apparent differential benefits of efonidipine compared with conventional L-CCBs in reducing proteinuria.

The above clinical benefits may be attributable to differential vascular expression of L- and T-channels. Gustafsson et al⁶ demonstrated the presence of T-channel mRNA but an absence of detectable levels of L-channel mRNA in microvessels <40 μm in diameter. However, in contrast to these findings, Moosmang et al⁷ demonstrated that mibefradil's blood pressure lowering and increased hindlimb perfusion effects were absent in an L-channel conditional knockout mouse model, thereby proposing that mibefradil's vascular effects were mediated via the L-channel only.

Received October 31, 2008; first decision November 26, 2008; revision accepted January 21, 2009.

From the Cardiology Research Laboratory, Queen Elizabeth Hospital (C.J.B., D.P.W., S.P.T., J.F.B.), and Department of Physiology, School of Molecular and Biomedical Science (D.P.W., D.A.S., J.F.B.), University of Adelaide, Adelaide, Australia.

Correspondence to John F. Beltrame, Cardiology Research Laboratory, Queen Elizabeth Hospital, University of Adelaide, 28 Woodville Rd, Woodville South, SA 5011, Australia. E-mail john.beltrame@adelaide.edu.au

© 2009 American Heart Association, Inc.

Hypertension is available at <http://hyper.ahajournals.org>

DOI: 10.1161/HYPERTENSIONAHA.108.125831

The above clinical, pathophysiological, and genetic studies suggest that there may be both species differences and perhaps a differential distribution of L- and T-channels in the vasculature. However, these findings have received little attention and, hence, there are no detailed comparative studies evaluating segmental heterogeneity in vascular Ca^{2+} channels. Thus, the primary objectives of this study were to determine, in human and rat models, whether there were functional differences in responses to L- and T-channel blockade based on vessels size and to identify the relative distribution of these channels in the large and small vessels.

Methods

To achieve the above objectives, both "functional" vasomotor studies using an *in vitro* myograph model and "structural" Ca^{2+} channel quantification studies using quantitative western blot analysis were undertaken. These studies were performed on rat vascular tissues derived from large (thoracic aorta) or small (mesenteric) vascular segments. Adult male Sprague-Dawley rats, aged 8 weeks and weighing ≈ 400 g, were euthanized under fluorothane anesthesia and 2-mm segments from the above vessels excised.

In addition to the rat vessels, human subcutaneous microvessels were obtained from patients undergoing elective lower abdominal surgery to determine the applicability of the microvascular vasomotor findings in a human model. Patients without a history of cardiovascular disease and not prescribed vasoactive agents were recruited preoperatively, and written consent was obtained. These investigations were approved by the institutional animal and human ethics committees, respectively.

Functional Vasomotor Studies

Myograph Preparation

Rat aorta (large) and mesenteric (small) vessels were mounted in a wire myograph (multi myograph model 610 M, Danish Myo Technology) and the resting tension normalized using the procedure described by Mulvany and Aalkjaer.⁸ This normalizing method provides a resting tension equivalent to a vessel circumference of 90% of the value at 100-mm Hg intraluminal pressure. Accordingly, comparisons between vessels of different sizes can be undertaken, because they have proportionate resting tensions. The vessels were continually bathed in Krebs solution at 37°C and gassed with Carbogen (95% oxygen, 5% carbon dioxide). The Krebs solution was of the following composition (mmol/L): NaCl (118), KH_2PO_4 (1.18), NaHCO_3 (25), MgCl_2 (1.05), CaCl_2 (2.34), EDTA (0.01), and glucose (5.56; pH 7.4). After a 30-minute equilibration, baseline contractile responses to a depolarizing solution, potassium physiological salt solution (112 mmol/L), were repetitively evaluated until reproducible responses were obtained. Potassium physiological salt solution was obtained by replacing the NaCl in Krebs with isosmolar potassium chloride (KCl). The mean of the final 2 potassium physiological salt solution responses was used as a reference value for other contractile responses.

After establishing a concentration-response curve to phenylephrine, vessels were precontracted to 75% of the maximal response and endothelial integrity assessed with incremental doses of an endothelium-dependent vasodilator (bradykinin [BK] 0.001 to 3.000 $\mu\text{mol/L}$ for human microvessels; acetylcholine [ACh] 0.001 to 30.000 $\mu\text{mol/L}$ for rat vessels). The endothelium was considered intact if the contractile response was reduced $>80\%$ by the endothelium-dependent vasodilator. To determine the influence of the endothelium on the CCB responses, the endothelium was removed in selected vessels, and loss of endothelial integrity was confirmed using ACh.

Study Protocol

The experimental protocol used a paired-sample design with 1 vascular segment incubated in the study CCB and the other in the drug vehicle, thereby providing both a temporal and vehicle control.

The vascular rings were incubated for a 30-minute period with an L-CCB (verapamil or nifedipine), a combined L- and T-channel blocker (efonidipine or mibefradil), or the corresponding vehicle control. After this incubation period, vasoconstrictor agents (endothelin-1 [Et-1] or KCl) were administered and contractile responses recorded using Chart 5 (ADI Instruments).

The study involved 4 series of experiments. The first set of experiments explored the vasomotor effects of various CCB concentration ranges. Concentrations equivalent to the therapeutic plasma levels in CCB clinical studies were initially used. These included verapamil 1 $\mu\text{mol/L}$ (Abbott), nifedipine 1 $\mu\text{mol/L}$ (Sigma-Aldrich), mibefradil 1 $\mu\text{mol/L}$ (Sigma-Aldrich), and efonidipine 0.021 $\mu\text{mol/L}$ (Nissan Chemical Industries, Ltd). Ten-fold higher and lower CCB concentrations were then used to assess the comparative concentration ranges.

The second series of experiments assessed the effect of the various CCBs at their respective plasma therapeutic concentrations on receptor-mediated vasoconstrictor responses. In these experiments, incremental doses of Et-1 were administered and concentration-response curves obtained. Et-1 was selected as the agonist because of its sustained contractile responses and clinical relevance.

In a third series of experiments, the effect of administering an L- and T-type channel blocker on constrictor responses, in vessels exposed to maximal L-channel blockade, was assessed. This later experiment endeavored to "pharmacologically reproduce" the L-channel conditional knockout model established by Moosmang et al⁷ and to shed light on the use of combined L- and T-channel blockade in patients on existing CCB therapy.

Finally, the effect of the various CCBs at their therapeutic plasma concentrations on depolarizing-mediated constrictor responses with 87 mmol/L of KCl was assessed.

Data Analysis

The inhibition of Et-1 and KCl contractions in response to the CCBs were expressed as a percentage of the mean potassium physiological salt solution responses. For Et-1 constrictor responses, sigmoid curves of best fit were constructed using nonlinear regression (GraphPad Prism, version 4.0a) with the EC_{50} and the concentration for maximal response (E_{max}) subsequently derived. For KCl-mediated depolarization responses, initial contraction was calculated for each CCB. Comparisons between CCBs in EC_{50} , E_{max} , and initial contraction were assessed using ANOVA with Bonferroni correction. Data were presented as means \pm SEMs, $P < 0.05$ was considered statistically significant, and "n" refers to the number of samples taken from independent experimental units.

Structural Quantification of Pore-Forming Subunits of Ca^{2+} Channels

Quantitative western blot analysis was used to identify the abundance of the pore-forming subunits of L- ($\text{Ca}_v1.2$) and T- ($\text{Ca}_v3.1$, $\text{Ca}_v3.2$) channels in the large and small vessels. Specific antibodies included the following: (1) anti- $\text{Ca}_v1.2$, which recognizes the $\alpha 1\text{C}$ subunit of the L-channel (polyclonal, rabbit IgG, Chemicon); (2) anti- $\text{Ca}_v3.1$, which recognizes the $\alpha 1\text{G}$ subunit of the T-channel (polyclonal, rabbit IgG, Sigma-Aldrich); and (3) anti- $\text{Ca}_v3.2$, which recognizes the $\alpha 1\text{H}$ subunit of the T-channel (polyclonal, rabbit IgG, Sigma-Aldrich).

Protein Extraction

The $\alpha 1$ subunits of the L-channel are known to be highly sensitive to proteases; therefore, to prevent degradation, all of the protein samples were extracted in the presence of Calpain Inhibitor 1 (Calbiochem) and broad-spectrum protease inhibitor Complete Mini tablets (Roche Applied Sciences). The vessels were extracted in an aqueous solution containing a 1:10 dilution of the calpain/protease inhibitor mix, 1 mmol/L of dithiothreitol, 50 mmol/L of Tris (pH 6.8), 30% glycerol, 0.001% bromophenol blue, and 2% sodium dodecyl sulfate. After extraction, the samples were heated to 70°C for 5 minutes.

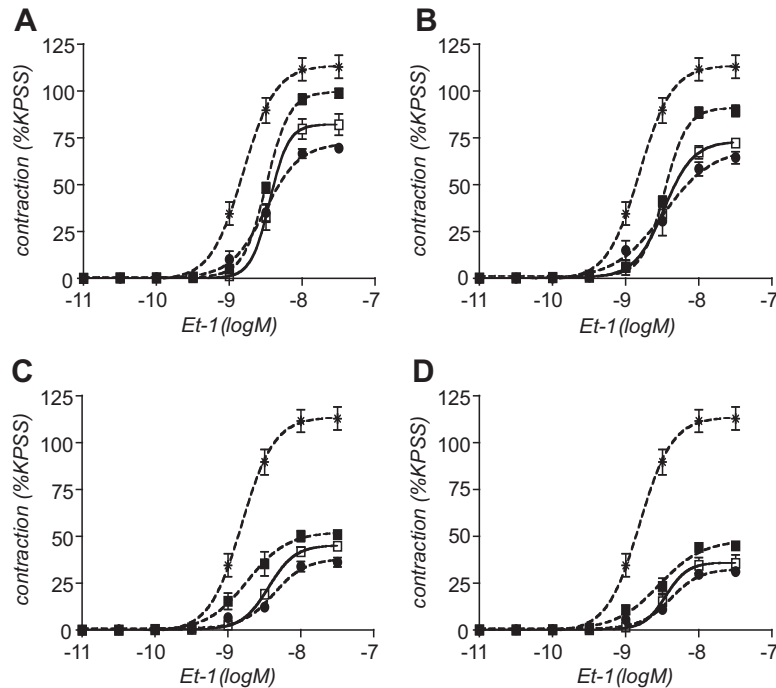


Figure 1. CCB dose-ranging study. Inhibition of Et-1 concentration response curves by (A) verapamil (■, 0.1 $\mu\text{mol/L}$; □, 1.0 $\mu\text{mol/L}$; ●, 10 $\mu\text{mol/L}$; *, 0 $\mu\text{mol/L}$), (B) nifedipine (■, 0.1 $\mu\text{mol/L}$; □, 1.0 $\mu\text{mol/L}$; ●, 10 $\mu\text{mol/L}$; *, 0 $\mu\text{mol/L}$), (C) efonidipine (■, 0.0021 $\mu\text{mol/L}$; □, 0.021 $\mu\text{mol/L}$; ●, 0.21 $\mu\text{mol/L}$; *, 0 $\mu\text{mol/L}$), and (D) mibefradil (■, 0.1 $\mu\text{mol/L}$; □, 1.0 $\mu\text{mol/L}$; ●, 10 $\mu\text{mol/L}$; *, 0 $\mu\text{mol/L}$). In each instance, □ represents the therapeutic plasma concentrations, and * represents control/solvent vehicle for rat mesenteric microvessels ($n=5$).

Western Blotting Procedure

Vessel samples were analyzed by SDS-PAGE, coomassie brilliant blue staining, and western blot. Densitometric scanning of stained gels and western blots enabled us to adjust sample volumes to ensure equal loading of samples and, importantly, to ensure that samples were in the linear range for quantitative western blot analysis. Total protein extracts were analyzed using 7.5% mini-gels and run with SDS-PAGE at 200 volts for 1 hour. Proteins were electrophoretically transferred onto 0.2- μm nitrocellulose membranes, followed by blocking of nonspecific antibody interacting sites using 5% nonfat dried milk powder in Tris-buffered saline (25 mmol/L of Tris-HCl [pH 7.5] and 150 mmol/L of NaCl) containing 0.01% Tween 20 (TBS-T), solution for 1 hour. Antibody detection of the pore-forming subunit of voltage-sensitive Ca^{2+} channels was carried out in solutions containing 1% nonfat dried milk powder in Tris-buffered saline with 0.01% Tween 20 containing the anti- $\text{Ca}_v1.2$ antibody (1:500 dilution), anti- $\text{Ca}_v3.1$ antibody (1:500), or anti- $\text{Ca}_v3.2$ antibody (1:2000) each for 1 hour. Membranes were washed and then incubated with an antirabbit IgG-horseradish peroxidase-conjugated secondary antibody for 1 hour (1:10 000 dilution). Blots were then briefly exposed to enhanced chemiluminescence reagents and signals detected using autoradiographic film.

Protein Quantification

To quantify the relative abundance of the pore-forming subunit of each Ca^{2+} channel present in the large and small vessels, the autoradiographic exposures of the western blots were scanned (BioRad GS-710 Imaging Densitometer) and the channel signal in each lane determined with the program QuantityOne. The coomassie blue stained gel was also scanned to identify equivalent protein loading in each lane. The abundance of all of the Ca^{2+} channels was represented as the ratio of optical density for T/L channels to account for minor differences in protein loading. Statistical differences were calculated using Student *t* tests with $P < 0.05$ taken to be significant and "n" referring to the number of samples taken from independent experimental units.

Results

Functional Vasomotor Studies

Ca^{2+} Channel Blocker Concentrations

The initial experiments exploring the CCB concentration ranges were undertaken in rat mesenteric vessels ($n=5$ per CCB) with

Et-1-induced constrictor responses. As illustrated in Figure 1, the maximal inhibition produced by the therapeutic plasma level equivalent concentration for verapamil and nifedipine was similar to that produced by the 10-fold higher concentration, suggesting near maximal effects for the L-CCBs at the therapeutic plasma level (E_{max} : verapamil 1 $\mu\text{mol/L}=82 \pm 6\%$, 10 $\mu\text{mol/L}=72 \pm 3\%$, $P > 0.05$; nifedipine 1 $\mu\text{mol/L}=76 \pm 3\%$, 10 $\mu\text{mol/L}=67 \pm 2\%$, $P > 0.05$). For the combined L- and T-CCBs, the therapeutic plasma concentrations used were also near maximal (E_{max} : efonidipine 0.021 $\mu\text{mol/L}=45 \pm 2\%$, 0.21 $\mu\text{mol/L}=41 \pm 4\%$, $P > 0.05$; mibefradil 1 $\mu\text{mol/L}=36 \pm 4\%$, 10 $\mu\text{mol/L}=29 \pm 2\%$, $P > 0.05$). Furthermore, there were no significant differences in the Et-1 EC_{50} s across the CCB concentration ranges for any of the CCBs. Hence, comparisons between the exclusive L-channel blockers (verapamil and nifedipine) with the combined L- and T-channel blockers (efonidipine and mibefradil) are both of pharmacodynamic and therapeutic relevance.

Receptor-Mediated Depolarization

Rat Aortic Vessel Responses

The aortic rings had a mean diameter of $2055 \pm 35 \mu\text{m}$ and intact endothelium-dependent vasodilator responses with a mean maximal ACh relaxation of $91 \pm 1\%$ ($n=7$). As shown in Figure 2A, pretreatment with verapamil, nifedipine, efonidipine, or mibefradil significantly reduced Et-1 contractile responses compared with control (E_{max} : $83 \pm 6\%$, $79 \pm 5\%$, $96 \pm 3\%$, and $100 \pm 4\%$ versus control $159 \pm 6\%$, respectively; $P < 0.05$). However, as shown in the Table, there is no difference between the CCBs in the extent of inhibition of the maximal Et-1 contractile responses.

Rat Microvascular Responses

Rat mesenteric microvessels had a mean diameter of $304 \pm 7 \mu\text{m}$ and intact endothelium-dependent vasodilator responses with a mean maximal ACh relaxation of $87 \pm 2\%$ ($n=6$). Pretreatment

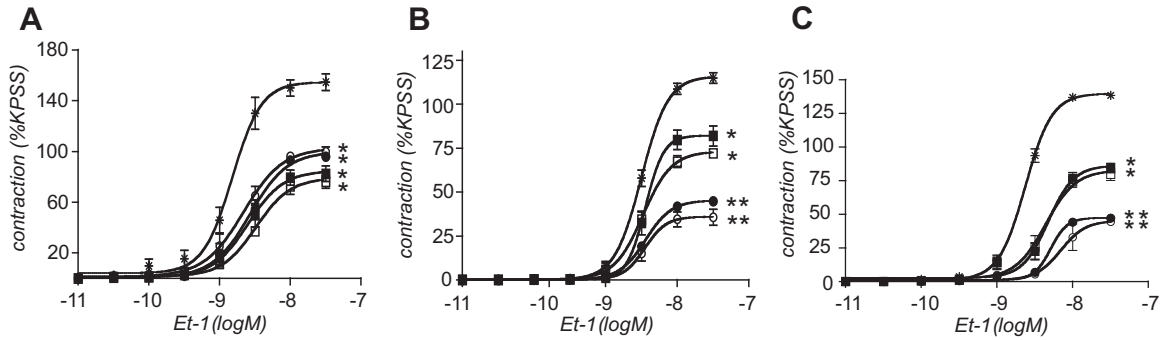


Figure 2. Et-1-mediated developed tension in rat aortic and mesenteric vessels in the presence of CCBs. Concentration-response curves to Et-1 after 30-minute incubation with verapamil (1 $\mu\text{mol/L}$, ■), nifedipine (1 $\mu\text{mol/L}$, □), efonidipine (0.021 $\mu\text{mol/L}$, ●), mibefradil (1 $\mu\text{mol/L}$, ○), or control/solvent vehicle (*). A, In rat aorta, there was a significant inhibition of the Et-1 E_{max} between the control and each of the CCBs, although the extent of inhibition was not different between the CCBs (n=7). B, In rat mesenteric microvessels, there was also a significant inhibition of the Et-1 E_{max} by each of the CCBs; however, the combined L- and T-channel blockers produced greater inhibition than the L-channel blockers (n=6). C, In endothelium-denuded rat mesenteric microvessels, the differential inhibitory effects of the combined L- and T-channel blockers compared with the L-channel blockers remained evident (n=6).

with verapamil, nifedipine, efonidipine, or mibefradil inhibited Et-1 contractile responses compared with control (E_{max} : $82 \pm 6\%$, $76 \pm 3\%$, $45 \pm 2\%$, and $36 \pm 4\%$ versus control $115 \pm 3\%$, respectively; $P < 0.05$; see Figure 2B). As shown in the Table, the combined L- and T-CCBs (efonidipine and mibefradil) inhibited Et-1 contractile responses almost twice as effectively as the L-CCBs (verapamil and nifedipine) in these microvessels.

In 6 independent experiments, the endothelium was removed from mesenteric microvessels (mean vessel diameter: $314 \pm 13 \mu\text{m}$) by gentle rubbing against the lumen of the vessel, and impaired endothelium-dependent vasodilatory responses were confirmed using ACh. Pretreatment with verapamil, nifedipine, efonidipine, or mibefradil in these endothelium-denuded vessels inhibited Et-1 contractile responses (E_{max} : $88 \pm 4\%$, $83 \pm 5\%$, $47 \pm 1\%$, and $45 \pm 3\%$, respectively, versus control $140 \pm 2\%$; $P < 0.05$; see Figure 2C). As shown in Figure 2C, the combined L- and T-CCBs (efonidipine and mibefradil) inhibited Et-1 contractile responses almost twice as effectively as the L-CCBs (verapamil and nifedipine) in these microvessels.

Human Subcutaneous Microvascular Responses

The 17 subjects (55 ± 4 years; 11 women) recruited to the study had no known history of cardiovascular disease, although several had cardiovascular risk factors, including hypercholesterolemia (29%), hypertension (24%), cigarette smoking (29%), and diabetes mellitus (12%). No patient was being prescribed vasodilator or statin therapy.

Subcutaneous microvessels were obtained during noncardiac surgery and mounted in the myograph. The mean vessel diameter (at resting normalized tension) was $289 \pm 14 \mu\text{m}$,

and endothelium-dependent vasodilator responses to BK were intact in all of the vessels with a mean maximal BK relaxation of $87 \pm 5\%$. The human microvascular responses to the CCBs were similar to those of the rat microvessels (Figure 3), with a significantly greater inhibitory effect on Et-1-mediated contractile responses by the combined L- and T-CCBs compared with L-channel blockade alone ($P < 0.05$; Table).

Inhibitory Effect of Efonidipine in Rat Microvessels With Maximal L-Channel Blockade

In rat mesenteric vessels pretreated with maximal L-channel blockers (either verapamil 10 $\mu\text{mol/L}$ or nifedipine 10 $\mu\text{mol/L}$), efonidipine was administered to ascertain whether there was incremental inhibition of the constrictor response with the combined L- and T-CCBs. Despite complete verapamil or nifedipine-mediated L-channel blockade, efonidipine produced incremental inhibition of Et-1 constrictor responses, suggesting that mechanisms other than L-channel blockade were involved (E_{max} difference relative to control: verapamil alone, $-49 \pm 3\%$; verapamil/efonidipine, $-64 \pm 3\%$; nifedipine alone, $-48 \pm 6\%$;

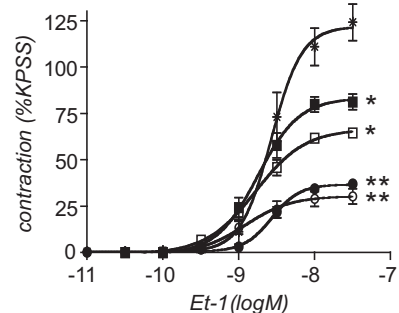


Figure 3. Effectiveness of L- and combined L- and T-channel blockade in human subcutaneous microvessels. Concentration-response curves to Et-1 in human subcutaneous microvessels after 30-minute incubation with verapamil (1 $\mu\text{mol/L}$, ■), nifedipine (1 $\mu\text{mol/L}$, □), efonidipine (0.021 $\mu\text{mol/L}$, ●), mibefradil (1 $\mu\text{mol/L}$, ○), or control/solvent vehicle (*). There was a significant inhibition of the Et-1 E_{max} between the control (123 \pm 8%) and each of the CCBs, verapamil (81 \pm 4%)*, nifedipine (66 \pm 1%)*, efonidipine (38 \pm 2%)**, and mibefradil (30 \pm 4%)** (* $P < 0.05$ vs control, ** $P < 0.05$ vs L-channel blockade; n=6).

Table. Change in Et-1 E_{max} by Various CCBs

ΔE_{max} Relative Control	L-Channel CCB		L- and T-Channel CCB	
	Verapamil	Nifedipine	Mibefradil	Efonidipine
Rat aorta	-69 \pm 1%	-75 \pm 11%	-68 \pm 9%	-65 \pm 9%
Rat microvessel*	-37 \pm 7%	-43 \pm 9%	-83 \pm 4%	-77 \pm 7%
Human microvessel*	-40 \pm 7%	-56 \pm 8%	-92 \pm 9%	-86 \pm 8%

*Data show the significant difference in reducing E_{max} by combined L- and T-channel blockers compared with L-channel blockers (ANOVA, $P < 0.05$).

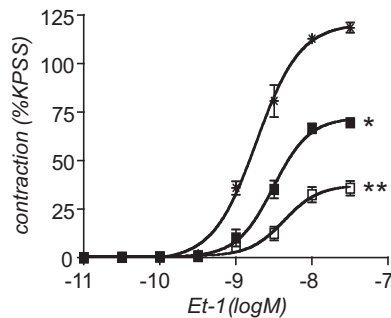


Figure 4. In the presence of maximal L-channel blockade, the addition of efonidipine reduces developed tension in rat mesenteric vessels. Concentration-response curves to Et-1 in the presence of verapamil (10 $\mu\text{mol/L}$, ■), verapamil (10 $\mu\text{mol/L}$)/efonidipine (0.21 $\mu\text{mol/L}$; □), or control/solvent vehicle (*) in rat mesenteric vessels. After incubation with the maximal verapamil concentration, there was a significant inhibition of the Et-1 E_{max} vs the control. However, in the presence of maximal verapamil followed by addition of efonidipine, there was a further significant inhibition of Et-1-mediated developed tension (verapamil alone: $70 \pm 2\%$ *; verapamil/efonidipine: $41 \pm 2\%$ ** vs control: $120 \pm 4\%$; * $P < 0.05$ vs control, ** $P < 0.05$ vs verapamil alone; $n = 5$).

nifedipine/efonidipine, $-67 \pm 2\%$; $P < 0.05$; $n = 5$; Figure 4, only verapamil data shown).

High Potassium-Mediated Depolarization

Rat Aorta Vessel Responses

As shown in Figure 5A, pretreatment with verapamil, nifedipine, efonidipine, or mibefradil significantly reduced the initial KCl contractile responses compared with control (KCl: $20 \pm 1\%$, $20 \pm 2\%$, $17 \pm 2\%$, $18 \pm 1\%$, respectively; $P < 0.05$; $n = 4$). However, there was no difference between the CCBs in the extent of inhibition of contraction.

Rat Mesenteric Vessel Responses

As expected, pretreatment with verapamil, nifedipine, efonidipine, or mibefradil significantly inhibited initial KCl contractile responses compared with control (KCl: $12 \pm 1\%$, $12 \pm 1\%$, $2 \pm 1\%$, and $3 \pm 2\%$, respectively; $P < 0.05$; $n = 4$; see Figure 5B). Furthermore, as observed with receptor-mediated responses, the combined L- and T-CCBs (efonidipine and mibefradil) inhibited KCl contractile responses to a greater extent than L-channel blockade alone (verapamil and nifedipine) in these microvessels.

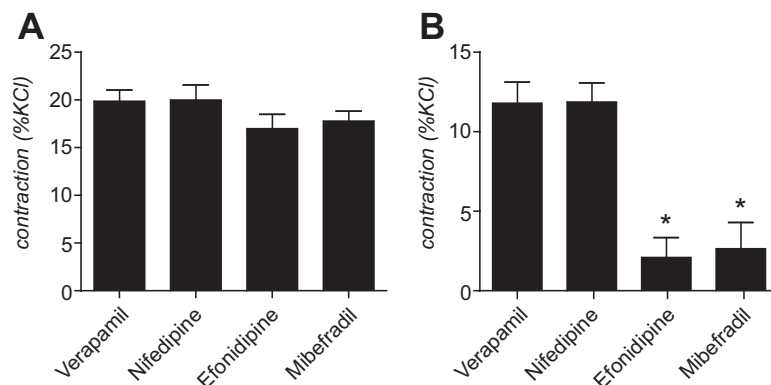


Figure 5. The role of L- and T-channels in depolarization-mediated extracellular Ca^{2+} entry in large and small vessels. Peak KCl contraction after 30-minute incubation with verapamil (1 $\mu\text{mol/L}$), nifedipine (1 $\mu\text{mol/L}$), efonidipine (0.021 $\mu\text{mol/L}$), mibefradil (1 $\mu\text{mol/L}$), or control/solvent vehicle. A, In rat aorta there was a significant inhibition of the peak KCl response between the control and individual CCBs but no difference between the CCBs ($n = 4$). B, In rat mesenteric microvessels, all of the CCBs significantly inhibited KCl contractile responses. Moreover, the combined L- and T-channel blockers (efonidipine and mibefradil) more effectively inhibited KCl responses compared with the L-channel blockers (* $P < 0.05$ L- and T-channel blockers vs L-channel blockade alone; $n = 4$).

Structural Ca^{2+} Channel Quantification Studies

Western Blotting Validation

To ensure accurate comparisons in quantitative western blotting, linear range experiments were performed for each tissue type and antibody. Sample loading beyond 10 μL was identified to be at saturation point, with the linear range for each tissue type between 5 and 10 μL and with r^2 values ranging from 0.98 to 1.00 (Figure 6).

Rat Vascular L- and T-Channel Abundance

Quantitative western blot analysis of $\text{Ca}_v1.2$ L-channel protein, $\text{Ca}_v3.1$ T-channel protein, and $\text{Ca}_v3.2$ T-channel protein in rat aorta revealed no relative differences in the amounts of channel expressed in these tissues. However, analysis of the rat mesenteric vessels identified a significant increase in the optical density of $\text{Ca}_v3.1$ T-channel (0.90 ± 0.05 OD) and $\text{Ca}_v3.2$ T-channel (1.23 ± 0.18 OD) compared with the $\text{Ca}_v1.2$ L-channel (0.47 ± 0.17 OD). Using radiometric analysis, these values equate to a significant increase of $112 \pm 38\%$ expression of the $\text{Ca}_v3.1$ T-channel and a significant increase of $163 \pm 48\%$ expression of the $\text{Ca}_v3.2$ T-channel ($n = 4$; Figure 7).

Discussion

The above experiments demonstrate segmental heterogeneity in vascular responses between conventional L-CCBs (verapamil and nifedipine) and newer agents with combined L- and T- Ca^{2+} channel-blocking properties (efonidipine and mibefradil). Specifically, we have identified that there were no differences between CCBs in the inhibition of contractile responses in the large conduit vessels; however, in the microvasculature of both humans and rats, combined L- and T-channel blockers were far more effective at attenuating contraction. The significance of this observation is further supported by the following: (1) a relative increase in the abundance of the pore-forming subunits $\text{Ca}_v3.1$ and $\text{Ca}_v3.2$ of the T-channel compared with the $\text{Ca}_v1.2$ subunit of the L-channel in the microvessels only (Figure 7); (2) consistent results in both human and animal models (Figures 2B and 3); (3) reproducibility with mechanistically different vasoconstrictor stimuli (ie, receptor-mediated Et-1 or depolarization-mediated KCl; Figures 2 and 5); (4) incremental inhibition of contractile responses by efonidipine in the presence of maximal L-channel blockade (Figure 4); (5) pairing of CCBs with similar effects on Ca^{2+} channels but different chemical structure (verapamil: phenylalkylamine; nifedipine and efonidipine: dihydro-

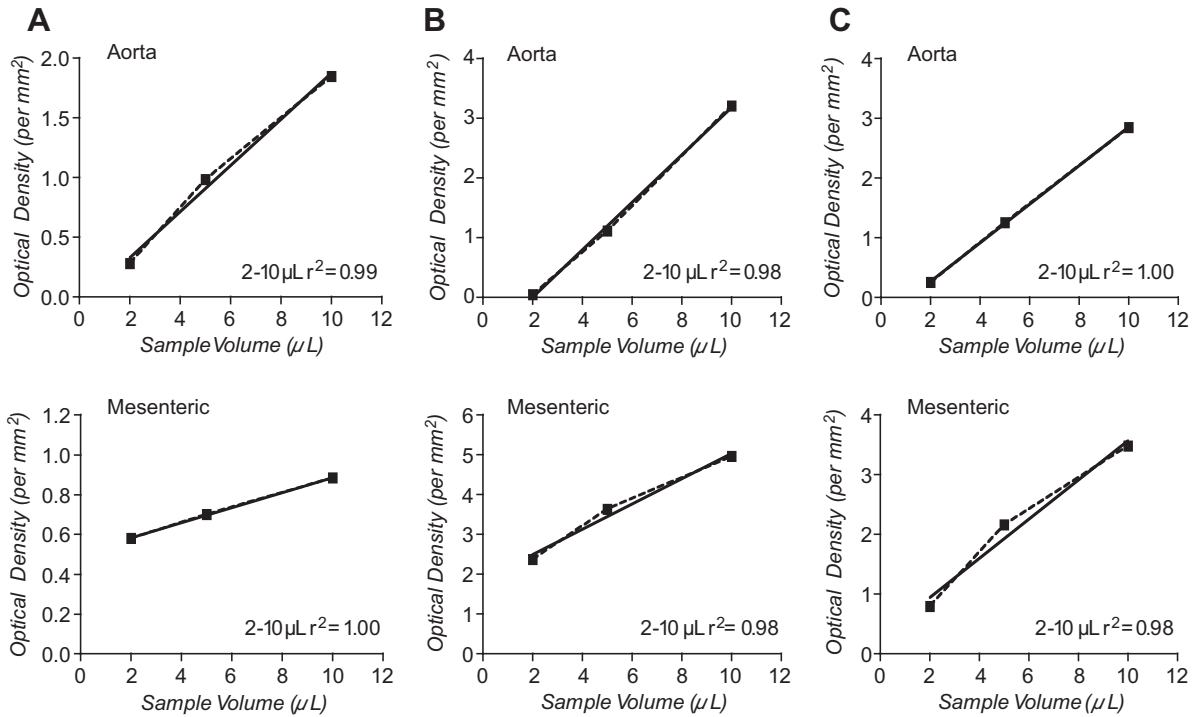


Figure 6. Relative quantitation of Ca^{2+} channels requires analysis of channels in the linear range. Linear analysis experiments for aorta and mesenteric tissue. A, Over a range of sample loadings, the L-channel demonstrated linearity for both the aorta and mesenteric tissue with r^2 values of 0.99 and 1.00, respectively. B, T-channel ($\text{Ca}_v3.1$) linear signal for the aorta and mesenteric tissue with r^2 values of 1.00 and 0.98, respectively. C, T-channel ($\text{Ca}_v3.2$) linear signal for the aorta and mesenteric tissue with r^2 values of 1.00 and 0.98, respectively.

pyridine; and mibefradil: benzimidazole); (6) the use of CCB concentrations that are near maximal for all of the CCBs and equivalent to their therapeutic plasma levels (Figure 1); and (7) exclusion of an endothelium-dependent mechanism (Figure 2B and 2C). These functional and structural findings suggest that

T-channels may play a significant role in human microvascular tone and provides a mechanism whereby combined L- and T-CCBs may have additional therapeutic benefits over conventional L-channel blockers.

Role of T-Channels in the Vasculature

Efonidipine^{9,10} and mibefradil¹¹ inhibit T-channel currents significantly more than the L-channel currents in isolated vascular smooth muscle preparations. Other investigators have also suggested that mibefradil may be more effective in the microvasculature. Kung et al¹² demonstrated that mibefradil dilates endothelin-contracted porcine small coronary vessels more effectively than larger coronary arteries. VanBavel et al¹³ showed that mibefradil is more potent than verapamil in inhibiting myogenic tone in rat cremasteric muscle arterioles.

Recently, Moosmang et al,⁷ using a conditional L-channel knockout mouse model, demonstrated a loss of mibefradil’s vasomotor effects, including impairment of its blood pressure-lowering effect and a reduction in its inhibition of vasoconstrictor effects in a hindlimb perfusion model. Appropriately, these researchers concluded that, in their mouse model, vasomotor effects of mibefradil were mediated exclusively via the L-channel. We have pharmacologically reproduced the inactivation of L-channels using maximal concentrations of the L-channel blockers (Figure 4). Our functional data with human and rat microvessels indicate that L-channel blockade inhibits contractile responses by approximately half. However, the addition of T-channel blockade in these microvessels results in a further 30% reduction in contractile responses. These data support the notion that there are species differences among both rodent models and humans.

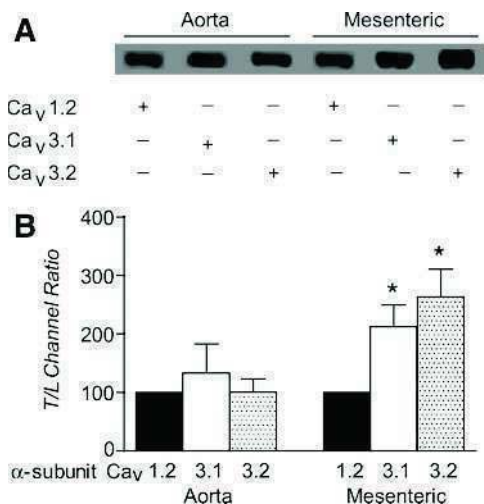


Figure 7. The relative abundance of the pore-forming subunits of $\text{Ca}_v1.2$ L-channel, $\text{Ca}_v3.1$ T-channel, and $\text{Ca}_v3.2$ T-channel in large and small vessels. A, Representative western blots using specific antibodies to the pore-forming subunits of $\text{Ca}_v1.2$, 3.1, or 3.2 in rat aorta and mesenteric vessels. B, To account for any variations in loading levels, cumulative data are expressed as a ratio of T/L channel abundance. There was a significant increase in the ratio of the pore-forming subunits of the 2 T-channels in small vessels; $\text{Ca}_v3.1$: $112 \pm 38\%$ increase*; $\text{Ca}_v3.2$: $163 \pm 48\%$ increase* vs L-channels but no difference in large vessels (* $P < 0.05$; $n = 4$).

Clinical Implications

The new-generation CCBs, which have combined L- and T-channel-blocking properties, appear to have incremental clinical benefits over the conventional L-CCBs. As demonstrated in this study, these 2 groups of CCB agents differ in their pharmacodynamic responses at the small resistance vessel level. Because these vessels play a pivotal role in the regulation of blood pressure, renal perfusion, and coronary blood flow, additional benefits of the newer agents could be expected in disorders relating to these circulations. For example, in a comparison of the antihypertensive effects of diltiazem (an L-channel blocker) and mibefradil, the combined L- and T-channel blocker reduced blood pressure to a greater extent than the L-channel blocker.¹⁴ Furthermore, efonidipine has also been shown to have these same antihypertensive effects.¹⁵

Studies of the glomerular microcirculation have demonstrated L-channels in the afferent but not the efferent arteriole, whereas T-channels are found in both types of glomerular microvessels.¹⁶ Thus, L-channel blockers predominantly dilate the afferent arteriole and may produce glomerular hypertension, whereas T-channel blockade does not. This may explain why efonidipine and mibefradil have been shown to reduce proteinuria in hypertensive patients with renal impairment, whereas L-channel blockers do not.⁵

The coronary slow-flow phenomenon is a coronary microvascular disorder characterized by the delayed passage of contrast during angiography reflecting the increased downstream resistance.¹⁷ Patients with this disorder on maintenance verapamil therapy still exhibit the angiographic phenomenon. However, the addition of mibefradil acutely improves angiographic flow.³ Furthermore, mibefradil was shown to alleviate the angina associated with this microvascular disorder.³ Mibefradil has also been shown to reduce myocardial ischemia more effectively than diltiazem in atherosclerotic coronary artery disease.² Our combination CCB experiments are consistent with these clinical findings such that the addition of efonidipine in the presence of maximal L-channel blockade produced incremental inhibition of microvascular constrictor responses.

Perspectives

The incremental microcirculatory benefits of the combined L- and T-channel blockers, efonidipine and mibefradil, over the conventional L-channel blockers are likely attributable to their additional T-channel blocking properties and the increased presence of T-channels compared with L-channels in the microvasculature of the rat. However, further studies aimed at quantifying T- and L-channels in the human vasculature and also defining the precise role of the T-channel with the newer CCBs and their role in the regulation of vascular tone are required. We believe that these studies provide a rational explanation for the beneficial effects of combined L- and T-channel blockers and provide the necessary data to warrant further investigation of the therapeutic value of these agents in cardiovascular conditions,

particularly in those involving increased microvascular resistance.

Acknowledgments

We acknowledge Nissan Chemical Industries Ltd (Tokyo, Japan) for their supply of the efonidipine.

Sources of Funding

C.J.B. is supported by a University of Adelaide and Queen Elizabeth Hospital Research Foundation Postgraduate Scholarship. J.F.B. is a National Heart Foundation of Australia Research Fellow.

Disclosures

None.

References

- Richard S. Vascular effects of calcium channel antagonists: new evidence. *Drugs*. 2005;65(suppl 2):1–10.
- Lee D, Goodman S, Dean D, Lenis J, Ma P, Gervais P, Langer A, PRIDE Investigators. Randomized comparison of T-type versus L-type calcium-channel blockade on exercise duration in stable angina: results of the Posicor Reduction of Ischaemia During Exercise (PRIDE) Trial. *Am Heart J*. 2002;144:60–67.
- Beltrame J, Turner S, Leslie S, Solomon P, Horowitz J. The angiographic and clinical benefits of mibefradil in the coronary slow flow phenomenon. *J Am Coll Cardiol*. 2004;44:57–62.
- Hayashi K, Kumagai H, Saruta T. Effect of efonidipine and ACE inhibitors on proteinuria in human hypertension with renal impairment. *Am J Hypertens*. 2003;16:116–122.
- Hayashi K, Wakino S, Sugano N, Ozawa Y, Homma K, Saruta T. Ca²⁺ channel subtypes and pharmacology in the kidney. *Circ Res*. 2007;100:342–353.
- Gustafsson F, Andreassen D, Salomonsson M, Jensen B, Holstein-Rathlou N. Conducted vasoconstriction in rat mesenteric arterioles: role for dihydropyridine-insensitive Ca(2+) channels. *Am J Physiol*. 2001;280:H582–H590.
- Moosmang S, Haider N, Bruderl B, Welling A, Hofmann F. Antihypertensive effects of the putative T-type calcium channel antagonist mibefradil are mediated by the L-type calcium channel Cav1.2. *Circ Res*. 2006;98:105–110.
- Mulvany M, Aalkjaer C. Structure and function of small arteries. *Physiol Rev*. 1990;70:921–961.
- Tanaka H, Shigenobu K. Efonidipine hydrochloride: a dual blocker of L- and T-type Ca(2+) channels. *Cardiovasc Drug Rev*. 2002;20:81–92.
- Lee T-S, Kaku T, Takebayashi S, Uchino T, Miyamoto S, Hadama T, Perez-Reyes E, Ono K. Actions of mibefradil, efonidipine and nifedipine block of recombinant T- and L-type Ca²⁺ channels with distinct inhibitory mechanisms. *Pharmacology*. 2006;78:11–20.
- Mishra S, Hermsmeyer K. Selective inhibition of T-type Ca²⁺ channels by Ro 40-5967. *Circ Res*. 1994;75:144–148.
- Kung C, Tschudi M, Noll G, Clozel J, Luscher T. Differential effects of the calcium antagonist mibefradil in epicardial and intramyocardial coronary arteries. *J Cardiovasc Pharmacol*. 1995;26:312–318.
- VanBavel E, Sorop O, Andreassen D, Pfaffendorf M, Jensen B. Role of T-type calcium channels in myogenic tone of skeletal muscle resistance arteries. *Am J Physiol*. 2002;283:H2239–H2243.
- Bittar N. Comparative antihypertensive effectiveness of once-daily mibefradil and diltiazem CD. Mibefradil hypertension study group. *Clin Ther*. 1997;19:954–962.
- Koh K, Quon M, Lee S, Han S, Ahn J, Kim J, Chung W, Lee Y, Shin E. Efonidipine simultaneously improves blood pressure, endothelial function, and metabolic parameters in nondiabetic patients with hypertension. *Diabetes Care*. 2007;30:1605–1607.
- Hansen P, Jensen B, Andreassen D, Skøtt O. Differential expression of T- and L-type voltage-dependent calcium channels in renal resistance vessels. *Circ Res*. 2001;89:560–562.
- Beltrame J. Chest pain and normal angiography. In: Braunwald E, ed. *Braunwald's Heart Disease Edition*. Vol 2006. Philadelphia, PA: Elsevier; 2006.

APPENDIX 2

JOURNAL OF THE AMERICAN HEART ASSOCIATION

Hypertension

Vascular Calcium L- & T-channel Distribution: A contributing factor to the observed efficacy of Combined L- and T-Blockers

David P. Wilson, Christine J Ball, Stuart P Turner, David A Saint, and John F. Beltrame
HYPERTENSION/2009/133850

You might find this additional information useful.

Topic Collections Articles on similar topics can be found in the following collections:
<http://hyper.ahajournals.org/cgi/collection>

Reviews You can submit your review by logging in at
<http://submit-hyper.ahajournals.org> and entering the Reviewer Area

Information about *Hypertension* can be found at:
<http://hyper.ahajournals.org>

To subscribe to *Hypertension*, please go to <http://hyper.ahajournals.org/subscriptions/>

Disclaimer: The manuscript and its contents are confidential, intended for journal review purposes only, and not to be further disclosed.

**Vascular Calcium L- & T-Channel Distribution:
A contributing factor to the observed efficacy of Combined L- and T-Blockers.**

Wilson, Combined Calcium L- & T-Channel Blockers.

David P. Wilson BSc (Hons), MSc, PhD^{1,2}

Christine J. Ball BSc (Hons)¹

Stuart P. Turner BMed, FRACP, PhD¹

David A. Saint BSc (Hons), PhD²

John F. Beltrame BSc, BMBS, FRACP, PhD, FESC, FACC, FCSANZ¹

1. Cardiology Research Laboratory, The Queen Elizabeth Hospital,
The University of Adelaide, Adelaide, Australia;

2. Department of Physiology, School of Molecular and Biomedical Science, The
University of Adelaide, Adelaide, Australia.

CORRESPONDENCE: Dr John F. Beltrame,
Cardiology Research Laboratory,
The Queen Elizabeth Hospital, University of Adelaide.
28 Woodville Road, Woodville South, SA 5011, Australia.
Phone: +61-8-8222 7632 Fax: +61-8-8222 6624
E-mail: john.beltrame@adelaide.edu.au.

WORD COUNT: 278

SUBJECT CODE: [118] Cardiovascular Pharmacology

MANUSCRIPT ID: HYPERTENSION/2009/133850 - Response to 133504

**Vascular Calcium L- & T-channel Distribution:
A contributing factor to the observed efficacy of Combined L- and T-Blockers.**

We acknowledge and endorse comments made by Professor Godfraind, that the response to calcium channel blockers (CCBs) is multifactorial. However, our data indicate that regional differences in calcium L- and T-channel abundance may be an important additional mechanism that accounts for differential responses to calcium channel blockers. Data from our previous and ongoing studies suggest that the greater inhibition of constrictor responses in microvessels by combined L- & T-channel blockers compared with the L-channel blockers, is independent of many of these alternate mechanisms.

Our studies focused upon the inhibition of constrictor responses by CCBs and therefore their ability to inhibit Ca^{++} channel activation and/or maintain an inactivated state. Both endothelin and depolarizing potassium solution responses were more effectively inhibited in microvessels by the combined L- & T-channel blockers than the L-channel blockers. We have also observed these differences with phenylephrine constrictor responses suggesting the inhibition of Ca^{++} channel activation (and/or maintenance of Ca^{++} channel inactivation) by the combined L- & T-channel blocker is more effective in the microvessels. Our ongoing studies are evaluating the relative contribution of the L- and T-channels in this phenomenon.

Regarding other non- Ca^{++} channel blocking effects of the CCBs, we excluded endothelial influences such as nitric oxide production by observing the phenomenon in endothelial denuded microvessels. Our ongoing studies are evaluating whether vascular disease states also influence the distribution of T- vs L-channels. These studies provide impetus for the further development of combined L- & T-channel blockers since these agents may provide incremental benefits in the treatment of cardiovascular disorders.

DP Wilson
CJ Ball
SP Turner
DA Saint
JF Beltrame

APPENDIX 3



DATE

CALCIUM L- AND T-CHANNEL DISTRIBUTION IN THE HUMAN
VASCULATURE

NAME

URN

DATE OF BIRTH.....

PROCEDURE

RISK FACTORS

Current Smoker	Y	Ncigs/d
Ex-Smoker	Y	Ncigs/d
Hypertension	Y	N
Diabetes	Y	N
Family History (CAD)	Y	N
Cholesterol > 5.5	Y	N

MEDICATIONS

B Blockers	Medication/Dosage details
CCB	Medication/Dosage details
ACE-inhibitors	Medication/Dosage details
Nitrates	Medication/Dosage details
Other	Medication/Dosage details

MEDICAL HISTORY

.....
.....
.....

REFERENCES

1. Davis M, Ferrer P, Gore R. Vascular anatomy and hydrostatic pressure profile in the hamster cheek pouch. *Am J Physiol* 1986;19(H291-303).
2. Johnson C. *Overview of the Microcirculation*. In: Tuma R, Duran W, Ley K, eds. *Handbook of Physiology: Microcirculation*. Oxford: Elsevier Science and Technology; 2008.
3. Schmid-Schoenbein G, Murakami H. Blood flow in contracting arterioles. *Int J Microcirc Clin Exp* 1985;4(4):311-28.
4. Merck. *Heart and Blood Vessel Disorders*. In: Tanser P, ed. *The Merck Manual: Home Health Handbook*; 1996.
5. Mulvany M. Investigations of resistance vessels. *Prog Appl Microcirc* 1985;8:1-6.
6. Davis M. Myogenic response gradient in an arteriolar network. *Am J Physiol* 1993;264(6 Pt 2):H2168-H79.
7. Fronck K, Zweifach B. Microvascular pressure distribution in skeletal muscle and the effect of vasodilation. *Am J Physiol* 1975;228(3):791-6.
8. Gore R, Bohlen H. Microvascular pressures in rat intestinal muscle and mucosal villi. *Am J Physiol* 1977;233(6):H685-H93.
9. Bohlen H, Gore R, Hutchins P. Comparison of microvascular pressures in normal and spontaneously hypertensive rats. *Microvasc Res* 1977;13(1):125-30.

10. Furchgott R, Zawadzki J. The obligatory role of endothelial cells in the relaxation of arterial smooth muscle by acetylcholine. *Nature* 1980;288:373-6.
11. Luscher T. Endothelium-derived vasoactive factors and regulation of vascular tone in human blood vessels. *Lung* 1990;168:27-34.
12. Luscher T, Richard V, Tschudi M, Yang Z, Boulanger C. Endothelial control of vascular tone in large and small coronary arteries. *JACC* 1990;15(3):519-27.
13. Munro J. Endothelial-leukocyte adhesive interactions in inflammatory disease. *Eur Heart J* 1993;14(Suppl K):72-7.
14. Stein C, Brown N, Vaughan D, Lang C, Wood A. Regulation of local tissue-type plasminogen activator release by endothelium-dependent and endothelium-independent agonists in human vasculature. *JACC* 1998;32(1):117-1122.
15. Murohara T, Horowitz J, Silver M, Tsurumi Y, Chen D, Sullivan A, Isner J. Vascular endothelial growth factor/vascular permeability factor enhances vascular permeability via nitric oxide and prostacyclin. *Circulation* 1998;97(1):99-107.
16. Sprague R, Bowles E, Hanson M, DuFaux E, Sridharan M, Adderley S, Ellsworth M, Stephenson A. Prostacyclin analogs stimulate receptor-mediated cAMP synthesis and ATP release from rabbit and human erythrocytes. *Microcirculation* 2008;15(5):561-471.

17. Kamata K, Hosokawa M, Matsumoto T, Kobayashi T. Acetylcholine-induced vasodilation in the perfused kidney of the streptozotocin-induced diabetic rat: role of prostacyclin. *J Smooth Muscle Res* 2006;42(5):159-70.
18. Peters K, De Vries C, Williams L. Vascular endothelial growth factor receptor expression during embryogenesis and tissue repair suggests a role in endothelial differentiation and blood vessel growth. *Proc Natl Acad Sci* 1993;90(19):8915-9.
19. Kubes P, Suzuki M, Granger D. Nitric oxide: an endogenous modulator of leukocyte adhesion. *Proc Natl Acad Sci* 1991;88(11):4651-5.
20. Gross P, Aird W. The endothelium and thrombosis. *Semin Thromb Hemost* 2000;26(5):463-78.
21. Wu K, Thiagarajan P. Role of endothelium in thrombosis and hemostasis. *Annu Rev Med* 1996;47:315-31.
22. Trepels T, Zeiher A, Fichtischerer S. The endothelium and inflammation. *Endothelium* 2006;13(6):423-9.
23. Pober J, Cotran R. The role of endothelial cells in inflammation. *Transplantation* 1990;50(4):537-44.
24. Maio-Ranta U, Yia-Herttuala S, Metsa-Ketela T, Jaakkola O, Moilanen E, Vuorinen P, Nikkari T. Nitric oxide donor GEA 3162 inhibits endothelial cell-mediated oxidation of low density lipoprotein. *FEBS Lett* 1994;337(2):179-83.

25. Jessup W, Mohr D, Giese S, Dean R, Stocker R. The participation of nitric oxide in cell free- and its restriction of macrophage-mediated oxidation of low density lipoprotein. *Biochim Biophys Acta* 1992;1180(1):73-82.
26. Ma X, Gao F, Liu G, Lopez B, Christopher T, Fukuto J, Wink D, Feelisch M. Opposite effects of nitric oxide and nitroxyl on postischemic myocardial injury. *Proc Natl Acad Sci* 1999;96(25):14617-22.
27. Marieb E. *The Cardiovascular System*. In: Essentials of Human Anatomy and Physiology (9th edition). San Francisco, California: Benjamin Cummins 2008.
28. Rosendorff C. Vascular hypertrophy in hypertension: role of the renin-angiotensin system. *Mt Sinai J Med* 1998;65(2):108-17.
29. O'Callaghan C, Williams B. The regulation of human vascular smooth muscle extracellular matrix protein production by alpha- and beta-adrenoceptor stimulation. *J Hypertens* 2002;20(2):287-94.
30. Majors A, Sengupta S, Jacobsen D, Pyeritz R. Upregulation of smooth muscle cell collagen production by homocysteine-insight into the pathogenesis of homocystinuria. *Mol Genet Metab* 2002;76(2):92-9.
31. Risler N, Castro C, Cruzado M, Gonzalez S, Miatello R. Proteoglycans production by aortic vascular smooth muscle cells from hypertensive rats. *Biocell* 2003;27(2):189-96.

32. Castro C, Cruzado M, Miatello R, Risler N. Proteoglycan production by vascular smooth muscle cells from resistance arteries of hypertensive rats. *Hypertension* 1999;34(4 Part 2):893-6.
33. Rafflenbeul W. Hypertension treatment and prevention of new atherosclerotic plaque formation. *Drugs* 1994;48(Suppl 1):11-5.
34. Hobara N, Nakamura A, Ohtsuka A, Narasaki M, Shibata K, Gomoita Y, Kawasaki H. Distribution of adrenomedullin-containing perivascular nerves in the rat mesenteric artery. *Peptides* 2004;25(4):589-99.
35. Scotland R, Vallance P, Ahluwalia A. Endogenous factors involved in regulation of tone of arterial vasa vasorum: implications for conduit vessel physiology. *Cardiovasc Res* 2000;46(3):403-11.
36. Laine P, Naukkarinen A, Heikkila L, Penttila A, Kovanen P. Adventitial mast cells connect with sensory nerve fibers in atherosclerotic coronary arteries. *Circulation* 2000;101(4):1665-9.
37. Laine P, Kaaerinen M, Penttila A, Panula P, Paavonen T, Kovanen P. Association between myocardial infarction and the mast cells in the adventitia of the infarct-related coronary artery. *Circulation* 1999;99(3):361-9.
38. Laflamme K, Roberge C, Grenier G, Remy-Zolghadri M, Poulliot S, Baker K, Labbe R, D'Orleans-Juste P, Auger F, Germain L. Adventitia contribution in vascular tone: insights from adventitia-derived cells in a tissue-engineered human blood vessel. *FASEB J* 2006;20:E516-E24.

39. Gonzalez M, Arribas S, Molero F, Fernandez-Alfonso M. Effect of removal of adventitia on vascular smooth muscle contraction and relaxation. *Am J Physiol Heart Circ Physiol* 2001;280(6):H2876-H81.
40. Darcy H. Les Fontaines Publiques de la Ville de Dijon. Dalmont, Paris; 1856.
41. Khan M, Furchgott R. *Additional evidence that endothelium-derived relaxing factor is nitric oxide*. In: Rand M, Roper C, eds. Pharmacology. Amsterdam: Elsevier; 1987.
42. Furchgott R. *Studies on relaxation of rabbit aorta by sodium nitrate: basis for the proposal that the acid-activatable component of the inhibitory factor from retractor penis is inorganic nitrate and the endothelium-derived relaxing factor is nitric oxide*. In: Vanhoutte P, ed. Mechanisms of Vasodilation. New York: Raven; 1988.
43. Moncada S, Gryglewski R, Bunting S, Vane J. An enzyme isolated from arteries transforms prostaglandin endoperoxides to an unstable substance that inhibits platelet aggregation. *Nature* 1976;263(5579):663-5.
44. Bolton T, Lang R, Takewaki T. Mechanisms of action of noradrenaline and carbachol on smooth muscle of guinea-pig anterior mesenteric artery. *J Physiol* 1984;351:549-72.
45. Lincoln T, Dey N, Sellak H. Invited review: cGMP-dependent protein kinase signaling mechanisms in smooth muscle: from the regulation of tone to gene expression. *J Appl Physiol* 2001;91(3):1421-30.

46. Terenghi G, Riveros-Moreno V, Hudson L, Ibrahim N, Polak J. Immunohistochemistry of nitric oxide synthase demonstrates immunoreactive neurons in spinal cord and dorsal root ganglion. *J Neurol Sci* 1993;118(1):34-7.
47. Ceccatelli S, Lundberg J, Zhang X, Aman K, Hokfelt T. Immunohistochemical demonstration of nitric oxide synthase in the peripheral autonomic nervous system. *Brain Res* 1994;646(2):381-95.
48. Seddon M, Melikian N, Dworakowski R, Shabeeh H, Jiang B, Byrne J, Casadei B, Chowienczyk P, Shah A. Effects of neuronal nitric oxide synthase on human coronary artery diameter and blood flow *in vivo*. *Circulation* 2009;119(20):2656-562.
49. Seddon M, Chowienczyk P, Brett S, Casadei B, Shah A. Neuronal nitric oxide synthase regulates basal microvascular tone in humans *in vivo*. *Circulation* 2008;117(15):1991-6.
50. Talman W, Nitschke Dragon D. Neuronal nitric oxide mediates cerebral vasodilation during acute hypertension. *Brain Res* 2007;1139:126-32.
51. Michel T, Lamas S. Molecular cloning of constitutive endothelial nitric oxide synthase: evidence for a family of related genes. *J Cardiovasc Pharmacol* 1992;20(Suppl 12):S45-S9.
52. Lamas S, Marsden P, Li G, Tempst P, Michel T. Endothelial nitric oxide synthase: molecular cloning and characterization of a distinct constitutive enzyme isoform. *Proc Natl Acad Sci* 1992;89(14):6348-52.

53. Balligand J, Kobzik I, Han X, Kaye D, Belhassen L, O'Hara D, Kelly R, Smith T, Michel T. Nitric oxide-dependent parasympathetic signaling is due to activation of constitutive endothelial (type III) nitric oxide synthase in cardiac myocytes. *J Biol Chem* 1995;270(24):14582-6.
54. Mehta J, Chen L, Kone B, Mehta P, Turner P. Identification of constitutive and inducible forms of nitric oxide synthase in human platelets. *J Lab Clin Med* 1995;125(3):370-7.
55. Takaki A, Morikawa K, Murayama Y, Tekes E, Yamagishi H, Ohashi J, Yada T, Yanahihara N, Shimokawa H. Crucial role of nitric oxide synthases system in endothelium-dependent hyperpolarisation in mice. *J Exp Med* 2008;205(9):2053-63.
56. Kleinert H, Schwarz P, Forstermann U. Regulation of the expression of inducible nitric oxide synthase. *Biol Chem* 2003;384(10-11):1343-64.
57. Kleinert H, Pautz A, Linker K, Schwartz P. Regulation of the expression of inducible nitric oxide synthase. *Eur J Pharmacol* 2004;500(1-3):255-66.
58. Korhonen R, Kankaanranta H, Lahti A, Lahde M, Knowles R, Molilanen E. Bi-directional effects of the elevation of intracellular calcium on the expression of inducible nitric oxide synthase in J774 macrophages exposed to low and high concentrations of endotoxin. *Biochem J* 2001;354(Pt 2):351-8.
59. Rapoport R, Draznin M, Murad F. Endothelium-dependent relaxation in rat aorta may be mediated through cyclic GMP-dependent protein phosphorylation. *Nature* 1983;306(5939):174-6.

60. Zhao G, Xu X, Ochoa M, Shen W, Hintze T. Interaction between prostacyclin and nitric oxide in the reflex control of the coronary circulation in conscious dogs. *Cardiovasc Res* 1996;32(5):940-8.
61. Gryglewski R, Moncada S, Palmer R. Bioassay of prostacyclin and endothelium-derived relaxing factor (EDRF) from porcine aortic endothelial cells. *Br J Pharmacol* 1986;87(4):685-94.
62. Chen G, Suzuki H, Weston A. Acetylcholine releases endothelium-derived hyperpolarising factor and EDRF from rat blood vessels. *Br J Pharmacol* 1988;95(4):1165-74.
63. Gainza F, Quintanilla N, Pijoan J, Delgado S, Urbizu J, Lampreabe I. Role of prostacyclin (epoprostenol) as anticoagulant in continuous renal replacement therapies: efficacy, security and cost analysis. *J Nephrol* 2006;19(5):648-55.
64. Langenecker S, Felfernig M, Werba A, Mueller C, Chiari A, Zimpfer M. Anticoagulation with prostacyclin and heparin during continuous venovenous hemofiltration. *Crit Care Med* 1994;22(11):1774-81.
65. Tan X, Chen Y, Liu Q, Gonzales-Crussi F, Liu X. Prostanoids mediate the protective effect of trefoil factor 3 in oxidant-induced intestinal epithelial cell injury: role of cyclooxygenas-2. *J Cell Sci* 2000;113(12):2149-55.
66. Blikslager A, Roberts M, Rhoads J, Argenzio R. Prostaglandins I2 and E2 have a synergistic role in rescuing epithelial barrier function in porcine ileum. *J Clin Invest* 1997;100(8):1928-33.

67. Yin H, Cheng L, Langenbach R, Ju C. Prostaglandin I(2) and E(2) mediate the protective effects of cyclooxygenase-2 in a mouse model of immune-mediated liver injury. *Hepatology* 2007;45(1):159-69.
68. Wang M, Sakon M, Miyoshi H, Umeshita K, Kishimoto S, Tanquchi K, Gotoh M, Imajoh-Ohmi S, Monden M. Prostacyclin analog-suppressed ischemia-reperfusion injury of the rat liver: evaluation by calpain mu activation. *J Surg Res* 1997;73(2):101-6.
69. Thiemermann C, Zacharowski K. Selective activation of E-type prostanoid(3)-receptors reduces myocardial infarct size. A novel insight into the cardioprotective effects of prostaglandins. *Pharmacol Ther* 2000;87(1):61-7.
70. Cargnoni A, Boraso A, Comini L, de Giuli F, Condorelli E, Pasini E, Ferrari R. Role of timing of administration in the cardioprotective effect of iloprost, a stable prostacyclin mimetic. *Eur J Pharmacol* 1991;199(2):165-78.
71. Reed M, Taylor B, Smith G, Phan T, Myers S. Splanchnic prostanoid production: effect of hemorrhagic shock. *J Surg Res* 1990;48(6):579-83.
72. Hocherl K, Schmidt C, Kurt B, Bucher M. Activation of the PGI(2)/IP system contributes to the development of circulatory failure in a rat model of endotoxic shock. *Hypertension* 2008;52(5):330-5.
73. Hajjar D. Prostaglandins and cyclic nucleotides: modulators of arterial cholesterol metabolism. *Biochem Pharmacol* 1985;34:295-300.

74. Willis A, Smith D, Vigo C, Kluge A. Effects of prostacyclin and orally stable mimetic agent RS-93427-007 on basic mechanisms of atherogenesis. *Lancet* 1987;2(8508):682-3.
75. Phillips P, Long L, Wilkins M, Morrell N. cAMP phosphodiesterase inhibitors potentiate effects of prostacyclin analogs in hypoxic pulmonary vascular remodeling. *Am J Physiol Lung Cell Mol Physiol* 2005;288(1):L103-L15.
76. Zellers T, Wu Y, McCormick J, Vanhoutte P. Prostacyclin-induced relaxations of small porcine pulmonary arteries are enhanced by the basal release of endothelium-derived nitric oxide through an effect on cyclic GMP-inhibited-cyclic AMP phosphodiesterase. *Acta Pharmacol Sci* 2000;21(2):131-8.
77. Yada T, Shimokawa H, Hiramatsu O, Kajita T, Shigeto F, Goto M, Ogasawara Y, Kajiya F. Hydrogen peroxide, an endogenous endothelium-derived hyperpolarizing factor, plays an important role in coronary autoregulation *in vivo*. *Circulation* 2003;107(7):1040-5.
78. Matoba T, Shimokawa H, Nakashima M, Hirakawa Y, Mukai Y, Hirano K, Kanaide H, Takeshita A. Hydrogen peroxide is an endothelium-derived hyperpolarizing factor in mice. *J Clin Invest* 2000;106(12):1521-30.
79. Villar I, Panayiotou C, Sheraz A, Madhani M, Scotland R, Nobles M, Kemp-Harper B, Ahluwalia A, Hobbs A. Definitive role of natriuretic peptide receptor-C in mediating the vasorelaxant activity of C-type natriuretic peptide and endothelium-derived hyperpolarising factor. *Cardiovasc Res* 2007;74(3):515-25.

-
80. Honing M, Smits P, Morrison P, Burnett J, Rabelink T. C-type natriuretic peptide-induced vasodilation is dependent on hyperpolarization in human forearm resistance vessels. *Hypertension* 2001;37(4):1179-83.
 81. Campbell W, Harder D. Endothelium-derived hyperpolarizing factors and vascular cytochrome P450 metabolites of arachidonic acid in the regulation of tone. *Circ Res* 1999;84(4):484-8.
 82. Randall M, Kendall D. Anandamide and endothelium-derived hyperpolarizing factor act via a common vasorelaxant mechanism in rat mesentery. *Eur J Pharmacol* 1998;346(1):51-3.
 83. Edwards G, Dora K, Gardener M, Garland C, Weston A. K⁺ is an endothelium-derived hyperpolarizing factor in rat arteries. *Nature* 1998;396(6708):269-72.
 84. Doughty J, Boyle J, Langton P. Potassium does not mimic EDHF in rat mesenteric arteries. *Br J Pharmacol* 2000;130(5):1174-82.
 85. Ceroni L, Ellis A, Wiehler W, Jiang Y, Ding H, Triggle C. Calcium-activated potassium channel and connexin expression in small mesenteric arteries from eNOS-deficient (eNOS ^{-/-}) and eNOS-expressing (eNOS ^{+/+}) mice. *Eur J Pharmacol* 2007;560(2-3):193-200.
 86. Si H, Heyken W, Wölfle S, Tysiac M, Schubert R, Grgic I, Villanovich L, Gieberg G, Maier T, Gross V, Bader M, de Wit C, Hoyer J, Kohler R. Impaired endothelium-derived hyperpolarizing factor-mediated dilations and increased blood pressure in mice deficient of the intermediate-conductance Ca²⁺-activated K⁺- channel. *Circ Res* 2006;99(5):537-44.
-

87. Parkington H, Chow J, Evans R, Coleman H, Tare M. Role of endothelium-derived hyperpolarizing factor in vascular tone in rat mesenteric and hindlimb circulations *in vivo*. *J Physiol* 2002;542(3):929-37.
 88. Miura H, Gutterman D. Human coronary arteriolar dilation to arachidonic acid depends on cytochrome P-450 monooxygenase and Ca²⁺-activated K⁺ channels. *Circ Res* 1998;83(5):501-7.
 89. Drummond G, Cocks T. Evidence for mediation by endothelium-derived hyperpolarizing factor of relaxation to bradykinin in the bovine isolated coronary artery independent of voltage-operated Ca²⁺ channels. *Br J Pharmacol* 1996;445:355-67.
 90. Nagao T, Vanhoutte P. Hyperpolarisation as a mechanism for endothelium-dependent relaxation in the porcine coronary artery. *J Physiol* 1992;445:355-67.
 91. Nagao T, Illiano S, Vanhoutte P. Calmodulin antagonists inhibit endothelium-dependent hyperpolarisations in canine coronary artery. *Br J Pharmacol* 1992;445:355-67.
 92. Dora K, Gallagher N, McNeish A, Garland C. Modulation of endothelial cell KCa3.1 channels during endothelium-derived hyperpolarizing factor signaling in mesenteric resistance arteries. *Circ Res* 2008;102(10):1247-55.
 93. Hilgers R, Todd J, Webb R. Regional heterogeneity in acetylcholine-induced relaxation in rat vascular bed: role of calcium-activated K⁺ channels. *Am J Physiol Heart Circ Physiol* 2006;291(1):H216-H22.
-

94. Coats P, Johnston F, MacDonald J, McMurray J, Hillier C. Endothelium-derived hyperpolarizing factor: identification and mechanisms of action in human subcutaneous resistance arteries. *Circulation* 2001;103(12):1702-8.
95. Inoue A, Yanagisawa M, Kimura S, Kasuya Y, Miyauchi T, Goto K, Masaki T. The human endothelin family: three structurally and pharmacologically distinct isopeptides predicted by three separate genes. *Proc Natl Acad Sci* 1989;86(8):2863-7.
96. Fagan K, McMurtry I, Rodman D. Role of endothelin-1 in lung disease. *Respir Res* 2001;2(2):90-101.
97. Lipa J, Neligan P, Perreault T, Baribeau J, Levine R, Knowlton R, Pang C. Vasoconstrictor effect of endothelin-1 in human skin: a role of ETA and ETB receptors. *Am J Physiol* 1999;276(2 Part 2):H359-H67.
98. Clarke J, Benjamin N, Larkin S, Webb D, Davies G, Maseri A. Endothelin is a potent long-lasting vasoconstrictor in men. *Am J Physiol* 1989;257(6 Part 2):H2033-H5.
99. Goto K, Kasuya Y, Matsuki N, Takuwa Y, Kurihara H, Ishikawa T, Kimura S, Yanagisawa M, Masaki T. Endothelin activates the dihydropyridine-sensitive, voltage-dependent Ca²⁺ channel in vascular smooth muscle. *Proc Natl Acad Sci* 1989;86(10):3915-8.
100. Yanagisawa M, Kurihara H, Kimura S, Tomobe Y, Kobayashi M, Mitsui Y, Yazaki Y, Goto K, Masaki T. A novel potent vasoconstrictor peptide produced by vascular endothelial cells. *Nature* 1988;332(6163):411-5.

101. Masuo Y, Ishikawa Y, Kozakai T, Uchide T, Komatsu Y, Saida K. Vasoactive intestinal contractor/endothelin-2 gene expression in the murine central nervous system. *Biochem Biophys Res Comm* 2003;300(3):661-8.
102. Takizawa S, Uchide T, Adur J, Kozakai T, Kotake-Nara E, Quan J, Saida K. Differential expression of endothelin-2 along the mouse intestinal tract. *J Mol Endocrinol* 2005;35(2):201-9.
103. Matsumoto H, Suzuki N, Onda H, Fujino M. Abundance of endothelin-3 in rat intestine, pituitary gland and brain. *Biochem Biophys Res Comm* 1989;164(1):74-80.
104. Terada Y, Tomita K, Nonoguchi H, Yang T, Marumo F. Expression of endothelin-3 mRNA along rat nephron segments using polymerase chain reaction. *Kidney Int* 1993;44(6):1273-80.
105. Sakamoto A, Yanagisawa M, Sakurai T, Takuwa Y, Yanagisawa H, Masaki T. Cloning and functional expression of human cDNA for the ETB endothelin receptor. *Biochem Biophys Res Comm* 1991;178(2):656-66.
106. Sakurai T, Yanagisawa M, Takuwa Y, Miyazaki H, Kimura S, Goto K, Masaki T. Cloning of a cDNA encoding a non-isopeptide-selective subtype of the endothelin receptor. *Nature* 1990;348(6303):732-5.
107. Kedzierski R, Yanagisawa M. Endothelin system: the double-edged sword in health and disease. *Annu Rev Pharmacol and Toxicol* 2001;41(851-876).

108. Simonson M, Herman W. Protein kinase C and protein tyrosine kinase activity contribute to mitogenic signaling by endothelin-1: cross-talk between G protein-coupled receptors and pp60c-src. *J Biol Chem* 1993;268:9347-57.
109. Ono K, Tsujimoto G, Sakamoto A, Eto K, Masaki T, Ozaki V, Satake M. Endothelin-A receptor mediators cardiac inhibition by regulating calcium and potassium currents. *Nature* 1994;370:301-4.
110. Kang H, Kang W, Lee C. Endothelin-B receptor-mediated Ca^{2+} signaling in human melanocytes. *Pflugers Arch* 1998;435(3):350-6.
111. Pang C, Zhang J, Xu H, Lipa J, Forrest C, Neligan P. Role and mechanism of endothelin-B receptors in mediating ET-1 induced vasoconstriction in pig skin. *Am J Physiol* 1998;275(4 Part 2):R1066-R74.
112. Guntupalli J, DuBose T. Effects of endothelin on rat renal proximal tubule Na^+ -Pi cotransport and Na^+ / H^+ exchange. *Am J Physiol* 1994;266(4 Part 2):F658-F66.
113. Eiam-Ong S, Hilden S, King A, Johns C, Madias N. Endothelin-1 stimulates the Na^+ / H^+ and Na^+ / HCO_3^- transporters in rabbit renal cortex. *Kidney Int* 1992;42(1):18-24.
114. Davie N, Haleen S, Upton P, Polak J, Yacoub M, Morrell N, Wharton J. ET(A) and ET(B) receptors modulate the proliferation of human pulmonary artery smooth muscle cells. *Am J Respir Crit Care Med* 2002;165(3):398-405.

115. Kohan D, Padilla E, Hughes A. Endothelin B receptor mediates ET-1 effects on cAMP and PGE2 accumulation in rat IMCD. *Am J Physiol* 1993;265(5 Part 2):F670-F6.
116. Mathison Y, Israel A. Endothelin ET(B) receptor subtype mediates nitric oxide/cGMP formation in rat adrenal medulla. *Brain Res Bull* 1998;45(1):15-9.
117. Higuchi H, Satoh T. Endothelin-1 induces vasoconstriction and nitric oxide release via endothelin ET(B) receptors in isolated perfused rat liver. *Eur J Pharmacol* 1997;328(2-3):175-82.
118. Godfraind T. Evidence for heterogeneity of endothelin receptor distribution in human coronary artery. *Br J Pharmacol* 1993;110:1201-5.
119. Garcia J, Fernandez N, Garcia-Villalon A, Monge L, Gomez B, Dieguez G. Coronary vasoconstriction by endothelin-1 in anesthetized goats: role of endothelin receptors, nitric oxide and prostanoids. *Eur J Pharmacol* 1996;315(2):179-86.
120. Toda N. Mechanisms of histamine action in human coronary arteries. *Circ Res* 1987;81:65-71.
121. Ginsburg R, Bristow M, Stinson E, Harrison D. Histamine receptors in the human heart. *Life Sci* 1980;26:2245-9.
122. Elhousseiny A, Hamel E. Sumatriptan elicits both constriction and dilation in human and bovine brain intracortical arterioles. *Br J Pharmacol* 2001;132(1):55-62.

123. Ullmer C, Schmuck K, Kalkman H, Lubbert H. Expression of serotonin receptor mRNAs in blood vessels. *FEBS Lett* 1995;370:215-21.
124. Calama E, Fernandez M, Moran A, Martin M, San Roman L. Vasodilator and vasoconstrictor responses induced by 5-hydroxytryptamine in the in situ blood autoperfused hindquarters of the anaesthetized rat. *Naunyn Schmiedebergs Arch Pharmacol* 2002;366(2):110-6.
125. Janiak P, Laine P, Grataloup Y, Luyt C, Bidouard J, Michel J, O'Conner S, Herbert J. Serotonin receptor blockade improves distal perfusion after lower limb ischemia in the fatty Zucker rat. *Cardiovasc Res* 2002;56(2):293-302.
126. Fernandez M, Moran A, Martin M, San Roman L. Mesenteric vasoconstrictor response to 5-hydroxytryptamine in the in situ blood autoperfused rat mesentery: involvement of 5-HT_{2B} and/or 5-HT_{2C} receptor activation. *Eur J Pharmacol* 2000;401(2):221-7.
127. Watts S, Baez M, Webb R. The 5-hydroxytryptamine 2B receptor and 5-HT receptor signal transduction in mesenteric arteries from deoxycorticosterone acetate-salt hypertensive rats. *J Pharmacol Exp Ther* 1996;277(2):1103-13.
128. Ishine T, Bouchelet I, Hamel E, Lee T. Serotonin 5-HT₇ receptors mediate relaxation of porcine pial veins. *Am J Physiol Heart Circ Physiol* 2000;278(3):H907-H12.
129. Lamping K, Kanatsuka H, Eastham C, Chilian W, Marcus M. Nonuniform vasomotor responses of coronary microcirculation to serotonin and vasopressin. *Circ Res* 1989;65:343-51.

130. Sarcevic B, Brooks V, Martin T, Kemp B, Robinson P. Atrial natriuretic peptide-dependent phosphorylation of smooth muscle cell particulate fraction proteins is mediated by cGMP-dependent protein kinase. *J Biol Chem* 1989;264(34):20648-54.
131. Singhal P, DeCandido S, Satriano J, Schlondorff D, Hays R. Atrial natriuretic peptide and nitroprusside cause relaxation of cultured rat mesangial cells. *Am J Physiol* 1989;257(1 Part 1):C86-C93.
132. Timmermans P, Smith R. Angiotensin-II receptor subtypes: selective antagonists and functional correlates. *Eur Heart J* 1994;15:79-87.
133. Dudley D, Panek R, Major T, Lu G, Bruns R, Klinkefus B, Hodges J, Weishaar R. Subclasses of angiotensin II binding sites and their functional significance. *Mol Pharmacol* 1990;38(3):370-7.
134. Chilian W, Harrison D, Haws C, Snyder W, Marcus M. Adrenergic coronary tone during submaximal exercise in the dog is produced by circulating catecholamines. Evidence of adrenergic denervation supersensitivity in the myocardium but not coronary vessels. *Circ Res* 1986;58(1):68-82.
135. Kemp P, Hubscher G, Hawthorne J. Phosphoinositides. 3. Enzymic hydrolysis of inositol-containing phospholipids. *Biochem J* 1961;79:193-200.
136. Iino M. Dynamic regulation of intracellular calcium signals through calcium release channels. *Mol Cell Biochem* 1999;190(1-2):185-90.

137. Ward J, Knock G, Snetkov V, Aaronson P. Protein kinases in vascular smooth muscle tone - role in pulmonary vasoconstriction. *Pharmacol Ther* 2004;104:207-31.
138. Kitazawa K, Eto K, Woodsome T, Brautigan D. Agonists trigger G protein-mediated activation of the CPI-17 inhibitor phosphoprotein of myosin light chain phosphatase to enhance vascular smooth muscle contractility. *J Biol Chem* 2000;275(14):9897-900.
139. Schmitz W, Eschenhagen T, Mende U, F. M, Scholz H. The role of alpha 1-adrenergic and muscarinic receptors in cardiac function. *Eur Heart J* 1991;12 (Suppl F):83-7.
140. Moreau M, Garbacki N, Molinaro G, Brown N, Marceau F, Adam A. The kallikrein-kinin system: current and future pharmacological targets. *J Pharmacol Sci* 2005;99(1):6-38.
141. Hadoke PW, McIntyre CA, Gray GA, Buckley CH. Functional heterogeneity of large and small resistance arteries isolated from biopsies of subcutaneous fat: implications for investigation of vascular pathophysiology. *Gen Pharmacol* 2000;35(3):119-27.
142. Pelc L, Gross G, Warltier D. Mechanisms of coronary vasodilation produced by bradykinin. *Circulation* 1991;83:2048-56.
143. Cowan C, Cohen R. Two mechanisms mediate relaxation by bradykinin of pig coronary artery: nitric oxide-dependent and -independent responses. *Am J Physiol* 1991;261:830-5.
-

144. Han E, MacFarlane R, Mulligan A, Scafidi J, Davis A. Increased vascular permeability in C1 inhibitor-deficient mice mediated by the bradykinin type 2 receptor. *J Clin Invest* 2002;109(8):1057-63.
145. Ishihara K, Kamata M, Hayashi I, Yamashina S, Majima M. Roles of bradykinin in vascular permeability and angiogenesis in solid tumor. *Int Immunopharmacol* 2002;2(4):499-509.
146. Sarker M, Hu D, Fraser P. Acute effects of bradykinin on cerebral microvascular permeability in the anaesthetized rat. *J Physiol* 2000;528(Pt 1):177-87.
147. Easton A, Abbott N. Bradykinin increases permeability by calcium and 5-lipoxygenase in the ECV304/C6 cell culture model of the blood-brain barrier. *Brain Res* 2002;953(1-2):157-69.
148. Furchgott R, Vanhoutte P. Endothelium-derived relaxing factor and contracting factors. *FASEB J* 1989;3:2007-18.
149. Palmer R, Ferrige A, Moncada S. Nitric oxide release accounts for the biological activity of endothelium-derived relaxing factor. *Nature* 1987;327(6122):524-6.
150. Kemp B, Cocks T. Evidence that mechanisms dependent and independent of nitric oxide mediate endothelium-dependent relaxation to bradykinin in human small resistance-like coronary arteries. *Br J Pharmacol* 1997;120:757-62.

151. Campos M, Souza G, Calixto J. Upregulation of B₁ receptor mediating des-Arg⁹-BK-induced rat paw oedema by systemic treatment with bacterial endotoxin. *Br J Pharmacol* 1996;117(5):793-8.
152. Perkins M, Kelly D. Induction of bradykinin B₁ receptors *in vivo* in a model of ultra-violet irradiation-induced thermal hyperalgesia in the rat. *Br J Pharmacol* 1993;110(4):1441-4.
153. Ferreira J, Beirith A, Mori M, Araujo R, Bader M, Pesquero J, Calixto J. Reduced nerve injury-induced neuropathic pain in kinin B₁ receptor knock-out mice. *J Neurosci* 2005;25(9):2405-12.
154. Rashid M, Inoue M, Matsumoto M, Ueda H. Switching of bradykinin-mediated nociception following partial sciatic nerve injury in mice. *J Pharmacol Exp Ther* 2004;308(3):1158-64.
155. Cunha T, Verri W, Fukada S, Guerrero A, Santodomingo-Garzon T, Poole S, Parada C, Ferreira S, Cunha F. NF- α and IL-1 β mediate inflammatory hypernociception in mice triggered by B₁ but not B₂ kinin receptor. *Eur J Pharmacol* 2007;573(1-3):221-9.
156. Vianna R, Calixto J. Characterization of the receptor and mechanisms underlying the inflammatory response induced by des-Arg⁹-BK in mouse pleurisy. *Br J Pharmacol* 1998;123(2):281-91.
157. Ehrenfeld P, Millan C, Matus C, Figueroa J, Burgos R, Nualart F, Bhoola K, Figueroa C. Activation of kinin B₁ receptors induces chemotaxis of human neutrophils. *J Leukoc Biol* 2006;80(1):117-24.

158. Araujo R, Kettritz R, Fichtner I, Paiva A, Pesquero J, Bader M. Altered neurophil homeostasis in kinin B₁ receptor-deficient mice. *Biol Chem* 2001;382(1):91-5.
159. Cocks T, Angus J. Endothelium-dependent relaxation of coronary arteries by noradrenaline and serotonin. *Nature* 1983;30:627-30.
160. Motta G, Rojkjaer R, Hasan A, Cines D, Schmaier A. High molecular weight kininogen regulates prekallikrein assembly and activation on endothelial cells: a novel mechanism for contact activation. *Blood* 1998;91(2):516-28.
161. Nishikawa K, Shibayama Y, Kuna P, Calcaterra E, Kaplan A, Reddigari S. Generation of vasoactive peptide bradykinin from human umbilical vein endothelium-bound high molecular weight kininogen by plasma kallikrein. *Blood* 1992;80(8):1980-8.
162. Kubo T, Fukuda K, Mikami A, Maeda A, Takahashi H, Mishina M, Haga T, Hata K, Ichiyama A, Kangawa K, Kojima M, Matsuo H, Hirose T, Numa S. Cloning, sequencing and expression of complementary DNA encoding the muscarinic acetylcholine receptor. *Nature* 1986;323(6087):411-6.
163. Bonner T, Buckley N, Young A, Brann M. Identification of a family of muscarinic acetylcholine receptor genes. *Science* 1987;237(4814):527-32.
164. Bonner T, Young A, Brann M, Buckley N. Cloning and expression of the human and rat m5 muscarinic acetylcholine receptor genes. *Neuron* 1988;1(5):403-10.

165. Caulfield M. Muscarinic receptors - characterization, coupling and function. *Pharmacol Ther* 1993;58(3):319-79.
166. Felder C. Muscarinic acetylcholine receptors: signal transduction through multiple effectors. *FASEB J* 1995;9(8):619-25.
167. Ashkenazi A, Winslow J, Peralta E, Peterson G, Schimerlik M, Capon D, Ramachandran J. An M₂ muscarinic receptor subtype coupled to both adenylyl cyclase and phosphoinositide turnover. *Science* 1987;238(4827):627-75.
168. Shimizu T, Rosenblum W, Nelson G. M₃ and M₁ receptors in cerebral arterioles *in vivo*: evidence for downregulated or ineffective M₁ when endothelium is intact. *Am J Physiol* 1993;264(3 Part 2):H665-H9.
169. Bohr D. Adrenergic receptors in coronary arteries. *Ann NY Acad Sci* 1967;139(3):799-807.
170. Guimaraes S, Moura D. Vascular adrenoceptors: an update. *Pharmacol Rev* 2001;53(2):319-56.
171. Civantos Calzada B, Aleixandre de Artinano A. Alpha-adrenoceptor subtypes. *Pharmacol Res* 2001;44(3):195-208.
172. Sun D, Huang A, Mital S, Kichuk M, Marboe C, Addonizio L, Michler R, Koller A, Hintze T, Kaley G. Norepinephrine elicits beta1-receptor-mediated dilation of isolated human coronary arterioles. *Circulation* 2002;106(5):550-5.
173. Gauthier C, Langin D, Balligand J. Beta3-adrenoceptors in the cardiovascular system. *Trends Pharmacol Sci* 2000;21(11):426-31.
-

174. Nakane T, Tsujimoto G, Hashimoto K, Chiba S. Beta-adrenoceptors in the canine large coronary arteries: beta-1 adrenoceptors predominate in vasodilation. *J Pharmacol Exp Ther* 1988;245:936-43.
175. Murphree S, Saffitz J. Delineation of the distribution of beta-adrenergic receptor subtypes in canine myocardium. *Circ Res* 1988;63:117-25.
176. Molenaar P, Chen L, Semmler A, Parsonage W, Kaumann A. Human heart beta-adrenoceptors: beta1-adrenoceptor diversification through 'affinity states' and polymorphism. *Clin Exp Pharmacol Physiol* 2007;34(10):1020-8.
177. Watts S, Kanagy N, Lombard J. *Receptor-Mediated Events in the Microcirculation*. In: Tuma R, Duran W, Ley K, eds. *Handbook of Physiology: Microcirculation*. Oxford: Elsevier Science and Technology; 2008.
178. Feigl E. Neural control of coronary blood flow. *J Vasc Res* 1998;35(2):85-92.
179. Bartelds B, Gratama J, Meuzelaar K, Dalinghaus M, Koers J, Helkens W, Zijlstra W, Kuipers J. Comparative effects of isoproterenol and dopamine on myocardial oxygen consumption, blood flow distribution and total body oxygen consumption in conscious lambs with and without an autopulmonary left to right shunt. *JACC* 1998;31(2):473-81.
180. Olanow C, Obeso J, Stocchi F. Continuous dopamine-receptor treatment of Parkinson's disease: scientific rationale and clinical implications. *Lancet Neurol* 2006;5(8):677-87.

181. Craig C, Stitzel R. *Modern Pharmacology*. Boston: Little, Brown and Company; 1994.
182. Jackisch R, Fehr R, Hertting G. Adenosine: an endogenous modulator of hippocampal noradrenaline release. *Neuropharmacology* 1985;24(6):499-507.
183. Ali S, Metzger W, Olanrewaju H, Mustafa S. Adenosine receptor-mediated relaxation of rabbit airway smooth muscle: a role for nitric oxide. *Am J Physiol* 1997;273(3 Part 1):L581-L7.
184. Buckwalter J, Hamann J, Clifford P. Vasoconstriction in active skeletal muscles: a potential role for P_{2X} purinergic receptors? *J Appl Physiol* 2003;95(3):953-9.
185. Burnstock G. Vascular control by purines with emphasis on the coronary system. *Eur Heart J* 1989;10:15-21.
186. Newhouse M, Hill C. A role for neuropeptide Y in rat iridial arterioles. *Am J Physiol* 1997;273(5 Pt 2):H2119-H27.
187. Neild T, Xia J. Mechanism of potentiation of vasoconstriction by neuropeptide Y in arterioles from the submucosa of the guinea-pig small intestine. *Clin Exp Pharmacol Physiol* 1997;24(3-4):217-22.
188. Maturi M, Greene R, Speir E, Burrus C, Dorsey L, Markie D, Maxwell M, Schmidt W, Goldstein S, Patterson R. Neuropeptide Y. A peptide found in human coronary arteries constricts primarily small coronary arteries to produce myocardial ischemia in dogs. *J Clin Invest* 1989;83:1217-24.

189. Crossman D, Larkin S, Fuller R, Davies G, Maseri A. Substance P dilates epicardial coronary arteries and increases coronary blood flow in humans. *Circulation* 1989;80:475-84.
190. Kuo L, Davis M, Chilian W. Longitudinal gradients for endothelium-dependent and -independent vascular responses in the coronary microcirculation. *Circulation* 1995;92(3):518-25.
191. Brain S, Williams T, Tippins J, Morris H, MacIntyre I. Calcitonin gene-related peptide is a potent vasodilator. *Nature* 1985;313(5997):54-6.
192. Sekiguchi N, Kanatsuka H, Sato K, Wang Y, Akai K, Komaru T, Takishima T. Effect of calcitonin gene-related peptide on coronary microvessels and its role in acute myocardial ischemia. *Circulation* 1994;89(1):366-74.
193. Roudenok V, Gutjar L, Antipova V, Rogov Y. Expression of vasoactive intestinal polypeptide and calcitonin gene-related peptide in human stellate ganglia after acute myocardial infarction. *Ann Anat* 2001;183(4):341-4.
194. Kallner G. Release and effects of calcitonin gene-related peptide in myocardial ischaemia. *Scand Cardiovasc J Suppl* 1998;49:1-35.
195. Murphy A. Signal transduction and regulation in smooth muscle: problems and progress. *Rev Physiol Biochem Pharmacol* 1999;134:1-6.
196. Meiss R. *Mechanics of smooth muscle contraction*. In: Kao C, Carsten M, eds. Cellular aspects of smooth muscle function. New York: Cambridge University Press; 1997.

197. Ishikawa T, Hidaka H. Molecular pharmacology of calcium, calmodulin-dependent myosin phosphorylation in vascular smooth muscle. *Am J Hypertens* 1990;3(8 Part 2):231S-4S.
198. Itoh T, Ikebe M, Kargacin G, Hartshorne D, Kemp B, Fay F. Effects of modulators of myosin light-chain kinase activity in single smooth muscle cells. *Nature* 1989;338(6211):164-7.
199. Driska S, Aksoy M, Murphy R. Myosin light chain phosphorylation associated with contraction in arterial smooth muscle. *Am J Physiol* 1981;240(5):C222-C33.
200. Garcia J, Lazar V, Gilbert-McClain L, Gallagher P, Verin A. Myosin light chain kinase in endothelium: molecular cloning and regulation. *Am J Respir Cell Mol Biol* 1997;16(5):489-94.
201. Watanabe H, Tran Q, Takeuchi K, Fukao M, Liu M, Kanno M, Hayashi T, Iguchi A, Seto M, Ohashi K. Myosin light-chain kinase regulates endothelial calcium entry and endothelium-dependent vasodilation. *FASEB J* 2001;15(2):282-4.
202. Kotlikoff M, Herrera G, Nelson M. Calcium permeant ion channels in smooth muscle. *Rev Physiol Biochem Pharmacol* 1999;134:147-99.
203. Fellner S, Arendshorst W. Voltage-gated Ca²⁺ entry and ryanodine receptor Ca²⁺-induced Ca²⁺ release in preglomerular arterioles. *Am J Physiol Renal Physiol* 2007;292(5):F1568-F72.

204. Raina H, Zacharia J, Li M, Wier W. Activation by Ca^{2+} /calmodulin of an exogenous myosin light chain kinase in mouse arteries. *J Physiol* 2009;587(Part 11):2599-612.
205. Matthew A, Schmygol A, Wray S. Ca^{2+} entry, efflux and release in smooth muscle. *Biol Res* 2004;37(4):617-24.
206. Webb R. Smooth muscle contraction and relaxation. *Adv Physiol Educ* 2003;27(1-4):201-6.
207. Marin J, Encabo A, Briones A, Garcia-Cohen E, Alonso M. Mechanisms involved in the cellular calcium homeostasis in vascular smooth muscle: calcium channels. *Life Sci* 1999;64(5):279-303.
208. Clapperton J, Martin S, Smerdon S, Gamblin S, Bayley P. Structure of the complex of calmodulin with the target sequence of calmodulin-dependent protein kinase I: studies of the kinase activation mechanism. *Biochemistry* 2002;41(50):14669-79.
209. Mitzuno Y, Isotani E, Huang J, Ding H, Stull J, Kamm K. Myosin light chain kinase activation and calcium sensitization in smooth muscle *in vivo*. *Am J Physiol Cell Physiol* 2008;295(2):C358-C64.
210. Woodsome T, Eto M, Everett A, Brautigam D, Kitazawa T. Expression of CPI-17 and myosin phosphatase correlates with Ca^{2+} sensitivity of protein kinase C-induced contraction in rabbit smooth muscle. *J Physiol* 2001;535(2):553-64.

211. Ruegg J. Smooth muscle: PKC-induced Ca^{2+} sensitisation by myosin phosphatase inhibition. *J Physiol* 1999;520(Part 1):3.
212. Walsh M, Susnjar M, Deng J, Sutherland C, Kiss E, Wilson D. Phosphorylation of the protein phosphatase type 1 inhibitor protein CPI-17 by protein kinase C. *Methods Mol Biol* 2007;365:209-23.
213. Hirano K, Hirano M, Kanaide H. Regulation of myosin phosphorylation and myofilament Ca^{2+} sensitivity in vascular smooth muscle. *J Smooth Muscle Res* 2004;40(6):219-36.
214. Riddick N, Ohtani K, Surks H. Targeting by myosin phosphatase-RhoA interacting protein mediates RhoA/ROCK regulation of myosin phosphatase. *J Cell Biochem* 2008;103(4):1158-70.
215. Bolz S, Vogel L, Sollinger D, Derwand R, de Wit C, Loirand G, Pohl U. Nitric oxide-induced decrease in calcium sensitivity of resistance arteries is attributable to activation of the myosin light chain phosphatase and antagonized by the RhoA/Rho kinase pathway. *Circulation* 2003;207(24):3081-7.
216. Walsh M, Horowitz A, Clement-Chomienne O, Andrea J, Allen B, Morgan K. Protein kinase C mediation of Ca^{2+} -independent contractions of vascular smooth muscle. *Biochem Cell Biol* 1996;74(4):485-502.
217. Hartshorne D, Ito M, Erdodi F. Myosin light chain phosphatase: subunit composition, interactions and regulation. *J Muscle Res Cell Motil* 1998;19:325-41.
-

218. Khalil R, Morgan K. Phenylephrine-induced translocation of protein kinase C and shortening of two types of vascular cells in the ferret. *J Physiol* 1992;455(585-599).
219. Khalil R, Morgan K. Imagine of protein kinase C distribution and translocation in living vascular smooth muscle cells. *Circ Res* 1991;69(6):1626-31.
220. Haller H, Smallwood J, Rasmussen H. Protein kinase C translocation in intact vascular smooth muscle strips. *Biochem J* 1990;270(2):375-81.
221. Bell R, Burns D. Lipid activation of protein kinase C. *J Biol Chem* 1991;266(8):4661-4.
222. Eto M, Kitazawa T, Yazawa M, Mukai H, Ono Y, Brautigan D. Histamine-induced vasoconstriction involves the phosphorylation of a specific inhibitor protein for myosin phosphatase by protein kinase C alpha and delta isoforms. *J Biol Chem* 2001;276(3):29072-8.
223. Kitazawa T, Polzin A, Eto M. CPI-17-deficient smooth muscle of chicken. *J Physiol* 2004;557(2):515-28.
224. Wang Y, Zheng X, Riddick N, Bryden M, Baur W, Zhang X, Surcks H. ROCK isoform regulation of myosin phosphatase and contractility in vascular smooth muscle cells. *Circ Res* 2009;104(4):531-40.
225. Johnson R, El-Yazbi A, Takeya K, Walsh E, Walsh M, Cole W. Ca²⁺ sensitization via phosphorylation of myosin phosphatase targeting subunit at

- threonin-855 by Rho kinase contributes to the arterial myogenic response. *J Physiol* 2009;587(Part 11):2537-53.
226. Wilson D, Susnjar M, Kiss E, Sutherland C, Walsh M. Thromboxane A₂-induced contraction of rat caudal arterial smooth muscle involves activation of Ca²⁺ entry and Ca²⁺ sensitization: Rho-associated kinase-mediated phosphorylation of MYPT1 at Thr-855, but not Thr-697. *Biochem J* 2005;389(3):763-74.
227. Leung T, Manser E, Tan L, Lim L. A novel serine/threonine kinase binding the Ras-related RhoA GTPase which translocates to peripheral membranes. *J Biol Chem* 1995;270(49):29051-4.
228. Niironen N, Koga Y, Ikebe M. Agonist-induced changes in the phosphorylation of the myosin-binding subunit of myosin light chain phosphatase and CPI17, two regulatory factors of myosin light chain phosphatase, in smooth muscle. *Biochem J* 2003;369(1):117-28.
229. Koyama M, Ito M, Feng J, Seko T, Shiraki K, Takase K, Hartshorne D, Nakano T. Phosphorylation of CPI-17, an inhibitory phosphoprotein of smooth muscle myosin phosphatase, by Rho-kinase. *FEBS Lett* 2000;475(3):197-200.
230. Dimopoulos G, Semba S, Kitazawa K, Eto M, Kitazawa T. Ca²⁺-dependent rapid Ca²⁺ sensitization of contraction in arterial smooth muscle. *Circ Res* 2007;100(1):121-9.

231. Hirano K. Current topics in the regulatory mechanism underlying the Ca²⁺ sensitization of the contractile apparatus in vascular smooth muscle. *J Pharmacol Sci* 2007;104(2):109-15.
232. Catterall W. Structure and regulation of voltage-gated Ca²⁺ channels. *Ann Rev Cell Dev Biol* 2000;16(521-555).
233. McFadzean I, Gibson A. The developing relationship between receptor-operated and store-operated calcium channels in smooth muscle. *Br J Pharmacol* 2002;135:1-13.
234. Ganitkevich V, Isenberg G. Depolarization-mediated intracellular calcium transients in isolated smooth muscle cells of guinea-pig urinary bladder. *J Physiol* 1991;435:187-205.
235. Cavero I, Spedding M. "Calcium antagonists": a class of drugs with a bright future. Part 1. Cellular calcium homeostasis and calcium as a coupling messenger. *Life Sci* 1983;33(26):2571-81.
236. Wesselman J, VanBavel E, Pfaffendorf M, Spaan J. Voltage-operated calcium channels regulate myogenic tone of resistance arteries. *J Vasc Res* 1997;33:32-41.
237. McCarron J, Crichton C, Langton P, MacKenzie A, Smith G. Myogenic contraction by modulation of voltage-dependent calcium currents in isolated rat cerebral arteries. *J Physiol* 1997;498(Part 2):371-9.

238. Schubert R, Mulvany M. The myogenic response: established facts and attractive hypotheses. *Clin Sci* 1999;96(4):313-26.
239. Hofmann F, Biel V, Flockerzi V. Molecular basis for Ca²⁺ channel diversity. *Ann Rev* 1994;17:399-418.
240. Perez-Reyes E, Kim H, Lacerda A, Horne W, Wei X, Rampe D, Campbell K, Brown A, Birnbaumer L. Induction of calcium current by the expression of the alpha₁ subunit of the dihydropyridine receptor from skeletal muscle. *Nature* 1989;340(6230):233-6.
241. Bootman M, Collins T, Peppiatt C, Prothero L, MacKenzie L, De Smit P, Travers M, Tovey S, Seo J, Berridge M, Ciccolini F, Lipp P. Calcium signalling - an overview. *Semin Cell Dev Biol* 2001;12:3-10.
242. Lacinova L. Voltage-dependent calcium channels. *Gen Physiol Biophys* 2005;24(Suppl 1):1-78.
243. Gurnett C, De Waard M, Campbell K. Dual function of the voltage-dependent Ca²⁺ channel alpha2delta subunit in current stimulation and subunit interaction. *Neuron* 1996;16(2):431-40.
244. Davies A, Hendrich J, Van Minh A, Wratten J, Douglas L, Dolphin A. Functional biology of the alpha2delta subunits of voltage-gated calcium channels. *Trends Pharmacol Sci* 2007;28(5):220-8.
245. Dolphin A. Beta subunits of voltage-gated calcium channels. *J Bioenerg Biomembr* 2003;35(6):599-620.

246. Birnbaumer L, Qin N, Olcese R, Tarellus E, Platano D, Costantin J, Stefani E. Structures and functions of calcium channel beta subunits. *J Bioenerg Biomembr* 1998;30(4):357-275.
247. Felix R, Gurnett C, De Waard M, Campbell K. Dissection of functional domains of the voltage-dependent Ca²⁺ channel alpha2delta subunit. *J Neurosci* 1997;17(18):6884-91.
248. Takahashi M, Seagar M, Jones F, Reber B, Catterall W. Subunit structure of dihydropyridine-sensitive calcium channels from skeletal muscle. *Proc Natl Acad Sci* 1987;84(15):5478-82.
249. Klugbauer N, Dai S, Specht V, Lacinova L, Marais E, Bohn G, Hofmann F. A family of gamma-like calcium channel subunits. *FEBS Lett* 2000;470(2):189-97.
250. Letts V, Felix R, Biddlecome G, Arikkath J, Mahaffey C, Valenzuela A, Bartlett F, Mori Y, Campbell K, Frankel W. The mouse stargazer gene encodes a neuronal Ca²⁺-channel gamma subunit. *Nat Genet* 1998;19(4):340-7.
251. Chu P, Robertson H, Best P. Calcium channel gamma subunits provide insights into the evolution of this gene family. *Gene* 2001;280(1-2):37-48.
252. Sandmann S, Unger T. L- and T-type calcium channel blockade - the efficacy of the calcium channel antagonist mibefradil. *J Clin Basic Cardiol* 1999;2(2):187-201.

253. Jagannathan S, Publicover S, Barratt C. Voltage-operated calcium channels in male germ cells. *Reproduction* 2002;123(2):203-15.
254. Randall A. The molecular basis of voltage-gated Ca²⁺ channel diversity: is it time for T? *J Membr Biol* 1998;161(3):207-13.
255. Perez-Reyes E. Molecular physiology of low-voltage-activated t-type calcium channels. *Nature* 2003;391(6670):896-900.
256. Cribbs L, Lee J, Yang J, Satin J, Zhang Y, Daud A, Barclay J, Williamson M, Fox M, Rees M, Perez-ryes E. Cloning and characterization of alpha_{1H} from human heart, a member of the T-type Ca²⁺ channel gene family. *Circ Res* 1998;83:103-9.
257. Perez-Reyes E, Cribbs L, Daud A, Lacerda A, Barclay J, Williamson M, Fox M, Rees M, Lee J. Molecular characterization of a neuronal low-voltage-activated T-type calcium channel. *Nature* 1998;391(6670):896-900.
258. Heady T, Gomora J, MacDonald T, Perez-Reyes E. Molecular pharmacology of T-type Ca²⁺ channels. *Jpn J Pharmacol* 2001;85(4):339-50.
259. Nowycky M, Fox A, Tsien R. Three types of neuronal calcium channel with different calcium agonist sensitivity. *Nature* 1985;316(6027):440-3.
260. Birnbaumer L, Campbell K, Catterall W, Harpold M, Hofmann F, Horne W, Mori Y, Schwartz A, Snutch T, Tanabe T, Tsien R. The Naming of Voltage-Gated Calcium Channels. *Neuron* 1994;13:505-6.

261. Ertel E, Campbell K, Harpold M, Hofmann F, Mori Y, Perez-Reyes E, Schwartz A, Snutch T, Tanabe T, Birnbaumer L, Tsien R, Catterall W. Nomenclature of voltage-gated calcium channels. *Neuron* 2000;25(3):533-5.
262. Franzini-Armstrong C, Protasi F. Ryanodine receptors of striated muscles: a complex channel capable of multiple interactions. *Physiol Rev* 1997;77(3):699-729.
263. Tanabe T, Mikami A, Numa S, Beam K. Cardiac type excitation-contraction coupling in dynamic skeletal muscle injected with cardiac dihydropyridine receptor cDNA. *Nature* 1990;344(6265):451-3.
264. Beam K, Tanabe T, Numa S. Structure, function and regulation of the skeletal muscle dihydropyridine receptor. *Ann NY Acad Sci* 1989;560:127-37.
265. Reuter H. A variety of calcium channels. *Nature* 1985;316(6027):391.
266. Schneider M, Chandler W. Voltage dependent charge movement of skeletal muscle: a possible step in excitation-contraction coupling. *Nature* 1973;242(5395):244-6.
267. Lipscombe D, Helton T, Xu W. L-Type calcium channels: the low down. *Neurophysiol* 2004;92(5):2633-41.
268. Flucher B, Franzini-Armstrong C. Formation of junctions involved in excitation-contraction coupling in skeletal and cardiac muscle. *Proc Natl Acad Sci* 1996;93(15):8101-6.

269. Tanabe T, Beam K, Powell J, Numa S. Restoration of excitation-contraction coupling and slow calcium current in dysgenic muscle by dihydropyridine receptor complementary DNA. *Nature* 1988;336(6195):134-9.
270. Koch W, Ellinor P, Schwartz A. cDNA cloning of a dihydropyridine-sensitive calcium channel from rat aorta. Evidence for the existence of alternatively spliced forms. *J Biol Chem* 1990;265(29):17786-91.
271. Biel M, Ruth P, Bosse E, Hullin R, Stuhmer W, Flockerzi V, Hofmann F. Primary structure and functional expression of a high voltage activated calcium channel from rabbit lung. *FEBS Lett* 1990;269(2):409-12.
272. Diebold R, Koch W, Ellinor P, Wang J, Muthuchamy M, Wieczorek D, Schwartz A. Mutually exclusive exon splicing of the cardiac calcium channel α_1 subunit gene generates developmentally regulated isoforms in the rat heart. *Proc Natl Acad Sci* 1992;89(4):1497-501.
273. Wang L, Bhattacharjee A, Fu J, Li M. Abnormally expressed low-voltage-activated calcium channels in beta-cells from NOD mice and related clonal cell line. *Diabetes* 1996;45(12):1678-83.
274. Soldatov N. Molecular diversity of L-type Ca^{2+} channel transcripts in human fibroblasts. *Proc Natl Acad Sci* 1992;89(10):4628-32.
275. Joux N, Chevaleyre V, Alonso G, Boissin-Agasse L, Moos F, Desarmenien M, Husey N. High voltage-activated Ca^{2+} currents in rat supraoptic neurones: biophysical properties and expression of the various channel α_1 subunits. *J Neuroendocrinol* 2001;13(7):638-49.
-

276. Reuter H, Porzig H, Kokubun S, Prod'hom B. Calcium channels in the heart. Properties and modulation by dihydropyridine enantiomers. *Ann NY Acad Sci* 1988;522:16-24.
277. Westenbroek R, Hoskins L, Catterall W. Localization of Ca²⁺ channel subtypes on rat spinal motor neurons, interneurons, and nerve terminals. *J Neurosci* 1998;18(16):6319-30.
278. Ihara Y, Yamada Y, Fujii Y, Gono T, Yano H, Yasuda K, Inahaki N, Seino Y, Seino s. Molecular diversity and functional characterization of voltage-dependent calcium channels (CACN4) expressed in pancreatic beta-cells. *Mol Endocrinol* 1995;9(1):121-30.
279. Kawano T, Matsuse H, Kondo Y, Machida I, Seeki S, Tomari S, Mitsuta K, Obase Y, Fukushima C, Shimoda T, Kohno S. Acetaldehyde induces histamine release from human airway mast cells to cause bronchoconstriction. *Int Arch Allergy Immunol* 2004;134(3):233-9.
280. Taylor W, Morgans C. Localization and properties of voltage-gated calcium channels in cone photoreceptors of *Tupaia belangeri*. *Vis Neurosci* 1998;15(3):541-52.
281. Habermann C, O'Brien B, Wassle H, Protti D. All amacrine cells express L-type calcium channels at their output synapses. *J Neurosci* 2003;23(17):6904-13.

-
282. Kollmar R, Fak J, Montgomery L, Hudspeth A. Hair cell-specific splicing of mRNA for the α_{1D} subunit of voltage-gated Ca^{2+} channels in the chicken's cochlea. *Proc Natl Acad Sci* 1997;94(26):14889-93.
283. Mangoni M, Traboulsie A, Leoni A, Couette B, Marger L, Le Quang K, Kupfer E, Cohen-Solal A, Villare J, Shin H, Escande D, Charpentier F, Nargeot J, Lory P. Bradycardia and slowing of the atrioventricular conduction in mice lacking $Ca_v3.1/\alpha_{1G}$ T-type calcium channels. *Circ Res* 2006;98(11):1422-30.
284. Mangoni M, Couette B, Bourinet E, Platzer J, Reimer D, Striessnig J, Nargeot J. Functional role of L-type $Ca_v1.3$ Ca^{2+} channels in cardiac pacemaker activity. *Proc Natl Acad Sci* 2003;100(9):5543-8.
285. Bernston A, Taylor W, Morgans C. Molecular identity, synaptic localization, and physiology of calcium channels in retinal bipolar cells. *J Neurosci Res* 2003;71(1):146-51.
286. Murakami M, Nakagawasai O, Fujii S, Kameyama K, Murakami S, Hozumi S, Esashi A, Taniguchi R, Yanagisawa T, Tan-No K, Tadano T, Kitamura K, Kisara K. Antinociceptive action of amlodipine blocking N-type Ca^{2+} channels at the primary afferent neurons in mice. *Eur J Pharmacol* 2001;419(2-3):175-81.
287. Xu W, Lipscombe D. Neuronal $Ca_v1.2$ α_1 L-type channels activate at relatively hyperpolarized membrane potentials and are incompletely inhibited by dihydropyridines. *J Neurosci* 2001;21(16):5944-51.
-

-
288. Koschak A, Reimer D, Huber I, Grabner M, Glossmann H, Engel J, Striessnig J. α_{1D} ($Ca_v1.3$) subunits can form l-type Ca^{2+} channels activating at negative voltages. *J Biol Chem* 2001;276(25):22100-6.
289. Koschak A, Reimer D, Walter B, Hoda J, Heinzie T, Grabner M, Striessnig J. $Ca_v1.4\alpha_1$ subunits can form slowly inactivating dihydropyridine-sensitive L-type Ca^{2+} channels lacking Ca^{2+} -dependent inactivation. *J Neurosci* 2003;23(14):6041-9.
290. Baumann L, Gerstner A, Zong X, Biel M, Wahl-Schott C. Functional characterization of the L-type Ca^{2+} channel $Ca_v1.2\alpha_1$ from mouse retina. *Invest Ophthalmol Vis Sci* 2004;45(7):708-13.
291. Helton T, Xu W, Lipscombe D. Neuronal L-type calcium channels open quickly and are inhibited slowly. *J Neurosci* 2005;25(44):10247-51.
292. Lee T-S, Kaku T, Takebayashi S, Uchino T, Miyamoto S, Hadama T, Perez-Reyes E, Ono K. Actions of mibefradil, efonidipine and nifedipine block of recombinant T- and L-type Ca^{2+} channels with distinct inhibitory mechanisms. *Pharmacology* 2006;78(1):11-20.
293. Tanaka H, Komikado C, Shimada H, Takeda K, Namekata I, Kawanishi T, Shigenobu K. The *R*(-)-enantiomer of efonidipine blocks T-type but not L-type calcium currents in guinea pig ventricular myocardium. *J Pharmacol Sci* 2004;96(4):499-501.
294. Tanaka H, Shigenobu K. Efonidipine hydrochloride: a dual blocker of L- and T-type Ca^{2+} channels. *Cardiovasc Drug Rev* 2002;20:81-92.
-

295. Masumiya H, Kase J, Tanaka Y, Tanaka H, Shigenobu K. Frequency-dependent blockade of T-type Ca^{2+} current by efonidipine in cardiomyocytes. *Life Sci* 2000;68:345-51.
296. Berk B, Weintraub W, Alexander R. Elevation of C-reactive protein in active coronary artery disease. *Am J Cardiol* 1990;65(3):168-72.
297. Mishra S, Hermsmeyer K. Selective inhibition of T-type Ca^{2+} channels by Ro 40-5967. *Circ Res* 1994;75(1):144-8.
298. Kung C, Tschudi M, Noll G, Clozel J, Luscher T. Differential effects of the calcium antagonist mibefradil in epicardial and intramyocardial coronary arteries. *J Cardiovasc Pharmacol* 1995;26(2):312-8.
299. VanBavel E, Sorop O, Andreasen D, Pfaffendorf M, Jensen B. Role of T-type calcium channels in myogenic tone of skeletal muscle resistance arteries. *Am J Physiol* 2002;283(6):H2239-H43.
300. Jensen L, Holstein-Rathlou N. Is there a role for T-type Ca^{2+} channels in regulation of vasomotor tone in mesenteric arterioles? *Can J Physiol Pharmacol* 2009;87(1):8-20.
301. Gustafsson F, Andreasen D, Salomonsson M, Jensen B, Holstein-Rathlou N. Conducted vasoconstriction in rat mesenteric arterioles: role for dihydropyridine-insensitive Ca^{2+} channels. *Am J Physiol* 2001;280(7):H582-H90.

-
302. Talley E, Cribbs L, Lee J, Daud A, Perez-Reyes E, Bayliss D. Differential distribution of three members of a gene family encoding low voltage-activated (T-type) calcium channels. *J Neurosci* 1999;16(6):1895-911.
303. Craig P, Beattie R, Folly E, Banerjee M, Reeves M, Priestley J, Carney S, Sher E, Perez-Reyes E, Volson S. Distribution of the voltage-dependent calcium channel α_{1G} subunit mRNA and protein throughout the mature rat brain. *Eur J Neurosci* 1999;11(8):2949-64.
304. Bohn G, Moosmang S, Conrad H, Ludwig A, Hofmann F, Klugbauer N. Expression of T- and L-type calcium channel mRNA in murine sinoatrial node. *FEBS Lett* 2000;481:73-6.
305. Monteil A, Chemin J, Bourinet E, Mennessier G, Lory P, Nargeot J. Molecular and functional properties of the human α_{1G} subunit that forms T-type calcium channels. *J Biol Chem* 2000;275(9):6090-100.
306. Hansen P, Jensen B, Andreasen D, Skott O. Differential expression of T- and L-type voltage-dependent calcium channels in renal resistance vessels. *Circ Res* 2001;89(7):560-2.
307. Jaleel N, Nakayama H, Chen X, Kubo H, MacDonnell S, Zhang H, Berretta R, Robbins J, Cribbs L, Molkentin J, Houser S. Ca^{2+} influx through T- and L-type Ca^{2+} channels have different effects on myocyte contractility and induce unique cardiac phenotypes. *Circ Res* 2008;103(10):1109-19.
308. Zhou Z, Lipsius S. T-type calcium current in latent pacemaker cells isolated from cat right atrium. *J Mol Cell Cardiol* 1994;26(9):1211-9.
-

309. Hagiwara N, Irisawa H, Kameyama M. Contribution of two types of calcium currents to the pacemaker potentials of rabbit sino-atrial node cells. *J Physiol* 1988;395:233-53.
310. Chemin J, Monteil A, Perez-Reyes E, Bourinet E, Nargeot J, Lory P. Specific contribution of human T-type calcium channel isoforms (α_{1G} , α_{1H} and α_{1I}) to neuronal excitability. *J Physiol* 2002;540(1):3-14.
311. Huguenard J. Low-threshold calcium currents in central nervous system neurons. *Annu Rev Physiol* 1996;58:329-48.
312. Rossier M, Burnay M, Brandenburger Y, Cherradi N, Vallotton M, Capponi A. Sources and sites of action of calcium in the regulation of aldosterone biosynthesis. *Endocr Res* 1996;22(4):579-88.
313. Arnoult C, Cardullo R, Lemos J, Florman H. Activation of mouse sperm T-type Ca^{2+} channels by adhesion to the egg zona pellucida. *Proc Natl Acad Sci* 1996;93(23):13004-9.
314. Williams M, Washburn M, Hans M, Urrutia A, Brust P, Prodanovich P, Harpold M, Stauderman K. Structure and functional characterization of a novel human low-voltage activated calcium channel. *J Neurochem* 1999;72(2):791-9.
315. Perchenet L, Benardeau A, Ertel E. Pharmacological properties of $Ca_v3.2$, a low voltage-activated Ca^{2+} channel cloned from human heart. *Naunyn Schmiedeberg's Arch Pharmacol* 2000;361(6):590-9.

-
316. Joksovic P, Nelson M, Jevtovic-Todorovic V, Patel M, Perez-Reyes E, Campbell K, Chen C, Todorovic S. $Ca_v3.2$ is the major molecular substrate for redox regulation of T-type Ca^{2+} channels in the rat and mouse thalamus. *J Physiol* 2006;574(2):415-30.
317. Schrier A, Wang H, Talley E, Perez-Reyes E, Barrett P. α_{1H} T-type Ca^{2+} channel is the predominant subtype expressed in bovine and rat zona glomerulosa. *Am J Physiol Cell Physiol* 2001;280(2):C265-C72.
318. Sarsero D, Fujiwara T, Molenaar P, Angus JA. Human vascular to cardiac tissue selectivity of L- and T-type calcium channel antagonists. *Br J Pharmacol* 1998;125(1):109-19.
319. Schmitt R, Clozel J, Iberg N, Buhler F. Mibefradil prevents neointima formation after vascular injury in rats. Possible role of the blockade of the T-type voltage-operated calcium channel. *Arterioscler Thromb Vasc Biol* 1995;15(8):1161-5.
320. Rossier M, Ertel E, Vallotton M, Capponi A. Inhibitory action of mibefradil on calcium signaling and aldosterone synthesis in bovine adrenal glomerulosa cells. *J Pharmacol Exp Ther* 1998;287(3):824-31.
321. Gomora J, Xu C, Enyeart J, Enyeart J. Effect of mibefradil on voltage-dependent gating and kinetic of the T-type Ca^{2+} channels in cortisol-secreting cells. *J Pharmacol Exp Ther* 2000;292(1):96-103.
322. Yunker A, Sharp A, Sundarraj S, Ranganathan V, Copeland T, McEnery M. Immunological characterization of T-type voltage-dependent calcium channel
-

-
- Ca_v3.1 (α_{1G}) and Ca_v3.3 (α_{1I}) isoforms reveal differences in their localization, expression, and neural development. *Neuroscience* 2003;117(2):321-35.
323. McRory J, Santi C, Hamming K, Mezeyova J, Sutton K, Baillie D, Stea A, Snuth T. Molecular and functional characterization of a family of rat brain T-type calcium channels. *J Biol Chem* 2001;276(6):3999-4011.
324. Monteil A, Chemin J, Leuranguer V, Altier C, Mennessier G, Bourinet E, Lory P, Nargeot, J. Specific properties of T-type calcium channels generated by the human α_{1I} subunit. *J Biol Chem* 2000;275(22):16530-5.
325. Lee J, Daud A, Cribbs L, Lacerda A, Pereverez A, Klockner U, Schneider T, Perez-Reyes E. Cloning and expression of a novel member of the low voltage-activated T-type calcium channel family. *J Neurosci* 1999;19(6):1912-21.
326. Murbartian J, Arias J, Perez-Reyes E. Functional impact of alternative splicing of human T-type Ca_v3.3 calcium channels. *J Neurophysiol* 2004;92(6):3399-407.
327. Randall A, Tsien R. Pharmacological dissection of multiple classes of calcium channels in the mouse AtT20 cell line. *Br J Pharmacol* 1994;111:194P.
328. Sather W, Tanabe T, Zhang J, Mori Y, Adams M, Tsien R. Distinctive biophysical and pharmacological properties of class A (BI) calcium channel α₁ subunits. *Neuron* 1993;11(2):291-303.
-

329. Hillman D, Chen C, Aung T, Cherksey B, Sugimori M, Llinas R. Localization of P-type calcium channels in the central nervous system. *Proc Natl Acad Sci* 1991;88(16):7076-80.
330. Starr T, Prystay W, Snutch T. Primary structure of a calcium channel that is highly expressed in rat cerebellum. *Proc Natl Acad Sci* 1991;88(13):5621-5.
331. Kukwa W, Macioch T, Szulczyk P. Stellate neurones innervating the rat heart express N, L and P/Q calcium channels. *J Auton Nerv Syst* 1998;74(2-3):143-51.
332. Braun M, Ramracheya R, Bengtsson M, Zhang Q, Karanauskaite J, Partidge C, Johnson P, Rorsman P. Voltage-gated ion channels in human pancreatic beta-cells: electrophysiological characterization and role in insulin secretion. *Diabetes* 2008;57(6):1618-28.
333. Sher E, Giovannini F, Codignola A, Passafaro M, Giorgi-Rossi P, Volsen S, Craig P, Davalli A, Carrera P. Voltage-operated calcium channel heterogeneity in pancreatic beta cells: physiopathological implications. *J Bioenerg Biomembr* 2003;35(6):687-96.
334. Glassmeier G, Hauber M, Wulfsen I, Weinsberg F, Bauer C, Schwarz J. Ca²⁺ channels in clonal rat anterior pituitary cells (GH3/B6). *Pflugers Arch* 2001;442(4):577-87.
335. Dunlap K, Luebke J, Turner I. Identification of calcium channels that control neurosecretion. *Science* 1994;266(5186):828-31.

-
336. Luebke J, Dunlap K, Turner I. Multiple calcium channel types control glutamatergic synaptic transmission in the hippocampus. *Neuron* 1993;11(5):895-902.
337. Mori Y, Nishida M, Shimizu S, Ishii M, Yoshinaga T, Ino M, Sawada K, Niidome T. Ca²⁺ channel α_{1B} subunit (Ca_v2.2) knockout mouse reveals a predominant role of N-type channels in sympathetic regulation of the circulatory system. *Trends Cardiovasc Med* 2002;12(6):270-5.
338. Stea A, Dubel S, Snutch T. α_{1B} N-type calcium channel isoforms with distinct biophysical properties. *Ann NY Acad Sci* 1999;868:118-30.
339. Westenbroek R, Hell J, Warner C, Dubel S, Snutch T, Catterall W. Biochemical properties and subcellular distribution of an N-type calcium channel subunit. *Neuron* 1992;9(6):1099-115.
340. Sluka K. Blockade of N- and P/Q-type calcium channels reduces the secondary heat hyperalgesia induced by acute inflammation. *J Pharmacol Exp Ther* 1998;287(1):232-7.
341. Williams M, Marubio L, Deal C, Hans M, Brust P, Philipson L, Miller R, Johnson E, Harpold M, Ellis S. Structure and functional characterization of neuronal α_{1E} calcium channel subtypes. *J Biol Chem* 1994;269(35):22347-57.
342. Soong T, Stea A, Hodson C, Dubel S, Vincent S, Snutch T. Structure and functional expression of a member of the low voltage-activated calcium channel family. *Science* 1993;260(5111):1133-6.
-

-
343. Mitchell J, Larsen, Best P. Identification of the calcium channel α_{1E} ($Ca_v2.3$) isoform expressed in atrial myocytes. *Biochim Biophys Acta* 2002;1577(1):17-26.
344. Tateyama M, Zong S, Tanabe T, Ochi R. Properties of voltage-gated Ca^{2+} channels in rabbit ventricular myocytes expressing Ca^{2+} channel α_{1E} cDNA. *Am J Physiol Cell Physiol* 2001;280(1):C175-C82.
345. Yassin M, Zong S, Tanabe T. G-protein modulation of neuronal class E (α_{1E}) calcium channel expressed in GH3 cells. *Biochem Biophys Res Comm* 1996;220(2):453-8.
346. Tottene A, Volsen S, Pietrobon D. α_{1E} subunits form the pore of three cerebellar T-type calcium channels with different pharmacological and permeation properties. *J Neurosci* 2000;20(1):171-8.
347. Dietrich D, Kirschstein T, Kukley M, Pereverzev A, von Brelie C, Schneider T, Beck H. Functional specialization of presynaptic $Ca_v2.3$ Ca^{2+} channels. *Neuron* 2003;39(3):483-96.
348. Pereverzev A, Salehi A, Mikhna M, Renstrom E, Hescheler J, Weiergraber M, Smyth N, Schnider T. The ablation of the $Ca_v2.3/E$ -type voltage-gated Ca^{2+} channel causes a mild phenotype despite an altered glucose induced glucagon response in isolated islets of Langerhans. *Eur J Pharmacol* 2005;511(1):65-72.
349. Jing X, Li D, Olofsson C, Salehi A, Surve V, Caballero J, Ivarsson R, Lundquist I, Pereverzev A, Schneider T, Rorsman P, Renstrom E. $Ca_v2.3$
-

- calcium channels control second-phase insulin release. *J Clin Invest* 2005;115(1):146-54.
350. Triggle D. *Basic Principles*. In: Epstein M, ed. *Calcium Antagonists in Clinical Medicine*. Philadelphia: Hanley and Belfus, Inc.; 1998.
351. Omote K, Iwasaki H, Kawamata M, Satoh O, Namiki A. Effects of verapamil on spinal anesthesia with local anesthetics. *Anesth Analg* 1995;80(3):444-8.
352. Reynolds N, Wagstaff A, Keam S. Trandolapril/verapamil sustained release: a review of its use in the treatment of essential hypertension. *Drugs* 2005;65(13):1893-914.
353. Frishman W, Klein N, Klein P, Strom J, Tawil R, Strair R, Wong B, Roth S, LeJemtel T, Pollack S, Sonnenblick E. Comparison of oral propranolol and verapamil for combined systemic hypertension and angina pectoris. A placebo-controlled double-blind randomized crossover trial. *Am J Cardiol* 1982;50(5):1164-72.
354. Prisant L. Verapamil revisited: a transition in novel drug delivery systems and outcomes. *Heart Dis* 2001;3(1):55-62.
355. Hjemdahl P, Eriksson S, Held C, Rehnqvist N. Prognosis of patients with stable angina pectoris on antianginal drug therapy. *Am J Cardiol* 1996;77(16):6D-15D.
356. Gaine S, Rubin L. Primary pulmonary hypertension. *Lancet* 1998;352(9129):719-25.
-

357. Wanstall J, Jeffrey T. Recognition and management of pulmonary hypertension. *Drugs* 1998;56(6):989-1007.
358. Levy S. Pharmacologic management of atrial fibrillation: current therapeutic strategies. *Am Heart J* 2001;142(2):S15-S21.
359. Channer K. The drug treatment of atrial fibrillation. *Br J Clin Pharmacol* 1991;32(3):267-73.
360. Johnson G, Leis L, Francis G. Disparate effects of the calcium-channel blockers, nifedipine and verapamil, on alpha₂-adrenergic receptors and thromboxane A₂-induced aggregation of human platelets. *Circulation* 1986;73(4):847-54.
361. Barnathan E, Addonizio V, Shattil S. Interaction of verapamil with human platelet alpha-adrenergic receptors. *Am J Physiol* 1982;242(1):H19-H23.
362. Bellamy W. P-glycoproteins and multidrug resistance. *Annu Rev Pharmacol and Toxicol* 1996;36:161-83.
363. Kyle D, Oduola A, Martin S, Milhous W. Plasmodium falciparum: modulation by calcium antagonists of resistance to chloroquine, desethylchloroquine, quinine, and quinidine *in vitro*. *Trans R Soc Trop Med Hyg* 1990;84(4):474-8.
364. Peterson B, Tanada T, Catterall W. Molecular determinants of high affinity dihydropyridine binding in L-type calcium channels. *J Biol Chem* 1996;271(10):5293-6.

365. Mancia G, Brown M, Castaigne A, de Leeuw P, Palmer C, Rosenthal T, Wagener G, Ruilope L. Outcomes with nifedipine GITS or Co-amilofidil in hypertensive diabetics and nondiabetics in Intervention as a Goal in Hypertension (INSIGHT). *Hypertension* 2003;41(3):431-6.
366. Aschermann M, Bultas J, Karetova D, Kolbel F, Fozakova M, Simper D. Randomized double-blind comparison of isosorbide dinitrate and nifedipine in variant angina pectoris. *Am J Cardiol* 1990;65(21):46J-9J.
367. Weir M, Elkins M, Liss C, Vrecenak A, Barr E, Edelman J. Efficacy, tolerability, and quality of life of losartan, alone or with hydrochlorothiazide, versus nifedipine GITS in patients with essential hypertension. *Clin Ther* 1996;18(3):411-28.
368. Frishman W, Garofalo J, Rothschild A, Rothschild M, Greenberg S, Soberman J. Multicenter comparison of the nifedipine gastrointestinal therapeutic system and long-acting propranolol in patients with mild to moderate systemic hypertension receiving diuretics. A preliminary experience. *Am J Med* 1987;83(6B):15-9.
369. Thompson A, Pope J. Calcium channel blockers for primary Raynaud's phenomenon: a meta-analysis. *Rheumatology (Oxford)* 2005;44(2):145-50.
370. Snider M, Nazum D, Veverka A. Long-acting nifedipine in the management of the hypertensive patient. *Vasc Health Risk Manag* 2008;4(6):1249-57.

371. Kloner R, Vetovec G, Materson B, Levenstein M. Safety of long-acting dihydropyridine calcium channel blockers in hypertensive patients. *Am J Cardiol* 1998;81(2):163-9.
372. King J, Flenady V, Papatsonis D, Dekker G, Carbonne B. Calcium channel blockers for inhibiting preterm labour; a systematic review of the evidence and a protocol for administration of nifedipine. *Aust N Z J Obstet Gynaecol* 2003;43(3):192-8.
373. Maggiorini M. High altitude-induced pulmonary oedema. *Cardiovasc Res* 2006;72(1):41-50.
374. Oelz O, Maggiorini M, Ritter M, Noti C, Waber U, Vock P, Bartsch P. Prevention and treatment of high altitude pulmonary edema by a calcium channel blocker. *Int J Sports Med* 1992;13(Suppl 1):S65-S8.
375. Mishra S, Hermsmeyer K. Inhibition of signal Ca^{2+} in dog coronary arterial vascular muscle cells by Ro 40-5967. *J Cardiovasc Pharmacol* 1994;24(1):1-7.
376. Martin R, Lee J, Cribbs L, Perez-Reyes E, Hanck D. Mibefradil block of cloned T-type calcium channels. *J Pharmacol Exp Ther* 2000;295(1):302-208.
377. Bittar N. Comparative antihypertensive effectiveness of once-daily mibefradil and diltiazem CD. Mibefradil hypertension study group. *Clin Ther* 1997;19(5):954-62.
378. Li JS, Sventek P, Schiffrin EL. Effect of antihypertensive treatment and N omega-nitro-L-arginine methyl ester on cardiovascular structure in

-
- deoxycorticosterone acetate-salt hypertensive rats. *J Hypertens* 1996;14(11):1331-9.
379. Davies G, Kobrin I, Caspi A, Reisin L, de Albuquerque D, Armagnijan D, Coelho O, Schneeweiss A. Long-term antianginal and antiischemic effects of mibefradil, the novel T-type calcium channel blocker: a multicenter, double-blind, placebo-controlled, randomized comparison with sustained-release diltiazem. *Am Heart J* 1997;134(2 Part 1):220-8.
380. Davies G, Tzivoni D, Kobrin I. Mibefradil in the treatment of chronic stable angina pectoris: comparative studies with other calcium antagonists. *Am J Cardiol* 1997;80(4B):34C-9C.
381. Beltrame J, Turner S, Leslie S, Solomon P, Horowitz J. The angiographic and clinical benefits of mibefradil in the coronary slow flow phenomenon. *JACC* 2004;44:57-62.
382. Major T, Dhamija S, Black N, Liachenko S, Morenko B, Sobocinski G, Okerberg C, Tinholt P, Madore S, Kowala M. The T- and L-type calcium channel blocker (CCB) mibefradil attenuates leg edema induced by the L-type CCB nifedipine in the spontaneously hypertensive rat: a novel differentiating assay. *J Pharmacol Exp Ther* 2008;325(3):723-31.
383. Boulanger C, Nakashima M, Olmos L, Joly G, Vanhoutte P. Effects of the Ca²⁺ antagonist RO 40-5967 on endothelium-dependent responses of isolated arteries. *J Cardiovasc Pharmacol* 1994;23(6):869-75.
-

384. Panner A, Wurster R. T-type calcium channels and tumor proliferation. *Cell Calcium* 2006;40(2):253-9.
385. Gray L, Perez-Reyes E, Gomora J, Haverstick D, Shattock M, McLatchie L, Harper J, Brooks G, Heady T, MacDonald T. The role of voltage gated T-type Ca^{2+} channel isoforms in mediating "capacitative" Ca^{2+} entry in cancer cells. *Cell Calcium* 2004;36(6):489-97.
386. Bertolesi G, Shi C, Elbaum L, Jollimore C, Rozenberg G, Barnes S, Kelly M. The Ca^{2+} channel antagonists mibefradil and pimozide inhibit cell growth via different cytotoxic mechanisms. *Mol Pharmacol* 2002;62(2):210-9.
387. Yamashita T, Masuda Y, Sakai T, Tanaka S, Kasuya Y. NZ-105, a new 1,4-dihydropyridine derivative: correlation between dihydropyridine receptor binding and inhibition of calcium uptake in rabbit aorta. *Jpn J Pharmacol* 1991;57(3):337-48.
388. Masuda Y, Iwama T, Yamashita T, Sakai T, Hibi M, Tanaka S, Shigenobu K, Kasuya Y. Vasorelaxing and receptor binding properties of NZ-105, a novel dihydropyridine derivative, in isolated rabbit aorta. *Arch Int Pharmacodyn Ther* 1991;312:86-103.
389. Masumiya H, Toshinori S, Tanaka T, Shigenobu K. Inhibition of myocardial L- and T-type Ca^{2+} currents by aranidipine: possible mechanism for its chronotropic effect. *Pharmacology* 1998;349:351-257.
390. Masuda Y, Tanaka S. Efonidipine hydrochloride: a new calcium channel antagonist. *Cardiovasc Drug Rev* 1994;12(2):123-35.
-

-
391. Furukawa T, Miura R, Honda M, Kamiya N, Mori Y, Takeshita S, Isshiki T, Nukada T. Identification of *R*(-)-isomer of efonidipine as a selective blocker of T-type Ca²⁺ channels. *Br J Pharmacol* 2004;143(8):1050-7.
392. Tanaka T, Tsutamoto T, Sakai H, Fujii M, Yamamoto T, Horie M. Comparison of the effects of efonidipine and amlodipine on aldosterone in patients with hypertension. *Hypertens Res* 2007;30(8):691-7.
393. Koh K, Quon M, Lee S, Han S, Ahn J, Kim J, Chung W, Lee Y, Shin E. Efonidipine simultaneously improves blood pressure, endothelial function, and metabolic parameter in nondiabetic patients with hypertension. *Diabetes Care* 2007;30(6):1605-7.
394. Harada K, Nomura M, Nishikado A, Uehara K, Nakaya Y, Ito S. Clinical efficacy of efonidipine hydrochloride, a T-type calcium channel inhibitor, on sympathetic activities. *Circ J* 2003;67(2):139-45.
395. Masuda Y, Takeguchi M, Arakawa C, Sakai T, Hibi M, Tanaka S, Shigenobu K, Kasuya Y. Antihypertensive and diuretic effects of NZ-105, a novel dihydropyridine derivative. *Arch Int Pharmacodyn Ther* 1990;304:247-64.
396. Jin H, Sato R, Higashino R, Fukuda D, Kurimoto T, Tamaki H. Spasmolytic effect of efonidipine hydrochloride in isolated canine coronary artery: comparison with the effects of nifedipine and nisoldipine. *Biol Pharm Bull* 1997;20(2):196-200.
397. Saito T, Fujii K, Takizawa T, Toyosaki T, Kuwabara Y, Kobayashi S, Ichikawa H, Karaki A, Yamazaki Y, Iwata J, Yamada K, Tomiya H, Takeda K,
-

- Inagaki Y. Effects of the new calcium antagonist efonidipine hydrochloride on resting and exercise hemodynamics in patients with stable effort angina. *Arzneimittelforschung* 1996;46(9):861-7.
398. Nomura S, Kanazawa S, Fukuhara S. Effects of efonidipine on platelet and monocyte activation markers in hypertensive patients with and without type 2 diabetes mellitus. *J Hum Hypertens* 2002;16(8):539-47.
399. Ishimitsu T, Kameda T, Akashiba A, Takahashi T, Ohta S, Yoshii M, Minami J, Ono H, Numabe A, Matsuoka H. Efonidipine reduces proteinuria and plasma aldosterone in patients with chronic glomerulonephritis. *Hypertens Res* 2007;30(7):621-6.
400. Hayashi K, Kumagai H, Saruta T. Effect of efonidipine and ACE inhibitors on proteinuria in human hypertension with renal impairment. *Am J Hypertens* 2003;16(2):116-22.
401. Sasaki H, Saiki A, Endo K, Ban N, Yamaguchi T, Kawana H, Nagayama D, Ohhira M, Oyama T, Miyashita Y, Shirai K. Protective effects of efonidipine, a T- and L-type calcium channel blocker, on renal function and arterial stiffness in type 2 diabetic patients with hypertension and nephropathy. *J Atheroscler Thromb* 2009;16(5):568-575.
402. Bolton T. Mechanism of action of transmitters and other substances on smooth muscle. *Physiol Rev* 1979;59(3):606-718.
403. Van Breemen C, Aaronson P, Loutzenhiser R. Sodium-calcium interactions in mammalian smooth muscle. *Pharmacol Rev* 1978;30(2):167-208.
-

404. Janssen L, Kwan C. ROCs and SOCs: what's in a name? *Cell Calcium* 2007;41(3):245-7.
405. Guibert C, Ducret T, Savineau J. Voltage-independent calcium influx in smooth muscle. *Prog Biophys Mol Biol* 2008;98(1):10-23.
406. Wang Y, Kotlikoff M. Signalling pathway for histamine activation of non-selective cation channels in equine tracheal myocytes. *J Physiol* 2000;523(1):131-8.
407. Vogalis F, Sanders K. Cholinergic stimulation activates a non-selective cation current in canine pyloric circular muscle cells. *J Physiol* 1990;429:223-36.
408. Kim S, Ahn S, So I, Kim K. Role of calmodulin in the activation of carbachol-activated cationic current in guinea pig gastric antral myocytes. *Pflugers Arch* 1995;430(5):757-62.
409. Aromolaran A, Albert A, Large W. Evidence for myosin light chain kinase mediating noradrenaline-evoked cation current in rabbit portal vein myocytes. *J Physiol* 2000;524(3):853-63.
410. Albert A, Aromolaran A, Large W. Agents that increase tyrosine phosphorylation activate a non-selective cation current in single rabbit portal vein smooth muscle cells. *J Physiol* 2001;530(2):207-17.
411. Oike M, Kitamura K, Kuriyama H. Protein kinase C activates the non-selective cation channel in the rabbit portal vein. *Pflugers Arch* 1993;424(2):159-64.

412. Ahn S, Kim S, So I, Kim K. Inhibitory effect of phorbol 12,13 dibutyrate on carbachol-activated nonselective cationic current in guinea-pig gastric myocytes. *Pflugers Arch* 1997;434(4):505-7.
413. Inoue R, Okada T, Onoue H, Hara Y, Shimizu S, Naitoh S, Ito Y, Mori Y. The transient receptor potential protein homologue TRP6 is the essential component of vascular α_1 -adrenoceptor-activated Ca^{2+} -permeable cation channel. *Circ Res* 2001;88(3):325-32.
414. Xu S, Beech D. TrpC1 is a membrane-spanning subunit of store-operated Ca^{2+} channels in native vascular smooth muscle cells. *Circ Res* 2001;88:84-7.
415. Facemire C, Arendshorst W. Calmodulin mediates norepinephrine-induced receptor-operated calcium entry in preglomerular resistance arteries. *Am J Physiol* 2005;289:F127-F36.
416. Zhang Y, Hoover D. Signaling mechanisms for muscarinic receptor-mediated coronary vasoconstriction in isolated rat hearts. *J Pharmacol Exp Ther* 2000;293(1):96-106.
417. Tunctan B, Altug S, Uludag O, Abacioglu N. Effects of econazole on receptor-operated and depolarization-induced contractions in rat isolated aorta. *Life Sci* 2000;67(19):2393-401.
418. Golovina V. Cell proliferation is associated with enhanced capacitative Ca^{2+} entry in human atrial myocytes. *Am J Physiol* 1999;277(2 Pt 1):C343-C9.

419. Jayadev S, Petranka J, Cheran S, Biermann J, Barrett J, Murphy E. Reduced capacitative calcium entry correlates with vesicle accumulation and apoptosis. *J Biol Chem* 1999;274(12):8261-8.
420. Parekh A, Penner R. Store depletion and calcium influx. *Physiol Rev* 1997;77(4):901-30.
421. Lepple-Wienhues A, Belka C, Laun T, Jekie A, Walter B, Wieland U, Welz M, Heil L, Kun J, Busch G, Weller M, Bamberg M, Gulbins E, Lang F. Stimulation of CD95 (Fas) blocks T lymphocyte calcium channels through sphingomyelinase and sphingolipids. *Proc Natl Acad Sci* 1999;96(24):13795-800.
422. Albert A, Large W. Store-operated Ca^{2+} -permeable non-selective cation channels in smooth muscle cells. *Cell Calcium* 2003;33(5-6):345-56.
423. Casteels R, Droogmans G. Exchange characteristics of the noradrenaline-sensitive calcium store in vascular smooth muscle cells of the rabbit ear artery. *J Physiol* 1981;317:263-79.
424. Ma J, Pan Z. Junctional membrane structure and store operated calcium entry in muscle cells. *Front Biosci* 2003;8:d242-d55.
425. Bergdahl A, Gomez M, Wihlborg A, Erlinge D, Eyjolfson A, Xu s, Beech D, Dreja K, Hellstrand P. Plasticity of TRPC expression in arterial smooth muscle: correlation with store-operated Ca^{2+} entry. *Am J Physiol Cell Physiol* 2005;288(4):C872-C80.

426. Sweeney M, McDaniel S, Platoshyn O, Zhang S, Yu Y, Lapp B, Zhao Y, Thistlethwaite P, Yuan J. Role of capacitative Ca^{2+} entry in bronchial contraction and remodeling. *J Appl Physiol* 2002;92(4):1594-602.
427. Golovina V, Platoshyn O, Bailey C, Wang J, Limsuwan A, Sweeney M, Rubin L, Yuan J. Upregulated TRP and enhanced capacitative Ca^{2+} entry in human pulmonary artery myocytes during proliferation. *Am J Physiol Heart Circ Physiol* 2001;280(2):H746-H55.
428. Xu S, Boulay G, Flemming R, Beech D. E3-targeted anti-TRPC5 antibody inhibits store-operated calcium entry in freshly isolated pial arterioles. *Am J Physiol Heart Circ Physiol* 2006;291(6):H2653-H9.
429. Roos J, DiGregorio P, Yeromin A, et al. STIM1, an essential and conserved component of store-operated Ca^{2+} channel function. *J Cell Biol* 2005;169(3):435-45.
430. Lopez J, Salido G, Pariente J, Rosado J. Interaction of STIM1 with endogenously expressed human canonical TRP1 upon depletion of intracellular Ca^{2+} stores. *J Biol Chem* 2006;281(38):28254-64.
431. Prakriya M, Feske S, Gwack Y, Srikanth S, Rao A, Hogan P. Orai1 is an essential pore subunit of the CRAC channel. *Nature* 2006;443(7108).
432. Feske S, Gwack Y, Prakriya M, et al. A mutation in Orai1 causes immune deficiency by abrogating CRAC channel function. *Nature* 2006;441(7090):179-85.

433. Nelson M, Quayle J. Physiological properties of potassium channels in arterial smooth muscle. *Am J Physiol* 1995;268(4 Part 1):C799-C822.
434. Albarwani S, Nemetz L, Madden J, Tobin A, England S, Pratt P, Rusch N. Voltage-gated K⁺ channels in rat small cerebral arteries: molecular identity of the functional channels. *J Physiol* 2003;551(Part 3):751-63.
435. Cheong A, Dedman A, Beech D. Expression and function of native potassium channel K_vα₁ subunits in terminal arterioles of rabbit. *J Physiol* 2001;534(3):691-700.
436. Xu C, Lu Y, Tang G, Wang R. Expression of voltage-dependent K⁺ channel genes in mesenteric artery smooth muscle cells. *Am J Physiol* 1999;277(5 Part 1):G1055-G63.
437. Beech D, Bolton T. A voltage-dependent outward current with fast kinetics in single smooth muscle cells isolated from rabbit portal vein. *J Physiol* 1989;412(397-414).
438. Yuan X, Wang J, Juhaszova M, Golovina V, Rubin L. Molecular basis and function of voltage-gated K⁺ channels in pulmonary arterial muscle cells. *Am J Physiol* 1998;274(4 Part 1):L621-L35.
439. Archer S, Souil E, Dihn-Xuan A, Schremmer B, Mercier J, El Yaagoubi A, Nguyen-Huu L, Reeve H, Hampl V. Molecular identification of the role of voltage-gated K⁺ channels, K_v1.5 and K_v1.2, in hypoxic pulmonary

-
- vasoconstriction and control of resting membrane potential in rat pulmonary artery myocytes. *J Clin Invest* 1998;101(11):2319-30.
440. Yuan X. Voltage-gated K⁺ currents regulate resting membrane potential and [Ca²⁺]_i in pulmonary arterial myocytes. *Circ Res* 1995;77(2):370-8.
441. Milesi V, Aiello E, Rebolledo A, Gomez Alvis A, Grassi de Gende A. Role of Ca²⁺-activated K⁺ current in the maintenance of resting membrane potential of isolated, human, saphenous vein in smooth muscle cells. *Pflugers Arch* 1999;437(3):455-61.
442. Mistry D, Garland C. Characteristics of single, large-conductance calcium-dependent potassium channels (BKCa) from smooth muscle cells isolated from the rabbit mesenteric artery. *J Membr Biol* 1998;164(2):125-38.
443. Balwierczak J, Krulan C, Kim H, DelGrande D, Weiss G, Hu S. Evidence that BKCa channel activation contributes to K⁺ channel opener induced relaxation of the porcine coronary artery. *Naunyn Schmiedebergs Arch Pharmacol* 1995;352(2):213-21.
444. Wu S. Large-conductance Ca²⁺-activated K⁺ channels: physiological role and pharmacology. *Curr Med Chem* 2003;10(8):649-61.
445. Barrett J, Magleby K, Pallotta B. Properties of single calcium-activated potassium channels in cultured rat muscle. *J Physiol* 1982;331:211-30.
-

446. Latorre R, Vergara C, Hidalgo C. Reconstitution in planar lipid bilayers of a Ca^{2+} -dependent K^+ channel from transverse tubule membranes isolated from rabbit skeletal muscle. *Proc Natl Acad Sci* 1982;79(3):805-9.
447. Loeb A, Godeny I, Longnecker D. Functional evidence for inward-rectifier potassium channels in rat cremaster muscle arterioles. *Microvasc Res* 2000;59(1):1-6.
448. Jackson W, Blair K. Characterization and function of Ca^{2+} -activated K^+ channels in arteriolar smooth muscle cells. *Am J Physiol* 1998;274(1 Part 2):H27-H34.
449. Paterno R, Faraci F, Heinstad D. Role of Ca^{2+} -dependent K^+ channels in cerebral vasodilation induced by increases in cyclic GMP and cyclic AMP in the rat. *Stroke* 1996;27(9):1603-7.
450. Brayden J, Nelson M. Regulation of arteriolar tone by activation of calcium-dependent potassium channels. *Science* 1992;256(5056):532-5.
451. Quayle J, Nelson M, Standen N. ATP-sensitive and inwardly rectifying potassium channels in smooth muscle. *Physiol Rev* 1997;77(4):1165-232.
452. Davis N, Standen N, Stanfield P. ATP-dependent potassium channels of muscle cells: their properties, regulation and possible functions. *J Bioenerg Biomembr* 1991;23(4):509-35.
453. Noma A. ATP-regulated K^+ channels in cardiac muscle. *Nature* 1983;305(5930):147-8.

454. Cao K, Tang G, Hu D, Wang R. Molecular basis of ATP-sensitive K⁺ channels in rat vascular smooth muscles. *Biochem Biophys Res Comm* 2002;296(2):463-9.
455. Cui Y, Tran S, Tinker A, Clapp L. The molecular composition of K_{ATP} channels in human pulmonary artery smooth muscle cells and their modulation by growth. *Am J Respir Cell Mol Biol* 2002;26(1):135-43.
456. Daut J, Maier-Rudolph W, von Beckerath N, Mehrke G, Gunther K, Goedel-Meinen L. Hypoxic dilation of coronary arteries is mediated by ATP-sensitive potassium channels. *Science* 1990;247(4948):1341-4.
457. Kanatsuka H, Sekiguchi N, Sato K, Akai K, Wang Y, Komuru T, Ahikawa K, Takishima T. Microvascular sites and mechanisms responsible for reactive hyperemia in the coronary circulation of the beating canine heart. *Circ Res* 1992;71(4):912-22.
458. Landry D, Oliver J. The ATP-sensitive K⁺ channel mediates hypotension in endotoxemia and hypoxic lactic acidosis in dogs. *J Clin Invest* 1992;89(6):2071-4.
459. Sun Park W, Kyoung Son Y, Kim N, Boum Youm J, Joo H, Warda M, Ko J, Earm Y, Han J. The protein kinase A inhibitor, H-89, directly inhibits K_{ATP} and Kir channels in rabbit coronary arterial smooth muscle cells. *Biochem Biophys Res Comm* 2006;340(4):1104-10.

460. Knot H, Zimmermann P, Nelson M. Extracellular K^+ -induced hyperpolarizations and dilatations of rat coronary and cerebral arteries involve inward rectifier K^+ channels. *J Physiol* 1996;492(2):419-30.
461. Quayle J, McCarron J, Brayden J, Nelson M. Inward rectifier K^+ currents in smooth muscle cells from rat resistance-sized cerebral arteries. *Am J Physiol* 1993;265(5 Part 1):C1363-C70.
462. Robertson B, Bonev A, Nelson M. Inward rectifier K^+ currents in smooth muscle cells from rat coronary arteries: block by Mg^{2+} , Ca^{2+} , and Ba^{2+} . *Am J Physiol* 1996;271(2 Part 2):H696-H705.
463. Edwards F, Hirst G, Silverberg G. Inward rectification in rat cerebral arterioles; involvement of potassium ions in autoregulation. *J Physiol* 1988;404:455-66.
464. Park W, Ko J, Kim N, Son Y, Kang S, Warda M, Jung I, Park Y, Han J. Increased inhibition of inward rectifier K^+ channels by angiotensin II in small diameter coronary artery of isoproterenol-induced hypertrophied model. *Arterioscler Thromb Vasc Biol* 2007;27(8):1768-75.
465. Park W, Son Y, Kim N, Ko J, Kang S, Warda M, Earm Y, Jung I, Park Y, Han J. Acute hypoxia induces vasodilation and increases coronary blood flow by activating inward rectifier K^+ channels. *Pflugers Arch* 2007;452(6):1023-30.
466. Eckman D, Nelson M. Potassium ions as vasodilators: role of inward rectifier potassium channels. *Circ Res* 2001;88(2):132-3.

467. Zaritsky J, Eckman D, Wellman G, Nelson M, Schwartz T. Targeted disruption of Kir2.1 and Kir2.2 genes reveals the essential role of the inwardly rectifying K⁺ current in K⁺-mediated vasodilation. *Circ Res* 2000;87(2):160-6.
468. Chissobolis S, Ziogas J, Chu Y, Faraci F, Sobey C. Role of inwardly rectifying K⁺ channels in K⁺-induced cerebral vasodilation *in vivo*. *Am J Physiol Heart Circ Physiol* 2000;279(6):H2704-H12.
469. Jentsch T, Stein V, Weinreich F, Zdekik A. Molecular structure and function of chloride channels. *Physiol Rev* 2002;82(2):503-68.
470. Lamb F, Volk K, Shibata E. Calcium-activated chloride current in rabbit coronary artery myocytes. *Circ Res* 1994;75(4):742-50.
471. Pacaud P, Loirand G, Lavie J, Mironneau C, Mironneau J. Calcium-activated chloride current in rat vascular smooth muscle cells in short-term primary culture. *Pflugers Arch* 1989;413(6):629-36.
472. Zygmunt A. Intracellular calcium activates a chloride current in canine ventricular myocytes. *Am J Physiol* 1994;267(5 Part 2):H1984-H95.
473. Zygmunt A, Gibbons W. Properties of the calcium-activated chloride current in heart. *J Gen Physiol* 1992;99(3):391-414.
474. Reisert J, Bauer P, Yau K, Frings S. The Ca-activated Cl channel and its control in rat olfactory neurons. *J Gen Physiol* 2003;122(3):349-63.

475. Lancaster E, Oh E, Gover T, Weinreich D. Calcium and calcium-activated currents in vagotomized rat primary vagal afferent neurons. *J Physiol* 2002;540(2):543-56.
476. Schumann M, Gardner P, Raffin T. Recombinant human tumor necrosis factor alpha induces calcium oscillation and calcium-activated chloride current in human neutrophils. The role of calcium/calmodulin-dependent protein kinase. *J Biol Chem* 1993;268(3):2134-40.
477. Nishimoto I, Wagner J, Schulman H, Gardener P. Regulation of Cl⁻ channels by multifactorial CaM kinase. *Neuron* 1991;6(4):547-55.
478. Jeulin C, Seltzer V, Bailbe D, Andreeau K, Marano F. EGF mediates calcium-activated chloride channel activation in the human bronchial epithelial cell line 16HBE14o-: involvement of tyrosine kinase p60c-src. *Am J Physiol Lung Cell Mol Physiol* 2008;295(3):L489-L96.
479. Hartzell C, Putzier I, Arrela J. Calcium-activated chloride channels. *Annu Rev Physiol* 2005;67:719-58.
480. Scott R, Sutton K, Griffin A, Stapleton S, Currie K. Aspects of calcium-activated chloride currents: a neuronal perspective. *Pharmacol Ther* 1995;66(3):535-65.
481. Large W, Wang Q. Characteristics and physiological role of the Ca²⁺-activated Cl⁻ conductance in smooth muscle. *Am J Physiol* 1996;271(2 Part 1):C435-C54.

482. Drexler H, Hornig B. Endothelial dysfunction in human disease. *J Mol Cell Cardiol* 1999;31:51-60.
483. Davey M, Luscher E. Actions of thrombin and other coagulant and proteolytic enzymes on blood platelets. *Nature* 1967;216(118):857-8.
484. Voss B, McLaughlin J, Holinstat M, Zent R, Hamm H. PAR1, but not PAR4, activates human platelets through a Gi/o/phosphoinositide-3 kinase signaling axis. *Mol Pharmacol* 2007;71(5):1399-406.
485. Ross R. Atherosclerosis - an inflammatory disease. *N Engl J Med* 1999;340(2):115-26.
486. Newby A. An overview of the vascular response to injury: a tribute to the late Russell Ross. *Toxicol Lett* 2000;112-113:519-29.
487. National Heart Foundation of Australia (Report by Vos T and Begg S, Centre for Burden of Disease and Cost-effectiveness, University of Queensland School of Population Health). *The burden of cardiovascular disease in Australia for the year 2003*. 2006.
488. Harrison D. Endothelial dysfunction in atherosclerosis. *Basic Res Cardiol* 1994;89(Suppl 1):87-102.
489. Kinlay S, Ganz P. Role of endothelial dysfunction in coronary artery disease and implications for therapy. *Am J Cardiol* 1997;80(9A):11I-6I.

490. Papapetropoulos A, Garcia-Cardena G, Madri J, Sessa W. Nitric oxide production contributes to the angiogenic properties of vascular endothelial growth factor in human endothelial cells. *J Clin Invest* 1997;100(12):3131-9.
491. Abrams J, Thadani U. Therapy of stable angina pectoris: the uncomplicated patient. *Circulation* 2005;112(15):e255-e9.
492. Thadani U. Treatment of stable angina. *Curr Opin Cardiol* 1999;14(4):349-58.
493. Specchia G, De Servi S, Falcone C, Bramucci E, Angoli L, Mussini A, Mariononi G, Montemartini C, Boppa P. Coronary arterial spasm as a cause of exercise-induced ST-segment elevation in patients with variant angina. *Circulation* 1979;59(5):948-54.
494. de Silva R, Fox K. The changing horizon of acute coronary syndrome. *Lancet* 2009;374(9696):1125-7.
495. Davies M, Woolf N, Robertson W. Pathology of acute myocardial infarction with particular reference to occlusive coronary thrombi. *Br Heart J* 1976;38(7):659-64.
496. Kawano H, Ogawa H. Endothelial function and coronary spastic angina. *Intern Med* 2005;44(2):91-9.
497. Miller D, Waters D, Warnica W, Szlachcic J, Kreeft J, Theroux D. Is variant angina the coronary manifestation of a generalised vasospastic disorder. *N Engl J Med* 1981;304:763-6.

498. Viles-Gonzalez J, Fuster V, Badimon J. Atherothrombosis: a widespread disease with unpredictable and life-threatening consequences. *Eur Heart J* 2004;25(14):1197-207.
499. Schmieder F, Comerota A. Intermittent claudication: magnitude of the problem, patient evaluation, and therapeutic strategies. *Am J Cardiol* 2001;87(12A):3D-13D.
500. Hiatt W. Pharmacologic therapy for peripheral arterial disease and claudication. *J Vasc Res* 2002;36(6):1283-91.
501. Dormandy J, Rutherford R. Management of peripheral artery disease (PAD). TASC Working Group. TransAtlantic Inter-Society Consensus (TASC). *J Vasc Surg* 2000;31(1 Part 2):S1-S296.
502. Depre C, Wijns W, Robert A, Renkin J, Havaux X. Pathology of unstable plaque: correlation with the clinical severity of acute coronary syndromes. *JACC* 1997;30(3):694-702.
503. Crea F, Lanza G. Angina pectoris and normal coronary arteries: cardiac syndrome X. *Heart* 2004;90(4):457-63.
504. Maseri A, Crea F, Kaski J, Crake T. Mechanisms of angina pectoris in syndrome X. *JACC* 1991;17(2):499-506.
505. Beltrame J. *Chest Pain and Normal Angiography*. In: Braunwald E, ed. Braunwald's Heart Disease Edition. Philadelphia: Elsevier 2006.

506. National Heart Foundation of Australia. *Guide to management of hypertension 2008*. 2008.
507. Kjeldsen S, Julius S, Hedner T, Hansson L. Stroke is more common than myocardial infarction in hypertension: analysis based on 11 major randomized intervention trials. *Blood Press* 2001;10(4):190-2.
508. Bronner L, Kanter D, Manson J. Primary prevention of stroke. *N Engl J Med* 1995;333(21):1392-400.
509. Tocci G, Sciarretta S, Volpe M. Development of heart failure in recent hypertension trials. *J Hypertens* 2008;26(7):1477-86.
510. Levy D, Larson M, Vasan R, Kannel W, Ho K. The progression from hypertension to congestive heart failure. *JAMA* 1996;275(20):1555-1562.
511. Sarnak M, Greene T, Wang X, Beck G, Kusek J, Collins A, Levey A. The effect of lower target blood pressure on the progression of kidney disease: long-term follow-up of the modification of diet in renal disease study. *Ann Intern Med* 2005;142(5):342-51.
512. Leys D. Atherothrombosis: a major health burden. *Cerebrovasc Dis* 2001;11(Suppl 2):1-4.
513. Albers G, Easton J, Sacco R, Teal P. Antithrombotic and thrombolytic therapy for ischemic stroke. *Chest* 1998;114(Suppl 5):683S-98S.
514. Aiyagari V, Badruddin A. Management of hypertension in acute stroke. *Expert Rev Cardiovasc Therapy* 2009;7(6):637-46.
-

515. van Gijn J, Rinkel G. Subarachnoid haemorrhage: diagnosis, causes and management. *Brain* 2001;124(Part 2):249-78.
516. Almgren T, Persson B, Wilhelmsen L, Rosengren A, Andersson O. Stroke and coronary heart disease in treated hypertension - a prospective study over three decades. *J Intern Med* 2005;257:496-502.
517. Easton JD, Saver J, Albers G, Alberts M, Chaturvedi S, Feldmann E, Hatsukami T, Higashida R, Johnston S, Kidwell C, Lutsep H, Miller E, Sacco R. Definition and evaluation of transient ischemic attack: a scientific statement for healthcare professionals from the American Heart Association/American Stroke Association Stroke Council; Council on Cardiovascular Surgery and Anesthesia; Council on Cardiovascular Radiology and Intervention; Council on Cardiovascular Nursing; and the Interdisciplinary Council on Peripheral Vascular Disease. The American Academy of Neurology affirms the value of this statement as an educational tool for neurologists. *Stroke* 2009;40(6):2276-93.
518. Oczkowski W, Turpie A. Antithrombotic treatment of cerebrovascular disease. *Baillieres Clin Haematol* 1990;3(3):781-813.
519. Kistler J, Ropper A, Heros R. Therapy of ischemic cerebral vascular disease due to atherothrombosis (1). *N Engl J Med* 1984;311(1):27-34.
520. Rothwell P, Warlow C. Timing of TIAs preceding stroke: time window for prevention is very short. *Neurology* 2005;64(5):817-20.

521. Lopez A, Mathers C, Ezzati M, Jamison D, Murray C. Global and regional burden of disease and risk factors, 2001: systematic analysis of population health data. *Lancet* 2006;367(9524):1747-57.
522. Manolio T, Cutler J, Furberg C, Psaty B, Whelton P, Applegate W. Trends in pharmacologic management of hypertension in the United States. *Arch Intern Med* 1995;155(8):829-37.
523. Millard R, Grupp G, Grupp I, DiSalvo J, DePover A, Schwartz A. Chronotropic, inotropic and vasodilator actions of diltiazem, nifedipine, and verapamil. A comparative study of physiological responses and membrane receptor activity. *Circ Res* 1983;52(Pt 2):I29-I39.
524. Van der Vring J, Cleophas T, Van der Wall E, Niemeyer M. T-channel-selective calcium channel blockade: a promising therapeutic possibility, only preliminarily tested so far: a review of published data. T-Channel Calcium Channel Blocker Study Group. *Am J Ther* 1999;6(4):229-33.
525. Massie B. Mibefradil: a selective T-type calcium antagonist. *Am J Cardiol* 1997;80(9A):23I-32I.
526. Lee D, Goodman S, Dean D, Lenis J, Ma P, Gervais P, Langer A, PRIDE Investigators. Randomized comparison of T-type versus L-type calcium-channel blockade on exercise duration in stable angina: results of the Posicor Reduction of Ischaemia During Exercise (PRIDE) trial. *Am Heart J* 2002;144(1):60-7.

527. Moosmang S, Haider N, Bruderl B, Welling A, Hofmann F. Antihypertensive effects of the putative T-type calcium channel antagonist mibefradil are mediated by the L-type calcium channel Ca_v1.2. *Circ Res* 2006;98(1):105-10.
528. Sedeek M, Llinas M, Drummond H, Fortepiani L, Abram S, Alexander B, Reckelhoff J, Granger J. Role of reactive oxygen species in endothelin-induced hypertension. *Hypertension* 2003;42(4):806-10.
529. Mulvany M, Halpern W. Contractile properties of small arterial resistance vessels in spontaneously hypertensive and normotensive rats. *Circ Res* 1977;41:19-26.
530. Aalkjaer C, Mulvany M. Human and rat resistance vessels: a comparison of their morphological and pharmacological characteristics. *Gen Pharmacol* 1983;14:85-7.
531. McPherson G. Assessing vascular reactivity of arteries in the small vessel myograph. *Clin Exp Pharmacol Physiol* 1992;19(12):815-25.
532. Angus JA, Jennings GL, Sudhir K. Enhanced contraction to noradrenaline, serotonin and nerve stimulation but normal endothelium-derived relaxing factor response in skin small arteries in human primary hypertension. *Clin Exp Pharmacol Physiol Suppl* 1992;19:39-47.
533. McNally P, Watt P, Rimmer T, Burden A, Hearnshaw J, Thurston H. Impaired contraction and endothelium-dependent relaxation in isolated resistance vessels from patients with insulin-dependent diabetes mellitus. *Clin Sci* 1994;87(1):31-6.
-

534. Nissan Chemical Industries Ltd., Tokyo. *Efonidipine Hydrochloride Pharmacokinetics*. Tokyo, Japan; 2005.
535. Welker H, Wiltshire H, Bullingham R. Clinical pharmacokinetics of mibefradil. *Clin Pharmacokinet* 1998;35(6):405-423.
536. Eichelbaum M, Echizen H. Clinical pharmacology of calcium antagonists: a critical review. *J Cardiovasc Pharmacol* 1984;6(Suppl 7):S963-S7.
537. Kates R. Calcium antagonists. Pharmacokinetic properties. *Drugs* 1983;25(2):113-24.
538. Hollenberg S, Shelhamer J, Cunnion R. Tachyphylaxis to the vasopressor effects of endothelin in rat aortic rings. *Am J Physiol* 1993;264(2 Pt 2):H352-H6.
539. Wang J, Chiou W, Gagne G, Wu-Wong J. Internalization of type-A endothelin receptor. *J Cardiovasc Pharmacol* 2000;36(5 Suppl 1):S61-S5.
540. Anderson R, Brown M, Beisiegel U, Goldstein J. Surface distribution and recycling of the low density lipoprotein receptor as visualized with antireceptor antibodies. *J Cell Biol* 1982;93(3):523-31.
541. Donnellan P, Kinsella B. Immature and mature species of the human Prostacyclin Receptor are ubiquitinated and targeted to the 26S proteasomal or lysosomal degradation pathways, respectively. *J Mol Signal* 2009;25(4):7.

542. Tsai J, Seeman M. *In vitro* characterization of the mechanism of insulin degradation and the effect of chloroquine. *Biochim Biophys Acta* 1981;673(3):259-69.
543. Wu-Wong J, Chiou W, Magnuson S, Oppenorth T. Endothelin receptor in human astrocytoma U373MG cells: binding, dissociation, receptor internalization. *J Pharmacol Exp Ther* 1995;274(1):499-507.
544. Hayashi K, Wakino S, Sugano N, Ozawa Y, Homma K, Saruta T. Ca²⁺ channel subtypes and pharmacology in the kidney. *Circ Res* 2007;100(3):342-53.
545. Bangalore R, Mehrke G, Gingrich K, Hofmann F, Kass R. Influence of L-type Ca channel alpha2delta-subunit on ionic and gating current in transiently transfected HEK293 cells. *Am J Physiol* 1996;270(5 Pt 2):H1521-H8.
546. Shistik E, Ivanina T, Puri T, Hosey M, Dascal N. Ca²⁺ current enhancement by alpha 2/delta and beta subunits in *Xenopus* oocytes: contribution of changes in channel gating and alpha 1 protein level. *J Physiol* 1995;489(Pt 1):55-62.
547. Huguenard J. Low-voltage-activated (t-type) calcium-channel genes identified. *Trends Neurosci* 1998;21(11):451-2.
548. Hermsmeyer K, Sturek M, Rusch N. Calcium channel modulation by dihydropyridines in vascular smooth muscle. *Ann NY Acad Sci* 1988;522:25-31.

549. Ikebe M, Koretz J, Hartshorne D. Effects of phosphorylation of light chain residues threonine 18 and serine 19 on the properties and conformation of smooth muscle myosin. *J Biol Chem* 1988;263(13):6432-7.
550. Means A, George S. Calmodulin regulation of smooth-muscle myosin light chain kinase. *J Cardiovasc Pharmacol* 1988;12(Suppl 5):S25-S9.
551. Hayashi K, Wakino S, Homma K, Sugano N, Saruta T. Pathophysiological significance of T-type Ca^{2+} channels: role of T-type Ca^{2+} channels in renal microcirculation. *J Pharmacol Sci* 2005;99(3):221-7.
552. Jensen L, Salomonsson M, Jensen B, Holstein-Rathlou N. Depolarization-induced calcium influx in rat mesenteric small arterioles is mediated exclusively via mibefradil-sensitive calcium channels. *Br J Pharmacol* 2004;142(4):709-18.
553. Feng M, Li M, Navar L. T-type calcium channels in the regulation of afferent and efferent arterioles in rats. *Am J Physiol* 2004;286(2):F331-7.
554. Arya M, Shergill I, Williamson M, Gommersall L, Arya N, Patel H. Basic principles of real-time quantitative PCR. *Expert Rev Mol Diagn* 2005;5(2):209-19.
555. Mamic T, Holman N. Pmca 1 mRNA expression in rat aortic myocytes: a real-time PCR study. *Biochem Biophys Res Comm* 2000;276(3):1024-7.
556. Livak K, Schmittgent D. Analysis of relative gene expression data using real-time quantitative PCR and the $2^{-\Delta\Delta\text{CT}}$ method. *Methods* 2001;25(402-408).

557. Ganesan A, Maack C, Johns D, Sidor A, O'Rourke B. Beta-adrenergic stimulation of L-type Ca^{2+} channels in cardiac myocytes requires the distal carboxyl terminus of $\alpha_1\text{C}$ but not serine 1928. *Circ Res* 2006;98(2):e11-e8.
558. Shao Y, Alicknavitch M, Farach-Carson M. Expression of voltage sensitive calcium channel (VSCC) L-type $\text{Ca}_v1.2$ ($\alpha_{1\text{C}}$) and T-type $\text{Ca}_v3.2$ ($\alpha_{1\text{H}}$) subunits during mouse bone development. *Dev Dyn* 2005;234(1):54-62.
559. Han W, Bao W, Wang Z, Nattel S. Comparison of ion-channel subunit expression in canine cardiac Purkinje fibers and ventricular muscle. *Circ Res* 2002;91(9):790-7.
560. Avila T, Hernandez-Hernandez O, Almanza A, Bermudez de Leon M, Urban M, Soto E, Cisneros B, Felix R. Regulation of $\text{Ca}_v3.1$ Channels by Glucocorticoids. *Cell Mol Neurobiol* 2009;Epub ahead of print.
561. Inagaki A, Ugawa S, Yamamura H, Murakami S, Shimada S. The $\text{Ca}_v3.1$ T-type Ca^{2+} channel contributes to voltage-dependent calcium currents in rat outer hair cells. *Brain Res* 2008;1201:68-77.
562. Maeda Y, Aoki Y, Sekiguchi F, Matsunami M, Takahashi T, Nishikawa H, Kawabata A. Hyperalgesia induced by spinal and peripheral hydrogen sulfide: evidence for involvement of $\text{Ca}_v3.2$ T-type calcium channels. *Pain* 2009;142(1-2):127-32.
563. Bourinet E, Alloui A, Monteil A, Barrere C, Couette B, Poirot O, Pages A, Mery J, Snutch T, Eschalier A, Nargeot, J. Silencing of the $\text{Ca}_v3.2$ T-type

- calcium channel gene in sensory neurons demonstrates its major role in nociception. *EMBO J* 2005;24(2):315-24.
564. De Jongh K, Colvin A, Wang K, Catterall W. Differential proteolysis of the full-length form of the L-type calcium channel α_1 subunit by calpain. *J Neurochem* 1994;63(4):1558-64.
565. Maruyama Y, Nakanishi Y, Walsh E, Wilson D, Welsh D, Cole W. Heteromultimeric TRPC6-TRPC7 channels contribute to arginine vasopressin-induced cation current of A7r5 vascular smooth muscle cells. *Circ Res* 2006;98(12):1520-7.
566. Laemmli U. Cleavage of structural proteins during the assembly of the head of bacteriophage T4. *Nature* 1970;227(5259):680-5.
567. Clarke D. *Regulation at the RNA level*. In: Marr D, ed. *Molecular Biology: Understanding the Genetic Revolution*. London: Elsevier Academic Press; 2005.
568. Houston M. *Protein Synthesis and Degradation*. In: Eckstein M, Evans J, eds. *Biochemistry Primer for Exercise Science*. Leeds: Human Kinetics Europe Ltd.; 1995.